A COMPARATIVE STUDY OF TRACE ELEMENT GEOCHEMISTRY AND MINERALOGY OF SOME URANIUM DEPOSITS OF LABRADOR, AND EVALUATION OF SOME URANIUM EXPLORATION TECHNIQUES

D. G. MINATIDIS


CENTRE FOR NFLD. STUDIES
JUN 2 1979
MEMORIAL UNIVERSITY
OF NEWFOUNDLAND

NOTICE

The quality of this microfiche is heavily dependent upon the quality of the original thesis submitted for microfilming. Every effort has been made to ensure the highest quality of reproduction possible.

If pages are missing, contact the university which granted the degree.

Some pages may have indistinct print especially if the original pages were typed with a poor typewriter ribbon or if the university sent us a poor photocopy.

Previously copyrighted materials (journal articles, published tests, etc.) are not filmed.

Reproduction in full or in part of this film is governed by the Canadian Copyright Act, R.S.C. 1970, c. C-30. Please read the authorization forms which accompany this thesis.

THIS DISSERTATION
HAS BEEN MICROFILMED
EXACTLY AS RECEIVED

AVIS

La qualité de cette microfiche dépend grandement de la qualité de la thèse soumise au microfilmage. Nous avons tout fait pour assurer une qualité supérieure de reproduction.

S'il manque des pages, veuillez communiquer avec l'université qui a conféré le grade.

La qualité d'impression de certaines pages peut laisser à désirer, surtout si les pages originales ont été dactylographiées à l'aide d'un ruban usé ou si l'université nous a fait parvenir une photocopie de mauvaise qualité.

Les documents qui font déjà l'objet d'un droit d'auteur (articles de revue, examens publiés, etc.) ne sont pas microfilmés.

La reproduction, même partielle, de ce microfilm est soumise à la Loi canadienne sur le droit d'auteur, SRC 1970, c. C-30. Veuillez prendre connaissance des formules d'autorisation qui accompagnent cette thèse.

LA THÈSE A ÉTÉ
MICROFILMÉE TELLE QUE
NOUS L'AVONS REÇUE

A COMPARATIVE STUDY OF TRACE ELEMENT GEOCHEMISTRY AND MINERALOGY OF SOME URANIUM DEPOSITS OF LABRADOR, AND EVALUATION OF SOME URANIUM EXPLORATION TECHNIQUES IN A GLACIAL TERRAIN

by

D. G. Minatidis, B.Sc.

A Thesis

Submitted in Partial Fulfilment

of the requirements for the Degree of

MASTER OF SCIENCE

MEMORIAL UNIVERSITY OF NEWFOUNDLAND

CONTENTS

Page

CHAPTER IV

EVALUATION OF URANIUM EXPLORATION TECHNIQUES IN GLACIATED TERRAIN

CHAPTER V

SUMMARY AND EXPLORATION APPLICATION

ABSTRACT

The Aillik Group of Aphebian metavolcanic and metasedimentary rocks is situated in the Makkovik subprovince of Labrador, north of the Grenville Front.

The Kaipokok volcanic and the Walker Lake-White Bear Mountain belts consist of flow-banded and porphyritic rhyolite lavas, quartzites, minor interbedded basalt lavas and volcanic tuff.

Metamorphism has remained in the greenschist and amphibolite facies throughout tectonism.

One hundred and seventy rock samples were collected from eight uranium showings in the map area and were analysed for 10 trace elements, namely Zr, Sr, Rb, Zn, Cu, Ba, Ni, Cr, U and Th. One hundred and ten thin sections were examined and autoradiographed. Uranium in these showings is present possibly in the following forms:

1) In uranium minerals of davidite composition.
2) In lenses of dark bituminous material.
3) As ions dispersed in such minerals as hornblende, quartz, feldspar and in part in some other minerals.
4) As ions adsorbed on to hematite.
5) As an isomorphous admixture in the minerals biotite, epidote, zircon and sphene.
6) As independant compounds within magnetite.
7) As submicroscopic inclusions of uranium minerals of unknown compositions within garnets, sodic amphiboles and feldspar porphyroblasts.

Results obtained from different uranium exploration techniques in a glaciated terrain, e.g. radon detection, nearshore lake sediment geochemistry, lake water and air-borne surveys, should be interpreted in conjunction with glacial geology and other physiographic factors affecting their applicability.

LIST OF FIGURES

LIST OF TABLES

LIST OF PLATES

ACKNOWLEDGMENTS

The writer would like to thank Dr. D.F. Strong for supervising the study and Dr. R.M. Slatt who provided guidance on the lake sediment analyses.

The projects carried out in Labrador were initiated by the writer.

Thanks are extended to G. Andrews, J. Vahtra, D. Press and D. Sasseville for help in the geochemical lab; to Dr. A.P. Beavan, Dr. R.G. Cawthorn, Dr. V.C. Barber, Mr. J.G. Malpas, Mr. D. Hawkins, Mr. J.B. Whalen and Mr. R.C. Smith for additional help, to F. Goudie of Atlantic Analytical Services, Springdale, Newfoundland for help and advice on uranium analyses, to W. Marsh, F. Thornhill, G. Ford, L. Warford and L. Murphy for help during the preparation of the thesis.

The writer wishes also to thank Drs. J. Cameron, O. Suschny and A.Y. Smith of the International Atomic Energy Agency for the uranium and thorium analyses.

The study was financed by International Atomic Energy Agency (IAEA), British Newfoundland Exploration Ltd. (BRINEX) and N.R.C. operating grant A-7975 to D.F. Strong.

CHAPTER I

GENERAL INTRODUCTION

1.1 General

The Labrador uranium area is located between latitudes 54°35' and 55°15' and longitudes 58°50' and 60°40' of Labrador (Fig. 1). The uranium deposits under investigation are located in the eastern half of the area. The present study is based on field work sponsored by the British Newfoundland Exploration Company Limited (BRINEX) during the summer of 1974.

1.2 Physiography

The topography of the area is essentially of low relief as the result of glacial action, although the coastline is generally rugged with some steep cliffs. Because of poor soil and strong winds, vegetation near the coast is sparse, with 90 per cent of the area treeless. Evidence of ice movement, e.g. boulder trains and their relative position to bedrock, elongated lakes, indicates that the glacial movement was in a generally southwest direction. The glacial drift is generally thicker inland and negligible near the coast. The glacial drift affects the applicability of exploration techniques in a number of ways, as explained in Chapter 4.

1.3 Previous Work

1.3.1 Previous work in Labrador and the Labrador uranium area.

Steinhauer (1814), Lieber (1860), Packard (1891), Daly (1902) and

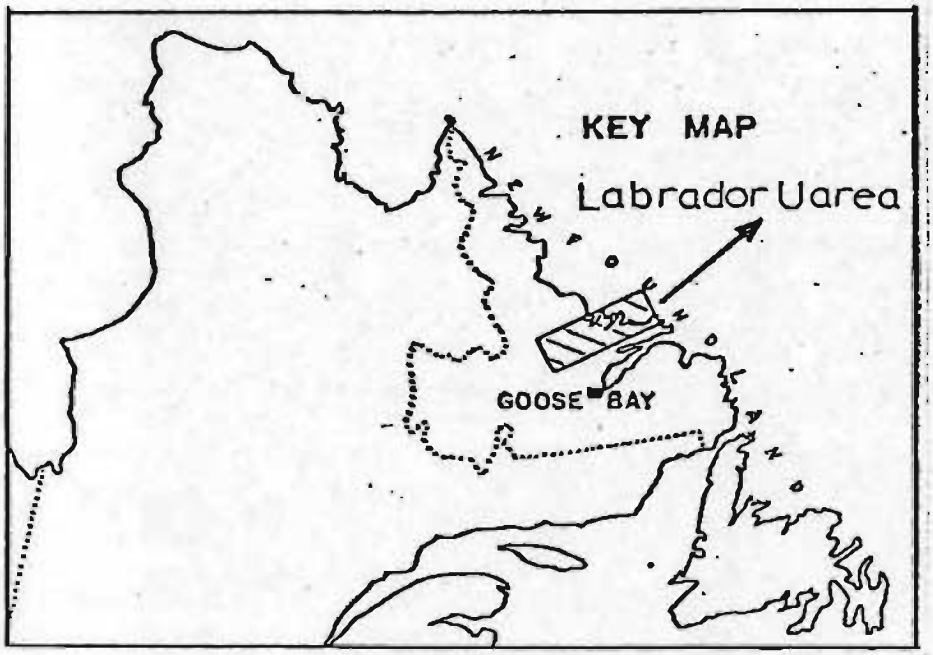

Figure 1. Index map showing the location of the Labrador uranium area.

others provided early interpretations of the regional and local geology. Observations were of a very general nature and were based on brief investigations of randomly scattered areas along the coast. Wheeler (1933 and 1935) studied the petrology of some diabase dykes and an amazonite aplite from the region. Kranck (1939, 1953) mapped the sediments of the Makkovik/Aillik coastal area and introduced the term "Aillik series" and "Hopedale gneiss" for Proterozoic supracrustal rocks and for the Archean basement respectively of the area. Douglas (1953) provided early interpretation of the regional and local geology.

The broad regional relationships of the Makkovik area, both within Labrador and in comparison with Greenland, have been reported by Douglas (1970), Bridgwater (1970), Greene (1972), Greene and McKillop (1972), Sutton (1972a, b), Sutton et al. (1971) and Sutton et al. (1972).

The Geological Survey of Canada has carried out regional geological mapping and radiometric age dating which has lead to numerous publications, e.g. Christie et al. 1953, Stevenson (1970), Taylor (1971, 1972a, b and c), Fahrig and Larochelle (1972), Lowden (1961), Leech et al. (1963), Stockwell (1964) and Wanless and Loveridge (1972).

Beavan (1958) summarized information on the Labrador uranium area and Gandhi et al. (1969) provided a comprehensive map and report on the geology and geochronology of the Makkovik Bay area.

Apart from these, there also exists several unpublished BRINEX reports as well as M.Sc. and Ph.D. theses concerning mainly petrographic studies and regional structural geology. These include, King (1963), Gill (1966), Barua (1969), Clark (1970, 1974).

1.3.2 Previous lithogeochemical studies.

The geological literature abounds with isolated references to economically oriented lithogeochemical studies. General references such as Bradshaw, et al. (1970), Boyle and Garrett (1970), Hawkes and Webb (1962) and Sakrison (1971) discuss the techniques and problems encountered in economic lithogeochemical surveys and refer to the various successes and failures of numerous individual studies. However most of the lithogeochemical studies have been concerned with base metal exploration, and little such work has been done for uranium.

To the knowledge of the writer few lithogeochemical-mineralogical studies have been done on the showings under investigation, although there are chemical analyses for some of them (BRINEX, unpublished data).

1.4 Purpose of the study

The main aim of this study was: (a) to determine the trace element geochemistry and the mineralogy in some of the main uranium deposits in Labrador with a view to understanding their origin and distribution, and (b) evaluate different techniques for uranium exploration in a glaciated terrain.

1.4.1 Methods of investigation

Rock samples were collected from the exposed part of the different deposits although in many cases much of the deposit is not exposed.

Fresh-looking samples were collected and at randomly chosen localities two rock samples were taken so as to provide an idea of sample variation on the outcrop scale, i.e. to evaluate sampling errors (Garrett, 1969).

Soil gas radon surveys were carried out in different areas using a radon emanometer and in one case the radon survey was carried out in conjunction with the Track Etch technique. Nearshore lake sediment samples were collected and analysed for U and Cu in order to compare the results obtained with the results of previous lake water geochemistry and air borne surveys.

1.5 Regional Geology

The majority of the main uranium deposits are located in the Aillik Group, a sequence of metasedimentary and metavolcanic rocks which overlie a complexly deformed banded gneiss, the Hopedale Gneiss (Kranck, 1953).

The rocks of the Aillik Group have been folded into a series of northerly trending folds and are intruded by gabbro, diorite, syenite and granite. Potassium/Argon age determinations range from approximately 1700 m.y. to 1800 m.y. for the Hopedale gneiss, which is considered to be partially remobilized Archean basement, and 1500 to 1600 m.y. for the metamorphosed sedimentary and volcanic rocks and intrusive granite gneiss and granite (Gandhi et al. 1969).

The area which lies north of the Grenville front was intruded by dykes (mainly diabase and lamprophyre dykes) of Grenvillian and later

age (Gandhi et al., 1960; King, 1963).

Four of the uranium showings under investigation (Michelin, Rainbow, M. Ben and McLean) are located in the Walker-Lake-White Bear Mountain area (S) and the other four (Witch, Nash, Kitts and Long Island) in the Kaipokok volcanic belt (N) (Fig. 2). Their local geological settings are shown in Figs. 3 and 4.

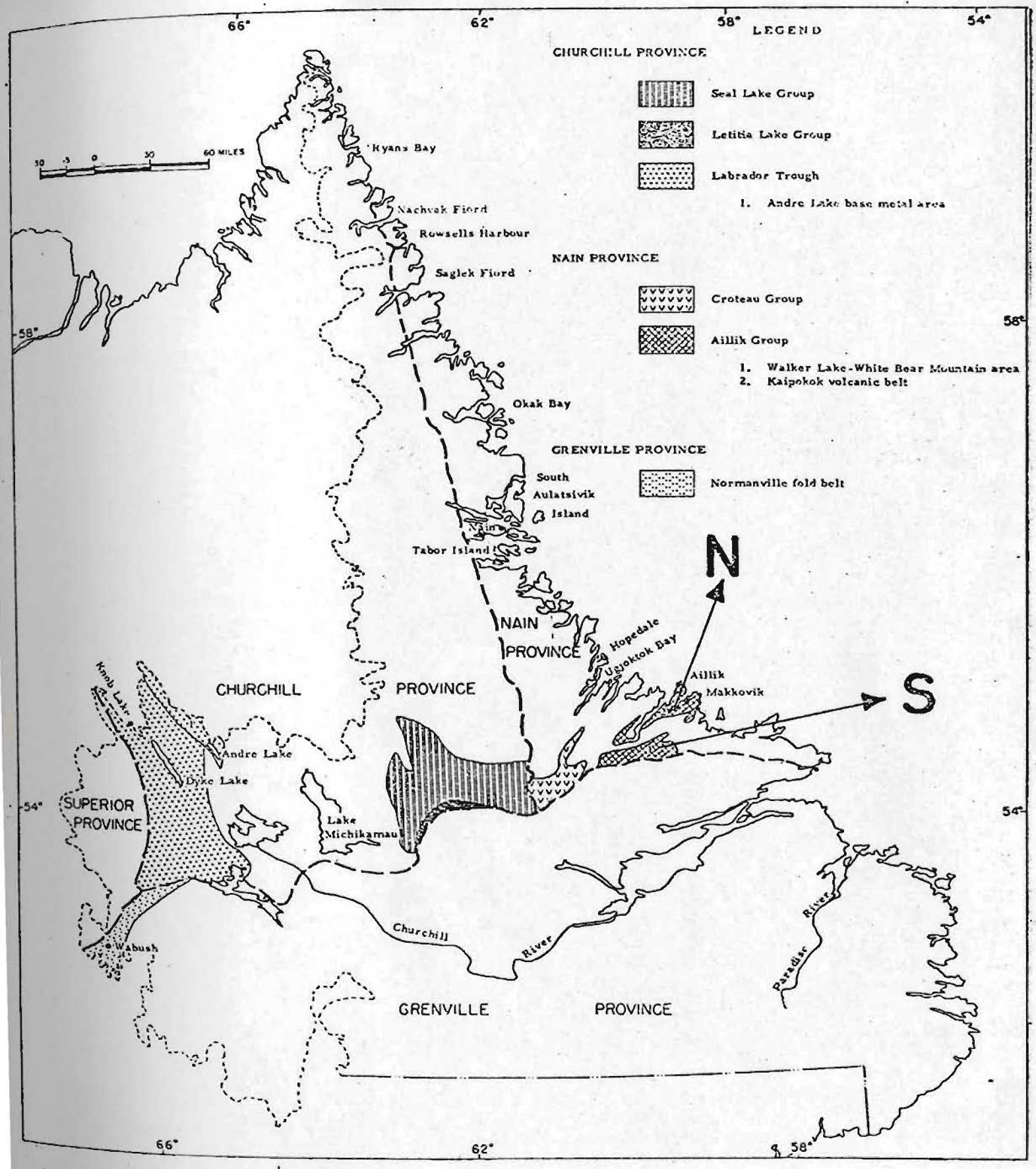

Figure 2. Map showing the principal areas of mineral exploration in Labrador and the location of Kaipokok volcanic belt (N) and Walker Lake-White Bear Mountain area (S) (after Greene, 1974).

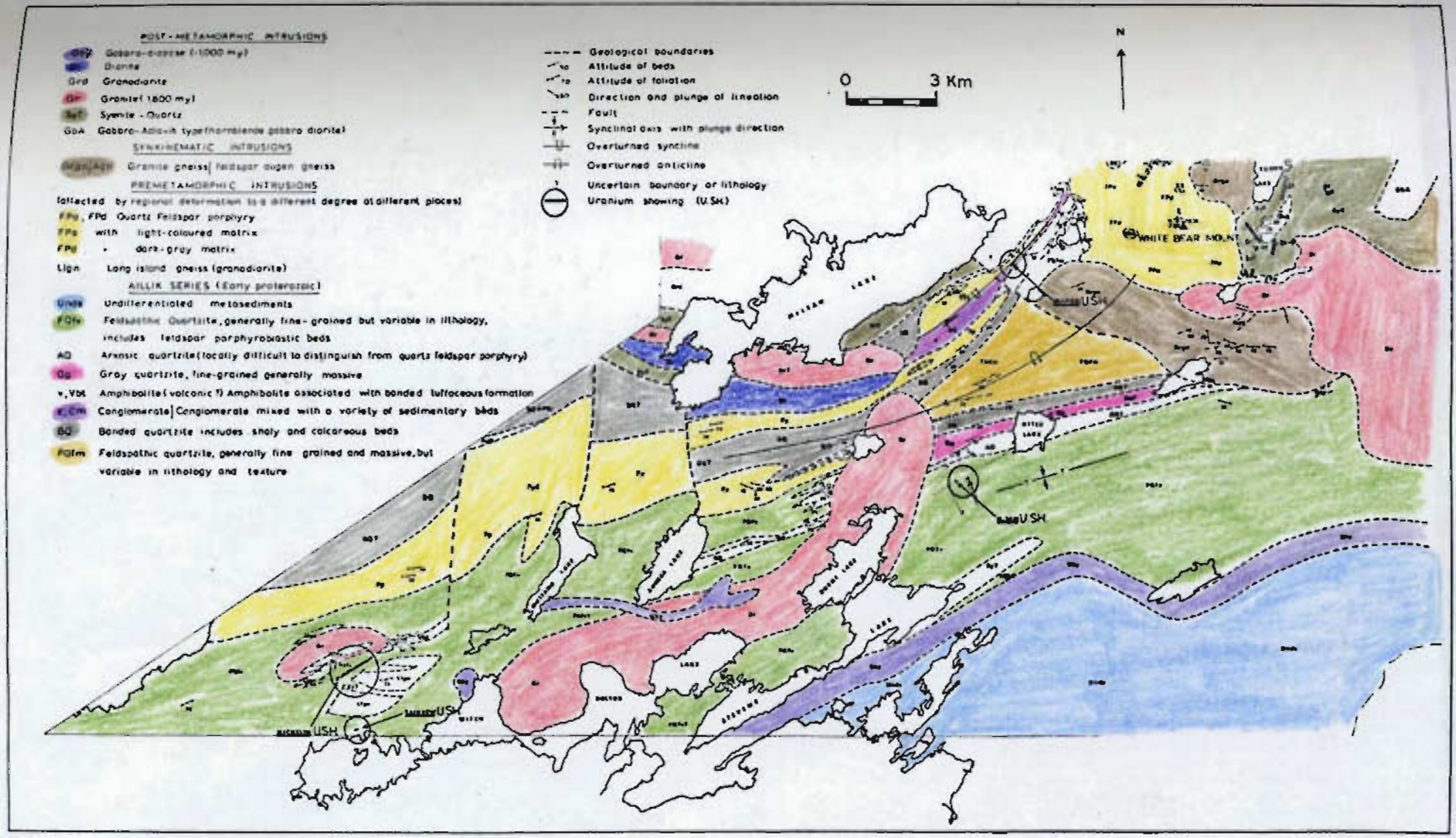

Figure 3. Map showing the regional geology of the Walker Lake-White Bear Mountain area, and the location of the investigated uranium deposits (after BRINEX unpublished compilation map).

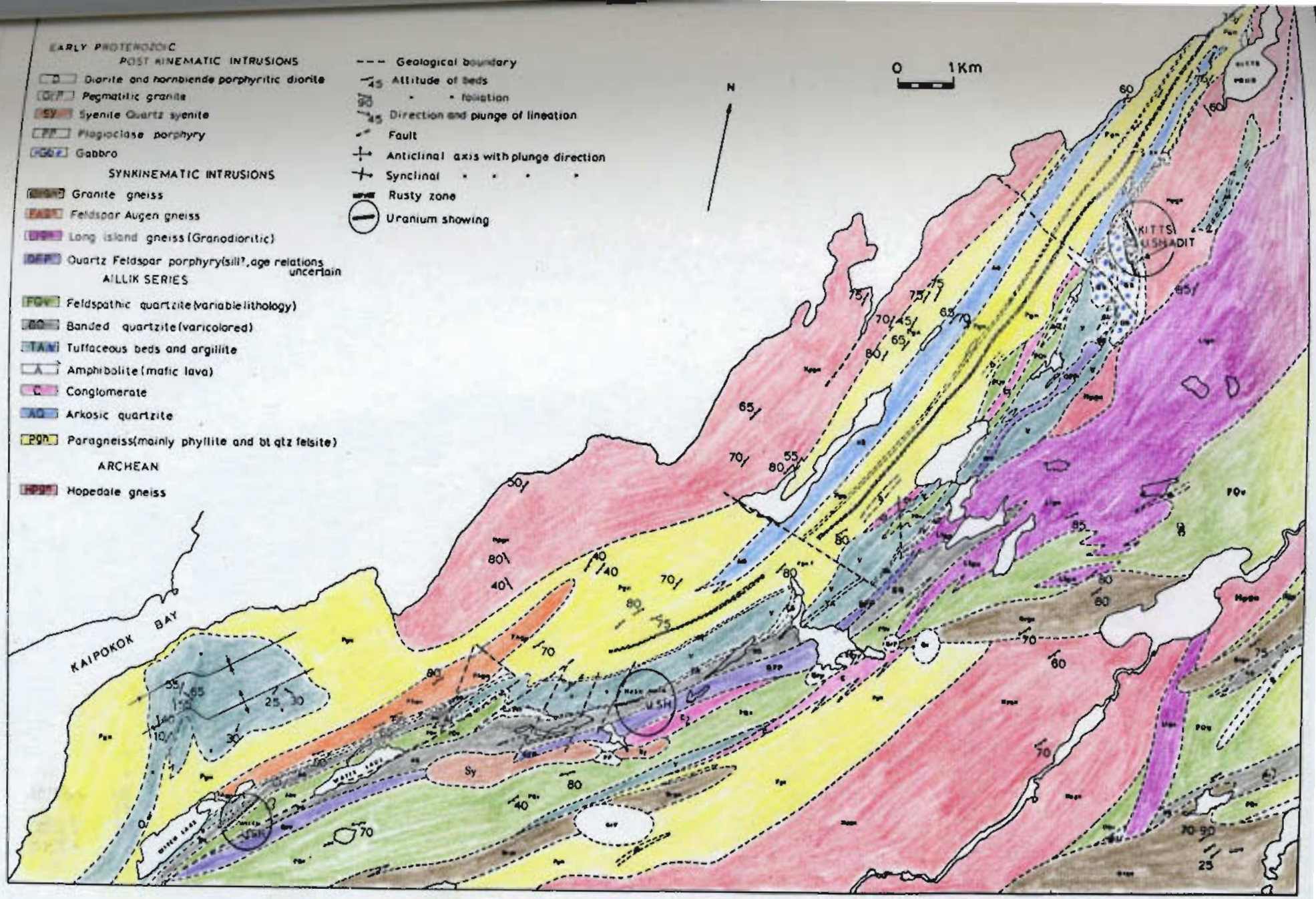

Fig. 4 Map showing the regional geology of the Kaipokok volcanic belt and the location of the investigated uranium deposits (after BRINEX unpublished compilation map).

CHAPTER II

A REVIEW OF THE GEOCHEMISTRY OF URANIUM AND THORIUM

More is known about uranium distribution in nature than about the distribution of many other elements because the radioactive properties of U and its disintegration products make it easy to detect and estimate in minute quantities. Emphasis is given in this chapter to the geochemistry of uranium because the showings under investigation appear to be depleted in thorium. Fig. 5 shows the relation between SiO_2, U, Th and K for the different types of igneous rocks listed in Table 1, showing that acid igneous rocks in general contain significantly higher proportions of Y and Th than basic igneous rocks.

The U^{+4} oxide ($U^{+4}O_2$) is very slightly soluble in water. The dissociation constant for the reaction

$$U^{+4}O_2 + 2H_2O \rightleftharpoons U^{+4} + 4OH^-$$

is but 10^{-52} at 25°C and 1 atmosphere pressure (Garrels, 1953) and little changed by increase in temperature up to 120°C. This great stability of $U^{+4}O_2$ (under reducing conditions) probably accounts for the preponderance of uraninite (UO_2) as a primary uranium ore mineral.

In glaciated areas and cold climates, such as the Canadian Shield, where oxidized surface zones are not well developed, a minimum amount of secondary minerals is found. However, where original uranium concentrations are exposed at the surface, uraninite oxidizes rapidly to give the soluble $(U^{+6}O_2)^{+2}$ complex. If the uraninite is associated

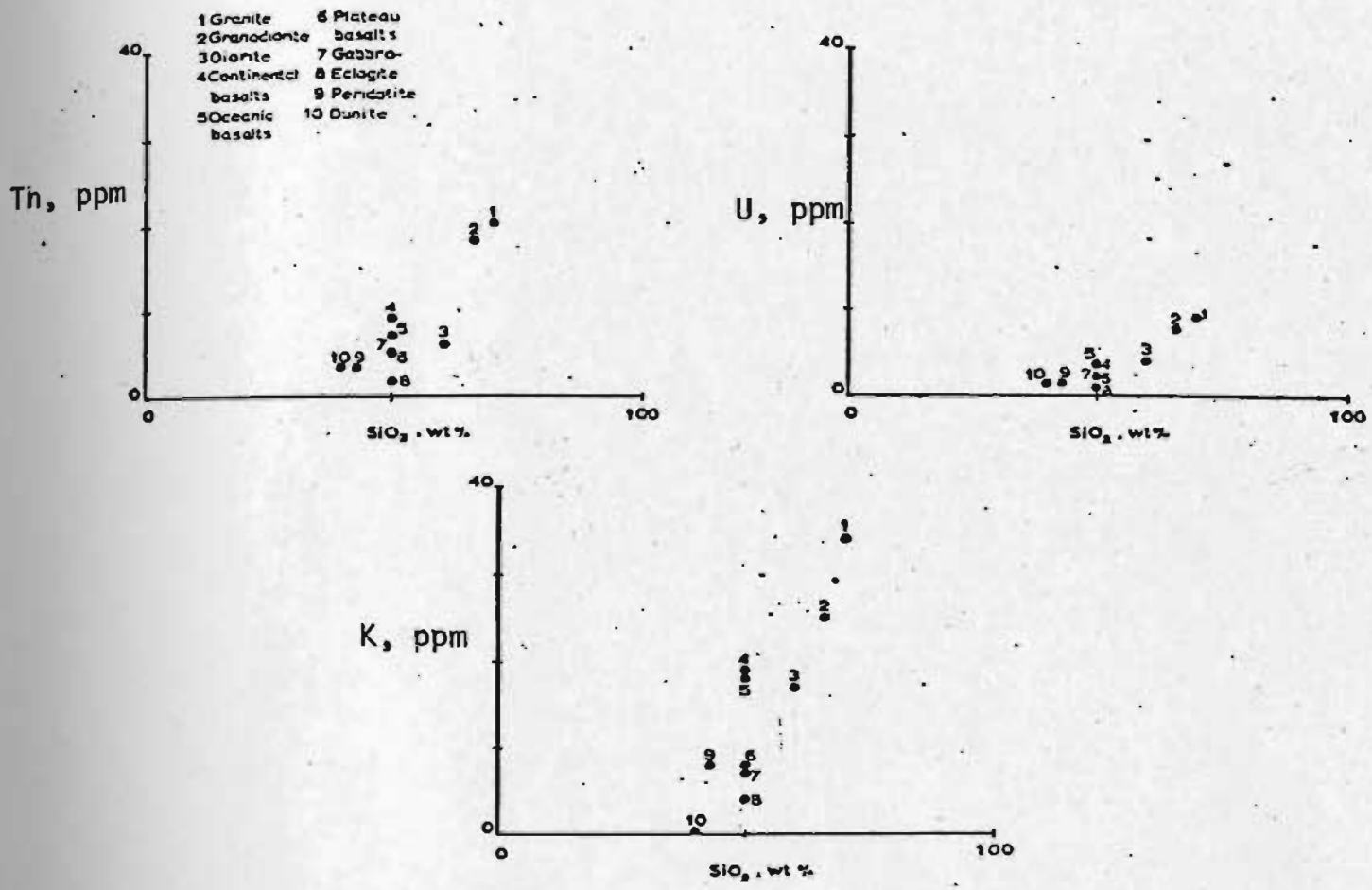

Figure 5. Relations between SiO_2, U, Th and K for the different types of rocks listed in Table I.

TABLE 1

Type of rock	SiO_2, Approx wt. %	Amount per metric ton (or ppm) Uranium, g	Thorium, g	Potassium, g
Granite	70	9.0	20.0	34
Granodiorite	66	7.7	18.0	25
Diorite	60	4.0	6.0	17
Central basalts	50			
Continental		3.5	9.1	19
Oceanic		3.6	7.1	18
Plateau basalt		2.2	5.0	8
Gabbro	50	2.4	5.1	7
Eclogite		1.0	1.8	4
Peridotite	43	1.5	3.3	8
Dunite	40	1.4	3.4	0.3

(After Katz and Rabinowitch, 1951)

is associated with iron sulfides, the $(U^{+6}O_2)^{+2}$ complex may be retained for sometime at the outcrop by its adsorption on the ferric oxide of the gossan (McKelvey et al., 1955). This might be one of the reasons why the radioactivity in the graphitic pyrite-bearing argillite in Kitts and Long Island showings is higher in localities where pyrite assemblages are covered by ferric oxide coatings.

After a study of the thermal stability of uranium oxides in the range UO_2 - U_3O_8, Perio (1953) concluded that the region of compounds of variable composition with the structures and parameters of UO_2 (corresponding to natural pitchblendes) extends to 140°C. In the region of higher temperatures, the compound UO_2 is stable in mixtures with other uranium compounds of constant composition.

Uraninite is easily oxidized and destroyed on weathering, but most of the other U^{+4} minerals are not. Presumably continued oxidation of the U^{+4} ion in fairly pure $U^{+4}O_2$ to the hexavalent state is permitted by the removal of friable and soluble oxidation products, whereas, in those compounds in which U^{+4} is a minor substituent, it is protected from attack by the surrounding unoxidizable ions (McKelvey et al., 1955).

One of the most striking and persistent features of uranium mineralization, particularly of uranium veins, is its association with hematitic alteration. The association of hematite with pitchblende is so consistent that, in many districts, hematite staining is widely used by prospectors as a guide in the search for uranium deposits. In igneous rocks (including pegmatites) uranium and thorium are intimately

associated, but hydrothermal uranium veins are notable for their low thorium content. In them, uranium occurs chiefly as uraninite. This segregation of uranium suggests the possibility that an oxidation of uranium to the hexavalent state may precede deposition in veins. In other words, an oxidation of U^{+4} to $(U^{+6}O_2)^{+2}$ at a late magmatic stage might permit the $(U^{+6}O_2)^{+2}$ to be carried away in solution, and separated from the unoxidizable Th^{+4}. In turn $(U^{+6}O_2)^{+2}$ might be reduced to form pitchblende in veins (McKelvey et al., 1955). Phair's (1952) studies of high and low uranium bostonite dikes indicates that uranium is released to vein solutions by an oxidation reaction.

The widespread association of uraninite and hematite in vein deposits also may be explained by such a hypothesis. The reaction:

$$3H_2O + 2Fe^{+2} + (U^{+6}O_2)^{+2} \longrightarrow Fe_2O_3 + U^{+4}O_2 + 6H^+$$

goes to completion ($(U^{+6}O_2)^{+2} K < 10^{-6}$) at 25°C at pH=4 and above, over a wide range of Fe^{+2} concentration (McKelvey et al., 1955)

Uranium, in the deposits under investigation, occurs in metasediments and/or metavolcanics, i.e. partly metamorphosed sedimentary and volcanic rocks, and although in general the effects of metamorphism on the distribution of trace elements are not well known, numerous studies (e.g. Taylor, 1965) have shown that transfer of material takes place over distances of a few centimeters. Heier and Adams (1965) found that high grade metamorphic rocks are significantly lower in Th and U than their chemical counterparts at lower metamorphic grade. They claim that the evidence for the metamorphic differentiation of Th and

U indicates that much of the Th and U in these rocks cannot be located in "inert" minerals such as zircon or other resistates. Pliler and Adams (1962) showed that Th in the Mancos shale was associated with the clay fraction, either in clay-size detrital resistate particles or adsorbed directly on the clay itself. Leaching experiments showed that most of the Th was available for leaching by acid, implying that Th is predominantly fixed in adsorption positions on the clay minerals, and does not necessarily occur in primary resistate minerals. In the case of U they found that the importance of the various sites for this element in the Mancos shale is extremely variable. It appeared that as much as 75 per cent and as little as 25 per cent of the U in the shales could be interpreted as being held in resistate minerals. This variation in "leachable" uranium within the same sedimentary rock may provide the explanation for the variable U concentrations in the paragneisses.

Progressive metamorphism leads to a gradual disappearance of "sheet silicates" which are the structures with the highest capacity for holding foreign ions to adsorption positions (Heier and Adams, 1965). According to them Granulite facies conditions mark the final breakdown of "micaceous" structures, and it is possible that proportionally a much more dominant part of Th and U is present in resistate minerals in these rocks. The behavior of U and Th during progressive metamorphism has been studied also by Yermolayev and Zhidikova (1966) and Yermolayev (1971, 1973). They found that uranium and thorium tend to migrate into the upper parts of the Earth's crust during extensive transformations of ancient sediments, and this trend is clear from uranium-lead isotope

measurements (Yermolayev and Zhidikova, 1966). Uranium begins to be mobilized and lost from rocks at low grades of regional metamorphism and with progressive contact metamorphism. As the grade of progressive metamorphism increases, thorium also becomes mobilized, and the Th/U ratio gradually falls during metamorphism as T and P increase. Extensive progressive metamorphism of sediments and volcanics cause the products in the initial stage of ultra-metamorphism to have extremely low concentrations of the radioelements; the uranium and thorium are carried into the upper part of the Earth's crust along with displaced water and carbon dioxide (Yermolayev, 1973). This tendency persists until the general melting of the rock during ultrametamorphism. High grade ultrametamrophism is accompanied by mobilization of U and Th, together with the production of melts with elevated radioactivity. The resulting crystalline rocks play a decisive part in the emplacement of the highly radioactive granite component of the Earth's continental crust. The retrogressive stage of regional or contact metamorphism represents a transitional link in the geochemistry of the radioelements from metamorphic to hydrothermal ore formation. Retrogressive metamorphism evolves, as regards U and Th, from regional radioelement migration to local metasomatic accumulation of radioelements (Yermolayev, 1973).

According to Yermolayev (1971) there are three types of extraction mechanism for U as progressive metamorphism increases:

(a) Recrystallization (blastesis), which produces temporary supersaturation

of intersitial solutions with uranium and other trace components;
(b) Uranium is adsorbed onto surface films and solutions in the pores, and is released from surface films into pore solutions, a process favoured by the considerable reduction in surface areas during recrystallization. According to Yermolayev, these two mechanisms predetermine the migration of uranium in areas of regional and contact metamorphism.
(c) Dissolution of uranium carrier minerals is promoted during ultra-metamorphism (granitization), which is accompanied by transport of some rock-forming components (Fe, Ti, Mg) to lower metamorphic grades
Original sedimentary composition controls uranium distribution in rock recrystallization. Uranium is least likely to be redeposited with substances having little affinity with uranium hydroxide and uranium ions (quartz and feldspars). Minerals of Fe, Ti, Zr and the Rare Earths actively take up U from the solution on recrystallization (Yermolayev, 1971).

Traces of ore elements are not released in recrystallization if the crystals are in equilibrium with the solutions, but this may occur if the recrystallization involves a medium with a different composition from the equilibrium solution (Yermolayev, 1971).

Adams et al. (1959) suggested that it would be of great interest to compare the distribution of thorium and uranium in the minerals of metamorphic rocks relative to their distribution in magmatic rocks. They state that the partial separation of thorium and uranium during weathering and erosion can be considered as the result of the three major processes

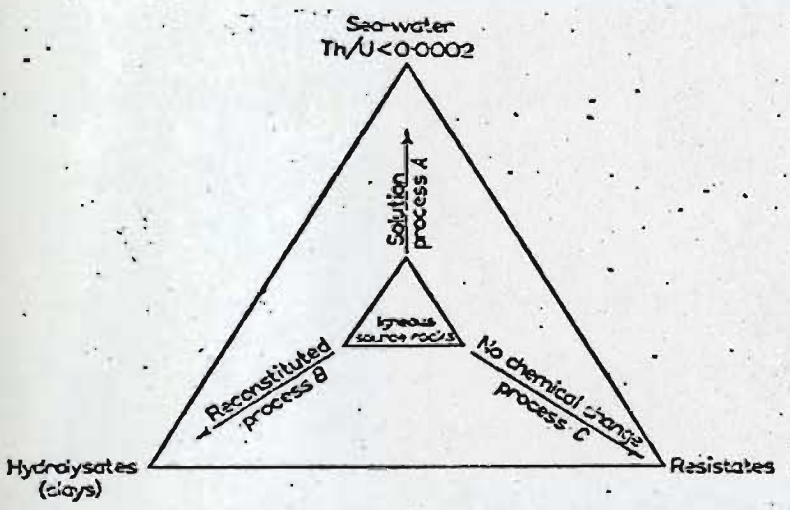

Figure 6. The fractionation of uranium and thorium during weathering and erosion (Adams et al., 1959).

diagrammed in Fig. 6.

According to them a considerable fraction, perhaps more than two-thirds, of the thorium and uranium from igneous source rocks is thought to be transported in resistate minerals such as zircon, monazite, etc.. These resistates are largely of silt and sub-silt size so that they are deposited mainly in the shales.

Adams et al. (1959) state that the small grain size of these resistates is indicated by auto-radiographic studies and the observation of the centres of pleochroic haloes. Further reduction in grain size would be caused by abrasion during transport and they claim that a well-mixed, homogeneous suite of fine-grained resistate minerals in common shales would explain the strong similarities observed in the thorium, uranium and zirconium contents of common shales as compared with the average igneous source rocks.

Leonova and Tauson (1958) have found that experiments in leaching of uranium from zircon showed that its presence cannot be ascribed to isomorphism with zirconium alone. The treatment of zircon with weak solvents gives almost no uranium, while treatment with concentrated HCl extracts about 30 per cent of the uranium. According to them the zircon is not decomposed by hydrochloric acid and the uranium extracted in this case must play a different role in the structure of this mineral. They found evidence that, of the uranium found in biotites, not more than 10 per cent can be credited to the inclusion of zircon and hence the main mass of uranium is in biotite itself. They treated biotite with different

solvents and they found that sorption plays an important role, but the possibility of isomorphous substitution is not excluded. The probability of the latter is increased by the fact that biotite is capable of capturing a number of rare elements. Their leaching experiments of uranium from quartz, potassium feldspar and plagiocalse showed that the extraction amounted to 100 per cent, with a complete preservation of the crystal lattice of the host mineral.

Leonova and Tauson (1958) also point out that the separation of uranium occurring in rocks into diadochic (structural uranium) and non-diadochic (leachable uranium) has a definite geochemical meaning, for it distinguishes uranium strongly bound in the lattices of the minerals from that which is not bound and may easily migrate from the rocks, under the action of specific natural or artificial solvents, without destruction of the lattices of the essential or accessory minerals. Also in their discussion they underlie the fact that the mineralogical character of the inclusions with non-diadochic uranium is very important. Neuerberg (1956) distinguishes six modes of uranium occurrence in rocks and in only one of these is uranium diadochic.

Leonova dnd Pogiblova (1961) examined the distribution of uranium among the minerals in syenites and alaskites. They found that the feldspars of syenites are from 2 to 3 times richer in uranium than the feldspars of the alaskites. Also in the alaskites biotite is always more radioactive than in hornblende but in syenites biotite is always poorer in uranium, while hornblende and pyroxene have a relatively high uranium content.

According to the same authors, in alaskites uranium is accumulated by biotite (15-20 per cent of total uranium), while in the syenites it is accumulated by hornblende and pyroxene.

Baranov and Du Lieh-T'ien (1961) found that most of the uranium, 67 per cent on the average, is concentrated in the accessory minerals, and the remaining 33 per cent appears in the essential minerals of Kyzyltan granites, USSR. They also found that the variation in the ratio of the uranium content in the accessory minerals to its content in the essential minerals, Ua/Ue, is related to the grain size of the rock, i.e. to the rate of crystallization of the magma. In the finer-grained rocks formed from rapidly crystallized magma the essential minerals captured more of the uranium present in the magma than did the same minerals of the coarse-grained rocks, in which by far the larger part of the uranium occurs in the accessory minerals.

Yermolayev (1973) states that the radioactive elements are removed from the host lattice by recrystallization and production of new structural groups. According to him, hydrohematite, b-FeO·OH releases the isostructural uranyl dehydrate when it is altered to hematite.

Krylov and Atrashenok (1959) examined the mode of occurrence of uranium in granites. They believe that for the understanding of the form of occurrence of dispersed uranium the leaching of magnetite is of special interest. It is improbable that uranium is diadochic in magnetite, but it must be present in it in the form of independent compounds. According to them, uranium is very probably present in magnetite as an oxide,

and if so, it should be easily leached out.

Autoradiographs of granites (Picciotto, 1950) indicate that thorium and uranium occur in very small mineral or liquid inclusions in the quartz, and the analysis of quartz in beach sands (Murray and Adams, 1958) indicates that about 5 per cent of the thorium and uranium in granites can be expected to be so fixed in the quartz.

It has been noted (Neuerburg, 1956; Gerasimovskiy, 1957) that uranium takes a variety of forms in rock-forming and accessory minerals. Neutron activation plus fission-track recording is a highly selective technique to determine the mode of uranium distribution. For instance, it has been shown (Komarov and Shukolyukov, 1966; Komarov et al., 1967) that most of the U in sphene and biotite is localized in the periphery of the grain and at the surface. This distribution indicates that U can be extracted by dissolution into the aqueous phase produced during metamorphism and also during recrystallization of a host mineral (concentrator) (Yermolayev , 1971).

Krauskoff (1967) states that metamorphism of fine grained rocks to hornfelses or phyllites produces no detectable change in rare-metal contnet, unless the rocks have been permeated by solutions during the metamorphic process. At higher grades of metamorphism the minor elements redistribute themselves locally among the growing crystals of new minerals, but again the overall concentrations do not change markedly unless movement of solutions has played an important role. Since some sedimentary rocks have unique assemblages of trace elements, e.g. shales, sandstones,

carbonates (see Turekian and Wedepohl, 1961) a study of these elements in metamorphic rocks provides a possible way to guess at the nature of the premetamorphic material. When metamorphism reaches the ultimate stage of partial melting, the minor elements go into the melt, and then recrystallize from the melt according to the pattern they follow for igneous rocks

None of the rock formations under investigation has reached the stage of partial melting since the main mineralogical assemblage in the Aillik series (albite, epidote, chlorite, hornblende, biotite, stilpnomelane, microcline, quartz, sphene and andradite) indicate regional metamorphism in the greenschist-amphibolite facies (Wedepohl, 1971; Turner, 1968). In this case it is expected that uranium may be present either in resitate minerals or adsorbed on sheet silicates.

The principal conclusion of this review is that the uranium content of each rock reflects a complicated history and a range of host mineralogy. Neuerburg (1956) has pointed out that the total uranium contents of igneous rocks are dynamic quantities that cannot be referred to any single event and that are probably changing from day to day by some infinitesimal amount.

The genesis of uranium deposits associated with the metamorphic rocks of Labrador appear to be complicated because the uranium has been affected by more than a single event and the mineralogical distribution of uranium is not highly variable.

CHAPTER III

TRACE ELEMENT GEOCHEMISTRY AND MINERALOGY OF SOME URANIUM DEPOSITS OF LABRADOR

3.1 Introduction

Beavan (1958) classified the uranium occurrences of Labrador as follows:

(a) Mineralization in fracture and shear zones in volcanic rocks, e.g. Rice Lake.

(b) Mineralization in sedimentary rocks (Kitts Pond showing).

(c) Mineralized fault zones (Pitch Lake showing), and

(d) Radioactive minerals in granitic rocks (Aillik).

Ruzicka (1971) classified the Labrador uranium occurrences into five genetic types:

1. Uraninite mineralization confined to granites and pegmatites (near Aillik).
2. A sedimentary-metamorphic type which is represented by disseminations, mainly confined to metamorphosed quartzites (Michelin showing).
3. Pitchblende mineralization in veins and disseminations (usually associated with quartz-carbonate gangue material) confined to graphitic argillites, tuffs and tuffites locally interbedded with amphibolites (Nash Lake showing).
4. Uranium mineralization in shear and fault zones (Rice Lake, Pitch Lake showing).
5. Pitchblende mineralization confined to granulites in which pitch-

blende is as a rule botryoidal and replaces hematite (No examples given and none found in the present study area).

According to Barua (1969), uranium mineralization in the Aillik series occurs in:

a) Felsic volcanic and less commonly subvolcanic rocks, and

b) tuffaceous and argillaceous horizons.

(a) Associations of uranium and felsic volcanic rocks predominate in the Michelin area and to a lesser extent in the Kaipokok-Aillik areas, e.g. Witch Lake showing, Sunil showing, etc. Uranium in these deposits originated in hydrothermal fluids which coexisted with volcanic activity, while later leaching and redeposition along shear planes and fractures was responsible for concentrating uranium. The superimposition of "shearing" and secondary enrichment (leaching and redeposition) on suitable felsic igneous rocks primarily enriched in U by synvolcanic metasomatic fluids may be prerequisite in producing uranium concentrations of economic interest.

(b) Uranium associated with tuffaceous and artillaceous horizons is found predominantly within the Kaipokok Belt and it is also a product of synvolcanic metasomatizing fluids. In these rocks a two stage process was envisioned by Barua (1969):

1. Primary precipitation of U with the deposition of tuffs and argillites (very fine grained basic tuffs), and
2. secondary leaching and concentration of uranium in bedding planes, fractures, etc.

As can be seen, there is a general classification of the uranium deposits on the basis of field observations but no systematic study of the chemistry and mineralogy has been done. However, this would appear necessary to a proper understanding of the mode of uranium occurrence and controls on its distribution in the variety of metasedimentary and metavolcanic rocks of the area.

Evidence of hydrothermal activity related with fluorite, copper and uranium mineralization in some showings, e.g. Michelin, Shoal Lake showing, gives rise to some pertinent questions, e.g.:

1. What were the physical and chemical properties of the ore-bearing solutions-temperature, pH, redox potential during transport and deposition?
2. By what means did they reach the sites of deposition?
3. What physical or chemical factors defined the favorable deposition conditions?
4. How were the solutions able to travel for some distances within the favorable formations without deposition taking place?

Nicholls (1958) and Nicholls and Loring (1962) have discussed the problems of interpreting trace element data in sediments. According to them, some elements will occur mainly in the detrital fraction, for example, zirconium. Taylor (1962) has considered the presence of high Zr in metamorphic rocks to be contributory evidence for a sedimentary parent. Other elements such as Rb and Sr may occur principally in the non-detrital fraction and according to Taylor (1965) Zr/Rb ratios should

indicate the relative proportions of detrital and non-detrital fractions, and should, in the ideal case, decrease from the margins of a basin towards the center. Based on these observations the ratio of $\frac{Zr}{Rb}$ was plotted versus uranium in an attempt to see if there is any correlation between the uranium content and the "detrital" and "non-detrital" portion of the samples.

Fig. 7 shows that in Michelin, M. Ben and McLean high uranium is concentrated in the "non-detrital" portions of the samples while in Rainbow high uranium is associated with the "detrital" portion of the samples. Such a subdivision was not made for the Witch, Nash, Kitts and Long Island showings.

Samples from three showings (Michelin, Rainbow and Witch Lake showings) were analysed for Ra in order to test the equilibrium Ra /U. The concept of equilibrium becomes important geologically when the amount of uranium in a rock sample is determined by measuring the radioactivity. If one or more of the daughters or parent is partially or completely removed from the series, a state of disequilibrium will occur. Then the measured radioactivity may not show the same relationship to the content of uranium (or the other series member) as it does under equilibrium conditions. If the absent nuclide is short-lived, thousands of years may be required to regain equilibrium (about 390,000 years after the parent U-283 is deposited).

The most important forms of uranium disequilibrium are:

1) deficiency of radium group nulides as a result of the migration of

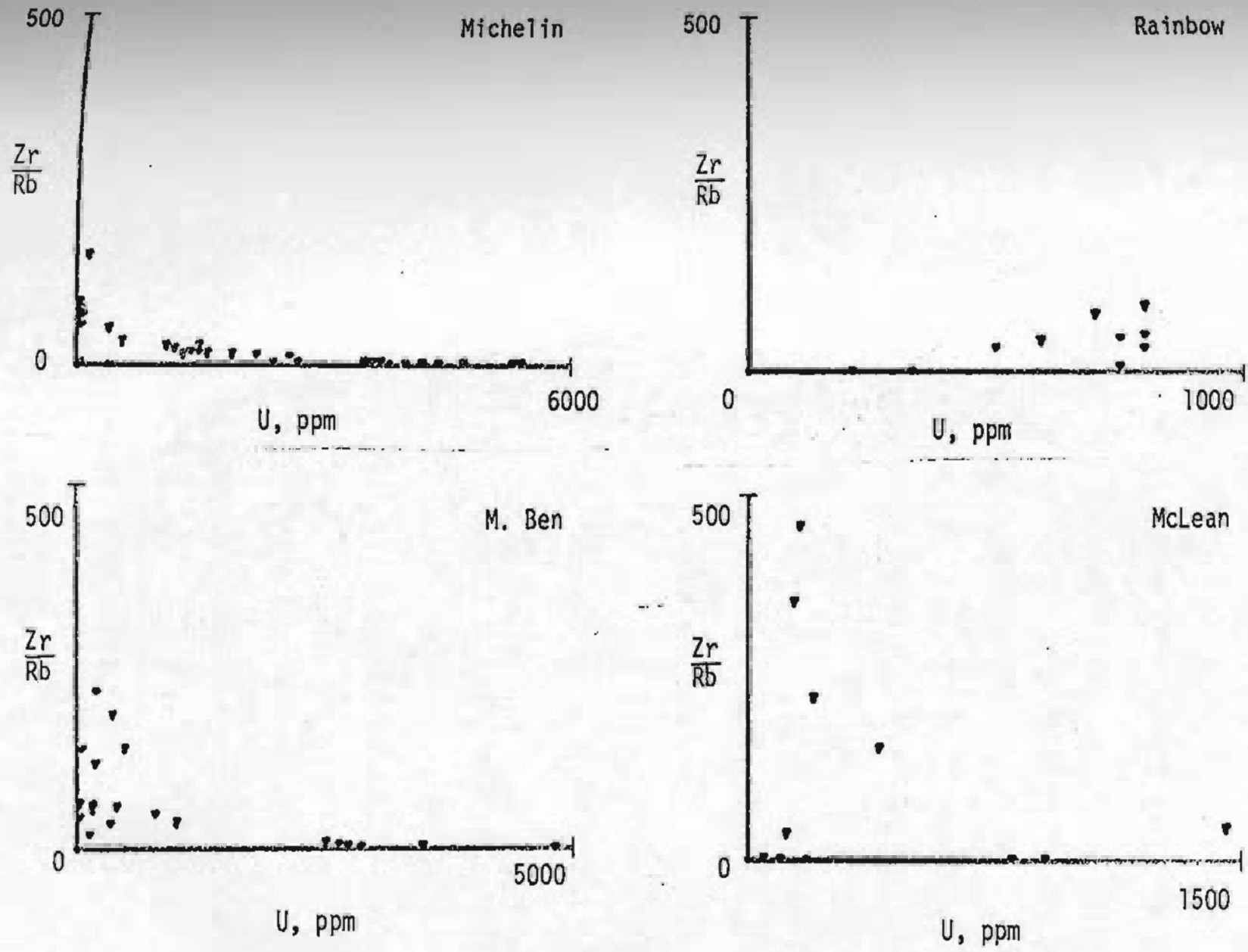

Figure 7. Plot of Zr/Rb versus U for Michelin, Rainbow, M. Ben and McLean uranium deposits (see text).

radon, the gaseous member of the uranium series;

2) deficiency of daughters, especially the radium group, as a result of insufficient time to attain equilibrium after deposition of the parent or leaching of the daughters;

3) deficiency of parent uranium because of preferential deposition of daughters, especially the radium group.

Certain of the radium group nuclides are the most strongly gamma-radioactive members of the uranium series while the uranium isotopes are only weakly radioactive. Hence, the first two types of uranium disequilibrium result in sources that are relatively enriched in uranium but relatively weak in gamma radioactivity. The third type of disequilibrium produces strongly radioactive sources with little or no uranium. Of course, uranium deposits in equilibrium will also be strongly radioactive (McPhar Geophysics, Geological Applications of Portable Gamma-ray Spectrometers, Parts I and II).

From the Ra /U ratios obtained, and from the fact that all the uranium deposits are strongly radioactive, it is concluded that uranium is in equilibrium with its daughter products. By taking into consideration the primary uranium mineralization and that the half-life of U^{238} is 4.51×10^9 years and that of U^{235} is 7.13×10^8 years, it cannot be argued that the uranium has been transported, redeposited and regained equilibrium since Precambrian times. This feature provides evidence for a syngenetic origin of these uranium deposits.

3.2 Michelin Uranium Deposit

The host rock of the Michelin uranium deposit is characterized by alternating bands of quartzofeldspathic material with a schistose texture usually dominated by hornblende, striking N 65°-80°E and dipping 45°-60° South. The bands are generally not continuous over long distances but lens out within 2-15 cm. They are, however, thin compared with their lateral extent. Feldspar porphyroblasts give an augen structure to the rock. The highly mineralized rock has a pink coloration due to disseminated hematite. The barren rock is white and consists predominantly of quartzo-feldspathic material.

The area has a relatively low relief and is drift-covered, with numerous boulders, which appear to be native to the area and close to their source. Some of the boulders are strongly radioactive and similar in lithology to the mineralized zone.

There is a distinct difference in mineralogy between the low and the highly mineralized rock as can be seen in Table II. The highly mineralized rocks are characterized by a higher content of common hornblende, sodic amphibole and the presence of zircon, pyroxene (aegirine-augite), biotite, hematite, stilpnomelane and minor calcite. The main radioactive mineral appears to be davidite rimmed by sphene and is found within the feldspar porphyroblasts and also associated with the amphiboles (Plates I, II and VI). Davidite, an ill-defined mineral chemically, containing chiefly oxides of Titanium and iron, plus variable amounts of rare earths of the Cerium Group, U, V and Cr (D' Arcy, 1947).

Alkali metamorphism is usually seen in the vicinity of carbonate alkali-syenite complexes (Mckie, 1966). Granite gneisses become transformed to fenites whose principal constituents are alkali feldspars (orthoclase or albite) and aegirine or sodic amphibole; and there are numerous cases in which the fenite envelope is clearly related to a carbonatite contact (e.g. Von Eckermann, 1961; Dawson, 1964; Sutherland, 1965, p. 367; Paarma, 1970). The mineralogical assemblage of the Michelin uranium deposit (sodic amphibole, sodic pyroxene, albite) and the presence of carbonatites in the vicinity of Makkovik (King, 1963; Hawkins, personal communication) suggest that fenitization processes might have taken place in the area.

The Ba content of the lithosphere (Turekian and Wedepohl, 1961 and Vinogradov, 1962) averages around 840 ppm for low Ca acidic rocks, 830 for granites, and alkalic rock such as syenites contain the most Ba (1600 ppm). Possibly an alkalic rock could be the original source of the Michelin uranium showing whose part of Ba was removed during weathering. Although fenitization seriously affected the Michelin host rock, its detrital nature is indicated by the round zircon crystals which are located mainly between grain boundaries.

Trace element concentrations and various statistical parameters for those rocks are given in Tables III to V. Compared to the average trace element concentrations of metasedimentary schists and quartzofeldspathic gneisses (Table VI), the quartz feldspar porphyry of the Michelin uranium deposit has a relatively higher Zr, Zn and Ba content

and lower Sr, Rb, Cu, Ni and Cr content.

Rubidium/strontium ratios in these rocks range from 0.04 to 5 (Fig. 8). The highly mineralized samples fall within the trachyte field and their Rb/Sr ratios range from 0.08 to 5. However, the full range of these samples outside igneous fields in Fig. 8 suggest that the protolith was not an igneous rock.

Patterns of other trace element distribution can be seen in Fig. 9-10. Some trends are comparable to those found in igneous rocks, e.g. positive correlation of Ba vs Sr (Fig. 9a) and presumably reflect residual igneous trends preserved in the clastic sediments.

There is no correlation between Cu-Sr, Ni-Sr and Cr-Sr, i.e. no variation in Cu, Ni, Cr (Fig. 9b, c, g) and no simple relations exist between Rb-Sr, Zr-Sr and Zn-Sr (Fig. 9d, e, f). Mineralogy and field evidence indicate fenitization processes; high uranium content is associated with higher content of sodic amphiboles and K-feldspars. If these minerals are the Rb-bearing minerals then the positive correlation of Rb vs U is explicable. The dominance of K-feldspars in the strongly mineralized samples could be responsible for the pattern Ba vs U (Fig. 10e). No simple relations exist between Sr-U and Zn-U (Fig. 10b, c) and there is no correlation between Cr-U, Zr-U, Cu-U or Ni-U (Fig. 10d, f, g, h). This poor Zr/U correlation, the existence of primary radioactive minerals, and the non-metamict nature of the zircon crystals indicate that no significant proportion of the uranium is held in the zircon, although the existing correlation could be attributed to uranium adsorbed onto the zircon crystals. The criteria for distinguishing the possible origins of

uranium mineralization in the Michelin showing are summarized below:

Syngenetic

- Daughter products of uranium in fresh looking rock samples are in radioactive equilibrium.
- Round zircon crystals between grain boundaries indicating detrital nature of the host rock.
- Uranium is more or less uniformly distributed laterally (parallel to stratification) but changes abruptly vertically (across stratification) with change in rock type.
- Stratiform shape of the deposit.

Epigenetic, metasomatic, hypogene

- Positive correlation U-Rb.
- Presence of purplish fluorite.
- Mineralogical assemblage indicating fenitization, especially euhedral riebeckite/aegirine.

TABLE II

Modal analyses of rock samples from Michelin; all values are expressed as volume percentages.

Sample Number	Low mineralized rock Michelin 32 (50 ppm)	High mineralized rock Michelin 23 (3700 ppm U)
Groundmass	76	43
Feldspar porphyroblasts (mostly plagioclases, albite-andesine), microcline	18	22
Common hornblende and sodic amphibole associated with radioactive opaque minerals	3	29
Opaques	5 (mostly pyrite and magnetite)	4 (mostly unidentified radioactive minerals) minor magnetite and pyrite.

Other minerals include zircon, pyroxene (intermediate between aegirine and augite) biotite, hematite, stilpnomelane, calcite.

The groundmass consists predominantly of quartz arranged in granoblastic-polygonal texture where straight boundaries and triple points are a common feature.

TABLE III

MICHELIN URANIUM DEPOSIT

(values in ppm)

Sample No.	Zr	Sr	Rb	Zn	Cu	Ba	Ni	Cr	U	Radioactivity C/S	Equilibrium Ra/U
1	840	32	27	146	4	194	20	3	1500		90
2	499	74	74	84	7	1306	19	8	10	50	100
3	715	50	99	240	1	384	24	6	4700	170	90
4	817	47	81	210	2	463	22	7	3500	480	90
4'	814	44	79	207	2	446	22	6	3500		90
5	962	45	46	234		171	22	9	1900	120	90
6	701	53	112	228	2	383	24	4	5400	270	100
7	667	47	97	239	1	408	23	6	5300	200	90
8	499	118	25	161	2	627	20	5	1300	270	90
9	808	46	45	205	1	254	21	7	2200	200	90
10	626	33	17	151	1	259	18	7	560	50	90
11	718	27	13	148	1	162	19	8	400	90	110
12	427	110	79	271	6	753	22	3	4000	300	100
12'	409	118	77	273	6	770	22	3	4300		90
13	447	101	67	42	3	639	22	3	3500	330	90
14	409	182	51	575	18	2055	22	4	2700	80	130
15	365	154	50	524	14	1414	22	3	2400		150
16	342	111	77	500	9	1194	23	3	3800	80	130
17	447	46	76	107	2	504	22	2	3500	230	100
17'	433	46	72	107	1	521	22	2	3600		100
18	470	65	3	99	3	1348	19	4	150		80
19	644	103	30	196		748	19	5	1500	130	140
20	610	93	28	275		634	19	4	1400	100	110
21	571	106	18	147	1	419	19	5	1100	90	100
22	520	89	68	152	8	893	22	2	3600	250	100
23	567	65	65	301	5	834	22	4	3700	240	100
24	659	135	30	125	1	713	20	4	1600	70	110
25	601	84	22	180	0	870	19	3	1200	100	140
26	844	47	56	231	0	182	21	7	2600	160	100

Continued.....

MICHELIN URANIUM DEPOSIT (Page 2)

Sample No.	Zr	Sr	Rb	Zn	Cu	Ba	Ni	Cr	U	Radioactivity C/S	Equilibrium Ra/U
27	596	181	74	256	7	2457	21	3	3700	210	110
27'	566	171	70	253	6	2516	21	2	3800		110
28	537	125	89	290	6	1866	21	2	4400	380	100
29	549	138	80	288	7	2049	22	2	4200	180	100
30	566	236	71	326	9	3039	21	1	3700	240	100
30'									4000		110
31	190	331	95	88	133	572	92	147	400	120	100
32	246	37	3	100	5	841	21	7	50	50	80
33	275	22	4	94	4	211	19	3	40	55	70
34	273	32	3	82	4	648	19	3	30	55	70
35	291	58	4	91	2	1369	19	4	80	50	80
36	232	35	4	72	4	812	19	5	60	50	80
37	342	58	134	93	4	1698	19	7	20	50	100
38	226	31	3	89	3	713	18	5	30		70

TABLE IV

MICHELIN URANIUM DEPOSIT

Correlation matrix calculation for 38 sets of data

Variable	Zr	Sr	Rb	Zn	Cu	Ba	Ni	Cr	U
Zr	1.000	-0.227	0.175	0.131	-0.356	-0.294	-0.247	-0.259	0.391
Sr		1.000	0.326	0.210	0.704	0.555	0.647	0.590	0.182
Rb			1.000	0.258	0.240	0.252	0.301	0.230	0.684
Zn				1.000	-0.035	0.196	-0.067	-0.149	0.468
Cu					1.000	0.043	0.980	0.973	-0.128
Ba						1.000	-0.071	-0.120	0.176
Ni							1.000	0.984	-0.041
Cr								1.000	-0.194

TABLE V

MICHELIN URANIUM DEPOSIT

Element	Mean	STD	95% Confidence Interval for Mean
Zr	528	32	463 - 592
Sr	88	10	66 - 109
Rb	50	5	38 - 62
Zn	193	20	151 - 234
Cu	7	3	0 - 14
Ba	897	113	671 - 1124
Ni	22	1	18 - 26
Cr	8	3	0 - 15
U	2111	284	1543 - 2679

TABLE VI

Average trace element concentrations (in parts per million) of metasedimentary schists, comparable averages for quartzofeldspathic gneisses, (After Bowes, 1972), and the uranium deposits under investigation.

	U	Zr	Sr	Rb	Zn	Cu	Ba	Ni	Cr
Metasedimentary schists		166	149	95	151	78	411	97	305
Quartzofeldspathic gneisses		127	497	61	33	44	903	18	50
Michelin	2111	517	90	50	197	7	897	22	8
Rainbow	623	1040	1080	48	128	10	350	39	54
M. Ben	1118	794	52	30	270	5	69	22	17
McLean	383	686	147	38	85	203	202	32	28
Witch	260	172	291	40	71	133	510	60	33
Nash	1570	91	314	54	209	113	158	94	327
Kitts	351	111	131	63	151	223	284	54	91
L. Island	157	69	127	63	325	232	316	74	98

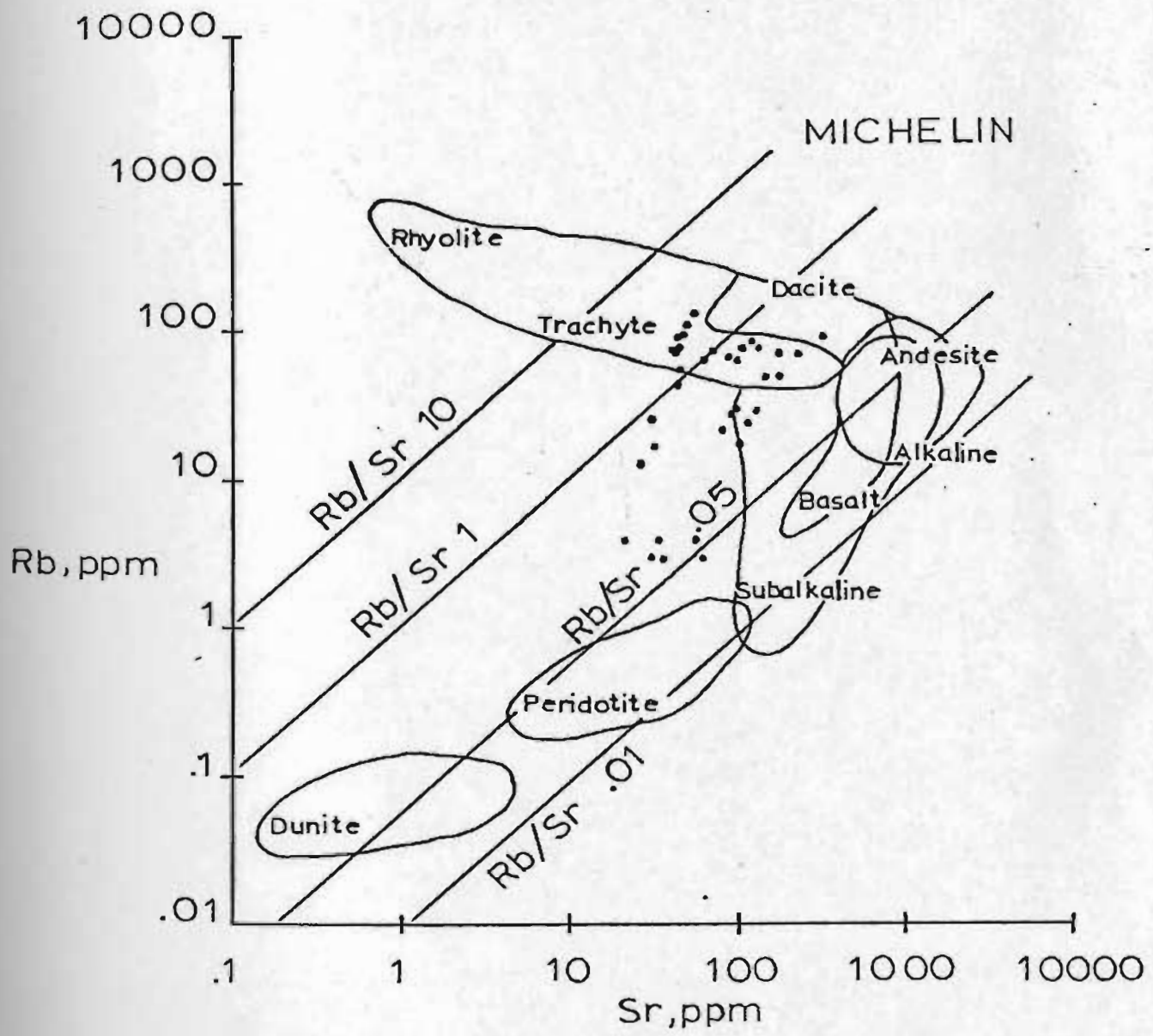

Figure 8. Plots of Rb vs Sr for the Michelin uranium deposit. (See text). (Diagram after Kistler and Peterman, 1973)

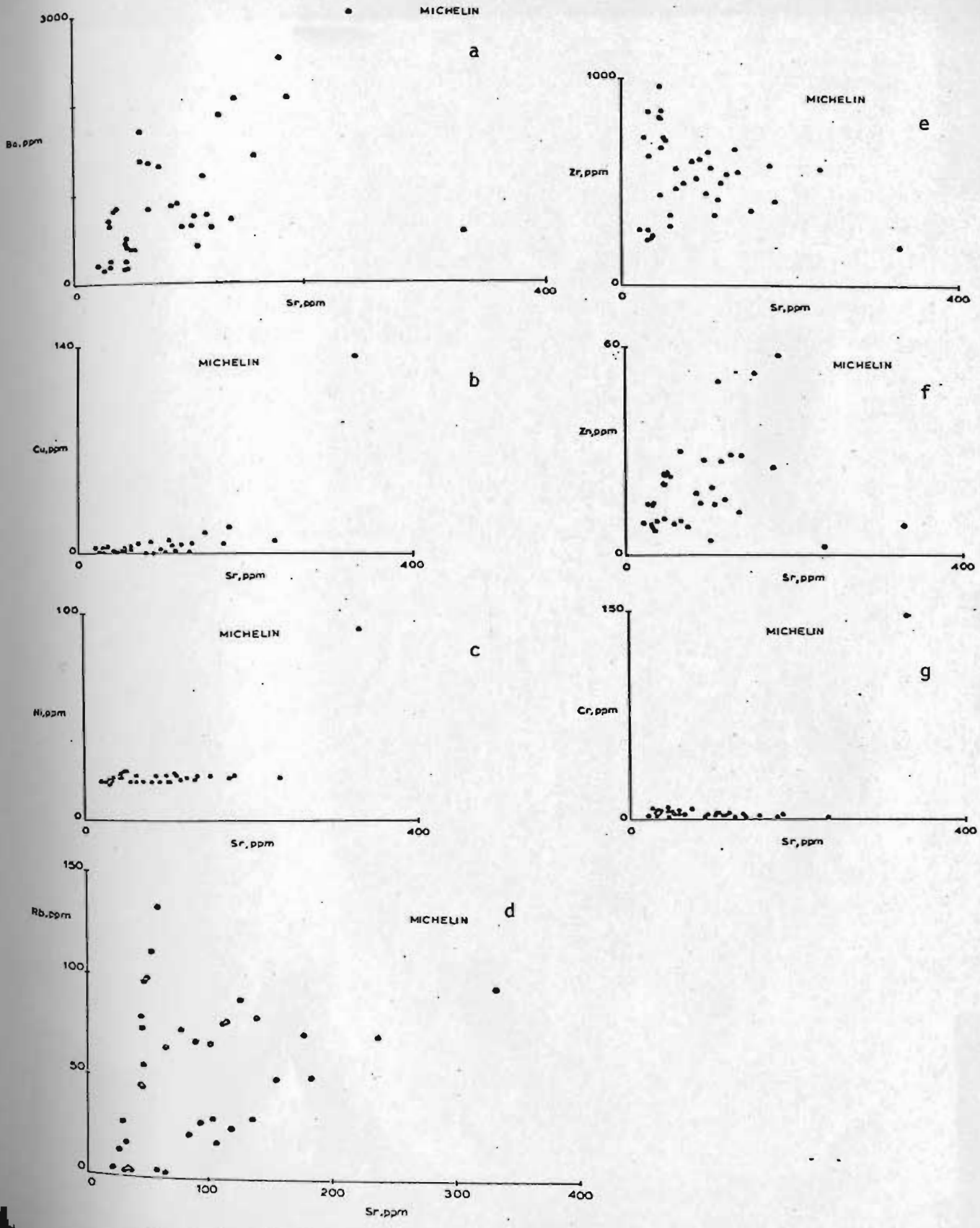

Figure 9. Plots of trace elements vs Strontium (see text).

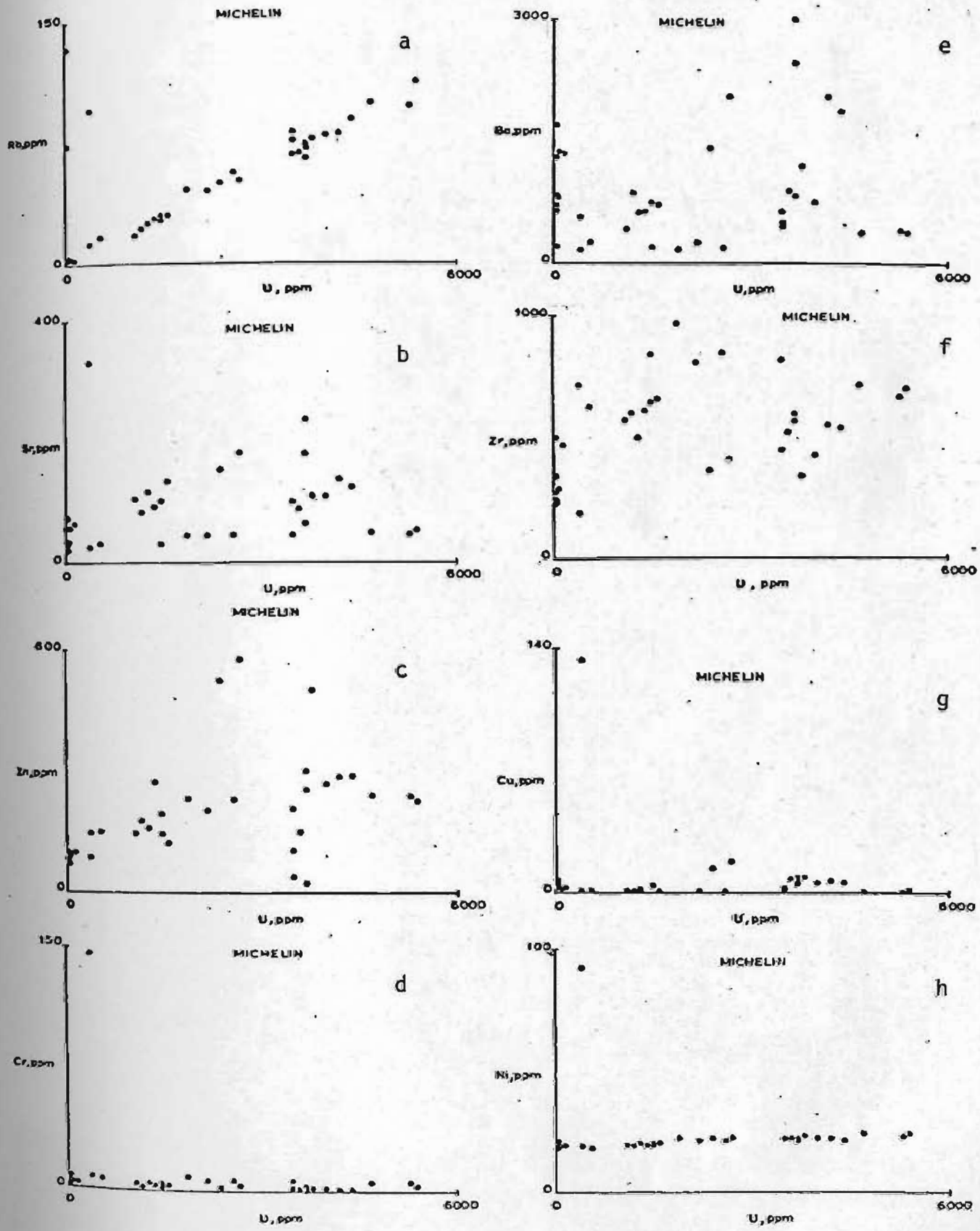

Figure 10. Plots of trace elements vs uranium (see text).

PLATE I

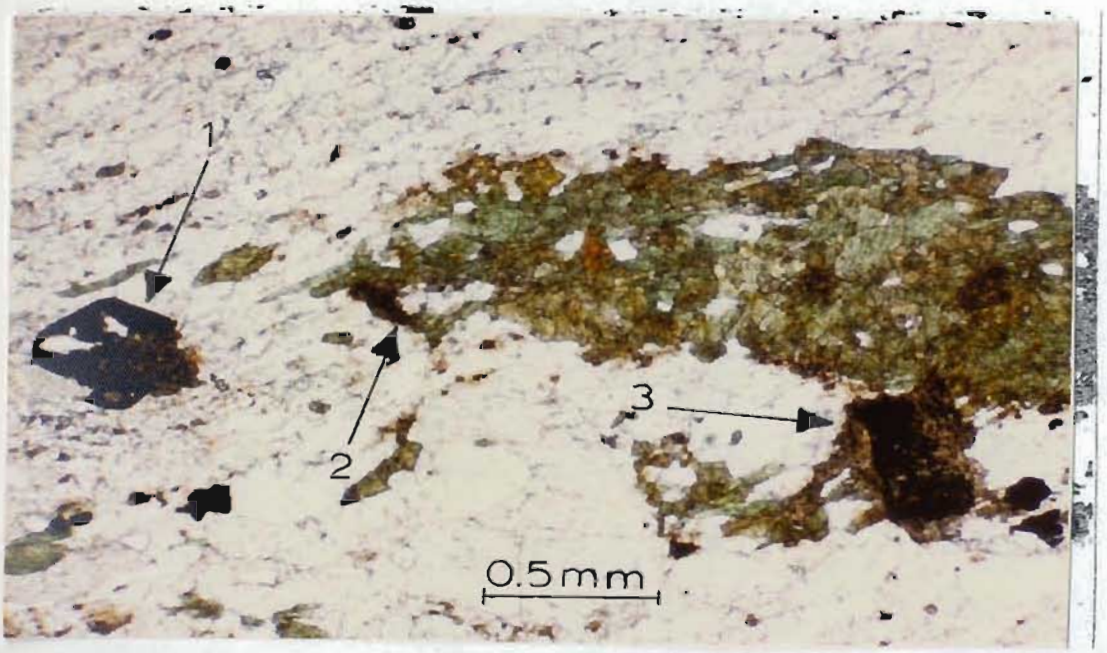

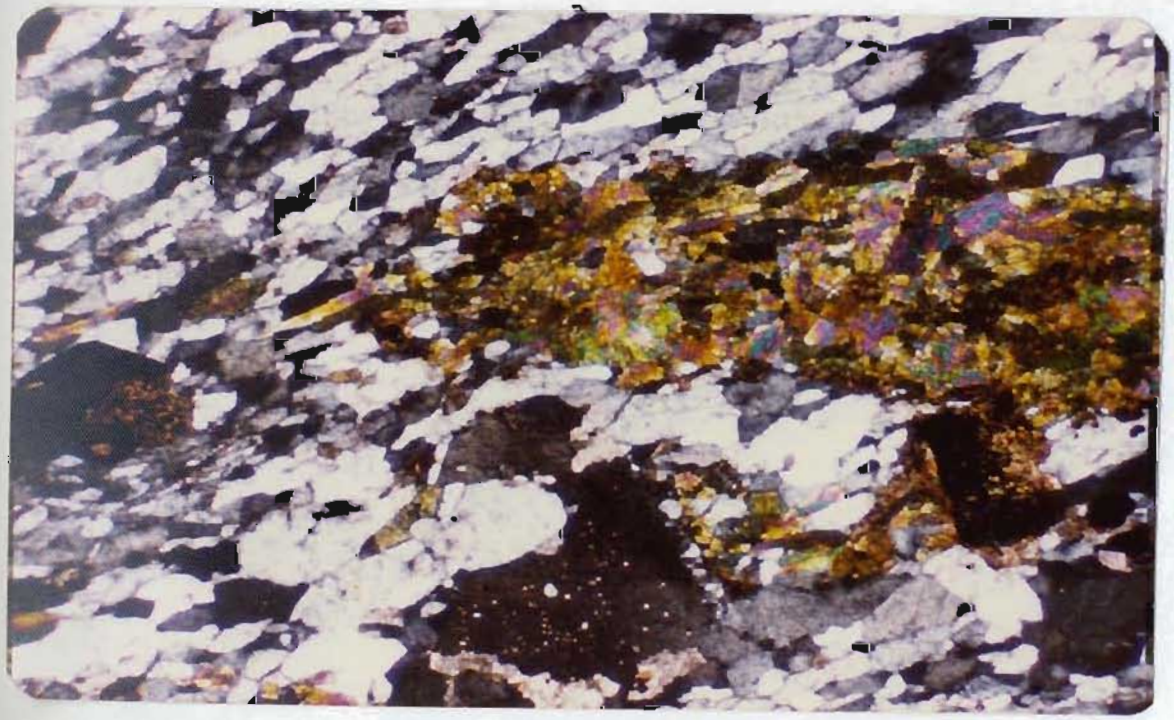

b

a. Arrows 1, 2 and 3 indicate radioactive opaque minerals identified by autoradiography (see PLATE III). Possibly davidite rimmed by sphene. Similar radioactive minerals are present in the green aggregate which consists mostly of hornblende.

b. Same as in (a) under crossed Nichols. Michelin uranium deposit.

PLATE II

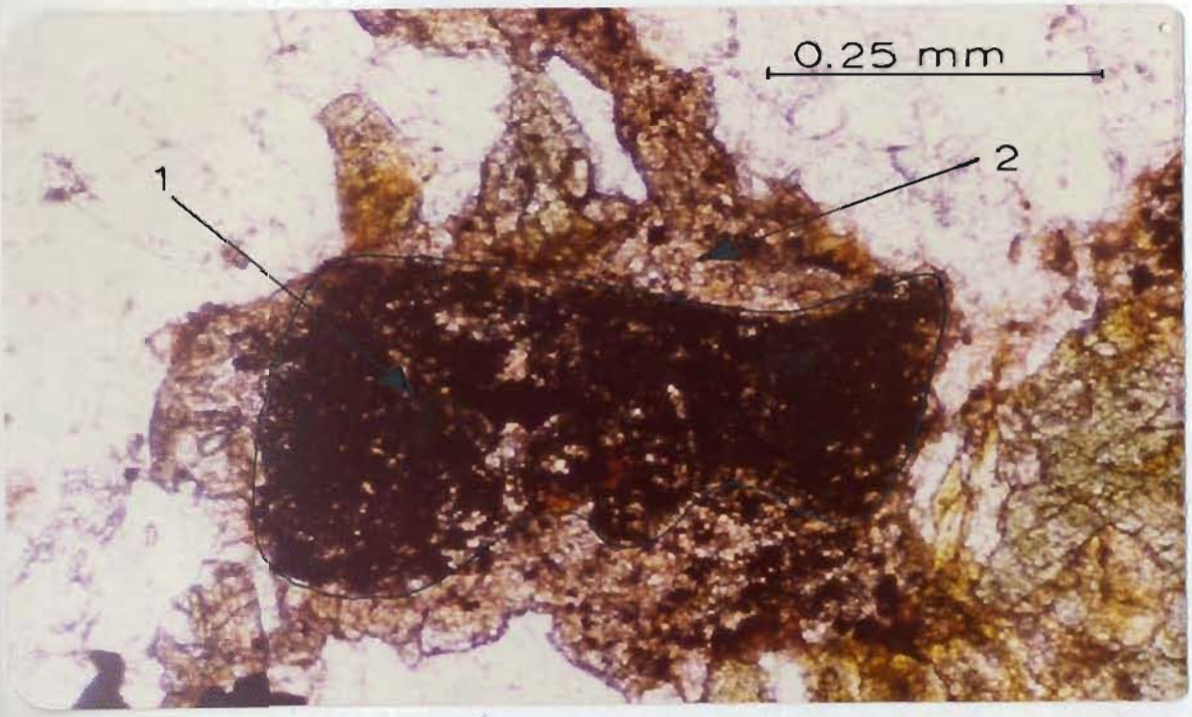

a

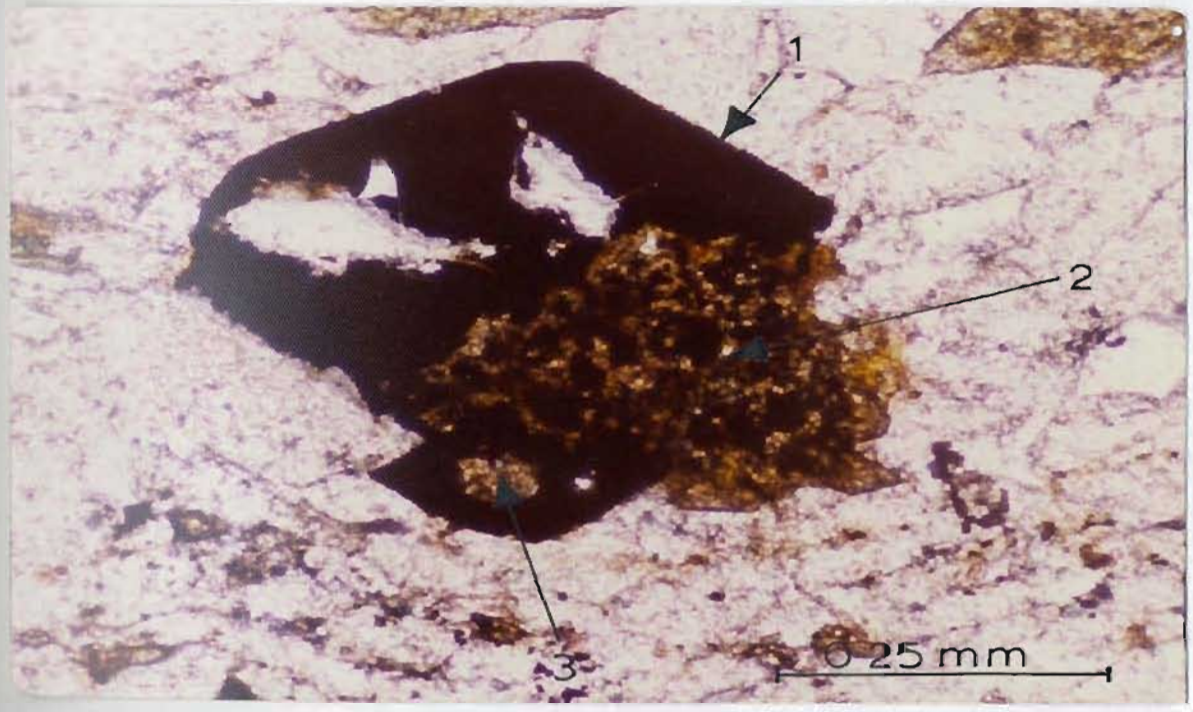

b

a. Radioactive mineral 3 indicated in PLATE I under higher magnification
   1. unidentified primary uranium mineral; possibly davidite
   2. sphene replacing davidite

b. Radioactive mineral 1 indicated in PLATE I
   1. possibly davidite
   2. sphene with remnants of the original davidite
   3. sphene surrounded by davidite

Michelin uranium deposit.

PLATE III

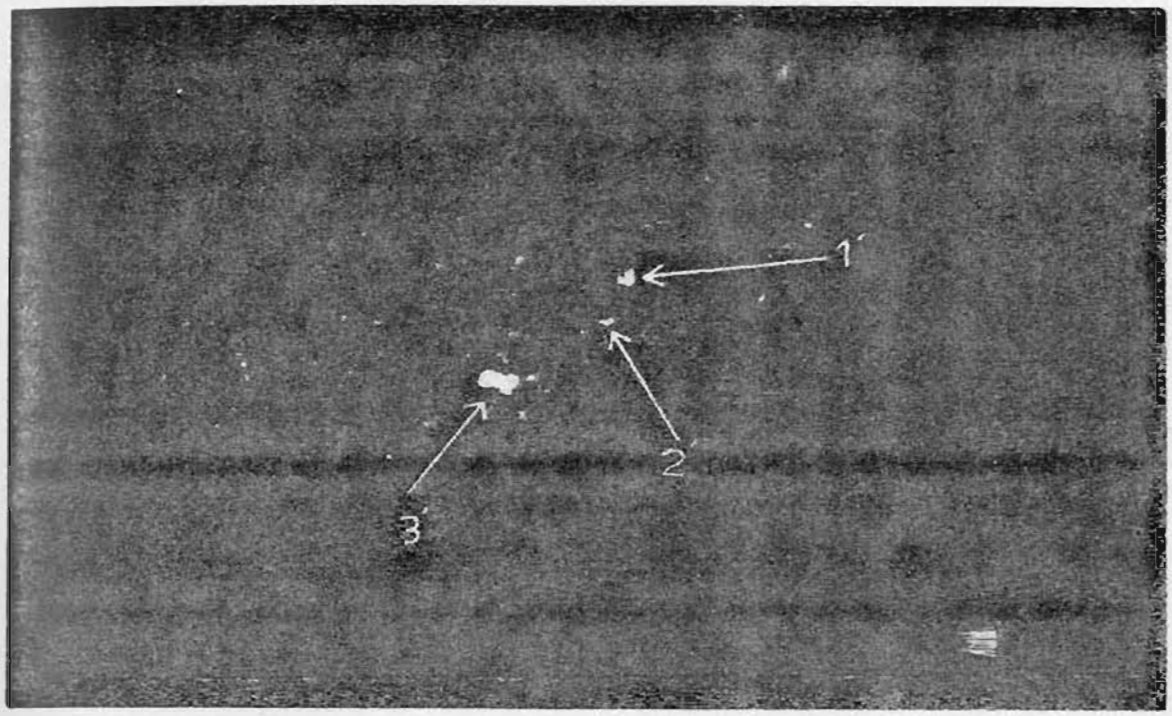

a

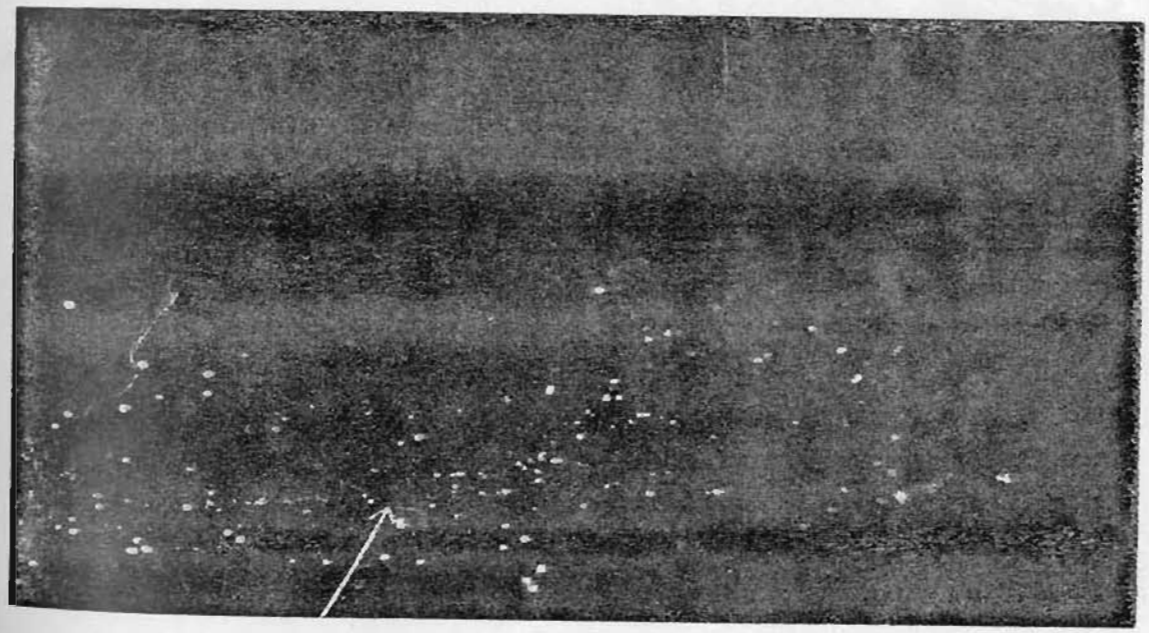

b

a. Autoradiograph of thin section shown in PLATE I. Arrows 1', 2' and 3' show minerals 1, 2 and 3 in PLATE I. Exposure 120 hours. Michelin uranium deposit, Labrador.

b. Autoradiograph of uranium rich boulder, Rainbow type (7,700 ppm). The radioactive minerals are not easily identified with conventional means. Arrow shows fracture filled with radioactive material.

PLATE IV

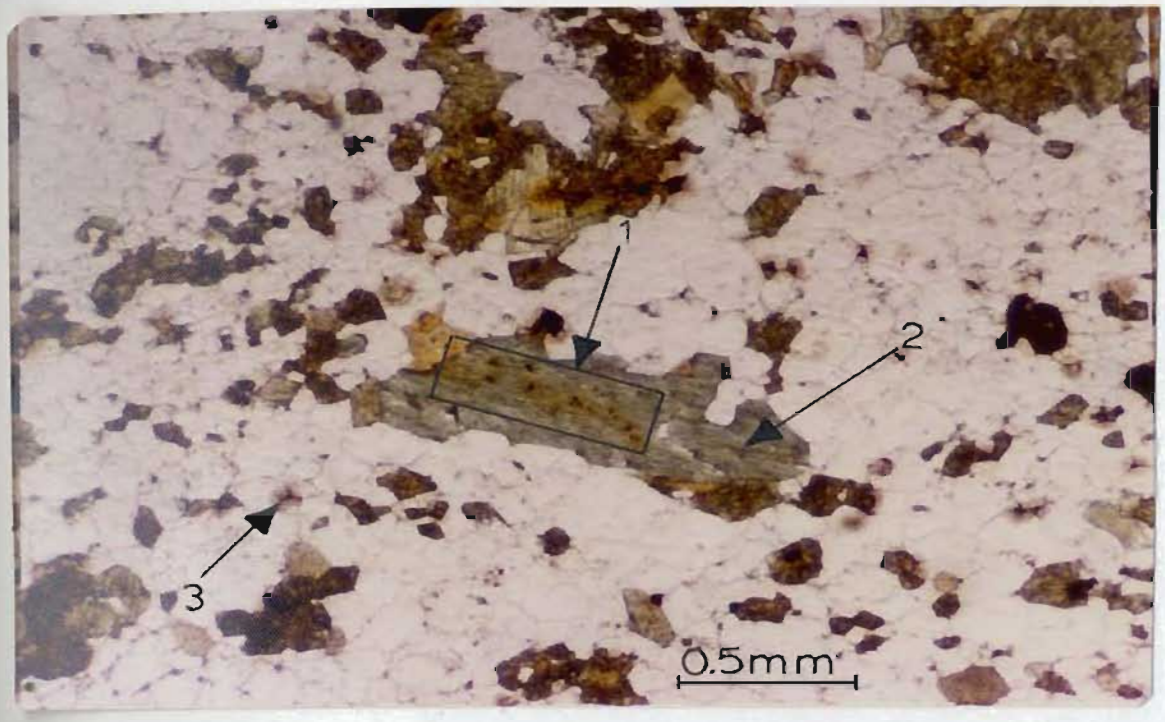

a

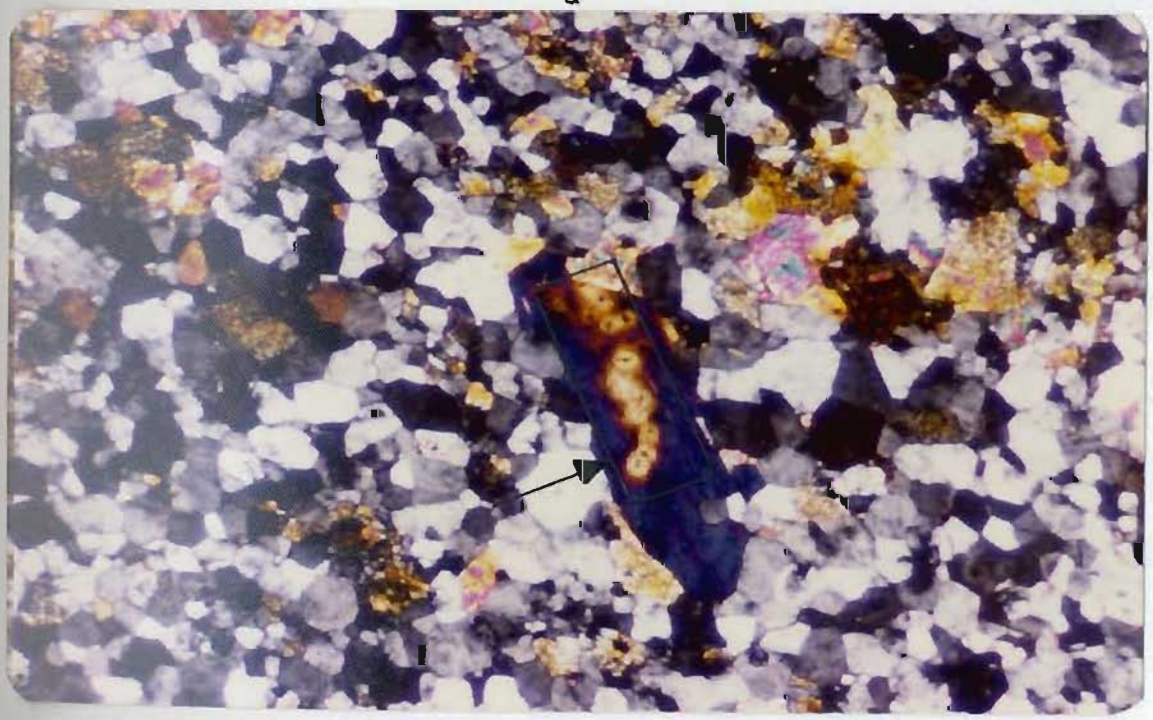

b

a. Arrow 2 shows sodic amphibole enclosing tiny opaque possibly radioactive minerals (Arrow 1).
Arrow 3 shows intergranular opaque radioactive material.

b. Same as in (a) under crossed Nicols. Michelin Uranium Deposit.

Note: The haloes may not be caused by radioactivity; see text.

PLATE V

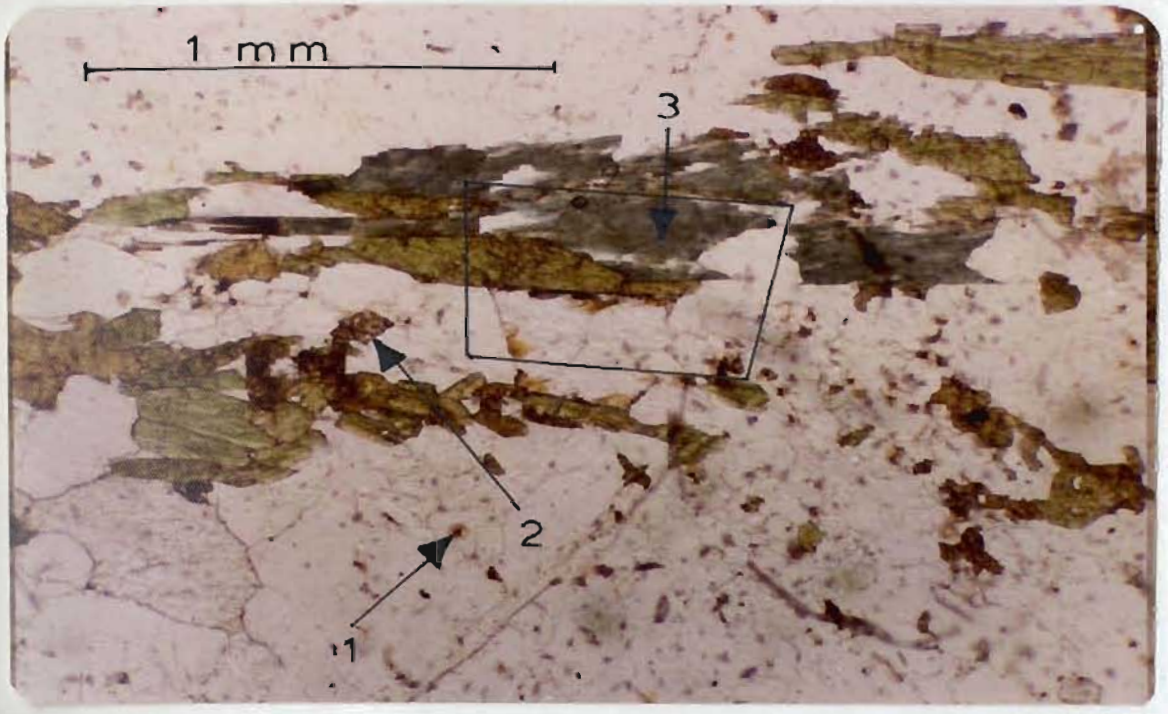

a

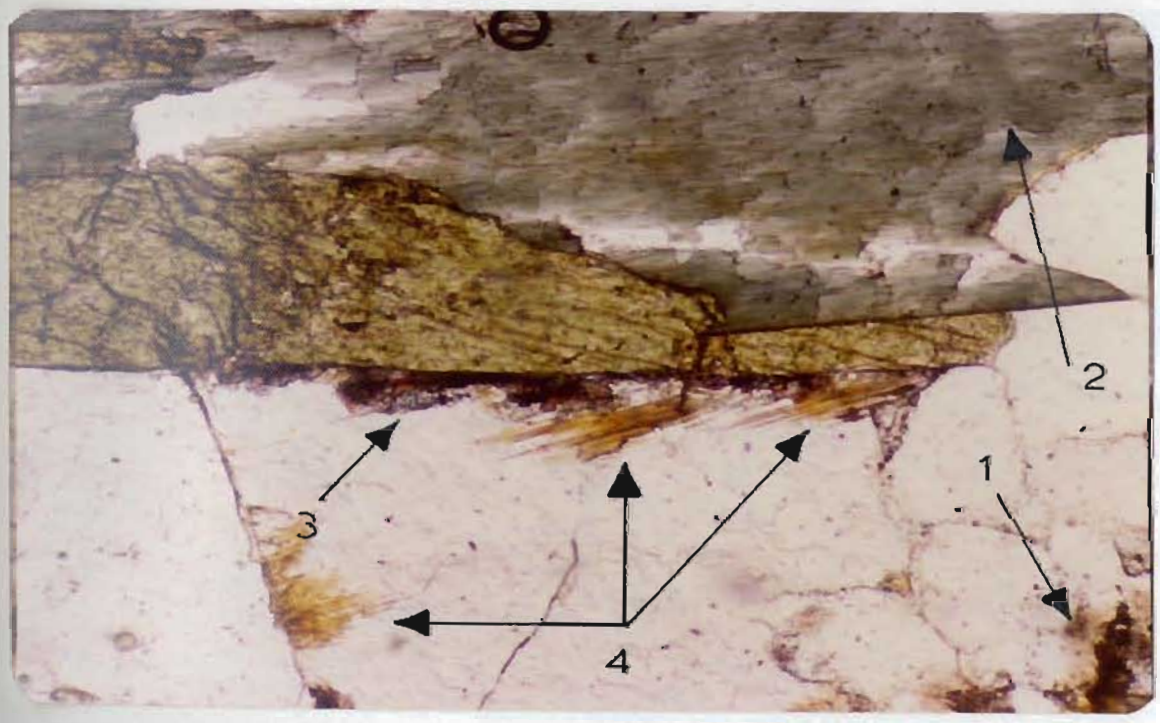

b

a. Typical mineral assemblage of the Michelin uranium deposit
   1. Possibly radioactive grain
   2. Sphene

b. Part 3 in (a) under higher magnification
   1. Radioactive aggregate 2. Sodic amphibole
   3. Hematite (possible source of leachable uranium)
   4. Stilplomelane

PLATE VI

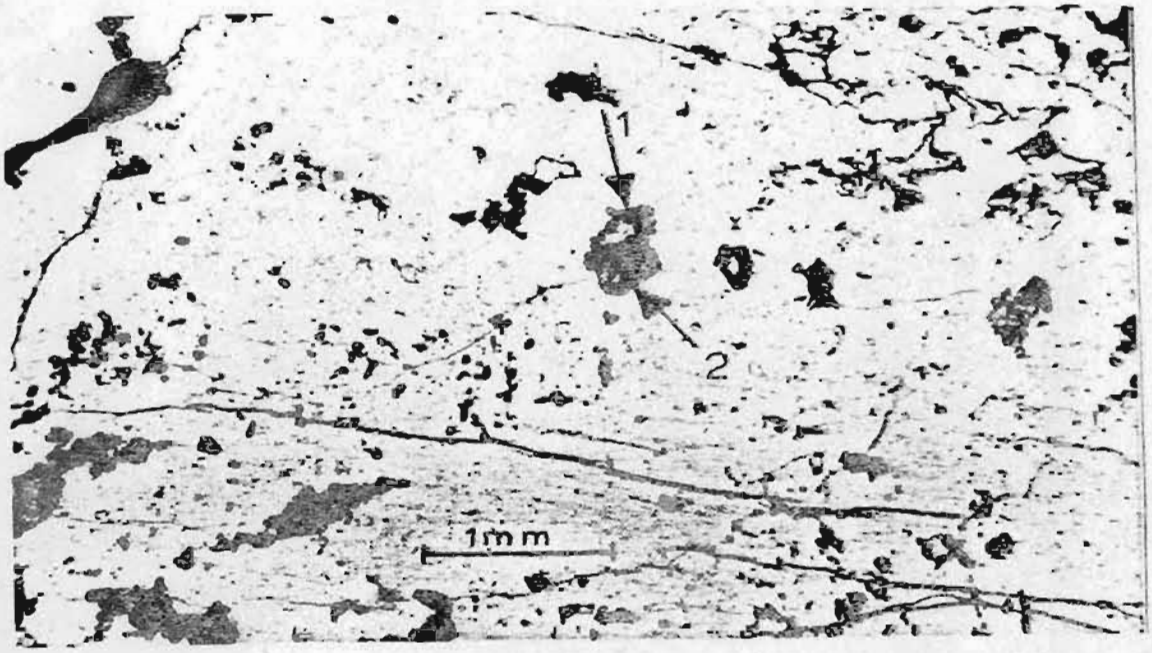

a

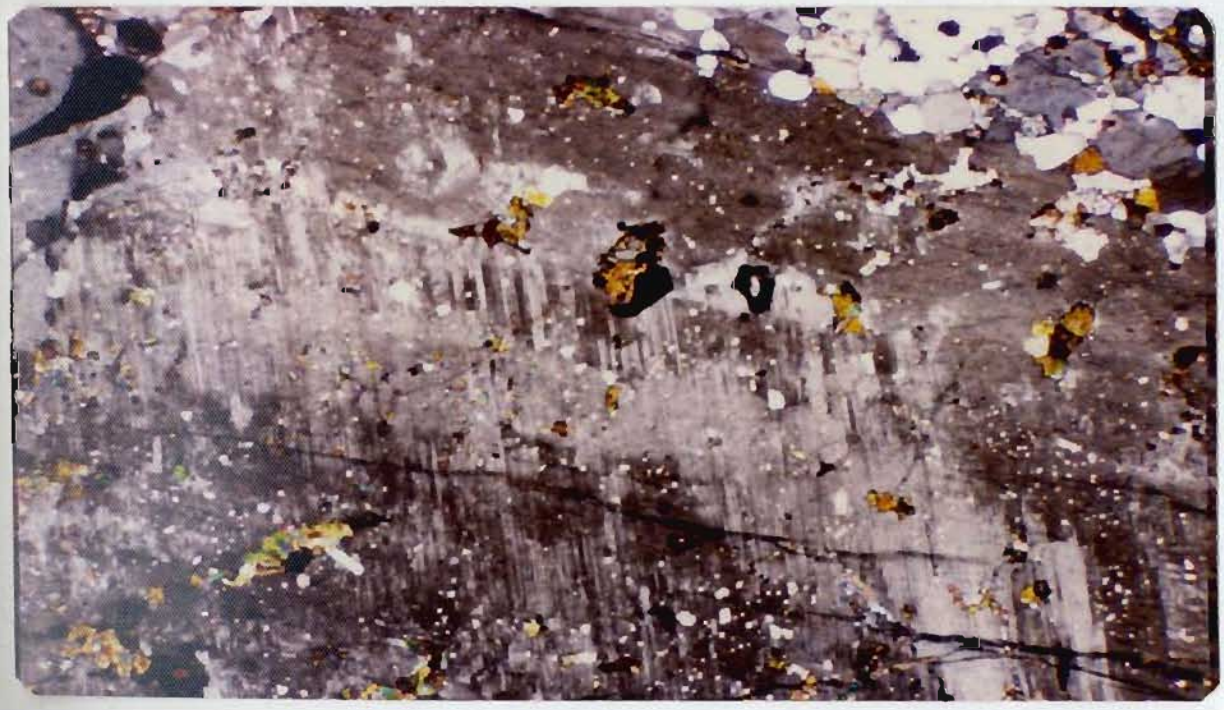

b

a. Radioactive opaque mineral partly altered to sphene, located within a plagioclase porphyroblast
   1. sphene
   2. opaque

b. Same as in (a) under crossed Nicols

Michelin uranium deposit

PLATE VII

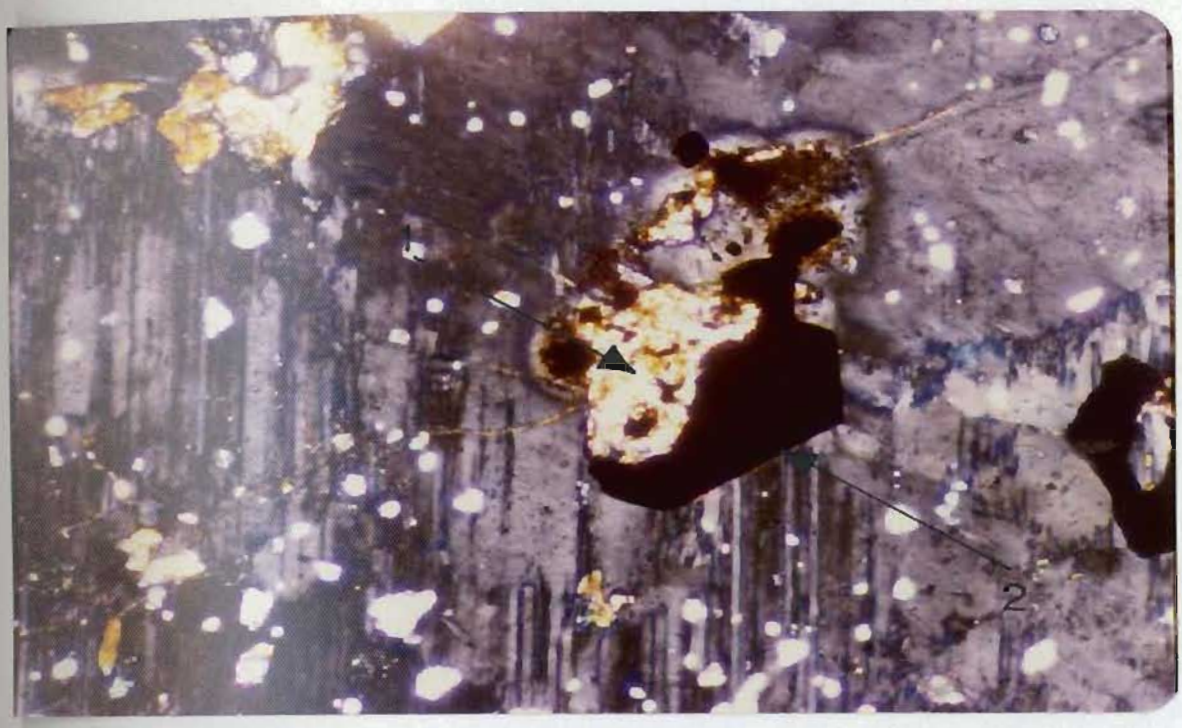

Radioactive mineral in PLATE VI under higher magnification. Note the similarity in the shape of the grain and the grain indicated by Arrow 1 in PLATE I.

Michelin uranium deposit.

PLATE VIII

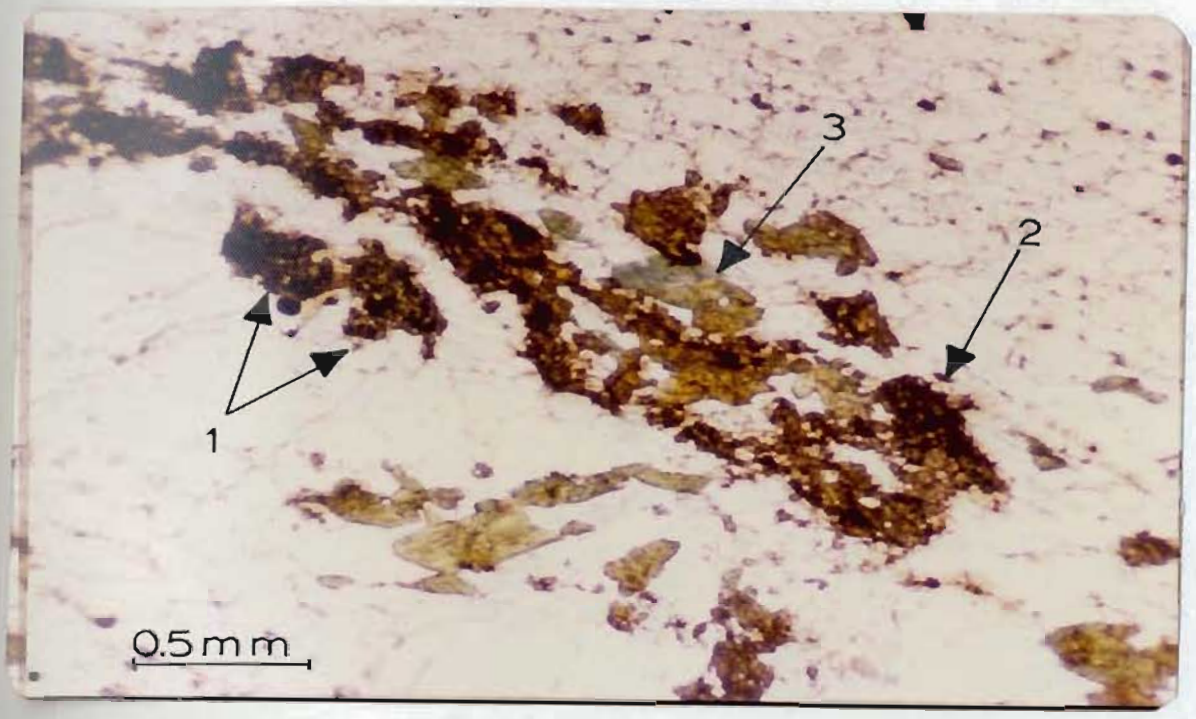

Arrows 1, and 2 show aggregates of radioactive minerals; 3 sodic amphibole.

Michelin uranium depsoit.

PLATE IX

Uraniferous feldspathic quartzite. Primary uranium mineralization of unknown composition (possibly davidite) is confined to quartzite and also to microfracture filling. Michelin uranium deposit.

PLATE X

a

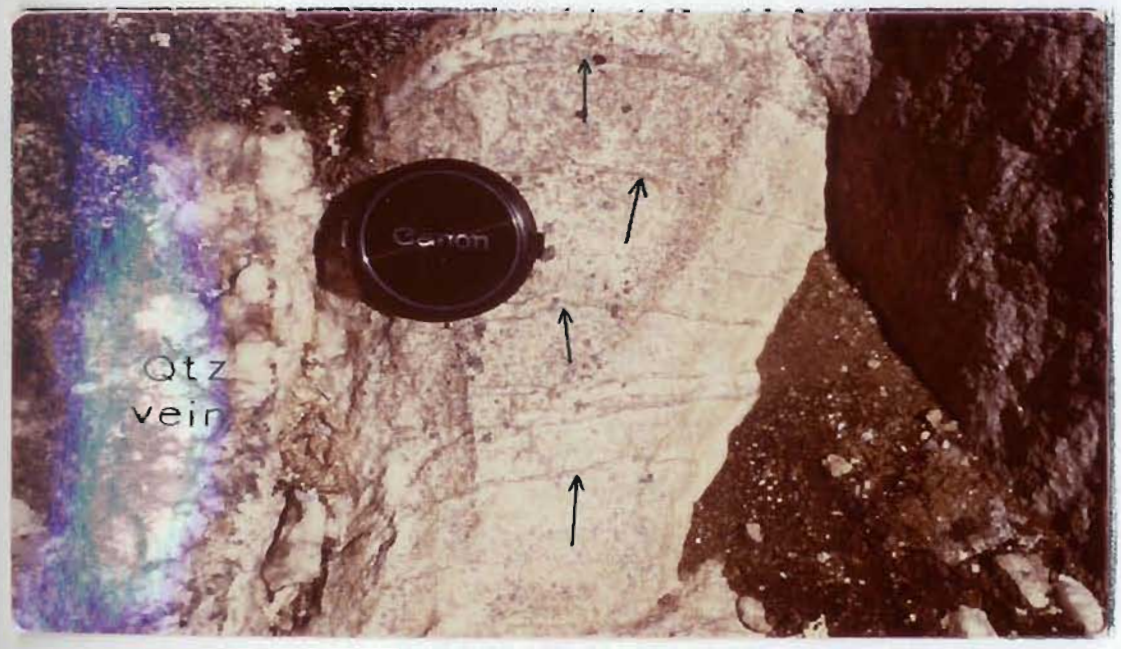

b

a. The latest manifestation of igneous activity in the area around the Michelin deposit are uranium depleted quartz veins from which a swarm of lateral apoyhyses cut the adjacent rock across the foliation.

b. Close up photo.

3.3 Rainbow Uranium Deposit

The Rainbow uranium deposit is found in a mafic metavolcanic rock which forms part of a NE striking series of acid and basic metavolcanic rocks dipping steeply to the south and lying unconformably on the gneissic basement. Uranium is more or less uniformly distributed laterally (parallel to stratification) but changes abruptly vertically (across stratification) with change in rock type.

A modal analysis of a representative mineralized rock sample from this showing is given in Table VII. Small opaque grains surrounded by a halo within the plagioclase and quartz crystals (Plate XI) are possibly the radioactive minerals in the Rainbow deposit, although no autoradiographs are available. However, an autoradiograph of a high mineralized boulder of "Rainbow type" (Plate III) indicated clearly the presence of similar radioactive grains.

Trace element concentrations and other statistical parameters are indicated in Tables VIII to X.

Plots of Rb vs Sr (Fig. II) range between Rb/Sr 0.01 and 0.05 and all of them fall within the andesite field. Compared to the average trace element concentrations of metasedimentary schists and quartzo-feldspathic gneisses (Table VI), the Rainbow metavolcanic rock is characterized by a relatively higher, Zr, Sr and Zn content and lower Rb, Cu, Ba, Ni and Cr content.

Patterns of other trace element distributions can be seen in Figs. 12-13. Some trends are difficult to explain since no simple relations

exist between trace elements vs Sr (Fig. 12). However, in some cases, similar trends for other showings are important and for consistency these diagrams are included here. The positive correlation between Zr-U (Fig. 13f) suggests that a significant proportion of the uranium in the Rainbow deposit is held in the structure of the minute inclusions of zircon crystals which occur within the amphiboles and between grain boundaries. The low mineralized samples are characterized by a lower sphene content. The principal substitutions in sphene ($CaTiSiO_4(O,OH,F)$) are:

Calcium: Na, Rare Earths, Mn, Sr, (Ba)

Titanium: Al, Fe^{+3}, Fe^{+2}, Mg, Nb, Ta, V, Cr

Oxygen: OH, F, Cl (Deer et al., 1971)

By taking into consideration that the amphibole (another mineral) which can accomodate Cr) content is more or less constant in the Rainbow samples, then the negative correlation of Cr-U (Fig. 13d) might be explicable by the slightly lower sphene content in the highly mineralized samples.

The criteria for distinguishing the possible origins of uranium mineralization in the Rainbow showing are summarized below:

Syngenetic

- Daughter products of uranium in fresh looking rock samples are in radioactive equilibrium
- Uranium is more or less uniformly distributed laterally (parallel to stratification) but changes abruptly vertically (across stratification)

with change in rock type.

- Stratiform nature of the deposit. 8

There is no evidence that this deposit might be epigenetic.

TABLE VII

Modal analyses of a representative mineralized rock sample from Rainbow Zone; all values are expressed as volume percentages.

Sample Number	Rainbow Zone 7 (750 ppm)
Hornblende	59
Plagioclase (An_{42}-An_{68})	31
Biotite (iron rich)	1
Opaques	6
Sphene, minor epidote	1

There are minute inclusions of zircon in the amphibole and the biotite and this accounts for the high Zr content of the Rainbow rock samples.

TABLE VIII

RAINBOW URANIUM DEPOSIT

(values in ppm)

Sample No.	Zr	Sr	Rb	Zn	Cu	Ba	Ni	Cr	U	Radioactivity C/S	Equilibrium Ra/U
1	528	1073	15	126	6	214	40	67	500	80	110
2	469	1110	42	117	27	352	36	75	750		80
3	758	1132	16	137	6	235	35	56	590		100
4	196	833	123	157	6	680	54	90	330	150	70
5	2200	1526	23	114	8	335	35	27	800	140	100
6	1586	1182	29	117	6	337	35	29	800	140	100
7	1197	1026	24	117	9	198	33	33	750		100
8	1516	1149	42	106	9	379	34	38	800	170	90
9	1756	1077	21	144	10	202	38	38	700	90	130
10	193	689	144	143	12	559	48	87	210	90	60
10'	200	685	135	120	8	540	45	80	200		90
11 Boulder Rainbow type									7700	500	

TABLE IX

RAINBOW URANIUM DEPOSIT

Correlation matrix calculation for 10 sets of data

Variable	Zr	Sr	Rb	Zn	Cu	Ba	Ni	Cr	U
Zr	1.000	0.791	-0.612	-0.527	-0.247	-0.486	-0.658	-0.937	0.784
Sr		1.000	-0.762	-0.650	-0.062	-0.523	-0.716	-0.743	0.808
Rb			1.000	0.579	0.078	0.915	0.865	0.734	-0.806
Zn				1.000	-0.208	0.460	0.808	0.632	-0.782
Cu					1.000	0.037	-0.118	0.295	0.145
Ba						1.000	0.825	0.648	-0.631
Ni							1.000	0.805	-0.886
Cr								1.000	-0.844

TABLE X

RAINBOW URANIUM DEPOSIT

Element	Mean	STD	95% Confidence Interval for Mean
Zr	1039	235	568 - 1511
Sr	1079	73	933 - 1226
Rb	47	15	17 - 78
Zn	127	5	116 - 138
Cu	9	2	5 - 14
Ba	349	58	242 - 455
Ni	38	2	34 - 43
Cr	54	8	37 - 70
U	623	70	481 - 764

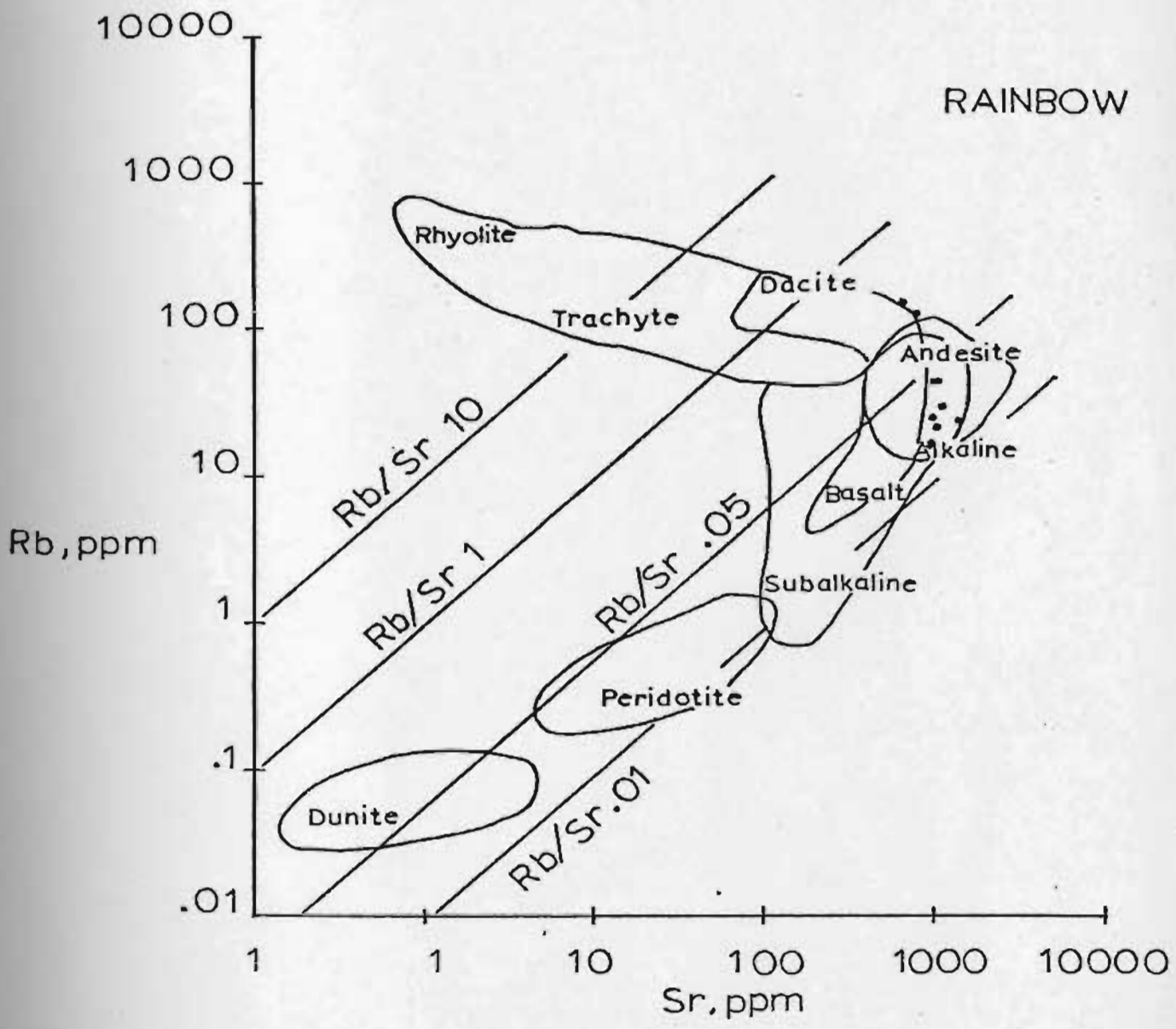

Figure 11. Plots of Rb vs Sr for the Rainbow deposit.

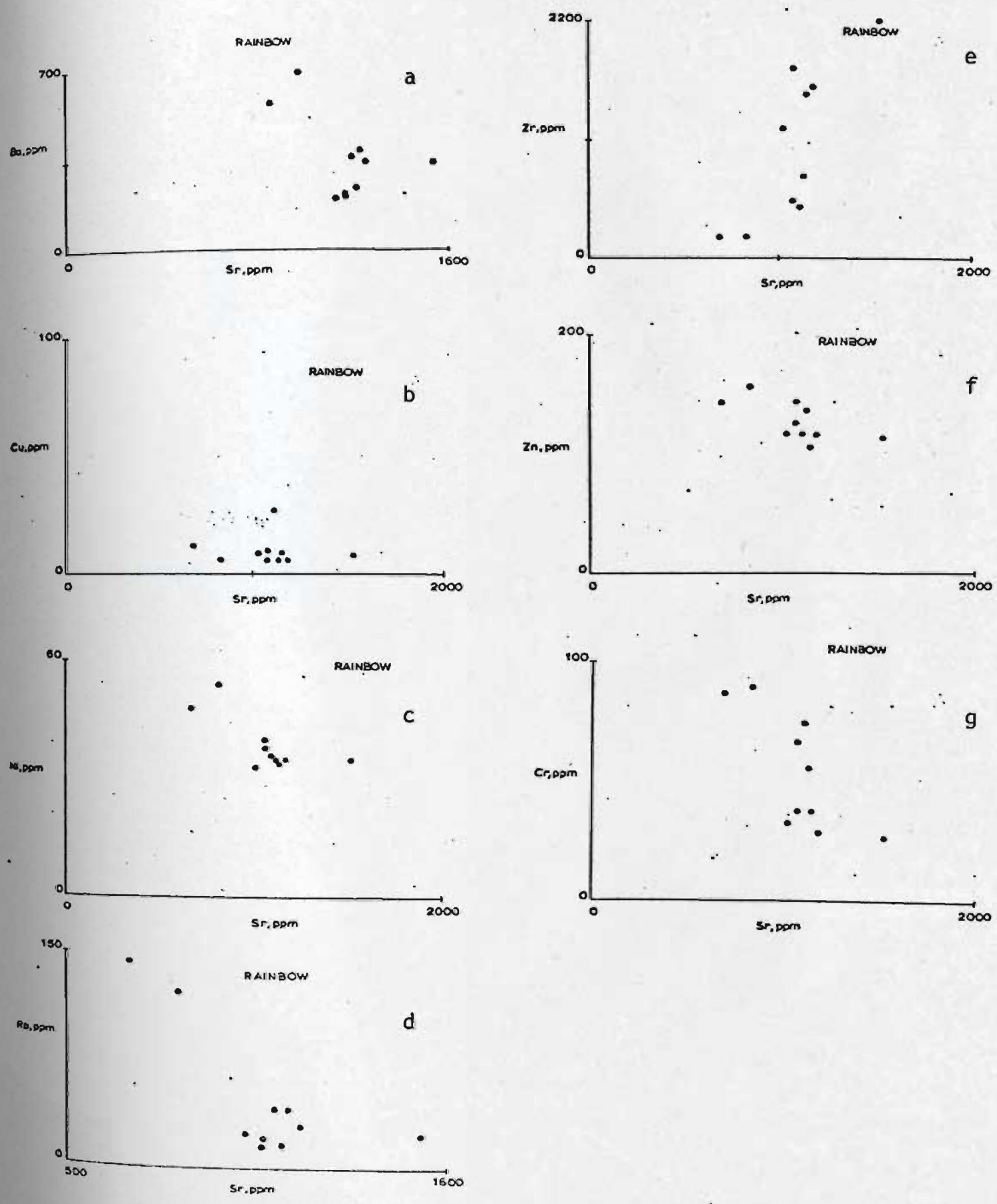

Figure 12. Plots of trace elements vs Sr (see text).

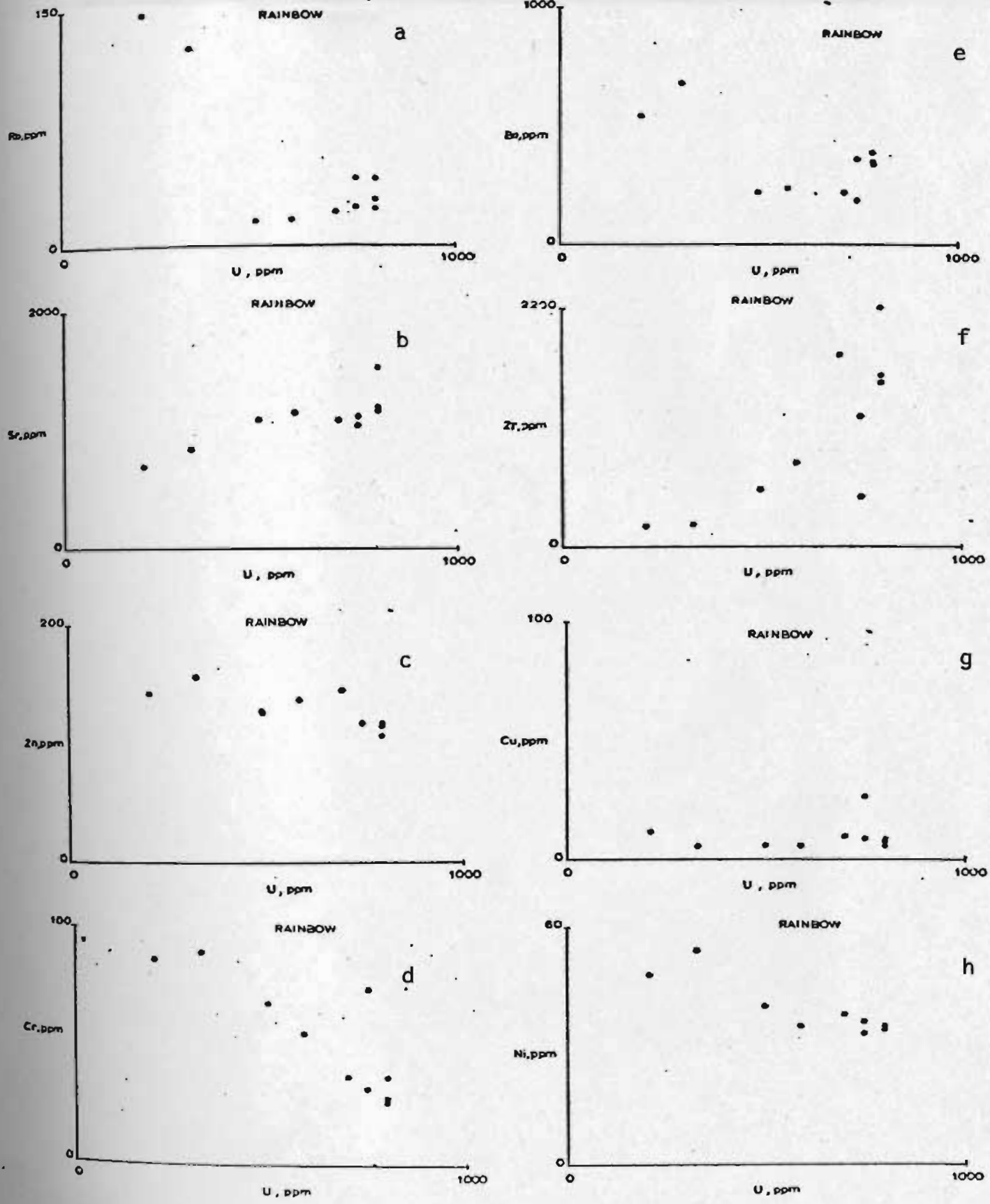

Figure 13. Plots of trace elements vs U (see text).

PLATE XI

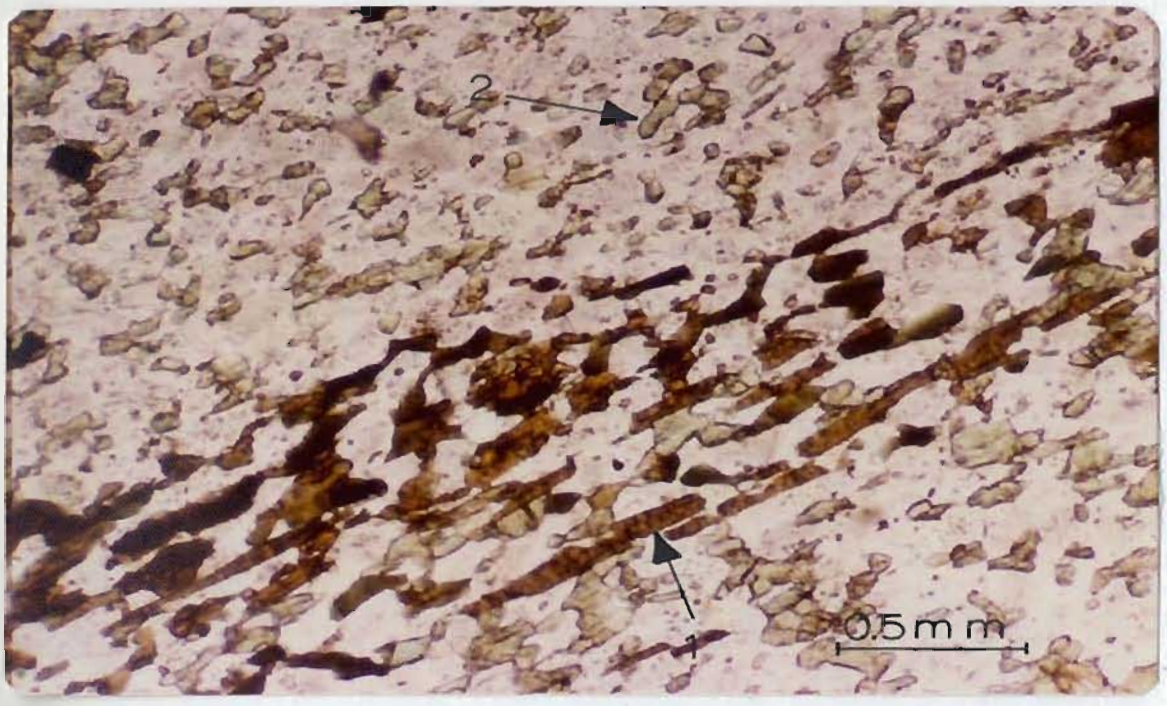

a

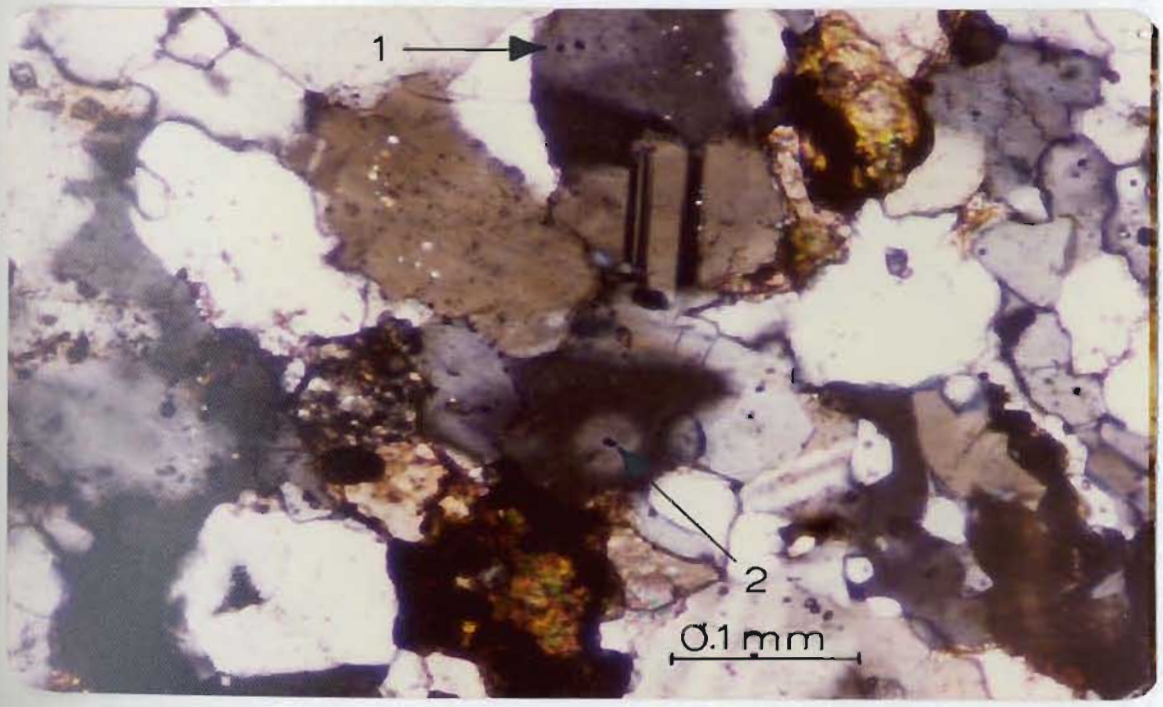

b

a. Granoblastic aggregate of quartz, biotite, metamorphic amphibole and plagioclase.
   1. iron-rich biotite 2. metamorphic amphibole

b. Small opaque inclusions within plagiocalse and quartz grains. Those indicated by Arrows 1 and 2 are surrounded by a halo, and can possibly be the radioactive minerals in the Rainbow deposit.

3.4 M. Ben Uranium Deposit

The M. Ben main uranium zone consists of small radioactive showings which are found in a fine to medium-grained feldspathic quartzite which varies in texture from massive to foliated. The strongly mineralized rock is a weakly banded quartzite, which lacks lenticular structure. It shows visible lithological variation from the unmineralized rock, with the presence of distinct mafic streaks consisting mainly of garnets (andradite) and hornblende with radioactive opaque minerals as inclusions.

The mineralized zone is generally striking ENE-WSW and dipping steeply to the south. The foliation shows the same trend. The Michelin uranium deposit is located 17 miles WSW of the M. Ben deposit and along with other radioactive showings (e.g. Burnt Lake showing) are found in feldspathic quartzites of generally similar lithology which constitute part of an extensive formation.

A post-deformational amphibolitic and a gabbroic dyke intruding the uraniferous quartzite is not radioactive. However, samples from the center of these dykes gave 24 and 3 ppm U respectively. The significance of these results becomes obvious from the following:

Page (1960) compiled evidence that most uranium districts of the world contain mafic dykes, referred to as diabase, basalt, lamprophyre, etc. These dike rocks may be slightly older or slightly younger than the uranium deposits, but they are all closely related in age. He states that such small bodies of igneous rocks themselves are obviously not the source of the uranium contained in the deposits, but they do represent

near surface parts of much larger adjacent igneous bodies that could furnish the uranium solutions. He concludes that intermediate to basic magmas are probably the source of most pitchblende-bearing solutions.

Many uranium veins, such as at the Eldorado Mine, Great Bear Lake, Canada, show little, if any, close associations with silicic igneous rock; commonly diabases are the only manifestations of igneous activity of comparable age. In addition, Mursky (1963 cited by Beck (1970) has found geochemical and geochronological evidence to support Page's contention that pitchblende ores of Great Bear Lake and the associated diabase dykes were derived from the same magmatic source. The probable age of pitchblende from the original discovery in Labrador, by lead isotope ratios, is 600 $\pm$ 30 m.y. (Beavan, 1958) and Lamprophyre dykes 500 to 600 m.y. (Leech et al., 1963), although King and McMillan (1975) found evidence that some lamprophyre dykes have an age not older than Lower Cretaceous.

The uranium content in amphibolites generally range from 2.6 to 4.1 ppm (Rodgers and Adams, 1969). The high uranium content (24 ppm) of the amphibolite dyke intruding the M. Ben main zone provides a further geochemical evidence that possibly the mafic dykes in the area are related to an original source of the uranium mineralization. The association of mafic dykes and uranium mineralization in the area is in agreement with Page's observations but the question of the primary source of uranium is still speculative, and it is not known whether it

wholly derived from crustal rocks by metamorphic remobilization or whether it has been partly introduced from depths.

Modal analyses of low and high mineralized rock samples from this showing are given in Table XI. As can be seen, the high mineralized rock is characterized by a high garnet (andradite) content which contains the opaque radioactive minerals.

Table XII shows analyses for total and leachable uranium of 18 samples from the M. Ben deposit. Total uranium was analysed with X-ray fluorescence which measures total uranium content regardless of mineralogy. Fluorimetry was used for the semi-quantitative analysis. By such an analytical approach one does not extract total uranium but only the acid leachable uranium. As can be seen in this table the amount of non leachable or structural uranium is relatively very high, exceeding in two cases 50% of the uranium content in these samples. Only in one case (sample E14) the non-leachable uranium is very low (5.4%). Fig. 14 indicates that there is poor correlation between Zr and diadochic uranium, which suggests that not much uranium is held in the crystal lattice of zircon. Obviously most of the diadochic uranium must be held in the structure of other minerals such as sphene, hornblende and possibly as inclusions within quartz, feldspars, magnetite and pyrite.

Trace element concentrations and various statistical parameters for these rocks are given in Tables XIII-XV. Plots of Rb vs Sr (Fig. 15) range between Rb/Sr 0.05 and 3. The highly mineralized samples have a high Rb content and they fall in the field between trachyte and dacite.

As in the Michelin deposit, the full range of those samples outside igneous fields in Fig. 15 suggest that the protolith was not an igneous rock and probably similar to the Michelin protolith.

Other trace element distribution patterns can be seen in Figs. 16a-g, 17a-h (numbers 24 and 26 represent samples from the amphibolitic and the gabbro dyke). As can be seen in Fig. 17a, a plot of Rb and U separated the low and the highly mineralized samples into two groups. A characteristic feature is the association of high uranium content with high andradite and hornblende contents. These minerals, particularly the andradite, contain the majority of radioactive submicroscopic inclusions in this showing. If amphiboles are the only Rb-bearing mineral, then the positive U-Rb correlation might be explicable from the presence of higher amphibole contents in the highly mineralized samples. Some trends are difficult to explain since no simple relations exist between trace elements. However, in some cases, similar trends for other showings are important and for consistency these diagrams are included here.

The criteria for distinguishing the possible origins of uranium mineralization in the M. Ben showing are summarized below.

Syngenetic

- Stratiform pockets of uranium mineralization.
- Absence of spatial association with major fault zones on igneous intrusives.

Epigenetic, hypogene

- Positive U-Rb correlation. (This can also reflect residual igneous trends preserved in the clastic sediments).

TABLE XI

Modal analyses of rock samples from M. BEN uranium showing; all values are expressed as volume percentages.

Sample Number	Low mineralized rock M. BEN 16 (32 ppm U)	High mineralized rock M. BEN 18A (4000 ppm U)
Groundmass (mostly quartzofeldspathic material)	79	64
Opaques (magnetite, pyrite, possibly other opaque minerals)	14	2
Andradite		29
Other minerals included zircon, sphene and hornblende	6	4

TABLE XII

M. BEN URANIUM DEPOSIT

Sample Number	Radio-activity (C/S)	Total U (XRF, ppm)	Leachable U (Fluorimetry, ppm)	Difference	% Non leachable U (Diadochic U)
E 1	100	320	200	120	37.5
E 2	55	100	57	43	43.0
E 3	70	630	370	260	41.2
E 4	55	550	340	210	38.1
E 5	75	400	193	207	51.7
E 6	130	1390	800	590	42.4
E 7	100	780	490	290	37.1
E 9	90	810	410	400	49.3
E 10	200	3730	2650	1080	28.9
E 11	60	310	160	150	48.3
E 12	60	220	130	90	40.9
E 13	60	360	167	193	53.5
E 14	450	3690	3490	200	5.4
E 15	550	4020	2740	1280	31.7
E 19	400	5600	4825	775	13.8
E 20	180	3690	2520	1170	31.7
E 21	160	1840	1010	830	45.1
E 23	200	4270	2870	1400	32.7

TABLE XIII

M. BEN URANIUM DEPOSIT

(values in ppm)

Sample No.	Zr	Sr	Rb	Zn	Cu	Ba	Mo	Ni	Cr	Ag	U	Radioactivity C/S
1	1310	25	6	69	5	40	1	20	17	.6	200	100
2	1255	19	9	120	7	29	1	18	23	.4	57	55
3	1869	20	10	89	3	30	1	21	20	.5	370	70
4	402	21	11	295	10	48	238	36	59	1.2	340	55
5	1322	22	11	108	2	38	2	19	18	.5	193	75
6	1316	32	26	285	7	180	2	20	16	9.6	800	130
7	1984	27	14	220	6	20	1	19	25	.6	490	100
8	276	30	6	43	4	22	2	20	12	.5	24	50
9	916	43	15	149	7	33	2	19	13	.6	410	90
10	616	41	68	429	2	85	1	21	7	2.6	2650	200
11	537	73	9	61	10	63	39	23	11	.6	160	60
12	153	69	7	59	7	44	82	21	14	1.6	130	60
13	443	30	7	143	5	56	1	19	12	.5	167	60
14	541	179	79	2131	17	293	2	27	13	8.5	3490	450
15	531	141	76	277	8	108	2	27	19	2.5	2740	550
16	331	32	5	70	3	34	1	20	14	.4	32	50
17												450
18												320
19	499	76	106	261	1	98	3	25	14	6.5	4825	400
19'	558	79	109	272	4	96	2	25	16	5.5	4900	
20	801	41	62	326	1	30	1	20	6	4.8	2520	180
21	1146	37	29	314	5	34	1	20	8	2.4	1010	160
22	224	58	3	36	4	30	N.D.	29	29	1.2	15	50
23	410	87	76	186	11	142	1	22	12	4.6	2870	200
24	205	215	28	176	26	420	2	55	53	1.0	24	50
25												50
26	191	275	34	176	17	711	1	61	42	.8	3	50

TABLE XIV

M. BEN URANIUM DEPOSIT

Correlation matrix calculation for 24 sets of data

Variable	Zr	Sr	Rb	Zn	Cu	Ba	Ni	Cr	U
Zr	1.000	-0.266	-0.026	0.039	-0.125	-0.205	-0.053	0.042	0.013
Sr		1.000	0.447	0.392	0.836	0.917	0.829	0.491	0.242
Rb			1.000	0.519	0.225	0.303	0.266	-0.044	0.966
Zn				1.000	0.386	0.296	0.167	-0.000	0.545
Cu					1.000	0.780	0.808	0.673	0.041
Ba						1.000	0.813	0.519	0.083
Ni							1.000	0.821	0.058
Cr								1.000	-0.192

TABLE . XV

M. BEN URANIUM DEPOSIT

Element	Mean	STD	95% Confidence Interval for Mean
Zr	666	112	441 - 890
Sr	61	13	34 - 88
Rb	26	6	14 - 39
Zn	232	80	70 - 393
Cu	6	1	4 - 8
Ba	99	31	36 - 162
Ni	22	2	17 - 27
Cr	17	2	11 - 23
U	904	270	363 - 1445

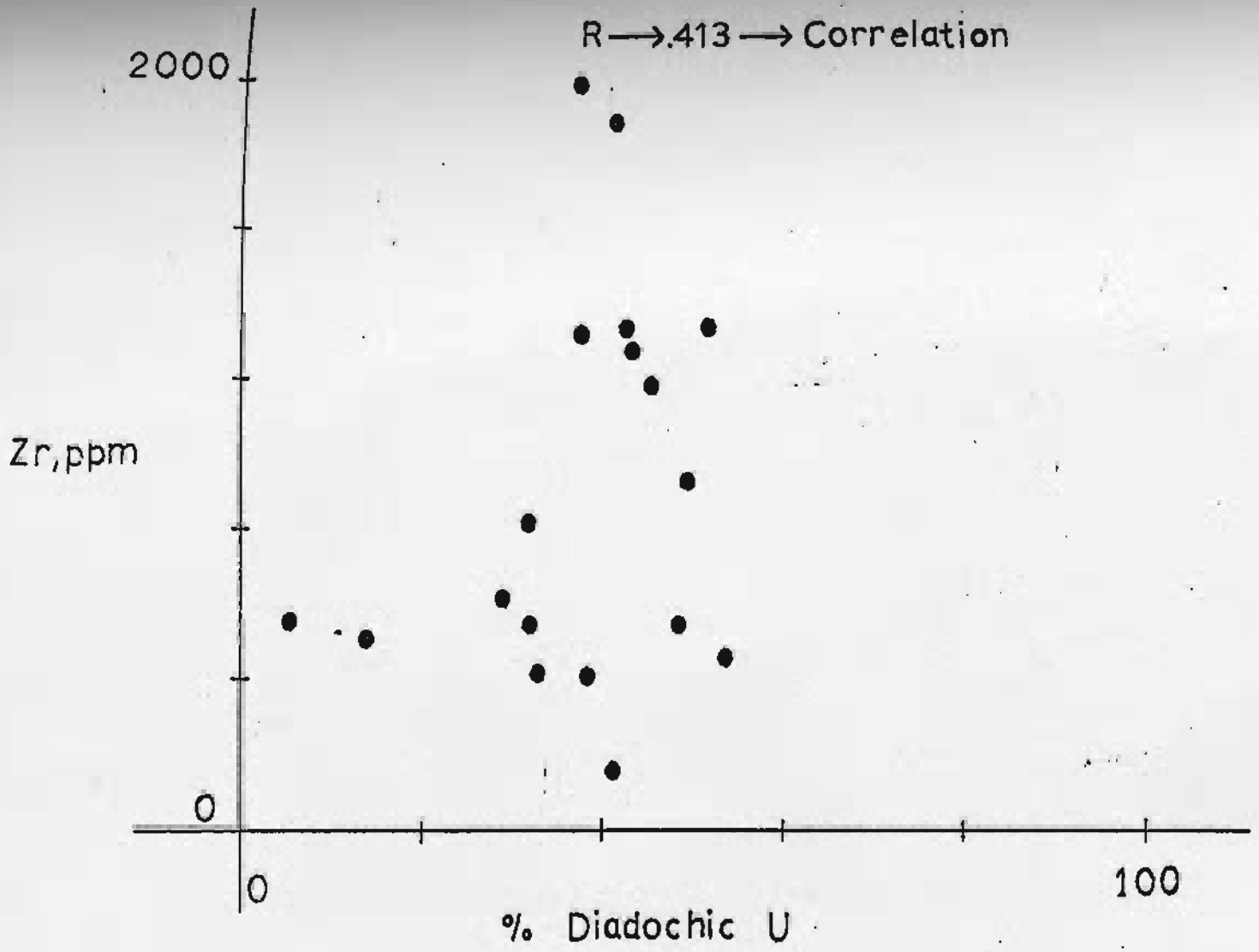

Figure 14. Plot of Zr vs. non-leachable uranium (see text).

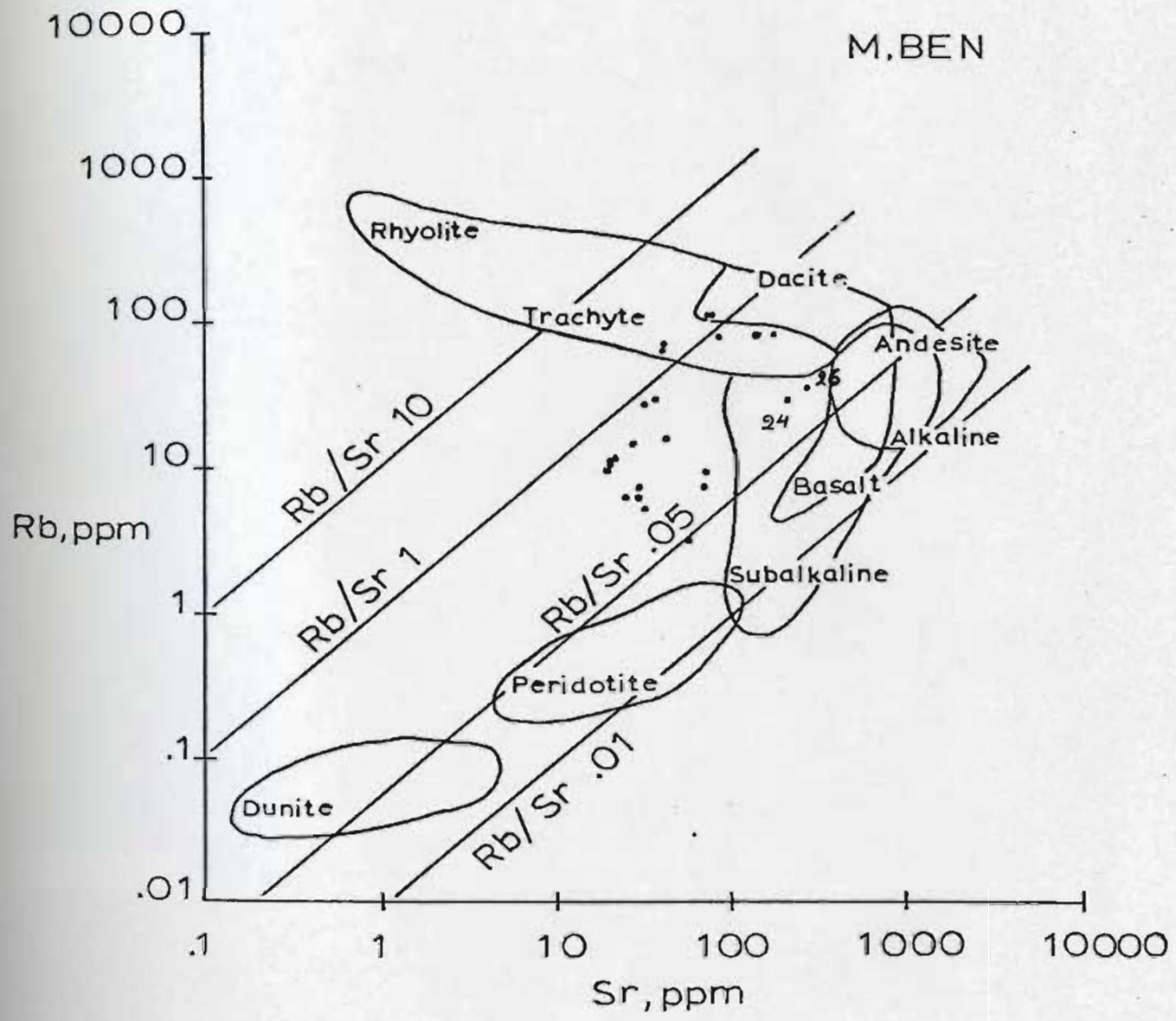

Figure 15. Plots of Rb vs Sr for the M. Ben uranium deposit (see text).

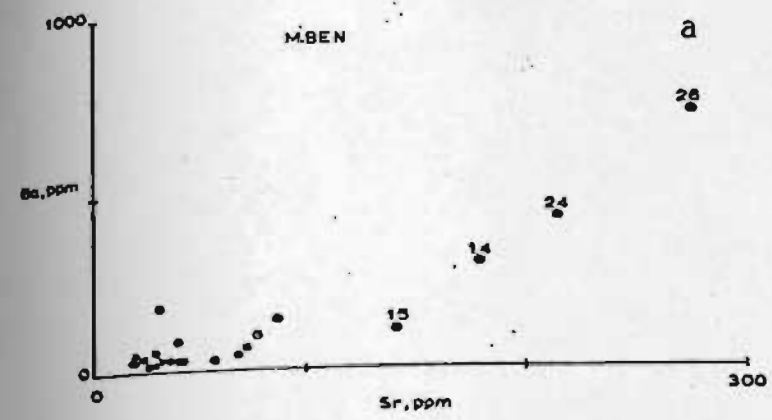

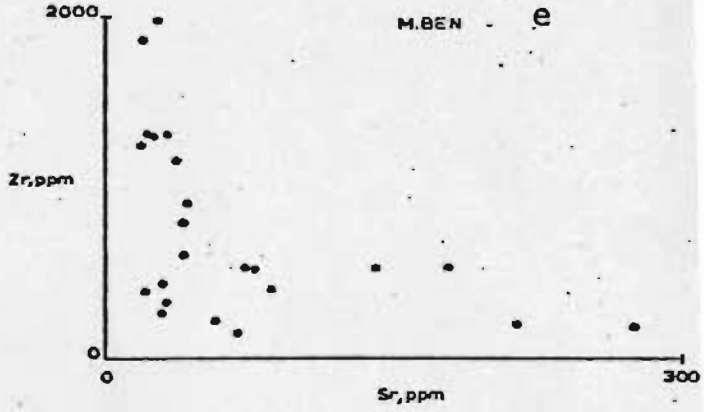

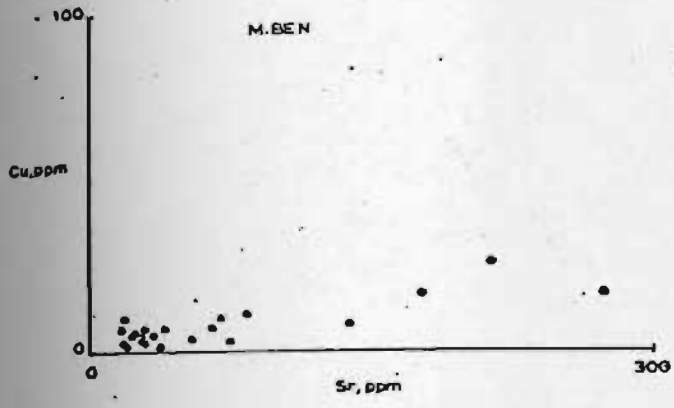

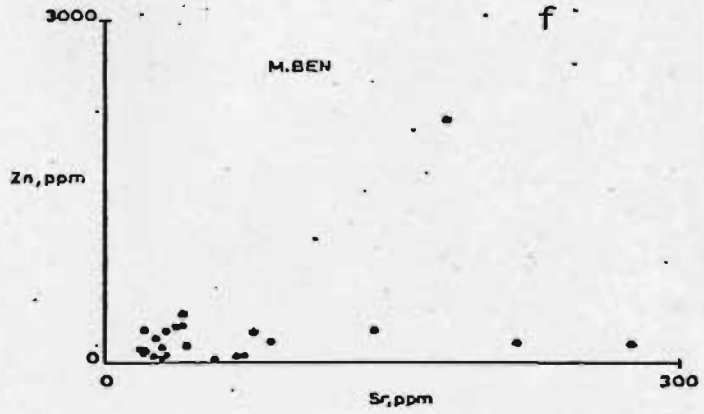

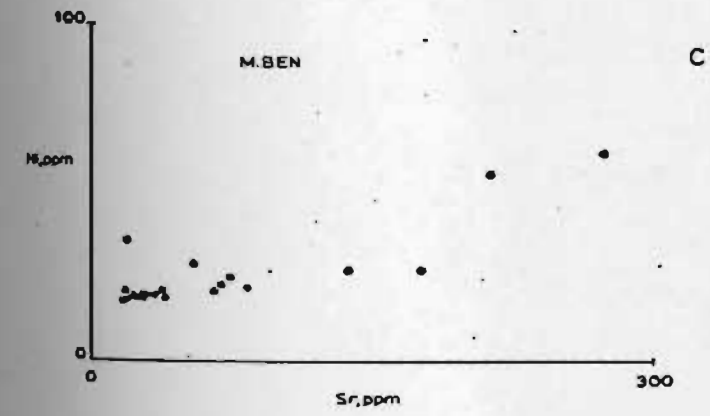

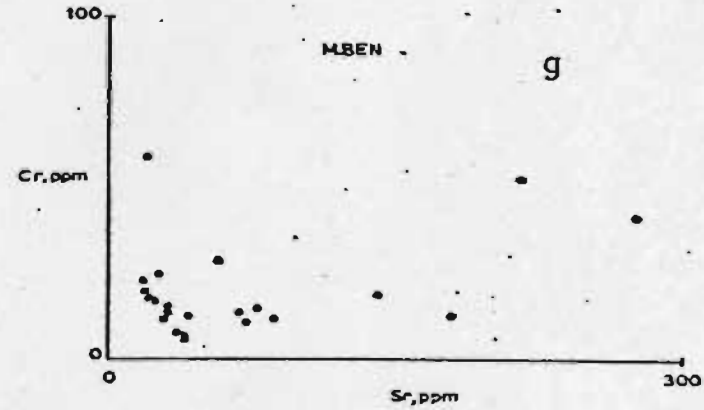

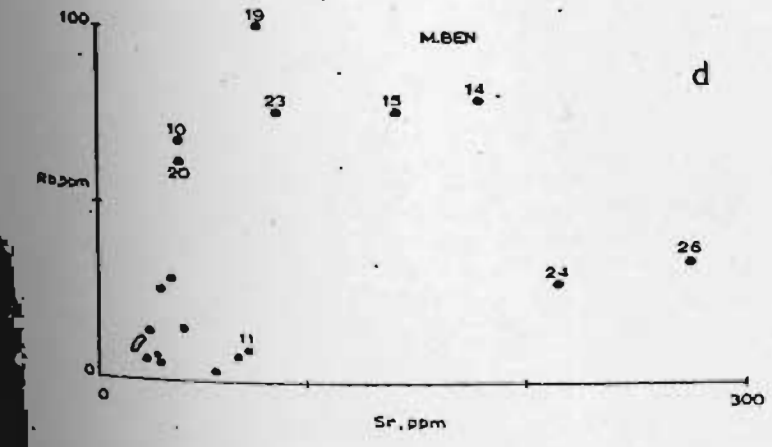

Figure 16. Plots of trace elements vs. Sr. (see text).

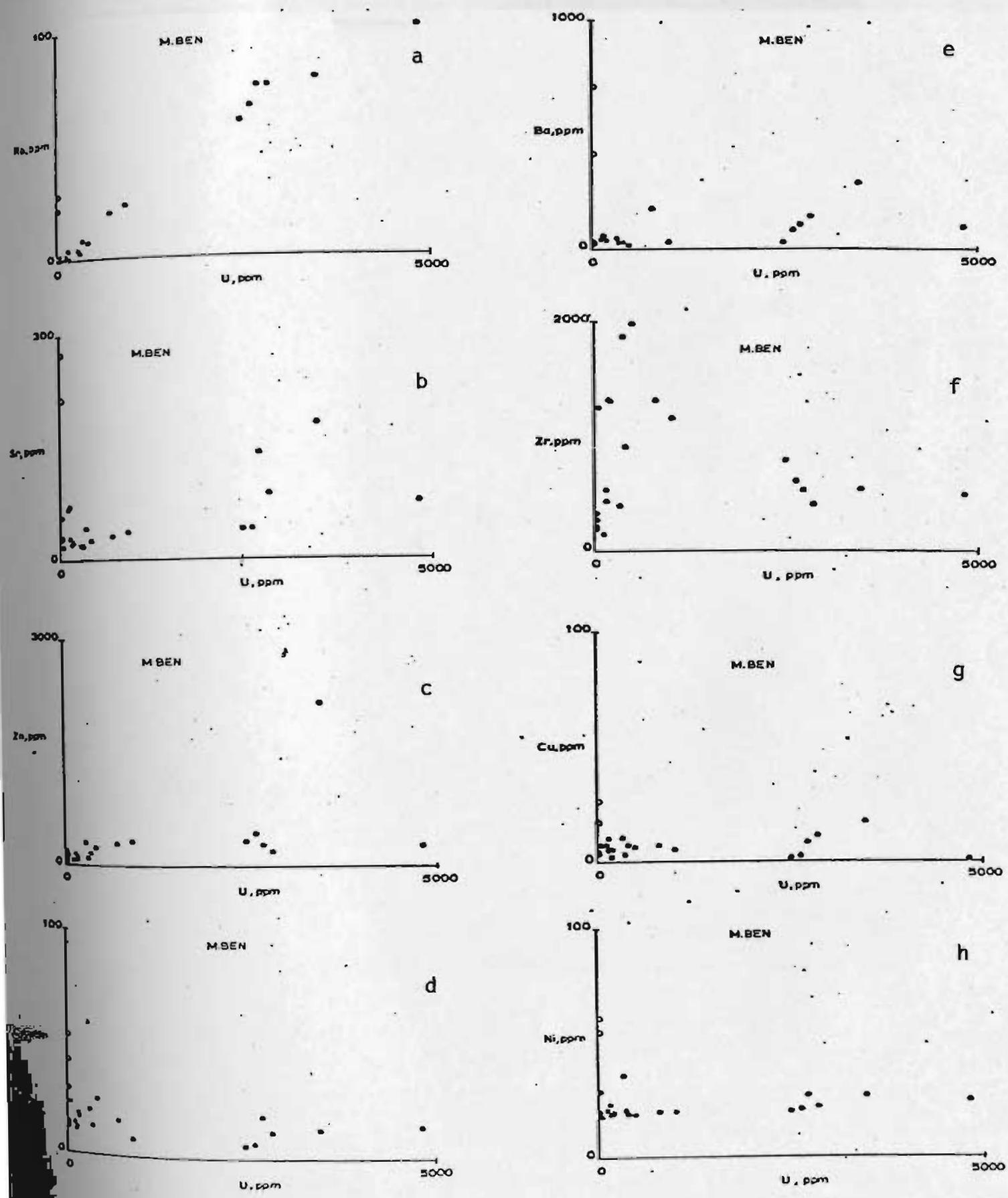

Figure 17. Plots of trace elements vs. U (see text).

PLATE XII

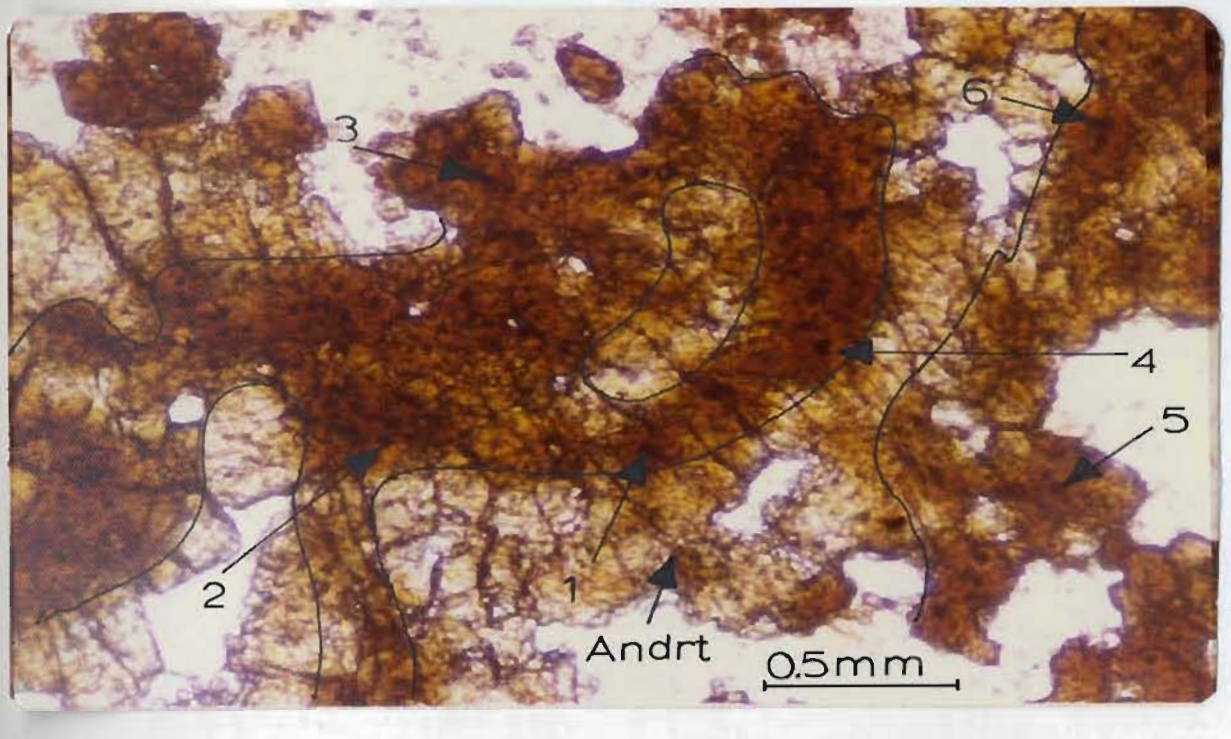

a

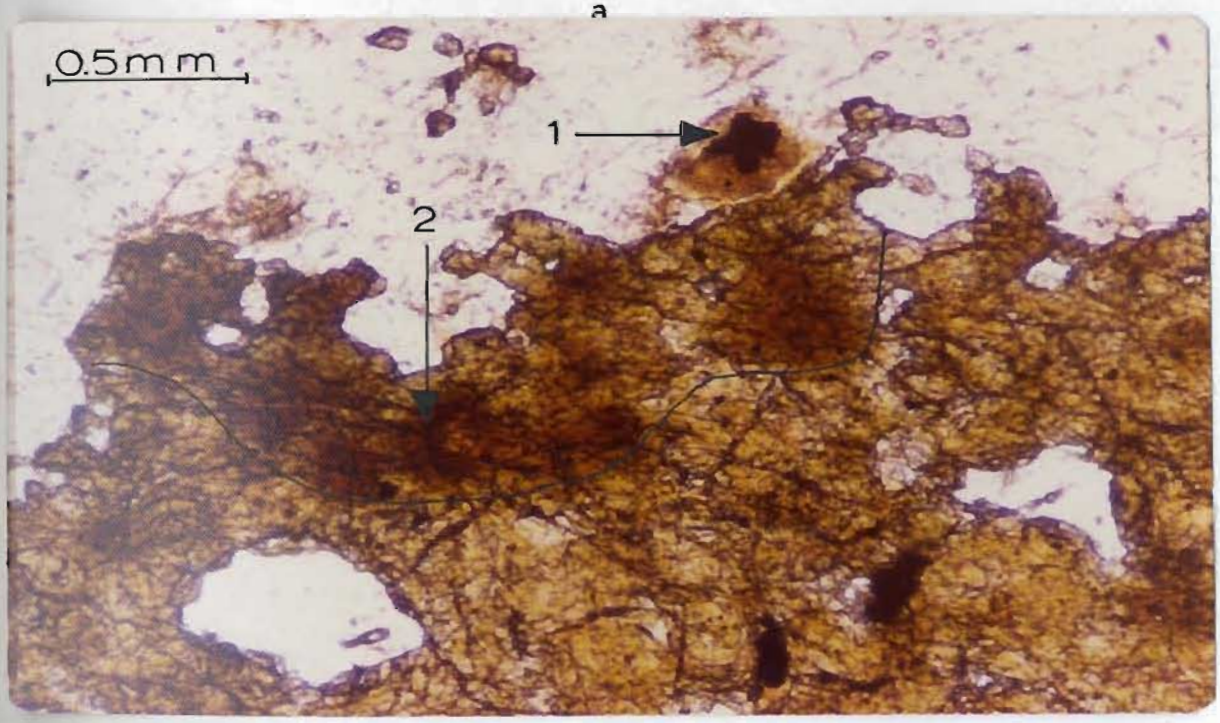

b

a. Garnet (andradite) with radioactive opaque inclusions. Arrows 1-6 show some of the opaque radioactive inclusions.

b. (Same thin section). Arrow 1 shows a larger opaque radioactive mineral.
M. BEN uranium deposit, Labrador.

3.5 McLean Uranium Deposit

The McLean uraniferous rock is weakly banded with mafic minerals which have been completely altered to chlorite. It is located within an extensive formation of the Aillik Group which includes mainly acidic volcanic rocks. The banding is striking in a general ENE-WSW and dipping to the southeast, and appears to be gradational into a well foliated grey and pink feldspar-quartz-hornblende-biotite granite gneiss.

Modal analysis of one rock sample from the McLean uranium deposit is indicated in Table XVI. Most of the rock consists of feldspars and minor quartz. Opaque minerals rimmed by sphene are possibly the radioactive minerals in the McLean showing. There appears to be a similarity in the mode of uranium mineralization between the Michelin and McLean uranium deposits, in both cases being in the form of davidite (Plate XIII).

Trace element concentrations and various statistical parameters for those rocks are given in Tables XVII to XIX. Plots of Rb vs Sr (Fig. 18) range between Rb/Sr 0.03 and 0.9 and they all, but one, fall in the field of subalkaline volcanic rocks; however, this showing is located in a feldspathic quattzite which differs locally in lithology. Compared to the average trace element concentrations of metasedimentary schists and quartzofeldspathic gneisses (Table VI) the McLean uranium bearing rock has a relatively lower Rb and Cr content and higher Zr and Cu content. Patterns of trace element distribution can be seen in Figs. 19a-g, 20a-h. No simple relations between the trace elements exist in this showing.

The main criterion for a syngenetic origin of the uranium mineralization is that uranium is more or less uniformly distributed laterally (parallel-to stratification) but changes abruptly vertically (across stratification) with change in rock type.

TABLE XVI

Modal analyses of rock sample from McLean; all values are expressed as volume percentages.

Sample Numbers	McLean 1
Feldspars (mostly plagiocalse An_{40}-An_{58}, Andesine-Labradorite	90
Hornblende and biotite altered to chlorite	5
Opaques (magnetite, pyrite and possibly primary radioactive minerals of unknown composition)	2.5
Sphene, zircon	2.0
Tiny opaque grains, possibly radioactive, rimmed by sphene	0.5

TABLE XVII

McLEAN URANIUM DEPOSIT

(values in ppm)

Sample No.	Zr	Sr	Rb	Zn	Cu	Ba	Ni	Cr	U
1	87	232	16	182	12	205	57	80	900
2	72	226	14	156	-58	184	56	75	800
3	1420	171	9	140	44	120	36	18	400
4	548	35	119	49	15	232	20	8	100
5									
6	420	88	69	32	10	422	19	7	50
7	126	305	38	163	80	454	41	49	180
8	377	27	137	41	40	166	20	10	100
9	489	111	12	71	31	138	28	20	120
10	1434	131	29	42	619	184	29	16	1450
11	904	155	4	56	345	102	27	18	200
12	1434	148	4	45	400	108	31	24	140
13	925	143	2	45	637	120	27	10	160
13'	940	150	2	50	640	125	30	15	165

TABLE XVIII

McLEAN URANIUM DEPOSIT

Correlation matrix calculation for 13 sets of data

Variable	Zr	Sr	Rb	Zn	Cu	Ba	Ni	Cr	U
Zr	1.000	-0.021	-0.213	-0.244	0.685	-0.281	-0.069	-0.387	0.213
Sr		1.000	-0.444	0.847	0.084	0.414	0.856	0.783	0.386
Rb			1.000	-0.211	-0.332	0.392	-0.257	-0.257	-0.212
Zn				1.000	-0.334	0.341	0.901	0.874	0.380
Cu					1.000	-0.239	-0.059	-0.249	0.310
Ba						1.000	0.269	0.249	-0.002
Ni							1.000	0.920	0.554
Cr								1.000	0.492

TABLE XIX

McLEAN URANIUM DEPOSIT

Element	Mean	STD	95% Confidence Interval for Mean
Zr	633	155	323 - 944
Sr	136	25	86 - 186
Rb	34	13	8 - 61
Zn	78	17	44 - 112
Cu	171	69	32 - 310
Ba	187	36	114 - 259
Ni	30	4	21 - 38
Cr	25	7	10 - 40
U	353	124	104 - 603

PLATE XIII

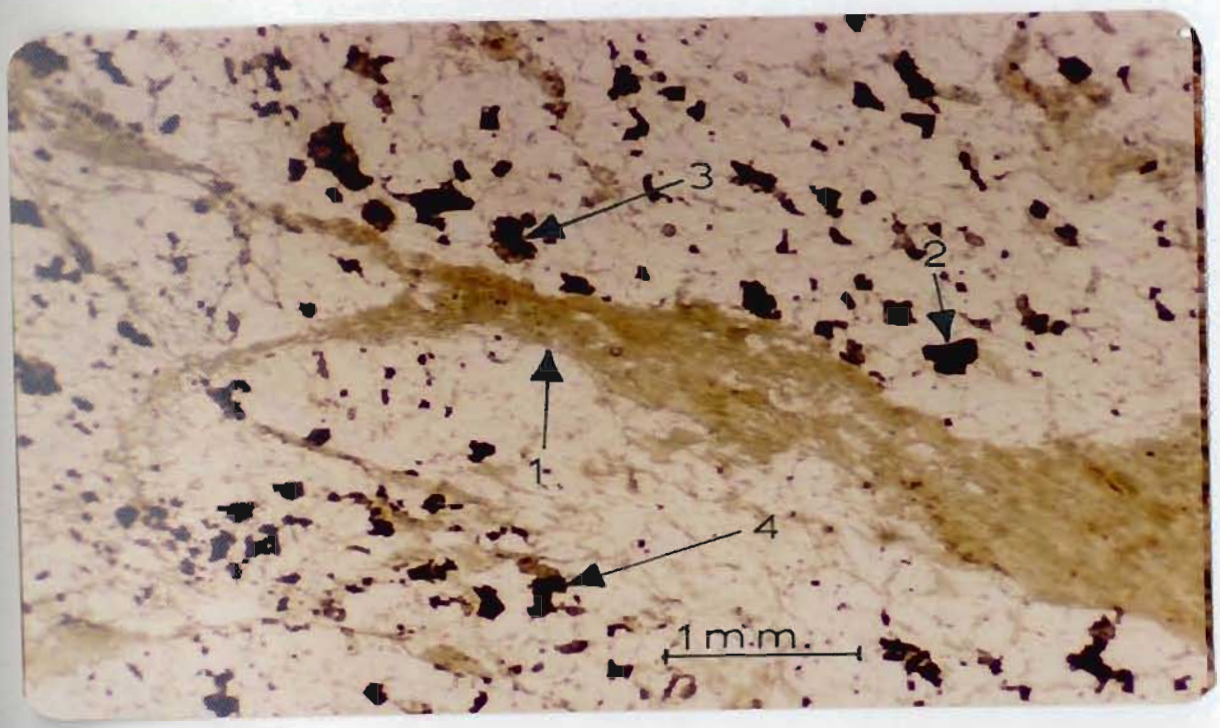

1, chlorite; 2, magnetite; 3 and 4 opaque grains partly rimmed by sphene: possibly the radioactive minerals in the showing. The white consists of feldspathic material.

McLean uranium deposit.

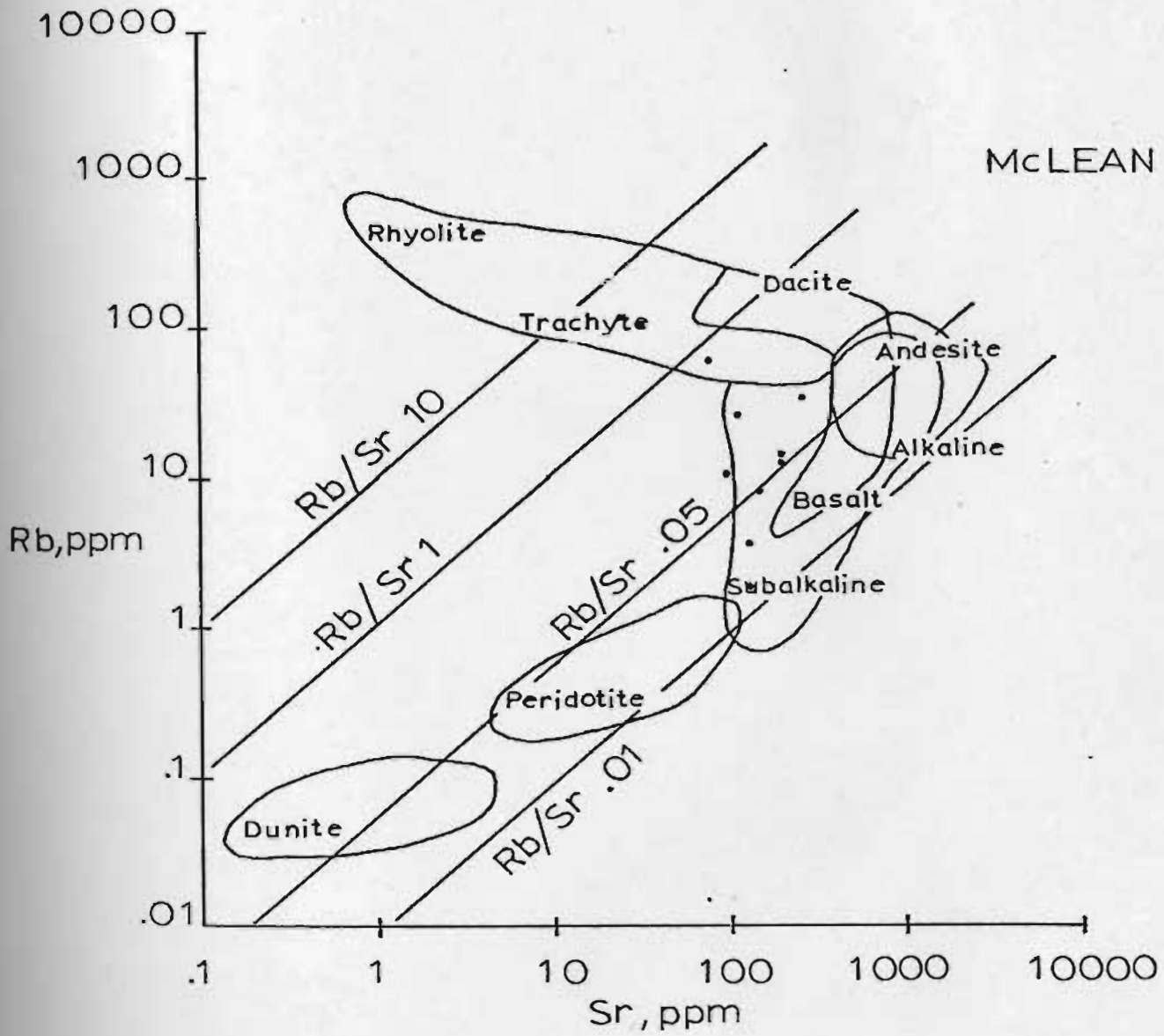

Figure 18. Plot of Rb vs. Sr for the McLean uranium deposit.

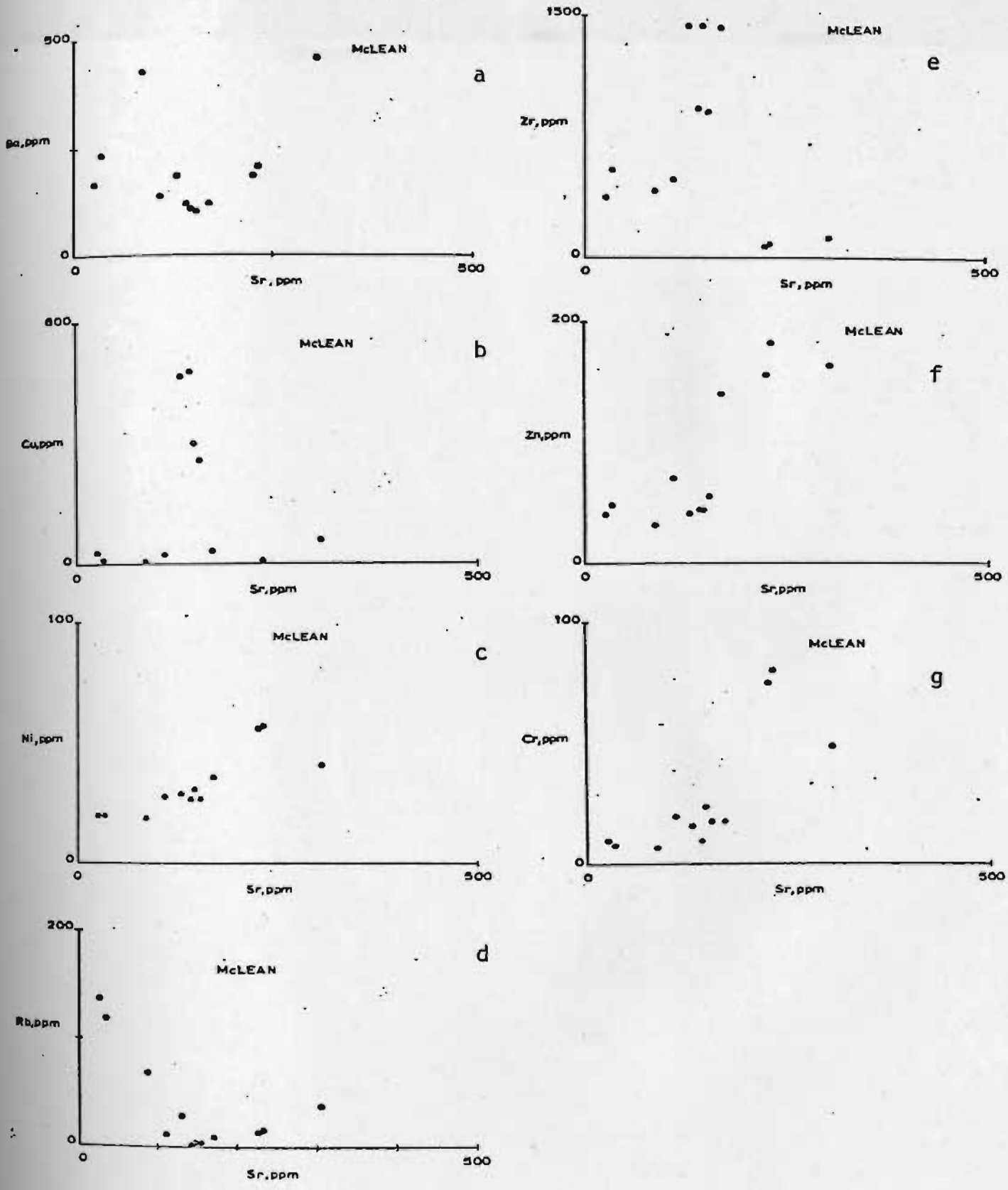

Figure 19. Plots of trace elements vs. Sr. (see text).

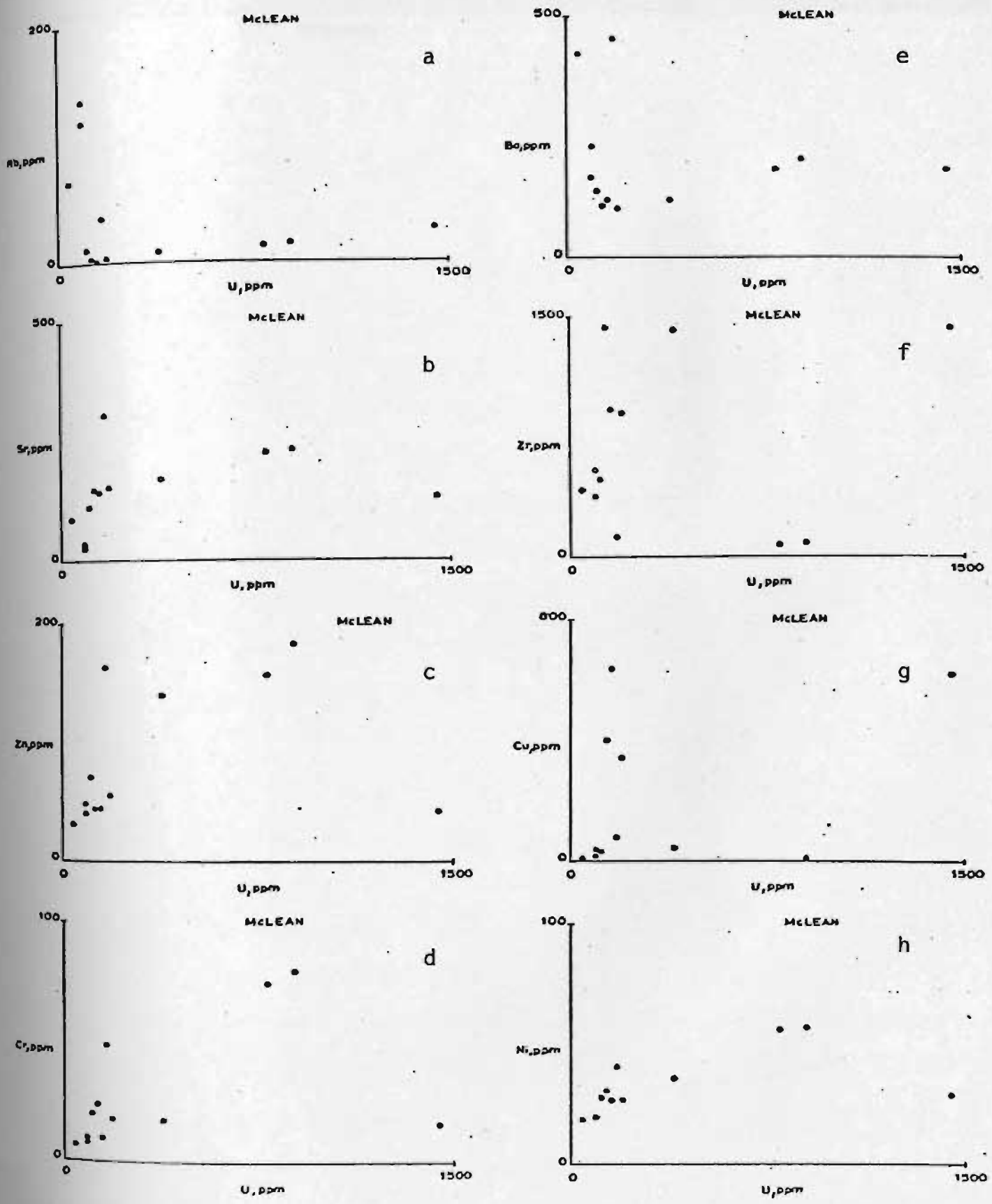

Figure 20. Plots of trace elements vs. U (see text).

3.6 Witch Lake Uranium Deposit

The Witch Lake uranium deposit occurs in a weakly banded and volcanic tuff, with the strongly mineralized rock characterized by distinct magnetite-rich streaks. The surface exposures of radioactive zones are few and small, but generally indicate a tabular deposit which is striking N70° - 80°E and steeply dipping to southeast. A banded feldspathic quartzite with variable lithology bounds the showing.

Modal analysis of a low and a high mineralized rock sample from this showing is indicated in Table XX. As can be seen, the highly mineralized samples are characterized by a high content of opaque minerals, particularly magnetite. This suggests that uranium is probably in the magnetite in the form of independant compounds, i.e. inclusions. Autoradiographs of the Witch samples did not indicate the existence of primary uranium minerals or interstitial radioactive material. The lack of interstitial radioactive material suggests that no uranium solutions have percolated through the Witch Lake host rock after original deposition of uranium mineralization and no extraction of uranium has taken place during recrystallization of this rock.

Trace element concentrations and various statistical parameters for those rocks are given in Tables XXI-XXIII. Plots of Rb vs Sr (Fig. 21) range between Rb/Sr 0.05 and 0.07. All the plots fall close to the dacite-andesite field. The highly mineralized rocks are characterized by higher Sr and Rb and lower Cu contents. Patterns of trace element distributions can be seen in Figs. 22a-g, 23a-h. The plot of Cu vs Sr (Fig. 22b) separated

the low from the highly mineralized samples of Witch Lake uranium showing; however, no simple relation between Rb and Sr exists.

The higher plagioclase content in the highly mineralized samples may be responsible for the positive correlation between Sr and U (Fig. 23b).

There is no correlation between Ba-Sr, Ni-Sr, Zr-Sr, Zn-Sr, Cr-Sr (Fig. 22a,c,e,f,g) and no simple relations between Cu-Sr and Rb-Sr (Fig. 22b,d). Also there is no correlation between Zn-U, Cr-U, Ba-U, Zr-U and Ni-U (Fig. 23c,d,e,f,h). The stratiform shape of the deposit, the radioactive equilibrium of uranium with its daughter products and the lack of interstitial radioactive material which would indicate passage of uraniferous solutions suggest a syngenetic origin of the uranium mineralization.

TABLE XX

Modal analyses of rock samples from Witch Lake Uranium Deposit; all values are expressed as volume percentages.

Sample Number	Low mineralized rock Witch 18 (20 ppm)	High mineralized rock Witch 7 (710 ppm)
Groundmass	20	41
Opaques (mostly magnetite, minor pyrite, possibly other unidentified opaques)	22	39
Quartz (sutured quartz boundaries due to slight post-crystalline deformation)	12	7
Plagioclases An_{74}-An_{60} (Bytownite-Labradorite)	27	28

The groundmass consists predominantly of sericite, chlorite, carbonates, fine grained opaques.

In the fine grained deformed tuff of Witch it is difficult to tell the plagioclases from strained quartz.

TABLE XXI

WITCH URANIUM DEPOSIT

(values in ppm)

Sample No.	Zr	Sr	Rb	Zn	Cu	Ba	Ni	Cr	U	Radioactivity C/S	Equilibrium Ra /U
1	175	308	43	68	154	462	29	25	390	140	160
2	156	327	57	88	157	480	31	32	40	75	100
3	163	306	59	92	142	508	33	35	340	120	90
4	180	236	26	52	17	630	28	41	90	60	90
5	169	414	48	91	40	383	32	33	590	150	100
6	162	372	42	84	8	340	32	39	890	140	90
7	171	345	59	92	89	415	37	56	710	250	90
8	158	287	16	67	73	429	33	42	10	50	200
9	163	170	17	75	48	428	26	23	20	50	100
10	185	385	54	87	81	423	33	40	730	220	100
11	172	388	58	118	10	384	35	30	740	75	100
12	164	239	18	40	29	756	23	24	90	60	100
13	164	319	62	111	207	573	43	54	140	60	100
14	194	263	20	49	23	607	25	26	80	50	100
15	187	246	22	32	53	725	24	28	10	50	200
16	169	250	20	33	54	802	26	28	40	50	150
17	191	301	17	45	44	568	26	29	90	50	110
18	181	199	15	80	43	339	30	29	20	40	80
19	183	285	26	51	25	613	22	19	50	40	100
20	148	180	19	68	33	310	29	30	140	50	110
20'	150	180	20	70	33	300	30	30	145		

TABLE XXII

WITCH URANIUM DEPOSIT

Correlation matrix calculation for 20 sets of data

Variable	Zr	Sr	Rb	Zn	Cu	Ba	Ni	Cr	U
Zr	1.000	0.045	-0.212	-0.368	-0.272	0.341	-0.035	-0.035	-0.061
Sr		1.000	0.762	0.554	0.194	-0.267	0.180	0.179	0.776
Rb			1.000	0.796	0.582	-0.310	0.316	0.315	0.664
Zn				1.000	0.397	-0.700	0.211	0.210	0.600
Cu					1.000	-0.006	0.106	0.106	-0.061
Ba						1.000	-0.156	0.155	-0.518
Ni							1.000	1.000	0.355
Cr								1.000	0.354

TABLE XXIII

WITCH URANIUM DEPOSIT

Element	Mean	STD	95% Confidence Interval for Mean
Zr	171	2	166 - 177
Sr	290	15	259 - 322
Rb	34	4	26 - 43
Zn	71	5	59 - 82
Cu	66	12	40 - 92
Ba	509	33	442 - 575
Ni	29	1	27 - 32
Cr	33	2	29 - 37
U	260	68	122 - 398

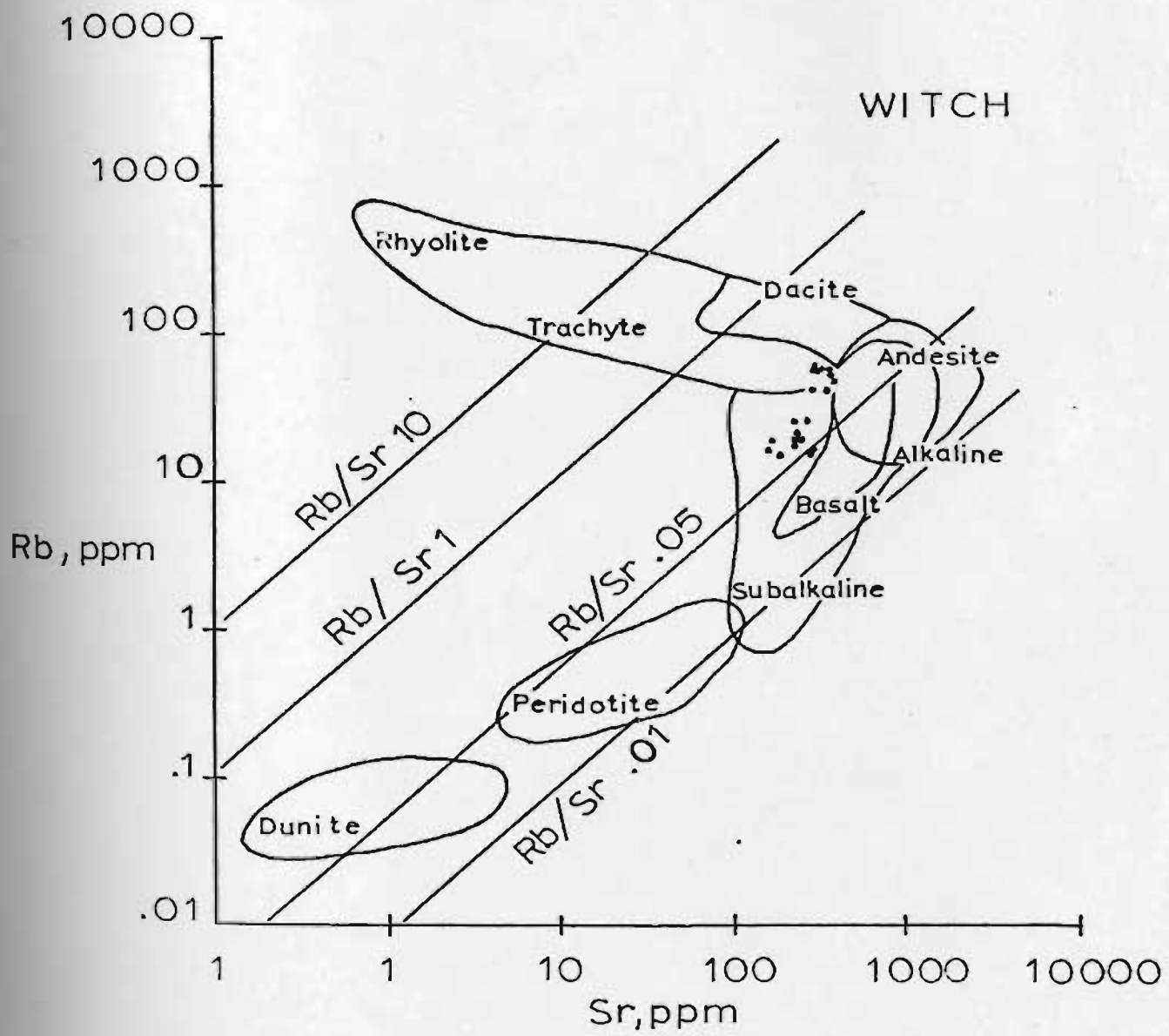

Figure 21. Plots of Rb vs. Sr for the Witch Lake uranium deposit.

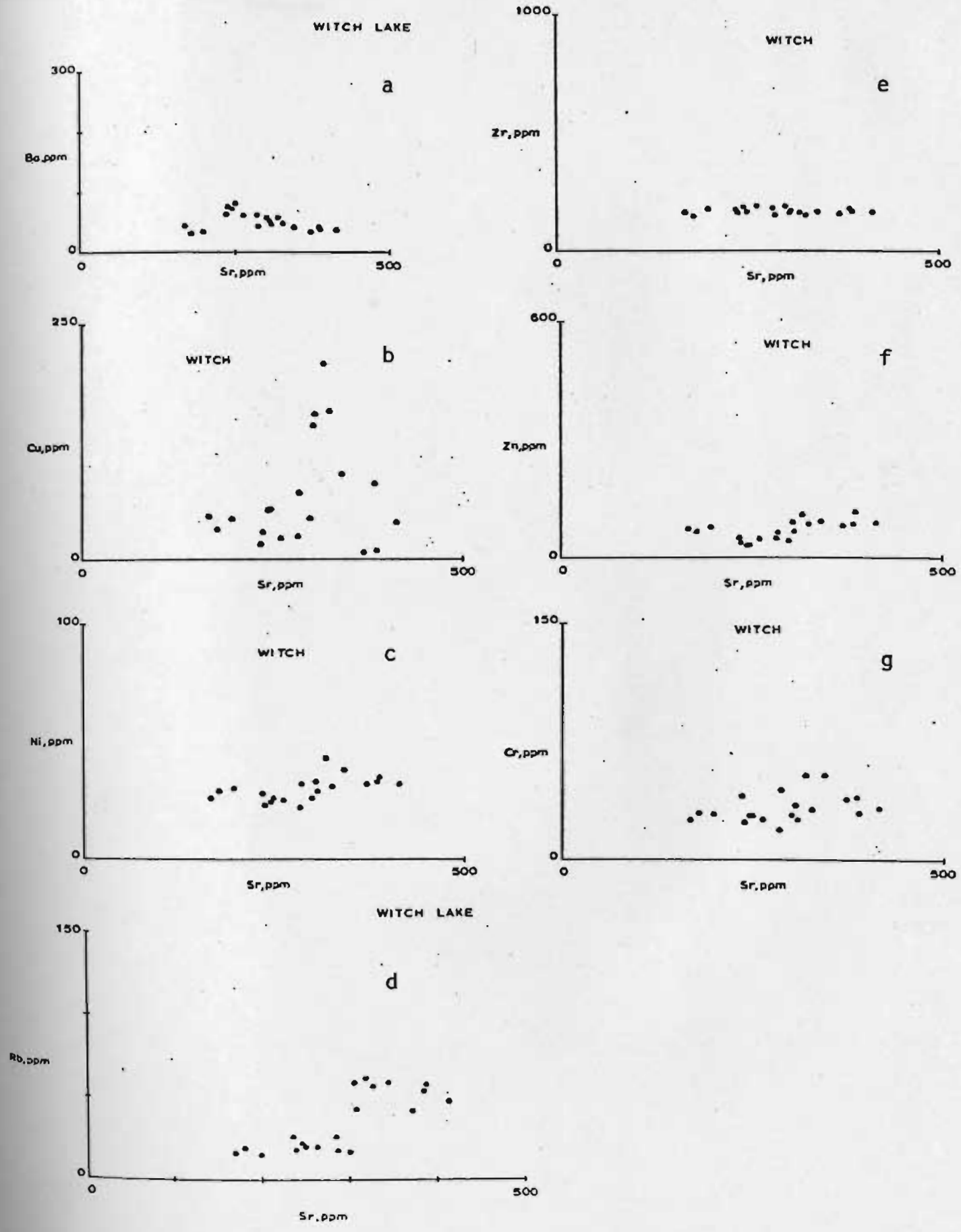

Figure 22. Plots of trace elements vs. Sr. (see text).

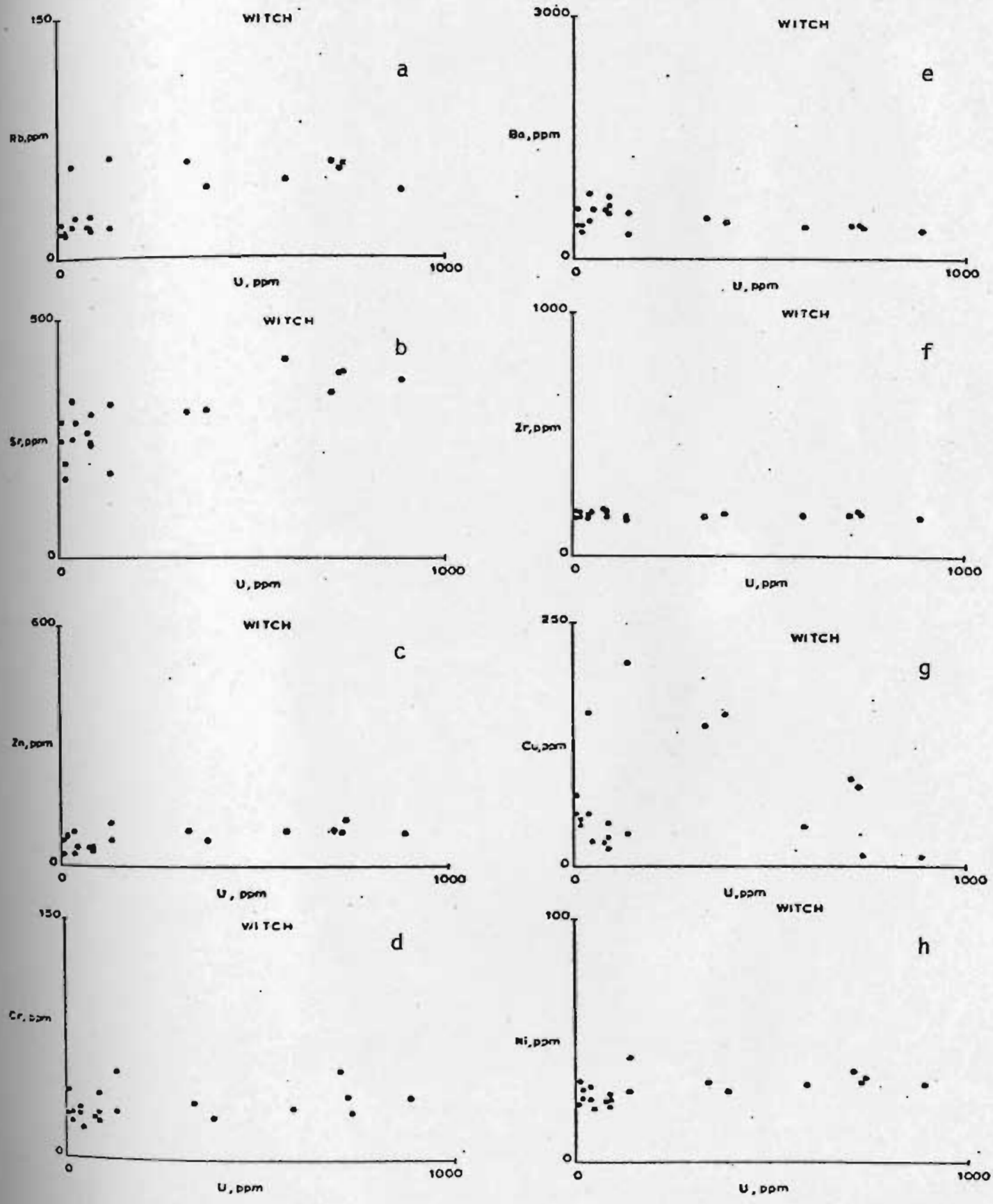

Figure 23. Plots of trace elements vs. U (see text).

PLATE XIV

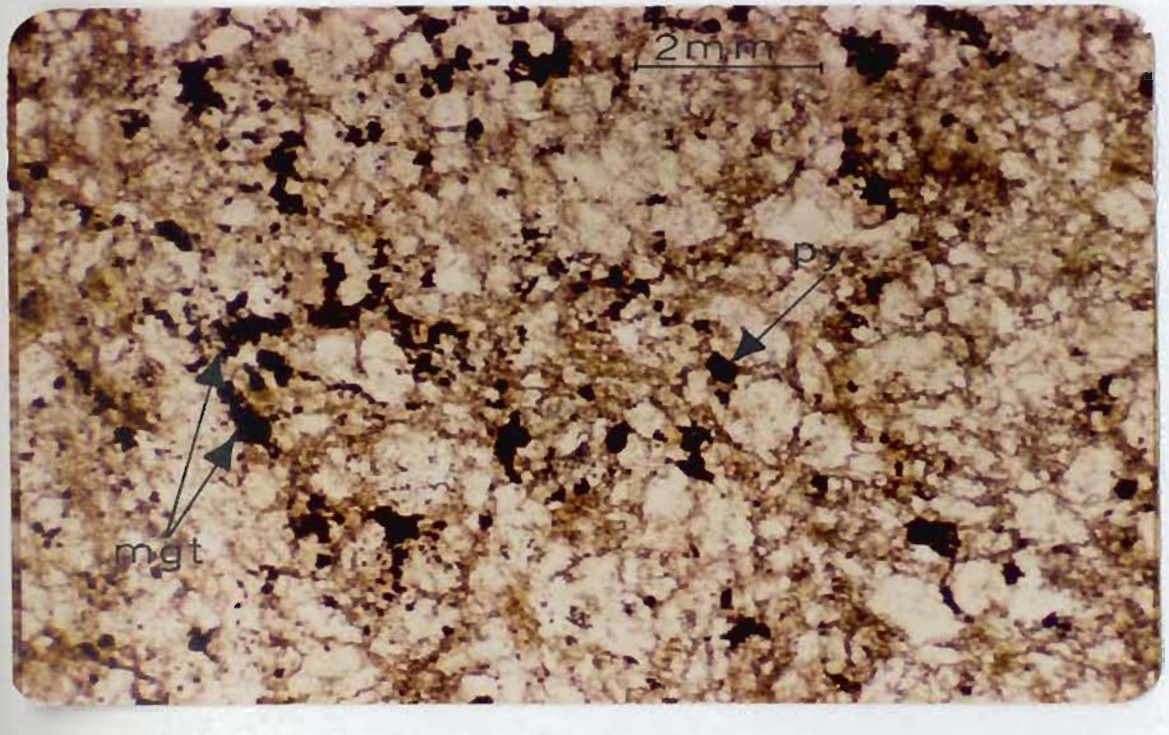

a

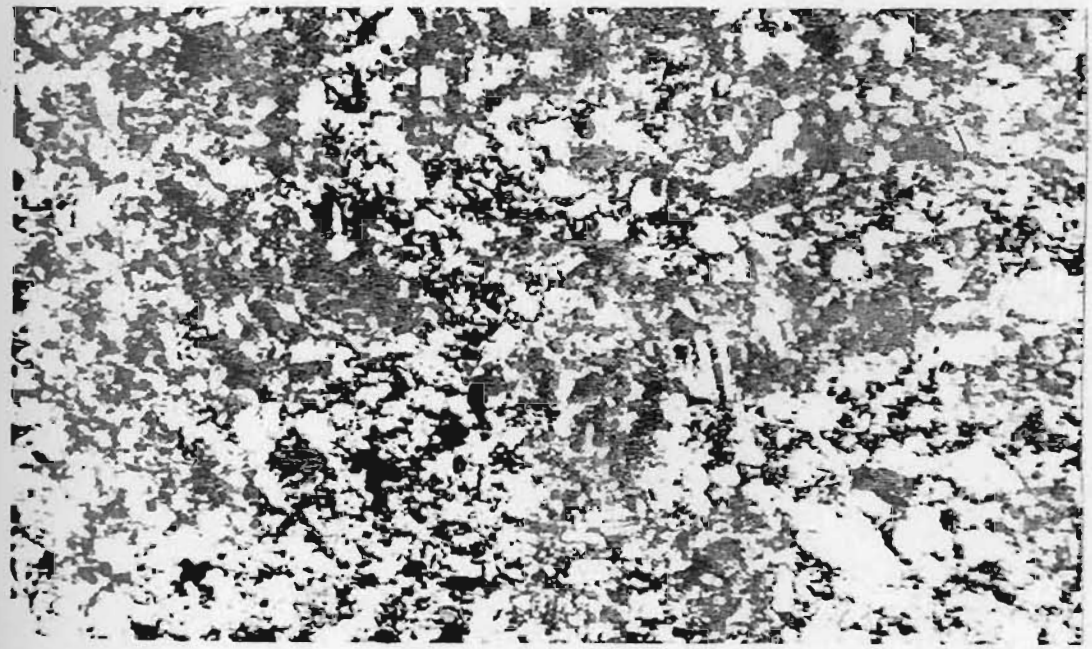

b

a. Plagioclase grains in a quartzofeldspathic groundmass with chlorite and opaques.

b. Same as (a) under crossed Nicols.

Witch Lake uranium deposit.

3.7 Nash Lake Uranium Deposit

A fine grained basic metavolcanic tuff hosts the uranium mineralization of the Nash Lake main zone. The zone is striking NE and dipping to the southeast and the uranium-bearing tuff grades northwards to a uranium-depleted amphibolite gneiss and southwards to a varicolored quartzite with slightly higher radioactivity. The radioactivity along the fractures is higher and this is due to a secondary coat of uranium minerals along the fractures.

Modal analysis of a low and a highly mineralized rock sample from this showing is indicated in Table XXIV. The strongly mineralized rocks are characterized in general by a high garnet (possibly andradite), hornblende and biotite content. The uranium possibly exists within the garnets as submicroscopic inclusions and/or adsorbed onto hematite which fills microfractures (Plate XV). Trace element concentrations and various statistical parameters for those rocks are given in Tables XXV-XXVII. Plots of Rb vs Sr (Fig. 24) range between Rb/Sr 0.02 and 1. The highly mineralized rock samples fall within the dacite field.

Compared to the average trace element concentrations of metasedimentary schists and quartzofeldspathic gneisses (Table VI), the Nash uranium bearing rock has a higher Zn, Cu, Cr content and lower Zr, Rb and Ba content. The higher hornblende and biotite content in the strongly mineralized rocks could account for the higher Rb, Cu and Ni content in these samples. No simple relations between the trace element and Sr exist (Fig. 25a-g). Plots of Rb, Sr, Zn, Cr, Ba and Zr vs U separated the samples of Nash in two groups; however, the relations between those elements are not simple (Fig. 26a-h).

TABLE XXIV

Modal analyses of rock samples from Nash uranium deposit; all values are expressed as volume percentages.

Sample Number	Low mineralized rock Nash SE (150 ppm U)	High mineralized rock Nash 24 (3500 ppm U)
Hornblende	53	17
Garnet (possibly andradite)	1	33
Opaques (magnetite + possibly other unidentified opaque minerals).	15	1
Quartz + feldspars (mostly plagiocalses, An_{60}-An_{68} Labradorite).	26	34
Others (sphene, epidote, biotite, chlorite)	3	13

TABLE XXV

NASH URANIUM DEPOSIT

(values in ppm)

Sample No.	Zr	Sr	Rb	Zn	Cu	Ba	Ni	Cr	Hg	U	Radioactivity C/S
WE 1	94	395	76	225	72	97	98	133	1.7	2160	220
2	193	581	11	357	5	106	90	298		1600	60
3	147	723	26	128	171	145	77	113		1700	80
4	115	308	7	157	14	95	57	127		110	70
5	101	294	10	312	32	122	83	312	.8	150	60
6	99	292	31	202	.6	265	82	301		800	60
7	109	382	30	216	12	251	87	283		300	60
R8N	69	293	93	118	18	103	106	291		20	40
N9C	92	325	10	152	21	100	64	120			50
10	77	245	13	245	12	43	64	148	.7	280	150
11	41	155	33	399	23	131	98	195		1650	250
12	72	282	110	184	169	193	94	365		3000	120
12'	80	300	100	190	170	193	90	365		2950	60
14	78	125	18	125	237	160	108	330		140	60
15	78	145	88	156	103	186	92	630		960	80
16											50
17	73	236	72	223	229	205	96	468		3000	130
18	73	420	69	207	170	105	114	227		3100	1000
19	59	189	151	198	206	319	117	611			100
20	79	181	53	158	15	155	84	559		400	70
21	56	301	85	200	390	140	119	450		3600	80
22	89	383	14	211	201	177	81	196		230	80
23	73	152	113	173	124	259	103	654		1300	130
24	90	290	132	223	171	227	181	461		3500	380

NASH URANIUM DEPOSIT (Page 2)

(values in ppm)

Sample No.	Zr	Sr	Rb	Zn	Cu	Ba	Ni	Cr	Hg	U	Radioactivity C/S
25	65	226	77	205	149	200	98	513		3400	120
26	72	308	114	178	266	184	121	373		4100	600
27	106	382	24	215	196	128	88	282		650	70
28	102	297	11	216	6	86	79	170			50
NE 29	171	574	7	270	37	101	76	243			60

TABLE XXVI

NASH URANIUM DEPOSIT

Correlation matrix calculation for 27 sets of data

Variable	Zr	Sr	Rb	Zn	Cu	Ba	Ni	Cr	U
Zr	1.000	0.856	-0.007	0.572	0.044	0.402	0.439	0.211	0.083
Sr		1.000	0.053	0.473	0.215	0.274	0.419	-0.004	0.271
Rb			1.000	0.144	0.503	0.570	0.735	0.705	0.734
Zn				1.000	0.088	0.406	0.586	0.322	0.324
Cu					1.000	0.385	0.556	0.420	0.669
Ba						1.000	0.697	0.749	0.407
Ni							1.000	0.666	0.640
Cr								1.000	0.438

TABLE XXVII

NASH URANIUM DEPOSIT

Element	Mean	STD	95% Confidence Interval for Mean
Zr	83	8	67 - 99
Sr	286	31	223 - 348
Rb	45	7	30 - 61
Zn	188	17	153 - 222
Cu	98	19	58 - 137
Ba	136	13	109 - 164
Ni	84	7	70 - 98
Cr	284	33	216 - 351
U	1246	260	726 - 1766

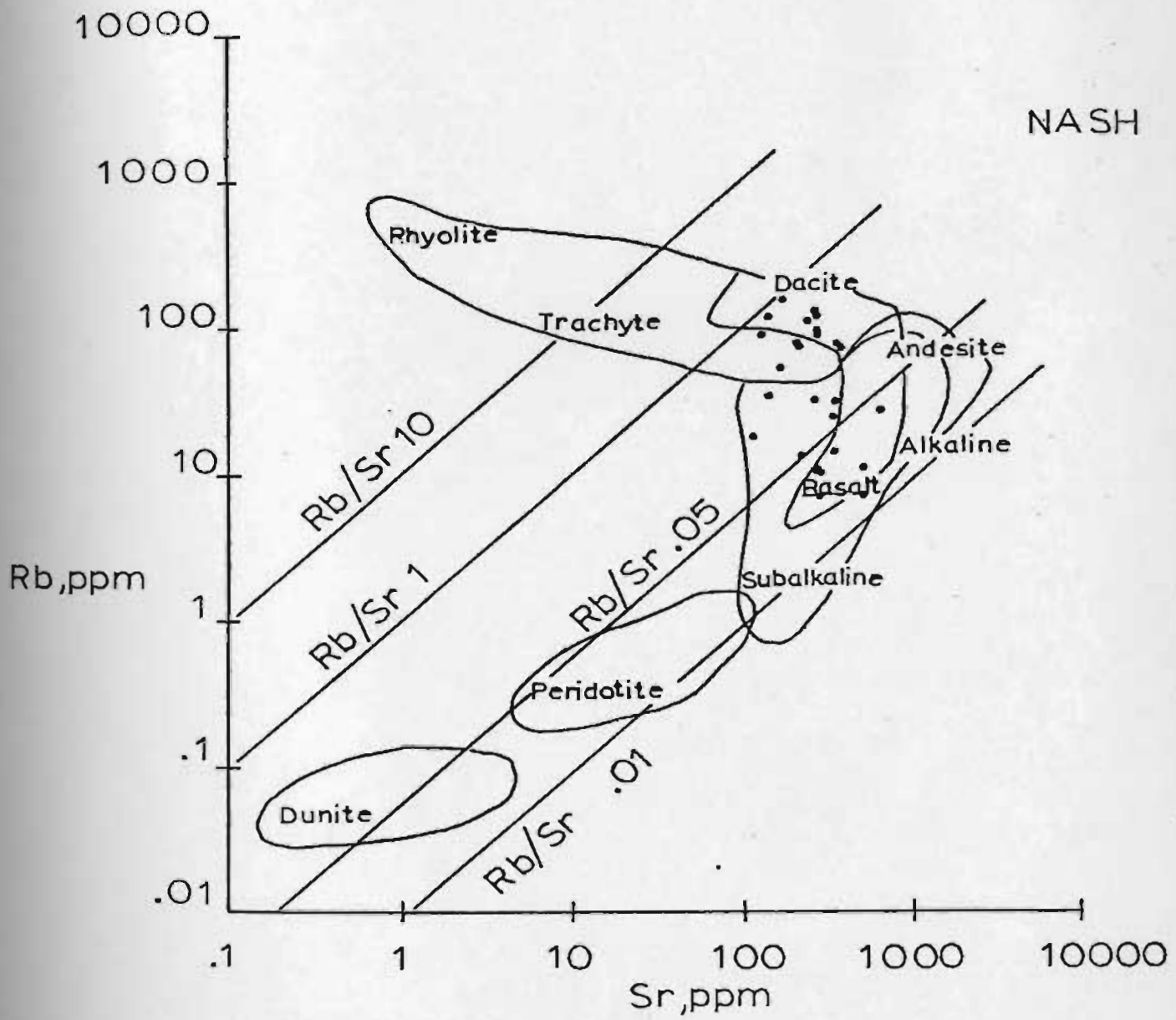

Figure 24. Plots of Rb vs. Sr for the Nash Lake uranium deposit.

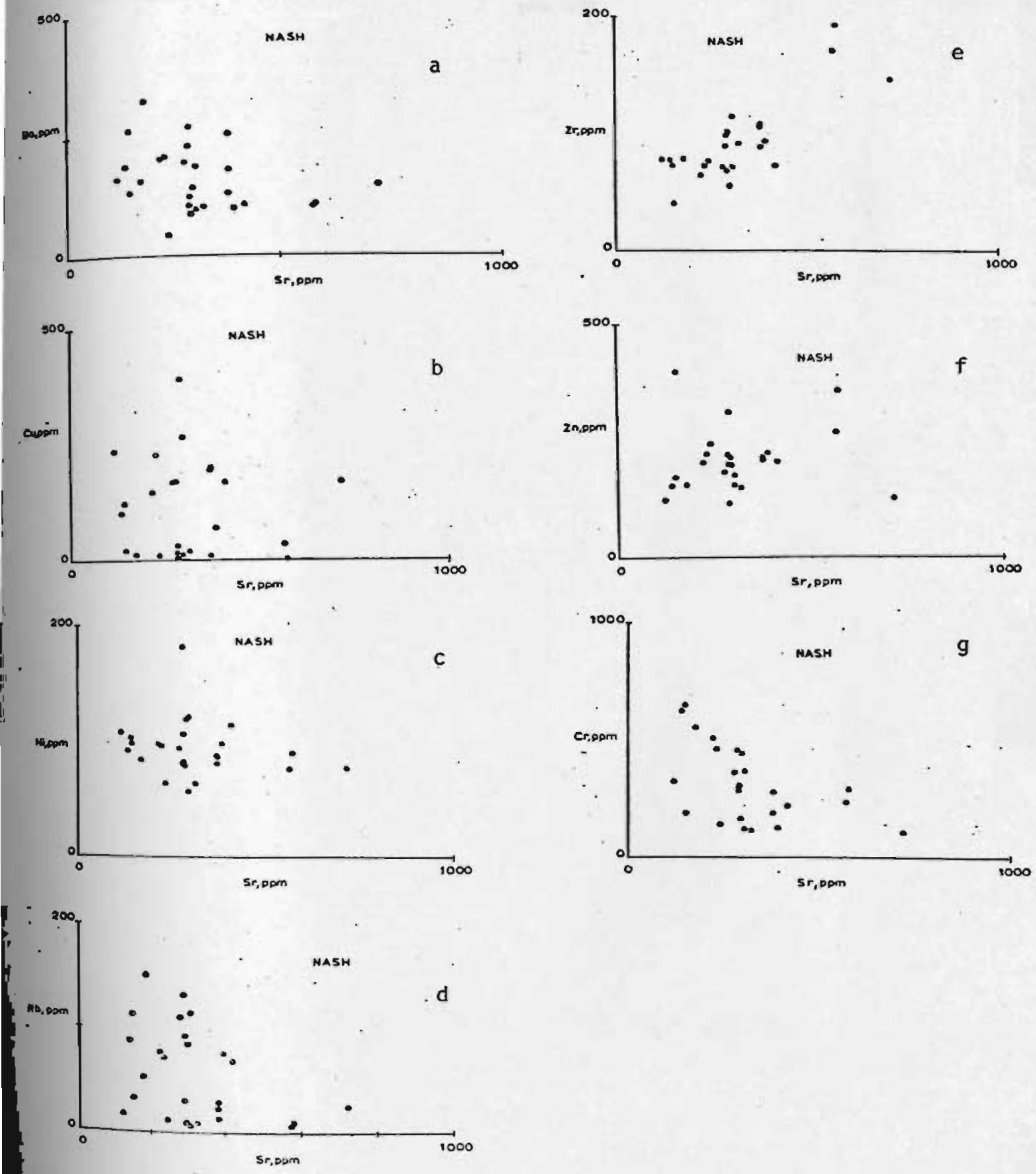

Figure 25. Plots of trace elements vs. Sr (see text).

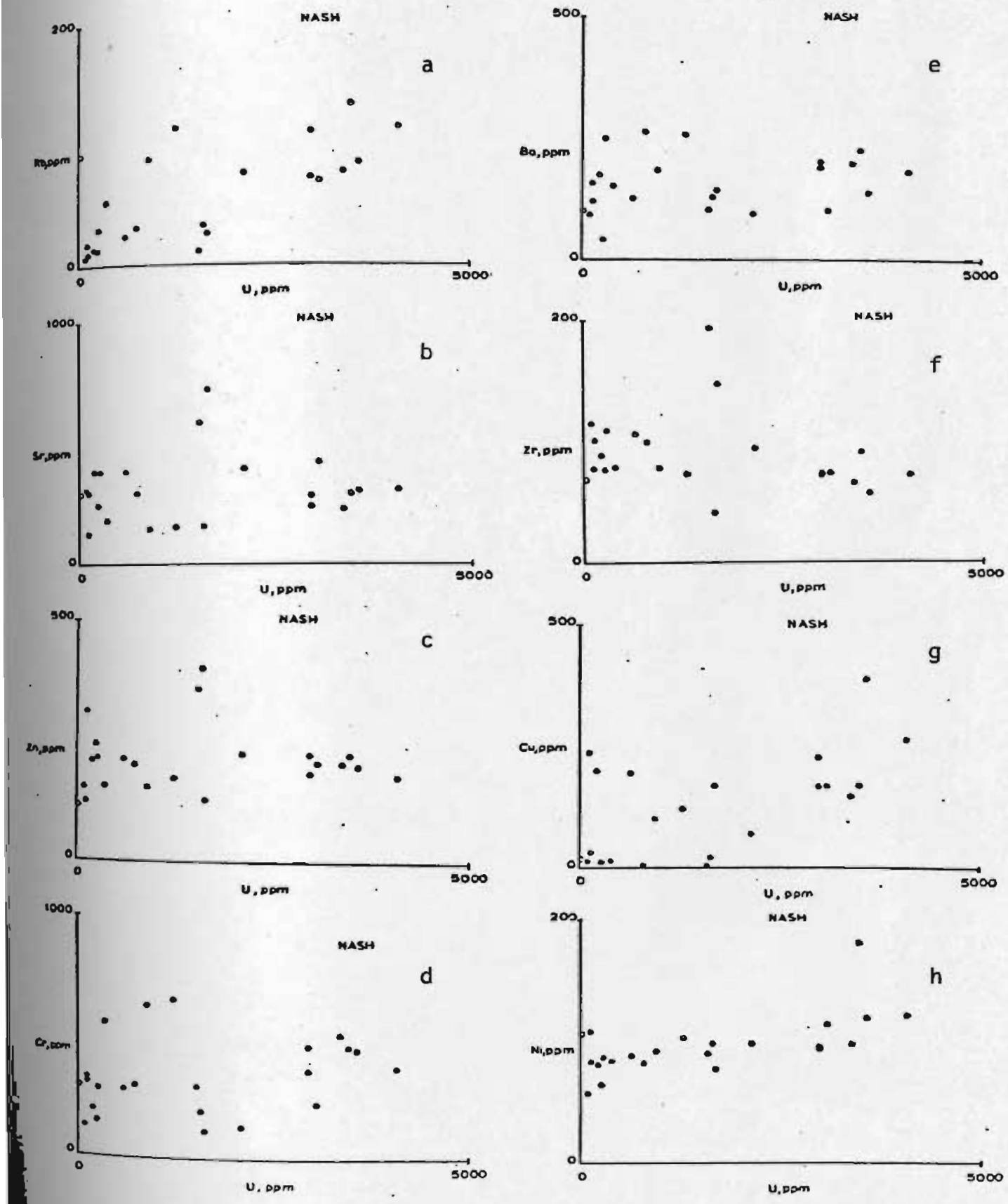

Figure 26. Plots of trace elements vs. U (see text).

PLATE XV

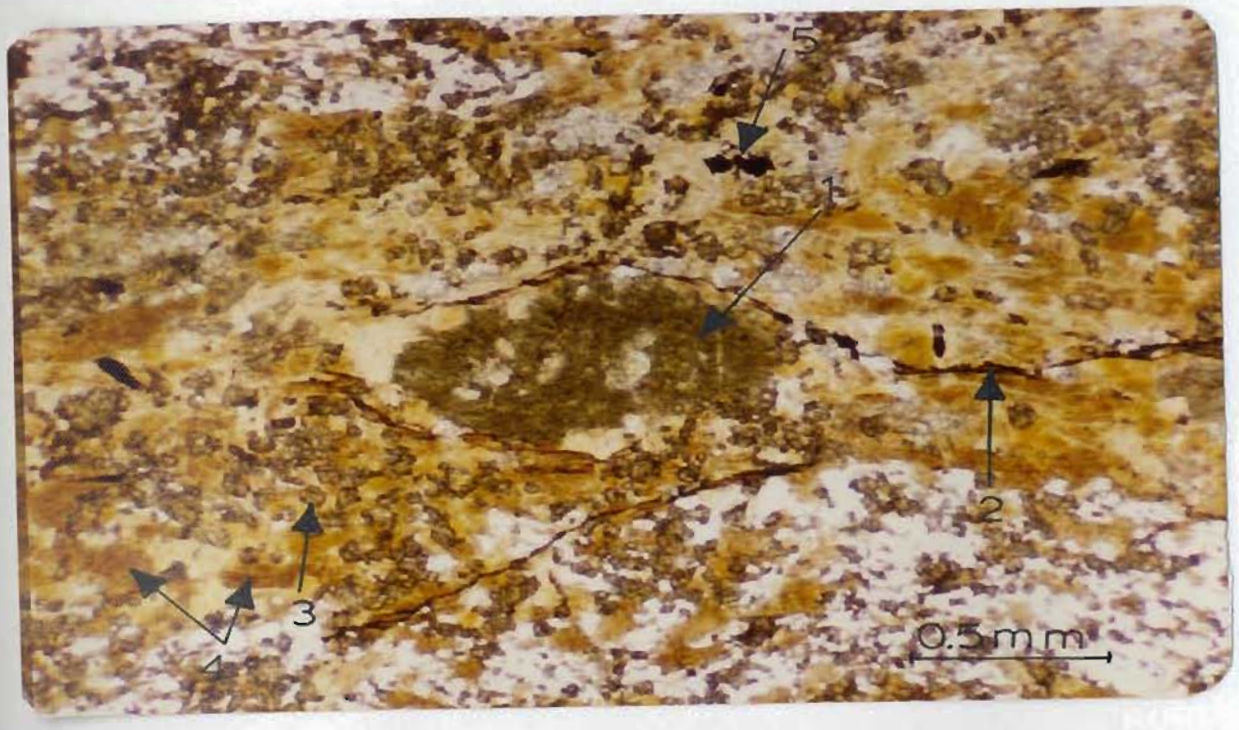

a

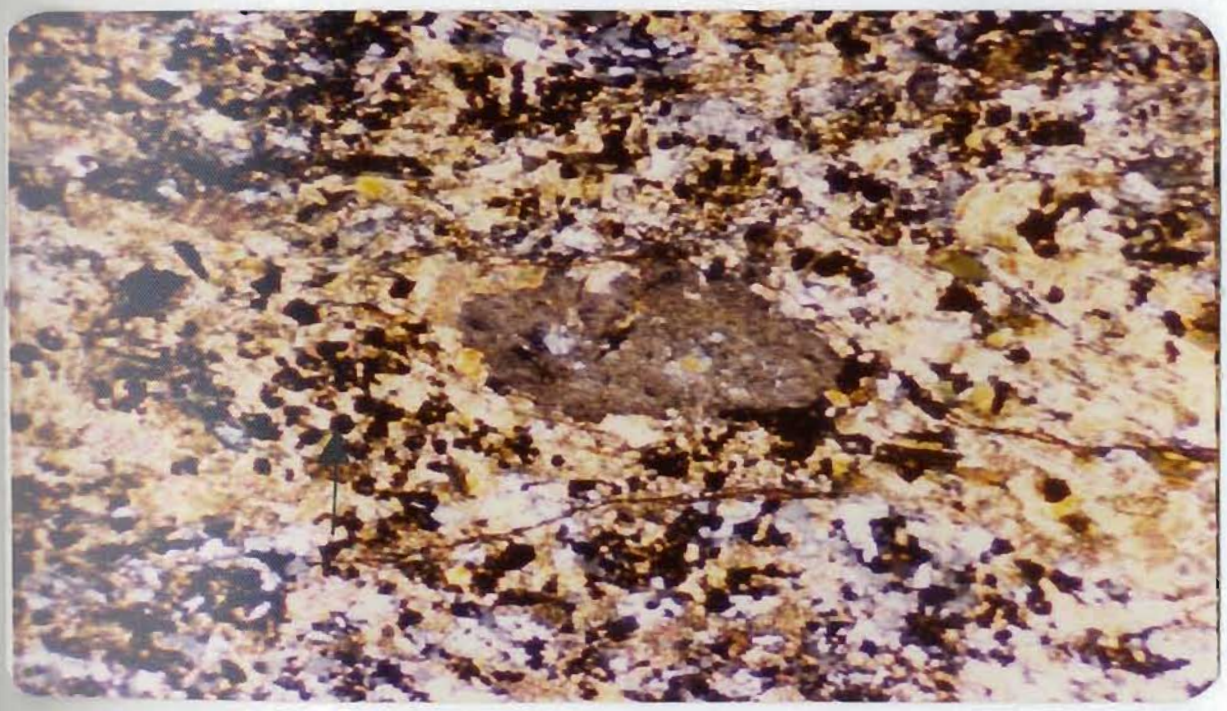

b

a. Arrow 1 shows a hornblende crystal partly altered to biotite (Arrow 4). Arrow 2 shows iron oxides within microfracture: Uranium may be accomodated here. 3, garnet (andradite); 5, magnetite.

b. Under crossed Nicols, Nash Lake uranium deposit.

3.8 Kitts Pond and Long Island Uranium Deposits

The Kitts Pond and Long Island uranium showings represent "black shale" type uranium deposits like the uranium deposits in the Upper Cambrian alum shale of Sweden (Svenke, 1956), the Devonian and Mississippian Chattanooga shale of Tennessee (Swanson, 1953), and the shale in the Pennsylvanian Hartville Formation in Wyoming (Duncan, 1953). Thus it is useful to present here some general information on the "black shale" type of uranium deposits for comparison with data from these two showings.

The uraniferous black shales are mainly of the sapropelic, rather than the humic variety, rich in sulfides, distillable hydrocarbons, and finely comminuted carbonaceous matter, and generally unfossiliferous except for species of plankton and nekton (Mckelvey et al., 1955). To the knowledge of the writer the mineral occuring in the black shales has not been established definitely. It is believed that the uranium in Kitts and Long Island showings is mainly in lenses of dark bituminous material and not in the form of pitchblende; however, more detailed studies are necessary to confirm this statement.

Whitehead (1952) reports that in the Micocene nodular shale of California and the Pensylvanian Cherokee shale in Oklahoma the net beta count increases with increasing phosphorus and carbon content (between which there is also a direct relation). Alpha-track studies of thin sections of these shales and of the Woodford shale show that the ratio of the number of alpha particles originating in inorganic material to these originating in organic material is 2.4 to 1. These studies therefore

suggest that uranium may be held both in phosphate and organic matter.

The largest amounts of uranium (as much as 0.5 per cent) in the alum shale of Sweden are in lenses of dark bitumen called "kolm". Because many forms of so-called amorphous carbon are graphitic in character, Fredrickson(1948) thinks it possible that the $(U^{+6}O_2)^{+2}$ ion "is adsorbed between the graphitic layers of carbonaceous material, forming a strong structure due to the stable UO_2^{++} ion holding the two lavers together".

Uranium in Kitts and Long Island showings is associated with pyrite and although no systematic relations were found between the uranium and the pyrite content in these showings, it has been suggested that in black shales the uranium content generally increases with the pyrite content but the pyrite itself contains little uranium (Mckelvey et al., 1955). Autoradiograph studies (Bates et al., 1954), however, show that much of the uranium in the Chattanooga Shale is in organic matter- pyrite assemblages.

There is an agreement for the syngenetic deposition of uranium in the black shales and that the bulk of the uranium was derived directly or indirectly from sea water, which contains 1.0 - 1.8 x 10^6 grams of uranium per liter. The question might be raised, however, as to whether the uranium has been locally derived or brought to the site of deposition through oceanic circulation. Strøm (1948) ahs postulated that the uranium is derived from adjacent granitic terraines, presumably during periods when chemical weathering is the dominant process of erosion. This is a reasonable assumption if the basins of deposition are restricted embayments, such as the Norwegian fiords on which Strøm's observations

were based. Probably restricted embayments or stagnant water conditions favored the formation of the Kitts and Long Island uranium showings.

Kitts Pond Uranium Deposit

The rock which hosts the uranium mineralization in Kitts uranium deposit is a pyrite-bearing graphitic argillite (black shale) and high radioactivity is in dark bituminous lenses. In hand specimen these lenses are confined to the schistosity planes along with visible pyrite aggregates.

Samples from an intrusive gabbro (hornblendite) approximately 10 cm away from the contact with the shale gave 40 ppm U; the high uranium content of hornblendite suggests that a migration of uranium has taken place from the argillite toward the gabbro during the intrusion of the latter.

A modal analysis of a representative rock sample from Kitts Pond deposit is given in Table XXVIII.

Trace element concentrations and various statistical parameters for these rocks are given in Tables XXIX-XXXI. Plots of Rb vs Sr (Fig. 27) range between Rb/Sr 0.06 and 6; however the full range of these plots does not indicate an original source of specific composition.

Average trace element values of the Kitts uranium deposit are listed in Table VI. It must be emphasized that the average uranium content of the mineralized rock is much higher since lenses of dark bitumen occur along the schistosity planes of the shale. However a

radioactive shale with an average uranium content ranging from 150 to 360 ppm (see also Long Island showing), with Rb/Sr ranging between 0.06 and 6 appears to be a stratigraphic horizon which should be investigated in detail for locating larger uranium concentrations.

Patterns of trace element distribution can be seen in Figs. 28-29; however no simple relations exist between the different trace elements.

Long Island Uranium Deposit

A pyrite-bearing graphitic argillite (black shale) host also the uranium mineralization in the Long Island showing. The formation grades to a paragneiss mainly phyllite and biotite quartz felsite.

The mineralogical assemblage of Long Island shale is similar to that of Kitts, except that the Kitts has a higher content of bituminous lenses and lower pyrite content than the Long Island.

Trace element concentrations and various statistical parameters for those rocks are given in Tables XXXII-XXXIV. Plots of Rb vs Sr (Fig. 30) range between Rb/Sr 0.07 and 6; however, the full range of these plots does not indicate an original source of specific composition.

Average trace element values for the Long Island showing are given in Table VI. As can be seen, the trace element concentrations for the Kitts and Long Island shale are similar, however, the uranium content in Kitts is higher and the Zn content lower than those in Long Island showing. This difference might be explicable by the higher content of radioactive bituminous lenses in Kitts Pond shale and lower

pyrite content in Long Island shale where uranium and Zn are expected to occur in the bituminous lenses and the pyrite respectively.

Trace element patterns are shown in Figs. 31-32, however no simple relations exist between the different trace elements, as would be expected from shales

TABLE XXVIII

Modal analysis of rock sample from Kitts Deposit; all values are expressed as volume percentages.

Sample Number	Kitts 113, Zone C
Hornblende	16
Graphite	44
Quartz	36
Opaques (mostly pyrite, plus other possibly primary unidentified radioactive minerals)	4

TABLE XXIX

KITTS POND URANIUM DEPOSIT

(values in ppm)

Sample No.	Zr	Sr	Rb	Zn	Cu	Ba	Ni	Cr	U	Radioactivity C/S
1. K111 ZC	84	147	32	130	97	199	62	89	100	
2. K113 ZC	176	351	54	122	163	222	90	100	300	60
3. KT3 109	95	172	12	97	245	38	52	74		
4. K101	194	206	49	71	3	432	19	14	420	
5. KZA 107	128	32	107	127	136	267	26	113	100	
6. K103	91	99	121	75	431	514	34	103	1500	
7. K106 ZA	75	55	50	102	357	135	61	85	70	
8. KT7 ZC	66	98	49	244	104	381	72	79	75	40
9. K110 ZA	98	82	36	95	482	230	60	106		
10. K99	20	18	7	128	1	48	212	696	40	
11. K108 ZA	105	75	127	332	198	369	62	140	500	350
12. K102 ZA	114	130	65	267	244	337	6	2104	100	
12' "	120	130	70	270	250	340	60	100	120	

TABLE XXX

KITTS POND URANIUM DEPOSIT

Correlation matrix calculation for 12 sets of data

Variable	Zr	Sr	Rb	Zn	Cu	Ba	Ni	Cr	U
Zr	1.000	0.708	0.261	-0.150	-0.109	0.403	-0.597	-0.613	0.158
Sr		1.000	-0.170	-0.173	-0.150	0.073	-0.192	-0.410	0.070
Rb			1.000	0.360	0.260	0.713	-0.488	-0.322	0.655
Zn				1.000	-0.156	0.246	0.086	0.008	-0.129
Cu					1.000	0.108	-0.343	-0.341	0.304
Ba						1.000	-0.547	-0.457	0.693
Ni							1.000	0.930	-0.291
Cr								1.000	-0.151

TABLE XXXI

KITTS URANIUM DEPOSIT

Element	Mean	STD	95% Confidence Interval for Mean
Zr	103	14	75 - 132
Sr	122	27	67 - 176
Rb	59	12	35 - 83
Zn	149	25	98 - 199
Cu	205	46	111 - 298
Ba	264	44	174 - 353
Ni	67	14	37 - 97
Cr	141	53	35 - 248
U	267	127	13 - 521

TABLE XXXIII

LONG ISLAND URANIUM DEPOSIT

Correlation matrix calculation for 13 sets of data

Variable	Zr	Sr	Rb	Zn	Cu	Ba	Ni	Cr	U
Zr	1.000	0.747	0.847	-0.041	-0.334	0.809	0.382	0.611	-0.048
Sr		1.000	0.508	0.108	0.278	0.669	0.213	0.842	0.153
Rb			1.000	-0.334	-0.283	0.684	0.475	0.488	-0.173
Zn				1.000	-0.287	-0.298	-0.450	0.254	-0.037
Cu					1.000	-0.284	0.342	-0.362	0.036
Ba						1.000	0.650	0.514	-0.067
Ni							1.000	0.236	-0.224
Cr								1.000	0.134

TABLE XXXII

LONG ISLAND URANIUM DEPOSIT

(values in ppm)

Sample No.	Zr	Sr	Rb	Zn	Cu	Ba	Ni	Cr	U	Radioactivity C/S
1	52	52	58	154	231	199	75	26	100	60
2	59	115	21	1116	192	109	61	110	160	
3	53	130	19	179	380	70	51	56	310	55
4	104	226	118	171	142	684	81	123	100	50
5	62	156	30	556	192	227	61	102	100	50
6	97	169	79	297	148	653	86	99	240	60
7	57	53	47	74	663	256	99	55	140	50
8	56	133	31	447	159	272	69	142	250	70
9	97	126	117	481	161	243	66	114	100	60
10	53	35	62	141	245	230	72	51	70	60
11	96	267	136	175	205	525	90	208	220	60
12	69	171	50	305	218	417	84	130	50	60
13	54	29	58	129	81	224	67	65	200	50
13'	60	15	45	100	75	200	60	60	230	

TABLE XXXIV

LONG ISLAND URANIUM DEPOSIT

Element	Mean	STD	95% Confidence Interval for Mean
Zr	69	5	58 - 81
Sr	127	21	85 - 169
Rb	63	11	41 - 85
Zn	325	81	162 - 487
Cu	232	42	147 - 317
Ba	316	56	203 - 428
Ni	74	3	66 - 81
Cr	98	14	70 - 126
U	156	23	110 - 203

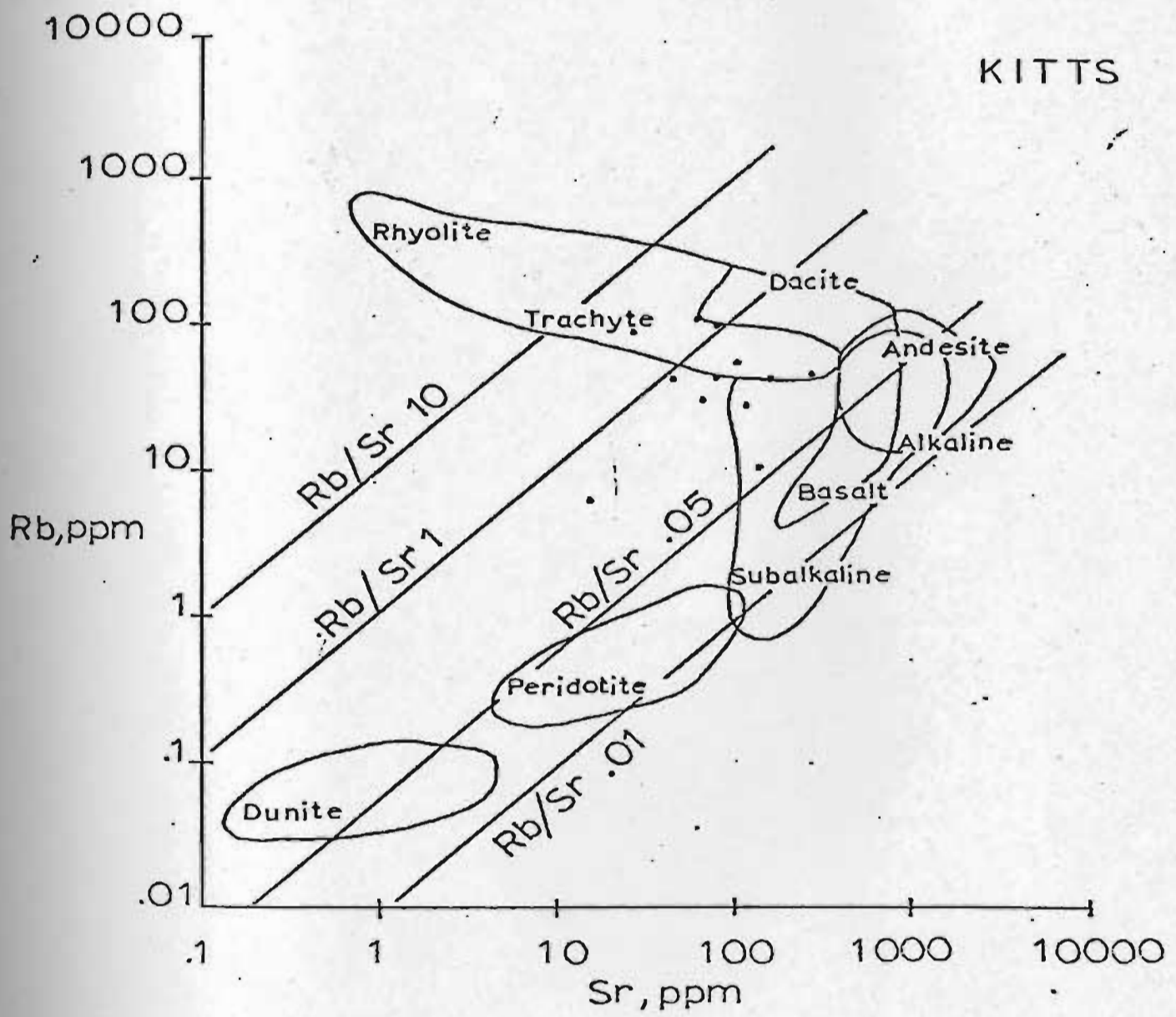

Figure 27. Plots of Rb vs Sr for the Kitts uranium deposit.

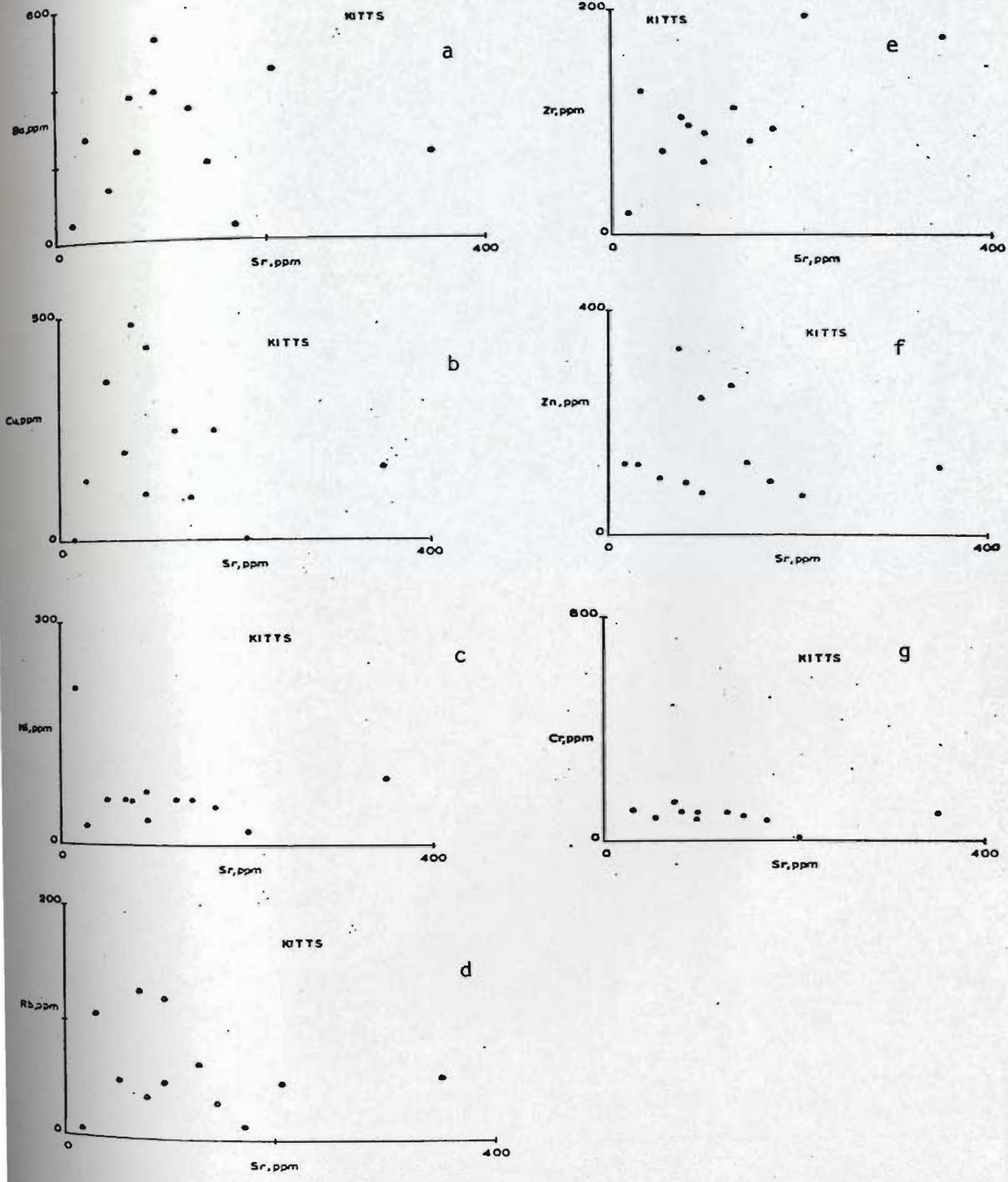

Figure 28. Plots of trace elements vs. Sr.

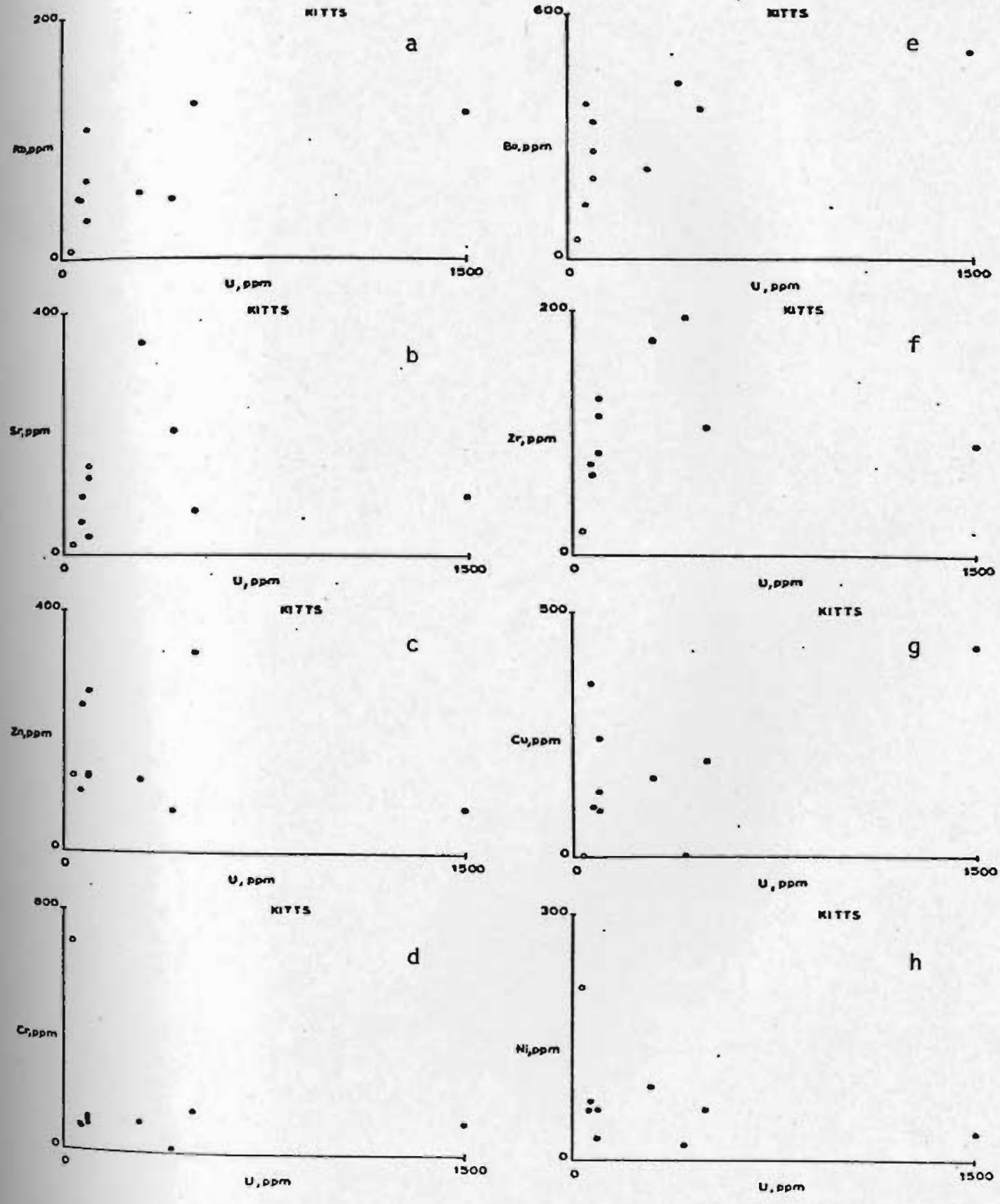

Figure 29. Plots of trace elements vs. U.

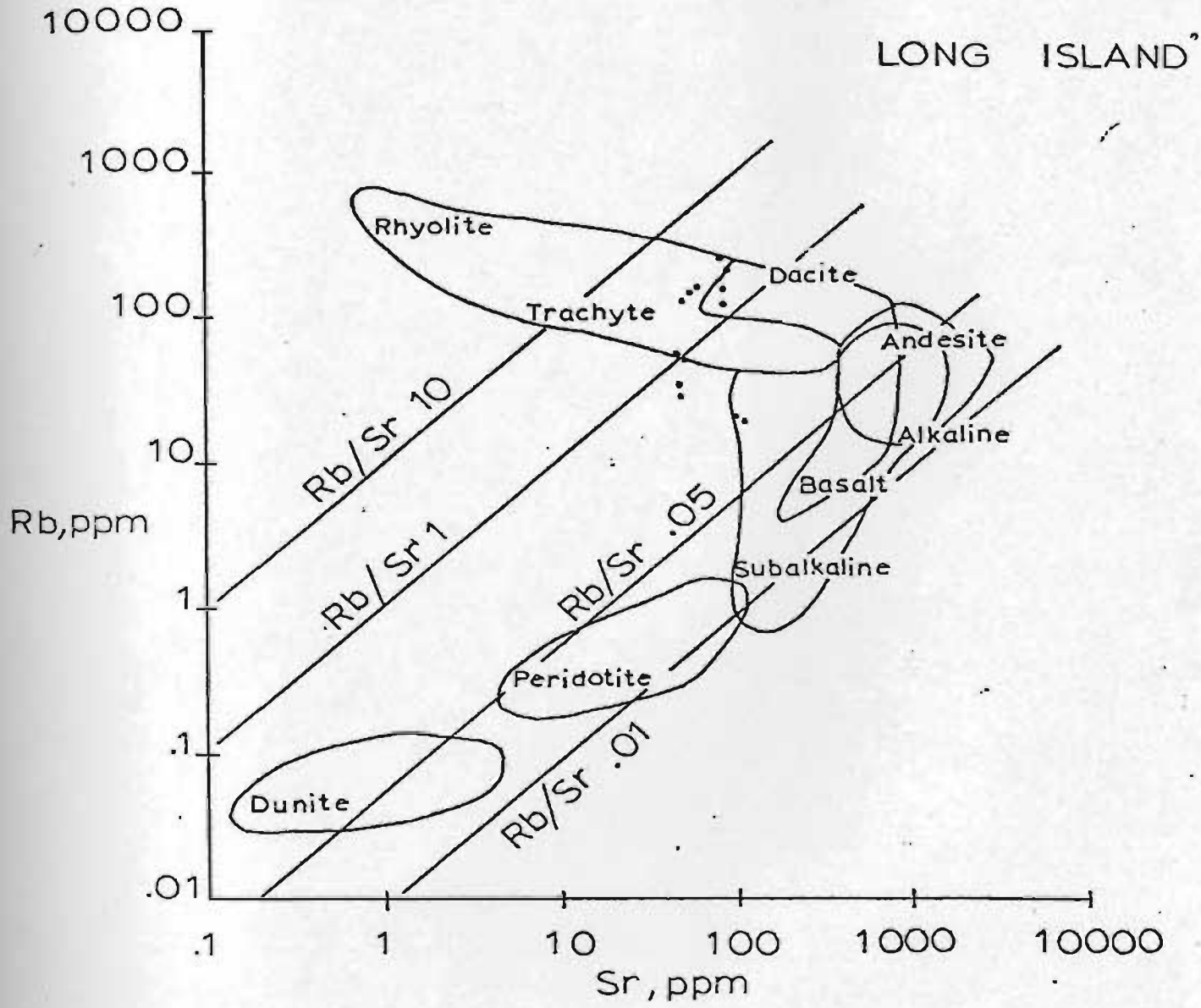

Figure 30. Plot of Rb vs Sr for the Long Island uranium deposit.

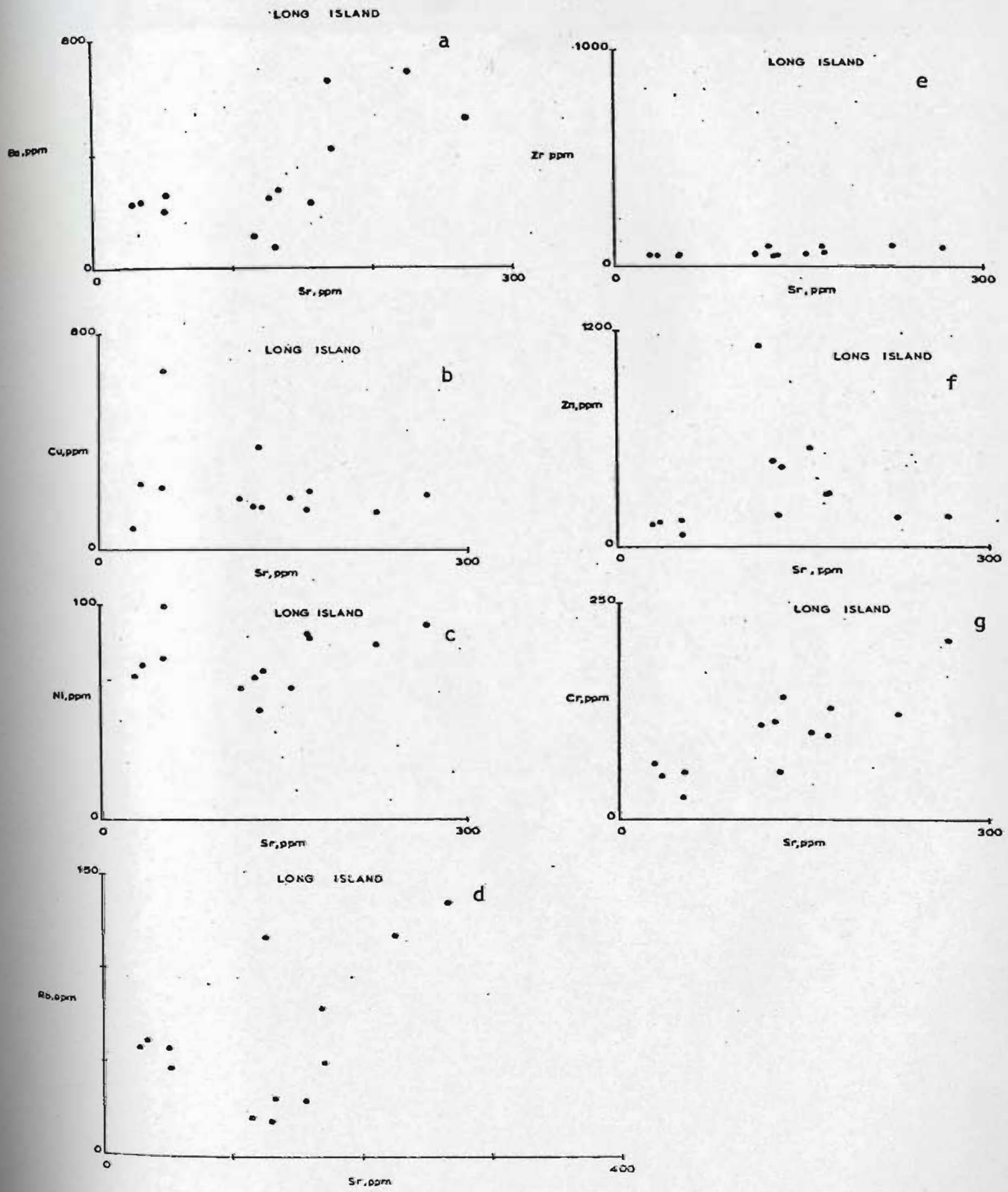

Figure 31. Plots of trace elements vs. Sr.

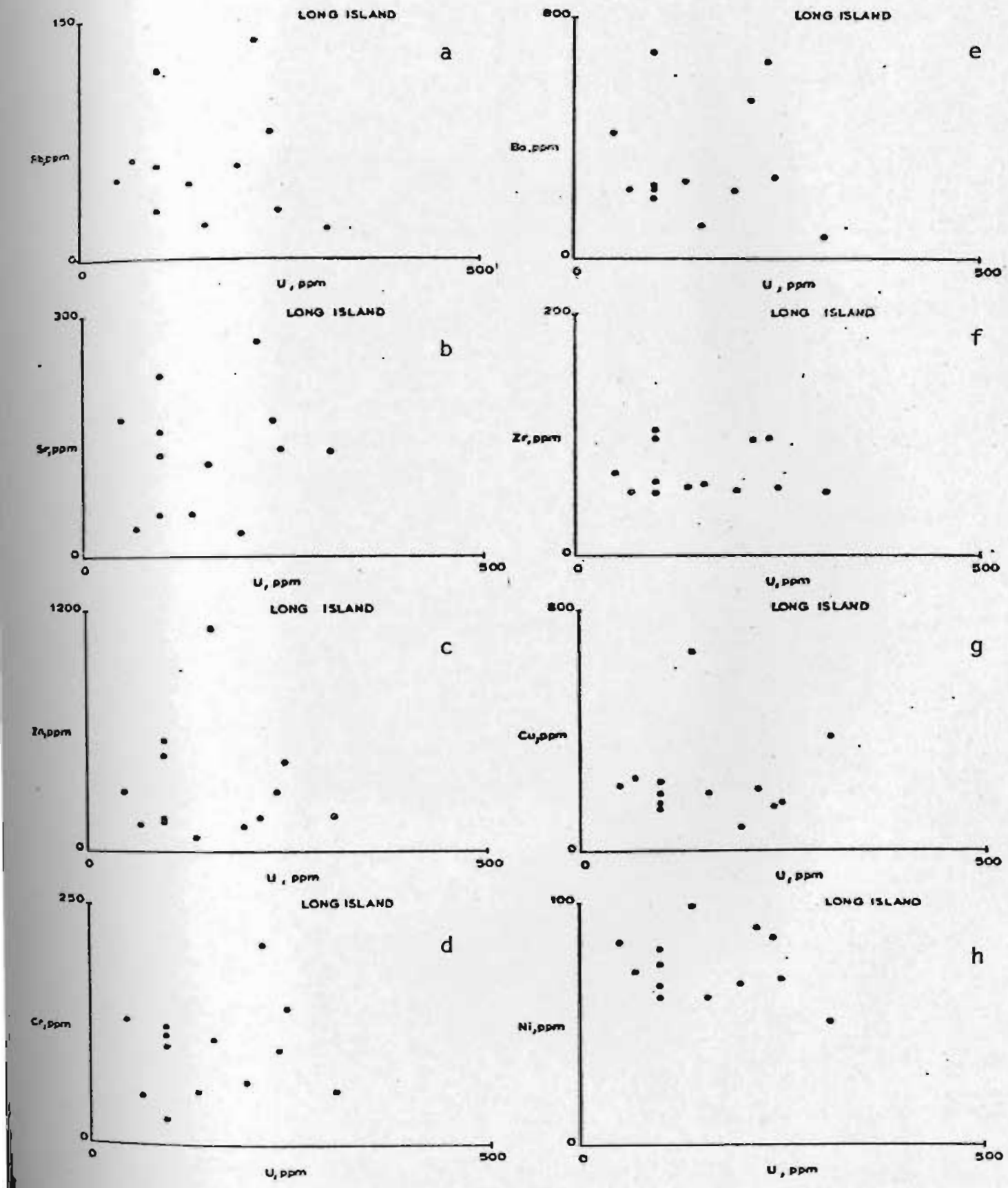

Figure 32. Plots of trace elements vs. U.

PLATE XVI

Uranium bearing argillite. The radioactivity in the dark areas is over 150 times the background.

Kitts uranium deposit.

3.9 Summary

Some trace element patterns for the showings under investigation have been summarized in Figs. 33-45. Diagrams marked by N are referred to the uranium showings located in the Kaipokok volcanic belt an diagrams marked by S to the uranium showings in the Walker Lake-White Bear Mountain area.

Among these the Michelin and M. Ben have similar Rb/Sr spreading, positive correlation between U and Rb, features suggesting detrital nature, e.g. presence of round zircon crystals and the pattern Zr-Rb-Sr (Fig. 33), similar U-Zr-Rb patterns (Fig. 35) and therefore geochemically belong to the same group of clastic metasediments.

The Rainbow, Witch and Nash Lake deposits appear to be colcanogenic syngenetic uranium deposit while the Kitts and Long Island showing represent "black shale" type uranium deposits, with the uranium being mainly concentrated in dark bituminous lenses.

The McLean uranium deposit is located in a feldspathic quartzite; however, plots of Rb/Sr suggest a subvolcanic source for the host rock of this showing.

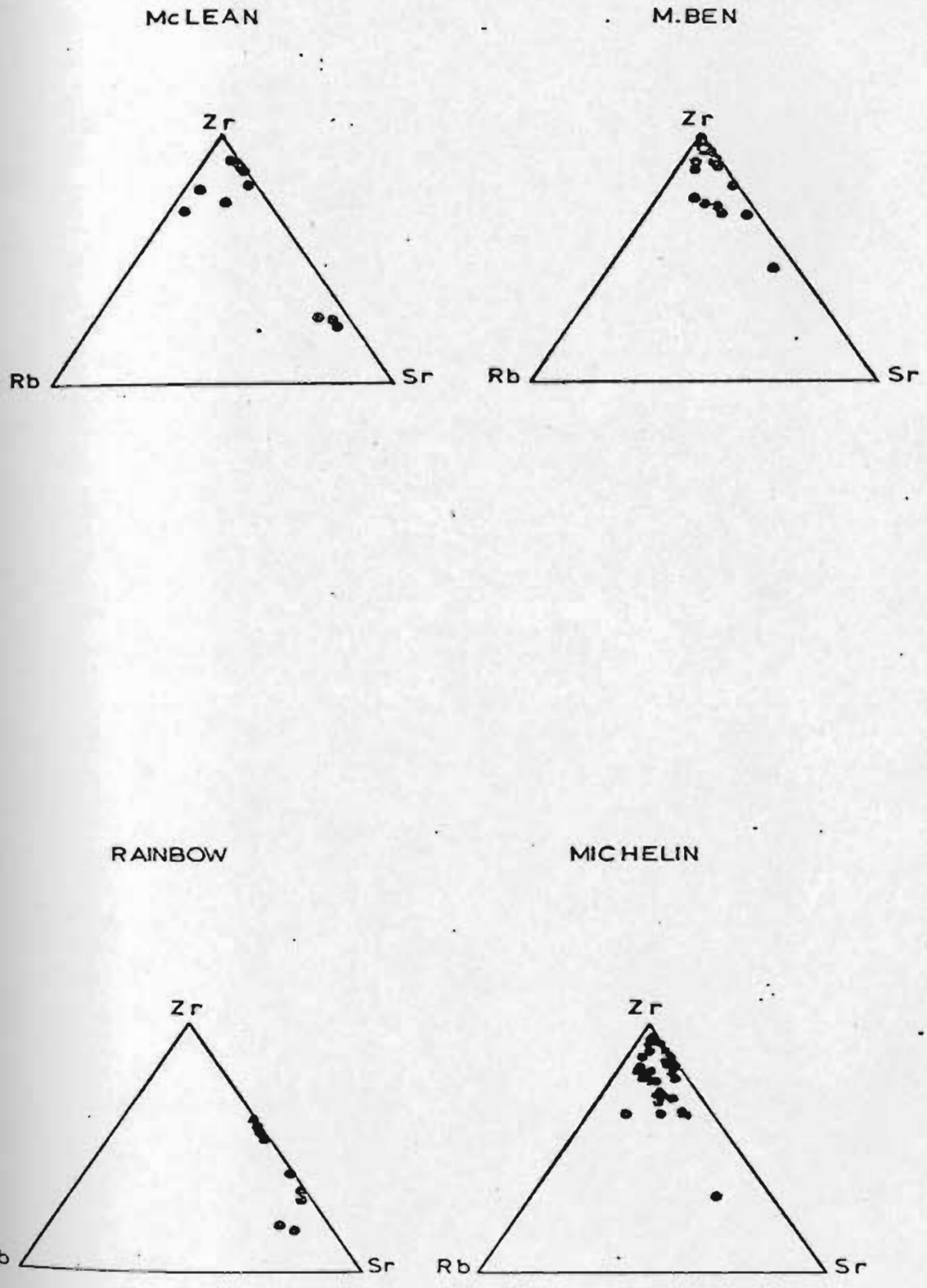

Figure 33. Ternary trace element diagrams of Zr-Rb-Sr of Michelin, Rainbow, McLean and M. Ben uranium deposits.

KITTS

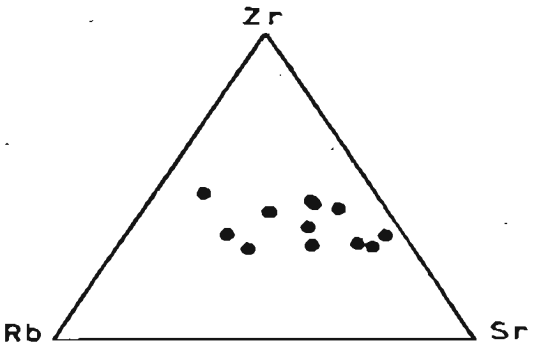

LONG ISLAND

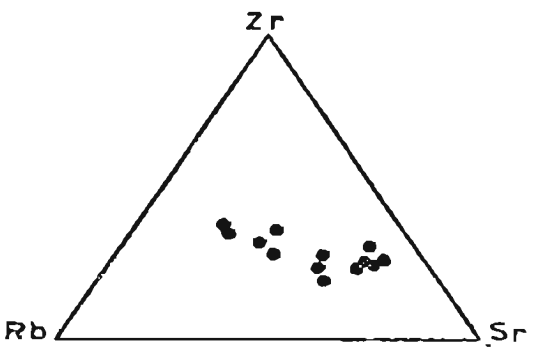

NASH

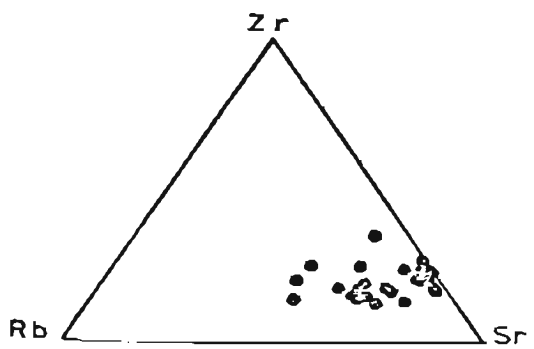

WITCH

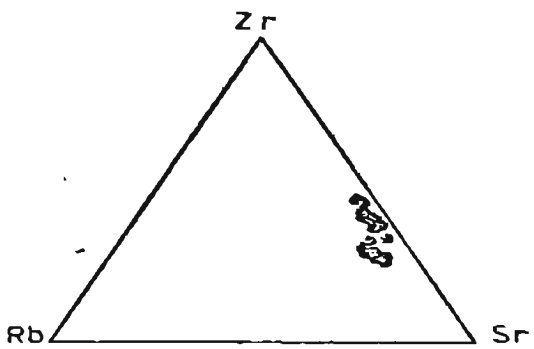

Figure 34. Ternary trace element diagrams of Zr-Rb-Sr of the Kitts, Long Island, Nash and Witch uranium deposits.

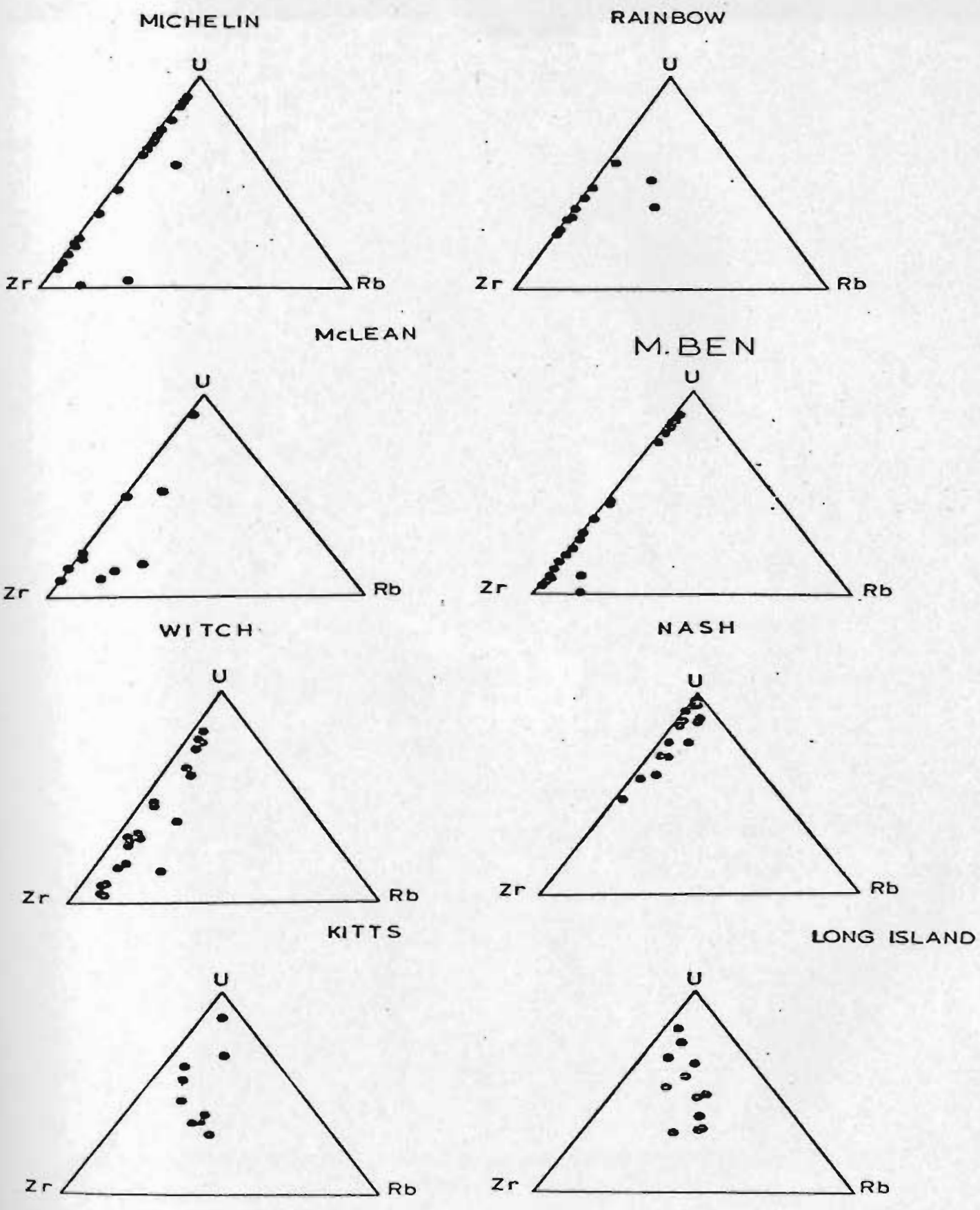

Figure 35. Ternary trace element diagrams of U-Zr-Rb of the examined uranium deposits.

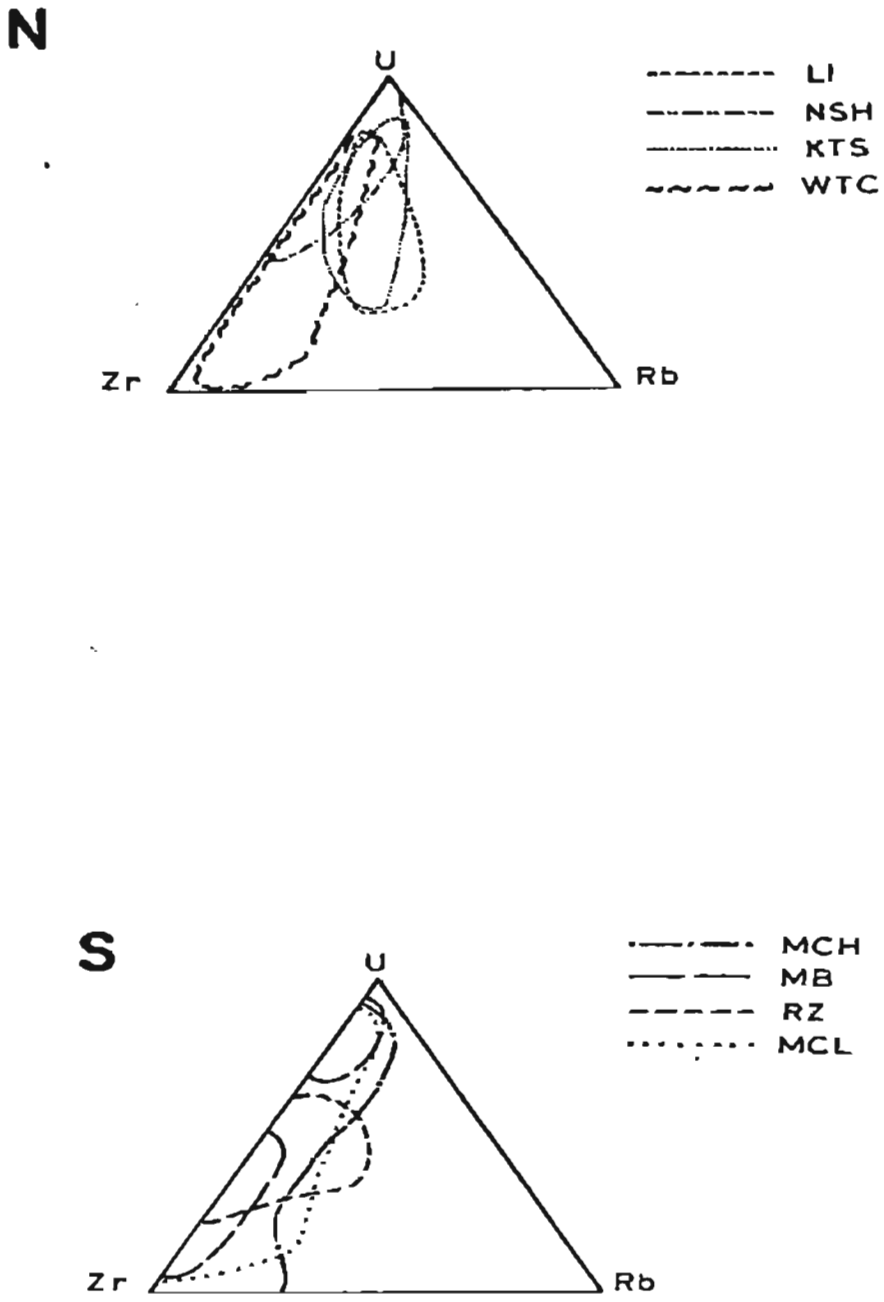

Figure 36. Summary of trace element patterns U-Zr-Rb of the examined uranium deposits.

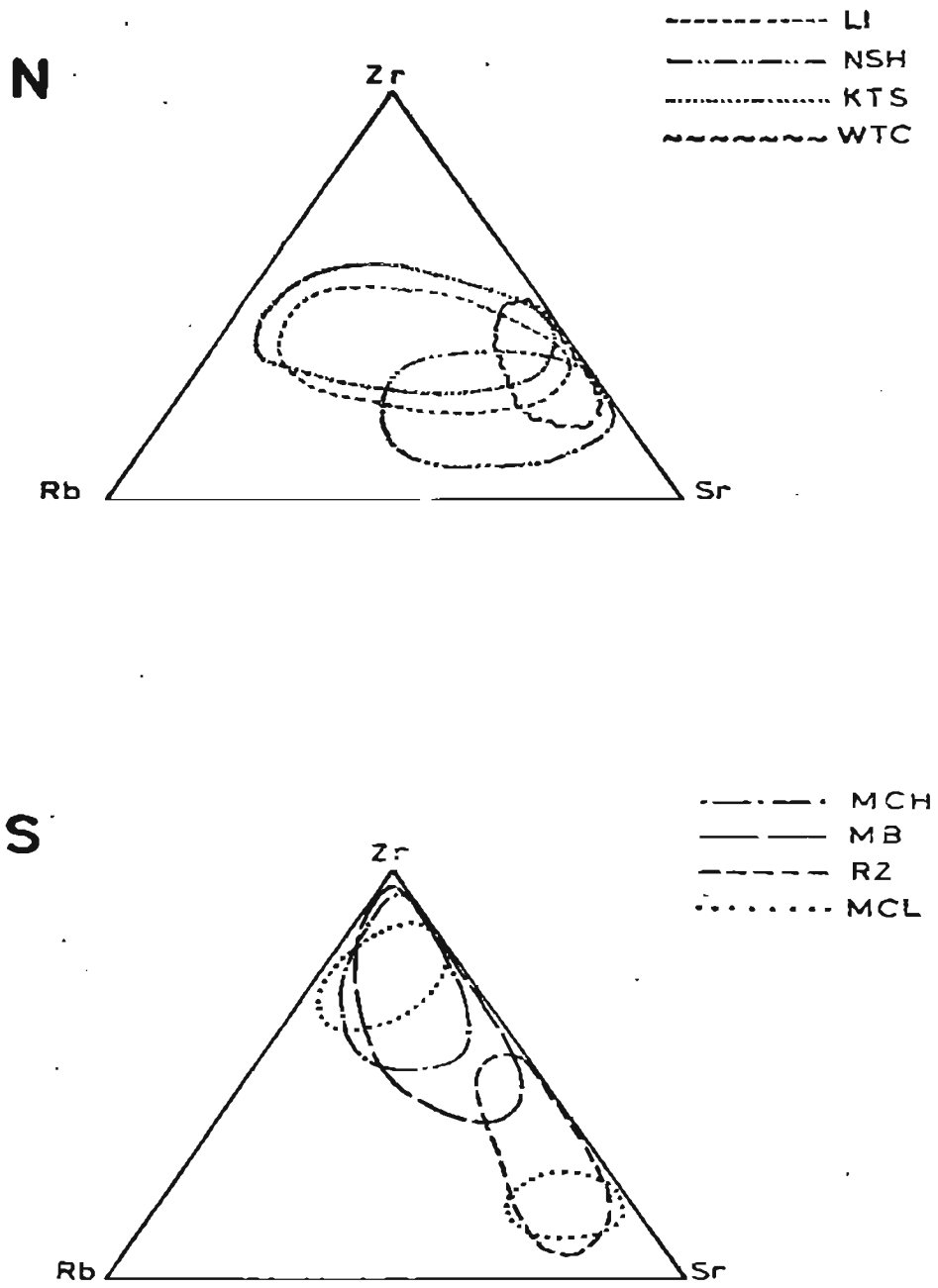

Figure 37. Summary of the trace element patterns Zr-Rb-Sr of the examined uranium deposits.

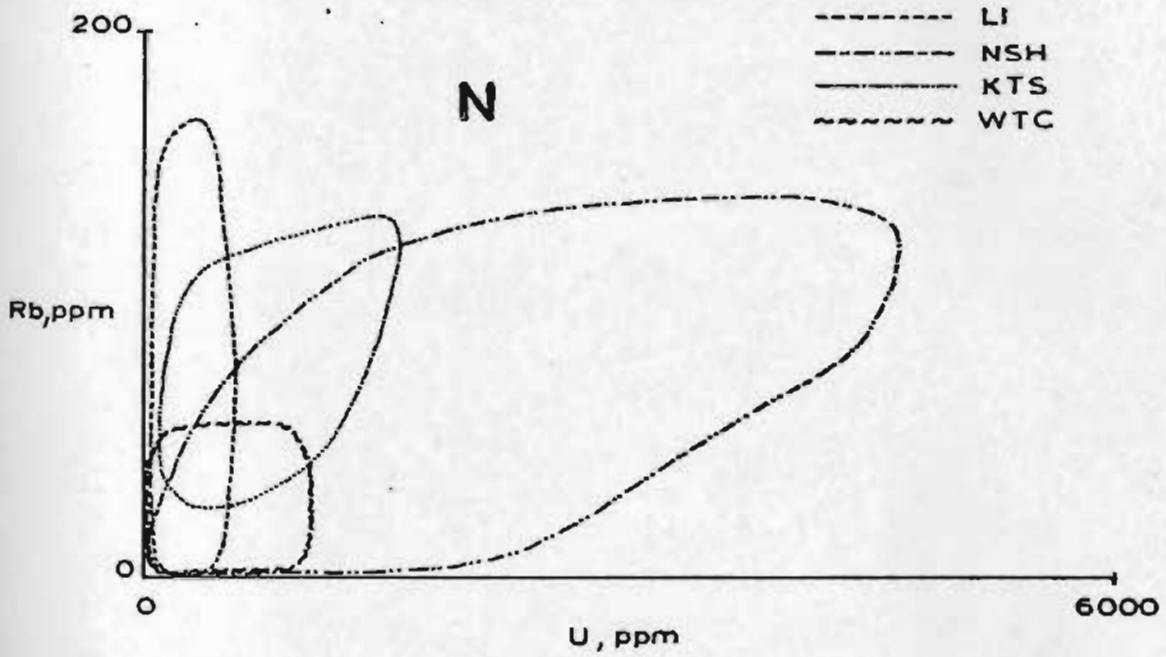

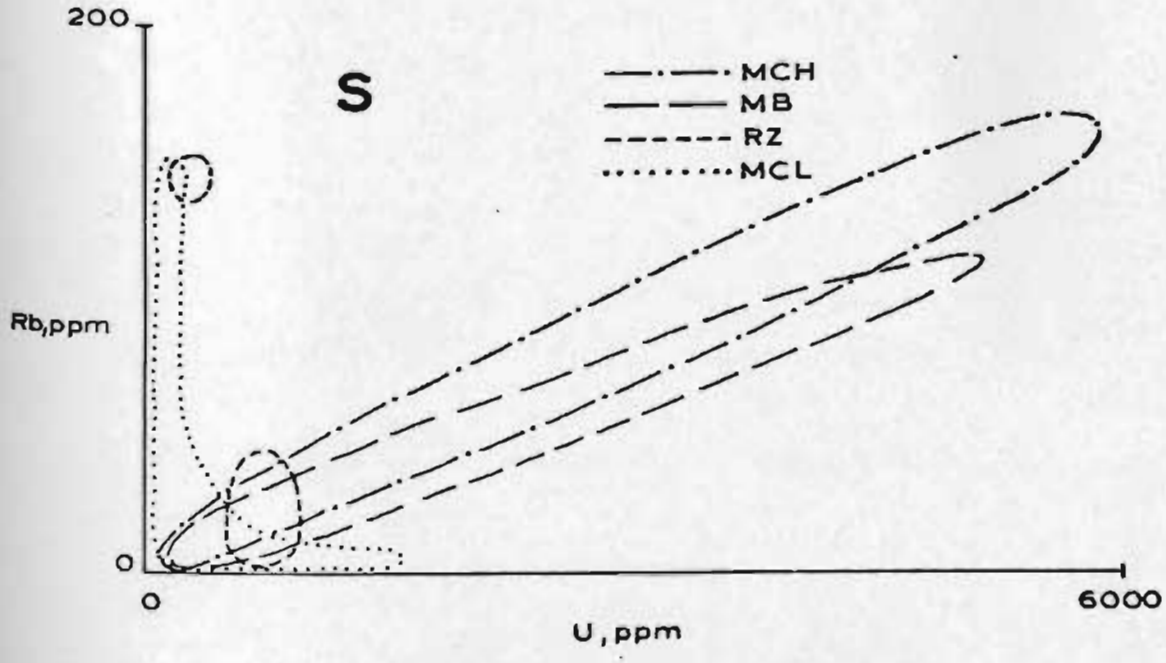

Figure 38. Summary of trace element patterns Rb-U of the examined uranium deposits.

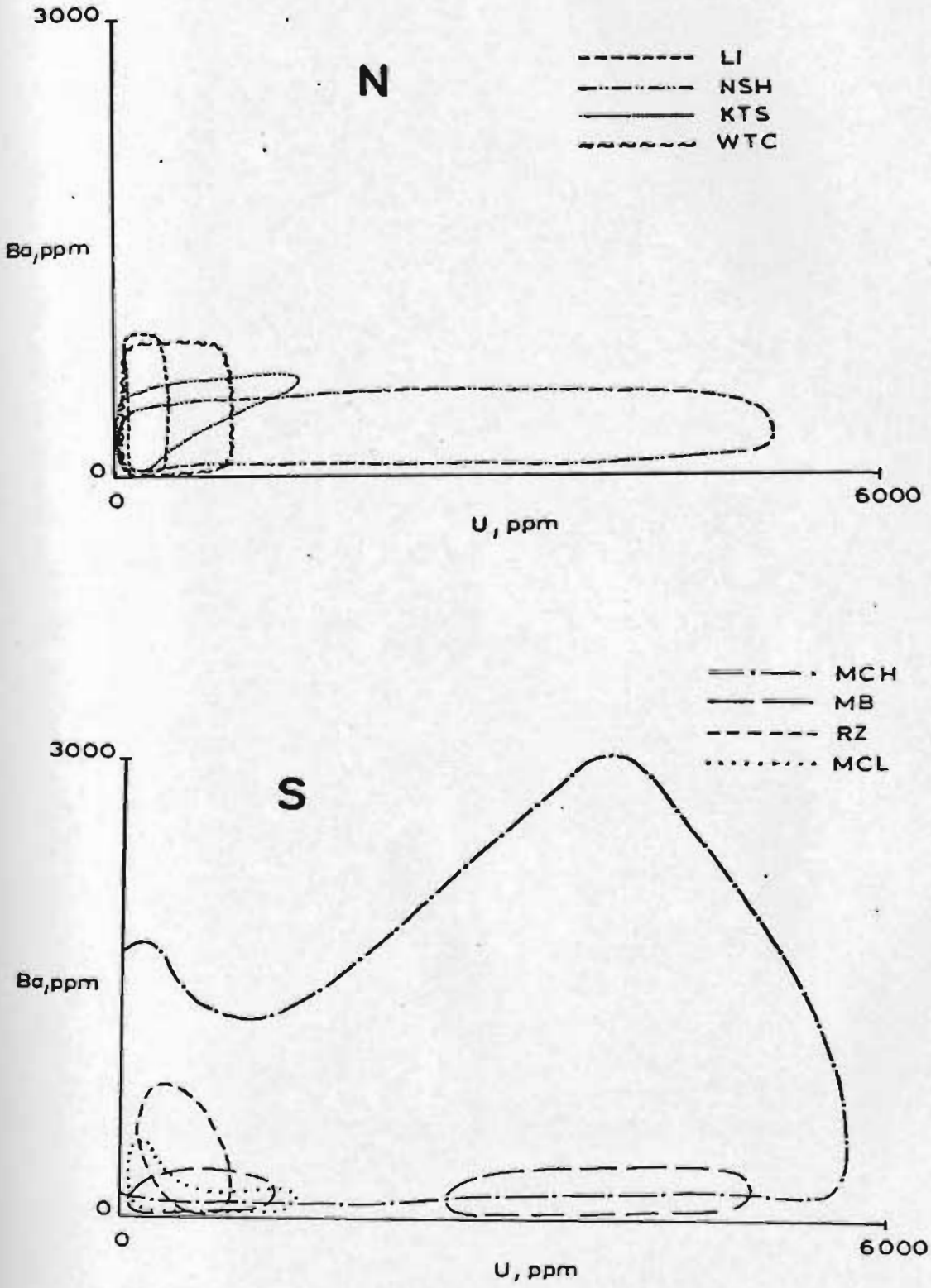

Figure 39. Summary of trace element patterns Ba-U of the examined uranium deposits.

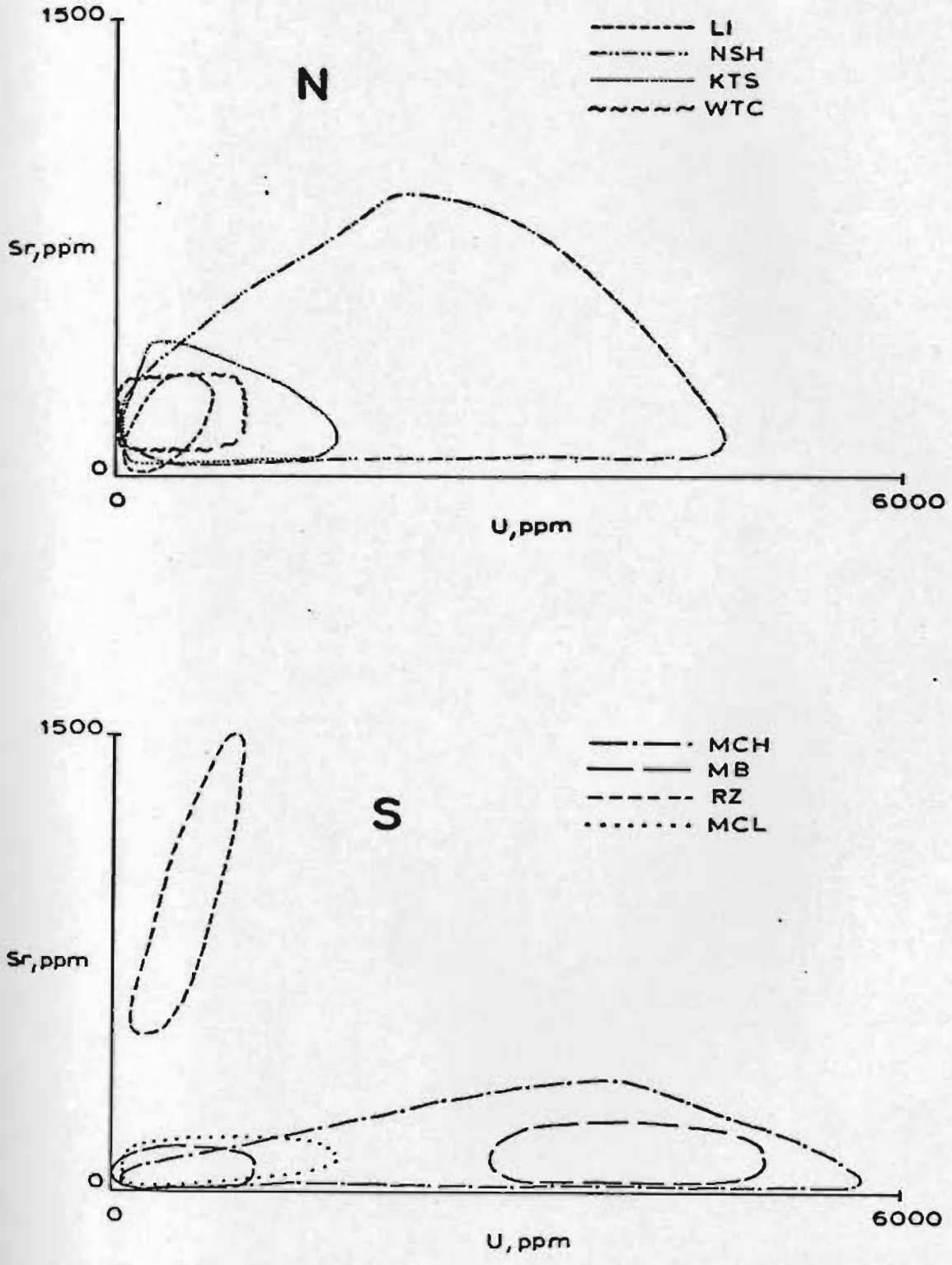

Figure 40. Summary of trace element patterns Sr-U of the examined uranium deposits.

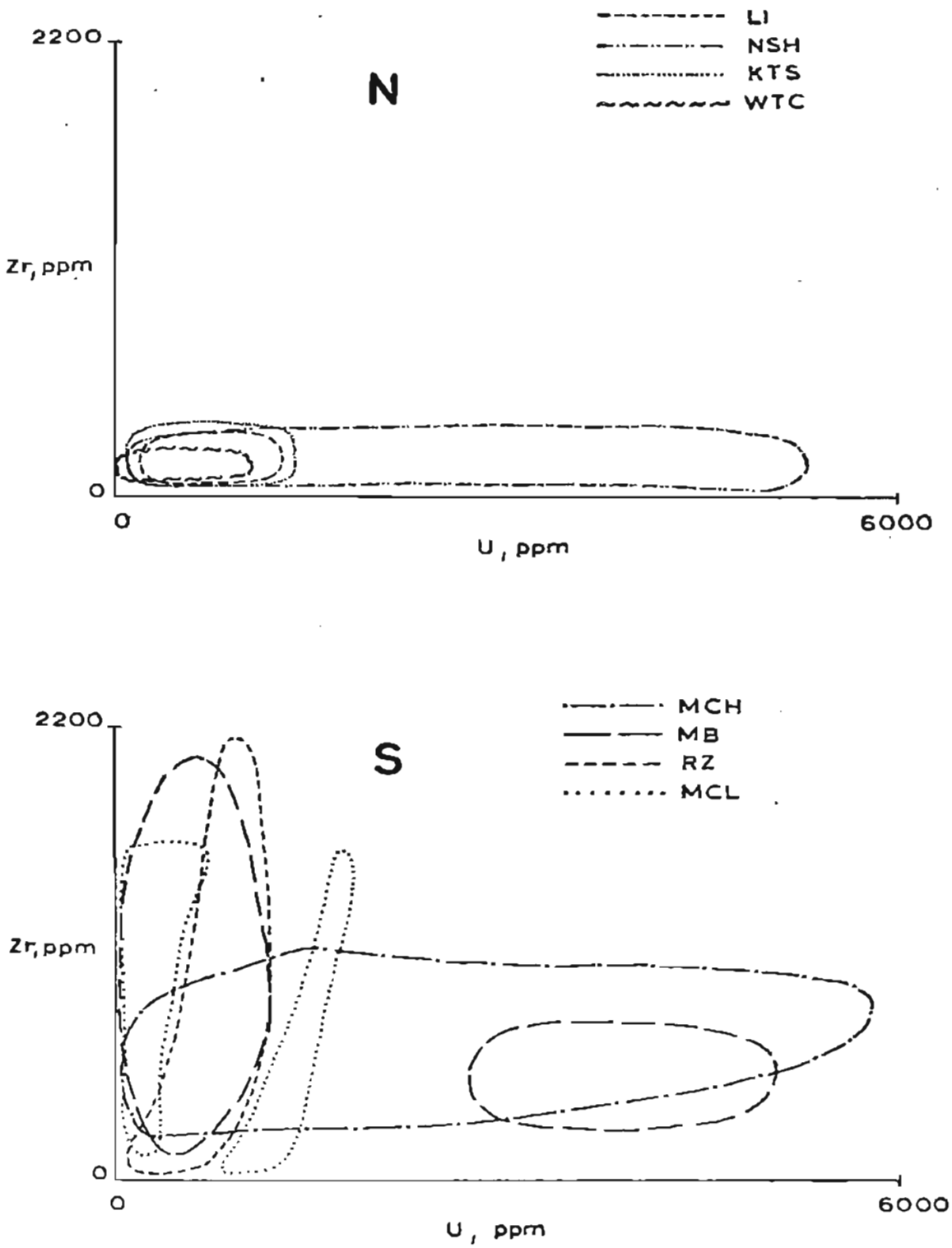

Figure 41. Summary of trace element patterns Zr-U of the examined uranium deposits.

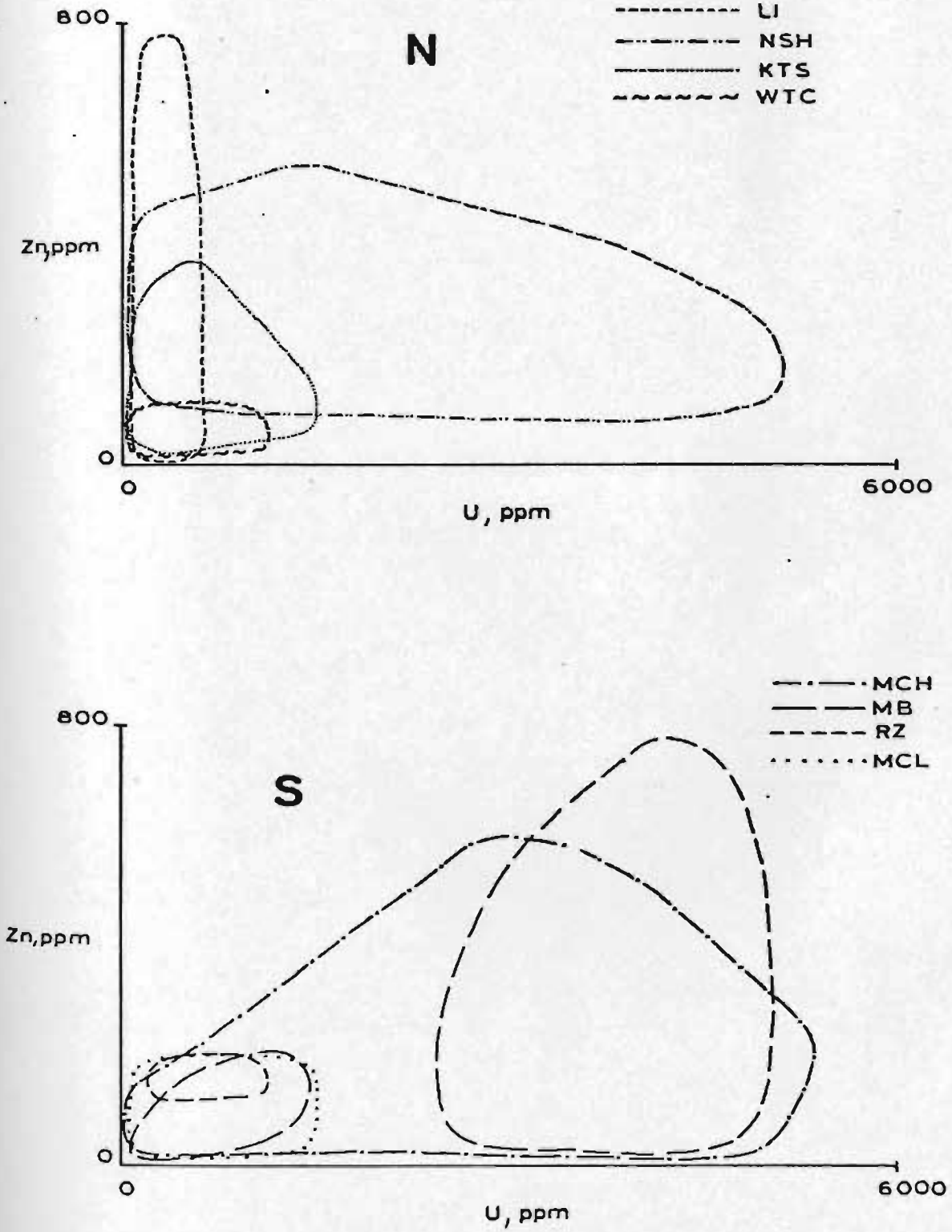

Figure 42. Summary of trace element patterns Zn-U of the examined uranium deposits.

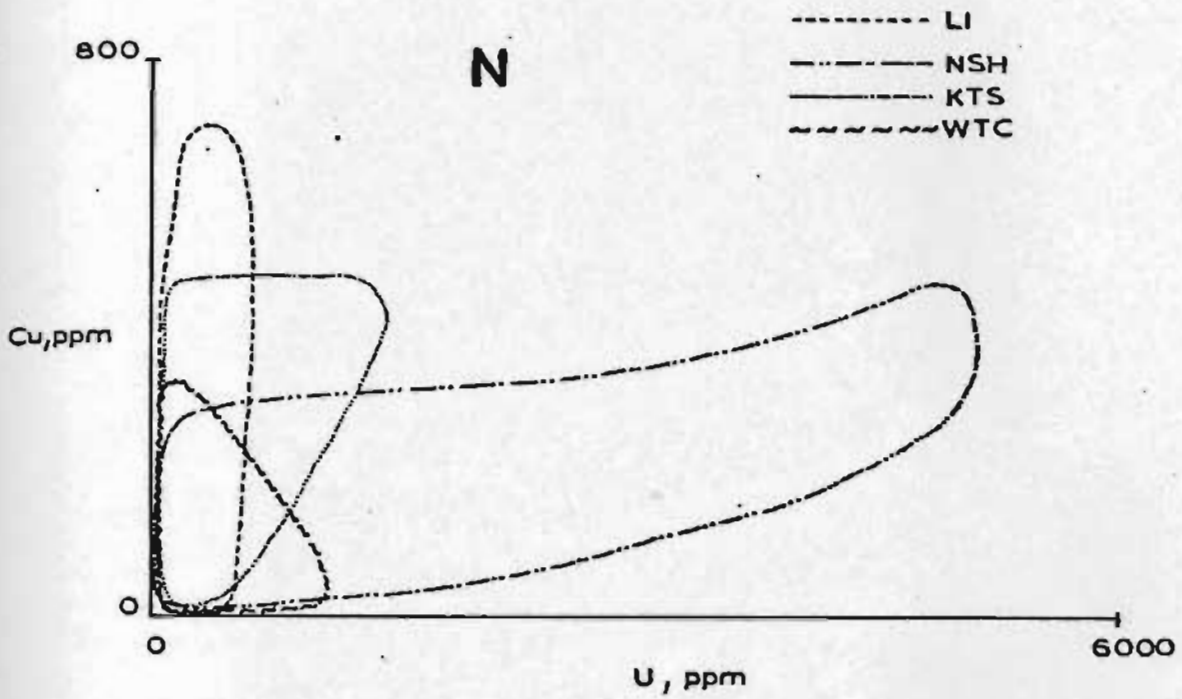

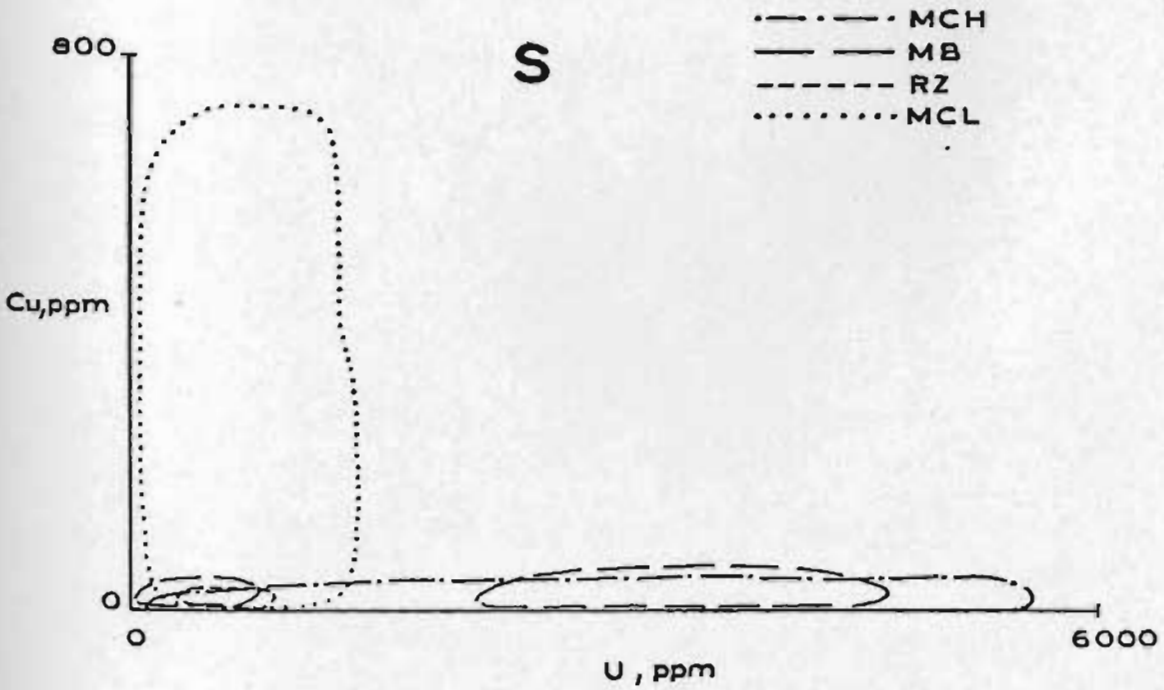

Figure 43. Summary of trace element patterns Cu-U of the examined uranium deposits.

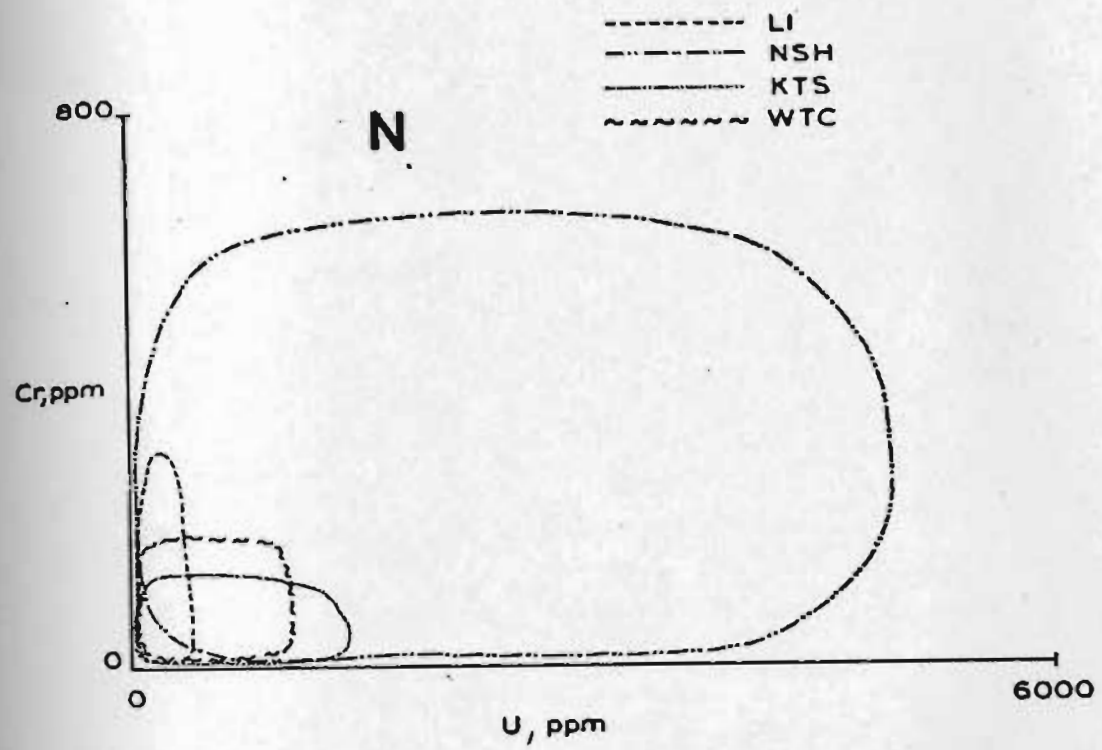

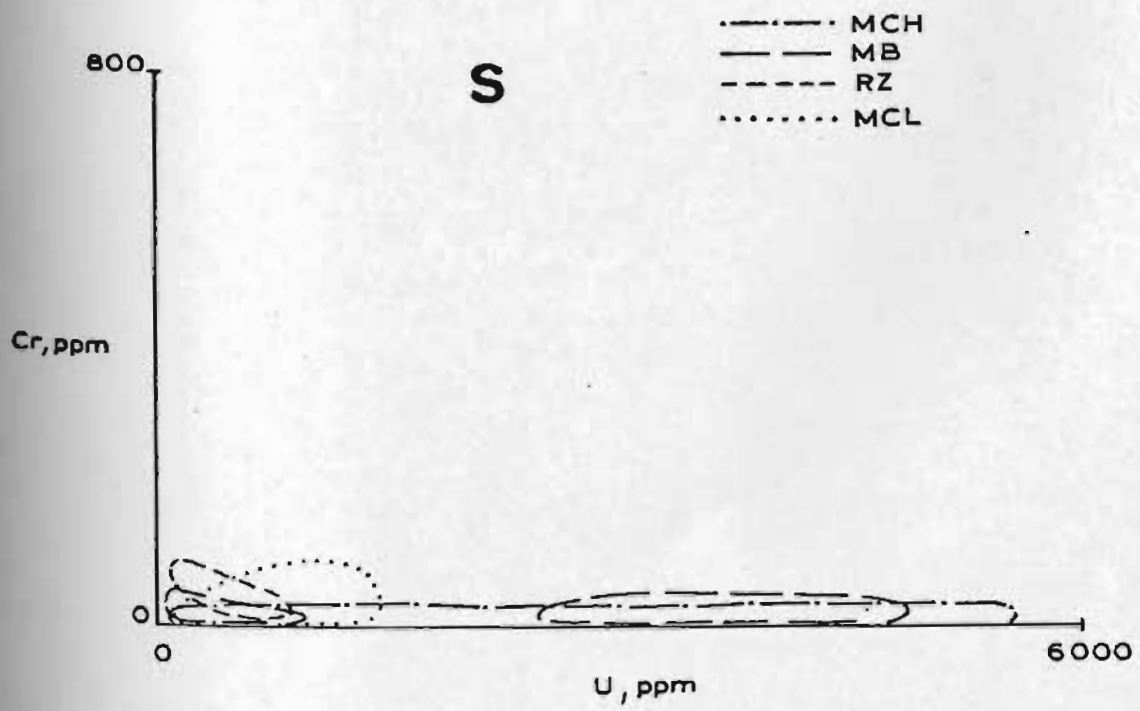

Figure 44. Summary of trace element patterns Cr-U of the examined uranium deposits.

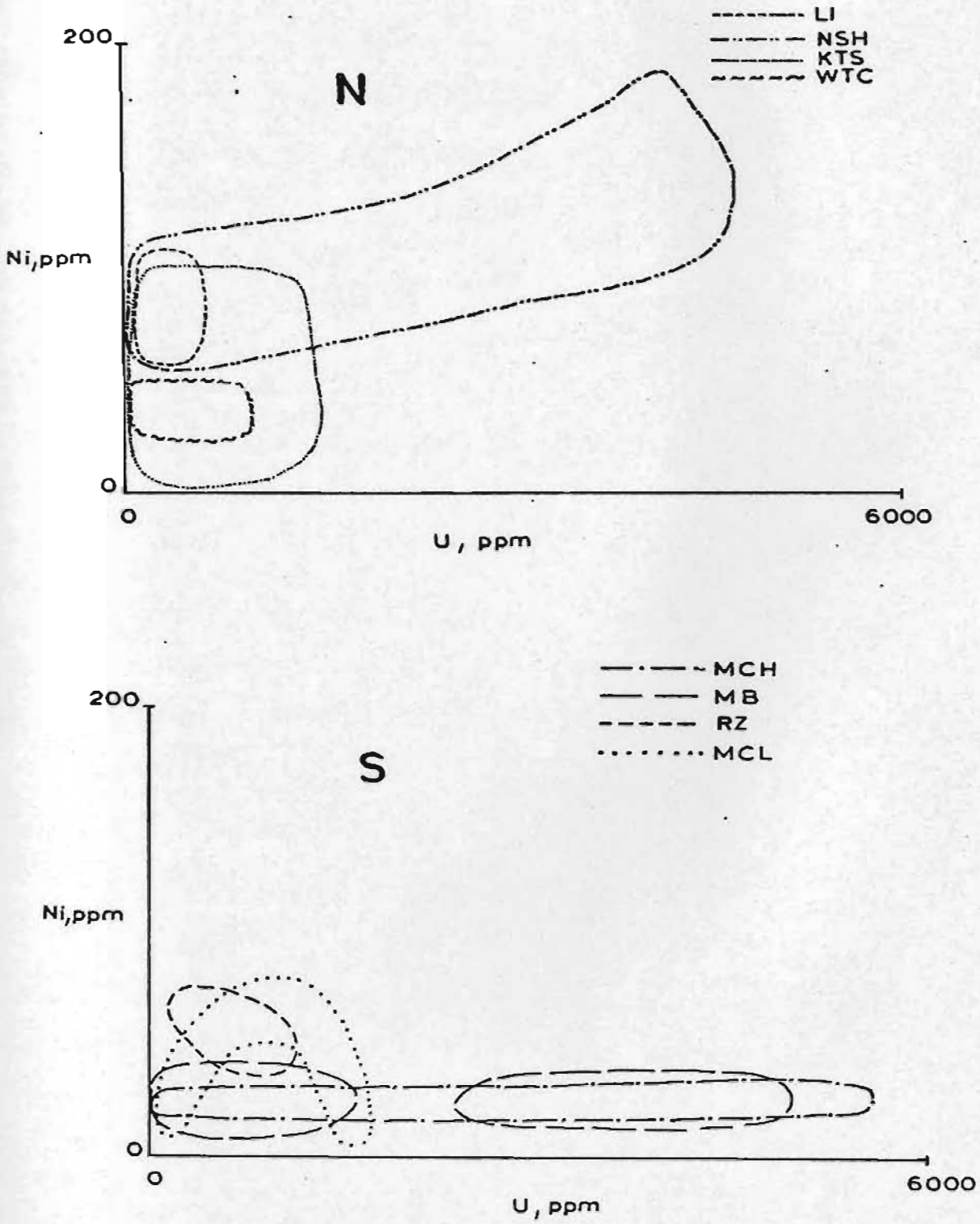

Figure 45. Summary of trace element patterns Ni-U of the examined uranium deposits.

CHAPTER IV

EVALUATION OF URANIUM EXPLORATION TECHNIQUES IN GLACIATED TERRAIN

Discussion of geochemical exploration in glaciated areas have been given by Bradshaw et al. (1972), Jones (1973), Kvalheim (1967) and Nichol and Bjorklund (1973). The purpose of this chapter is to prevent an evaluation of some uranium exploration techniques in part of central Labrador.

4.1 Terminology

A brief review of terminology in glacial geology is useful to understanding the significance of ice-transported material in exploration geochemistry.

According to Flint (1971) material which has been transported and deposited as a result of ice movement is known as glacial drift, which can be till (non-stratified) or stratified drift. Two types of till are recognized: lodgment till and ablation till. Lodgment till is deposited at the base of a glacier. Ablation till is deposited from drift in transport upon or within the terminal areas of a thinning and melting glacier. Transported rock fragments are called erratics (only if underlying lithology differs) and boulder trains consist of a series of erratics. Usually by mapping boulder trains the provenance can be determined and the direction of ice flow.

4.2 General

Geochemical anomalies in glacial overburden are generally

difficult to interpret in terms of bedrock source. Frequently the diversified nature and origin of glacial deposits and the complexity of the local glacial history tend to lead to a corresponding complexity of the dispersion processes and resulting geochemical patterns. Obviously, successful interpretation of such anomalies is largely dependent on a thorough knowledge of the glacial history. In other words one of the most basic problems in geochemical exploration in areas of glacial overburden is an adequate understanding of the glacial history, which can vary within an area on both a regional and local scale.

In this particular part of Labrador the glacial deposits, which are in the form of boulder clay and outwash material, generally cover the bedrock over extensive areas and it appears that they have not been moved very far from the source bedrock (Brinex, unpublished data). The glacial material forms a complete sequence from that deposited directly from ice to that deposited in running and quiet water. In some cases, as in the Rainbow Zone, there is a complete gradation of sizes from clay through sand and gravel to huge blocks , as well as a complete gradation of shapes from angular to perfectly round fragments.

The boulder trains appear either as lines of erratics or in a fan-shaped pattern, e.g. around the Michelin showing, with the apex at the place of origin although the origin of some of these is speculative and problematic.

Lundberg (1972) presented information on the range of different exploration methods used in Uranium exploration in northern Sweden (Fig.46-47). One significant point which can be seen in these figures is the sequence

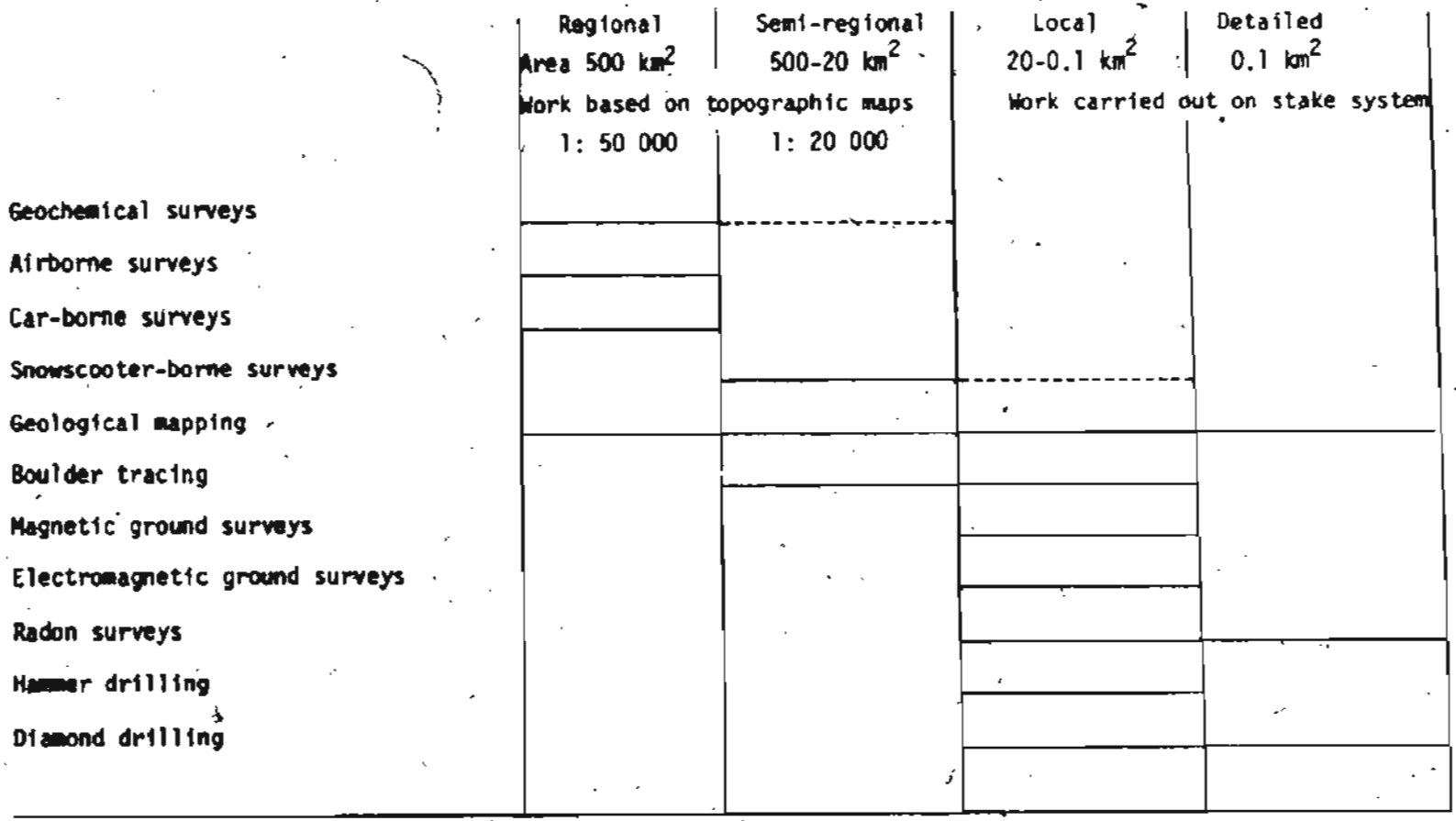

Figure 46. Outline of range of different exploration methods used in uranium exploration in northern Sweden (after Lundberg, 1972).

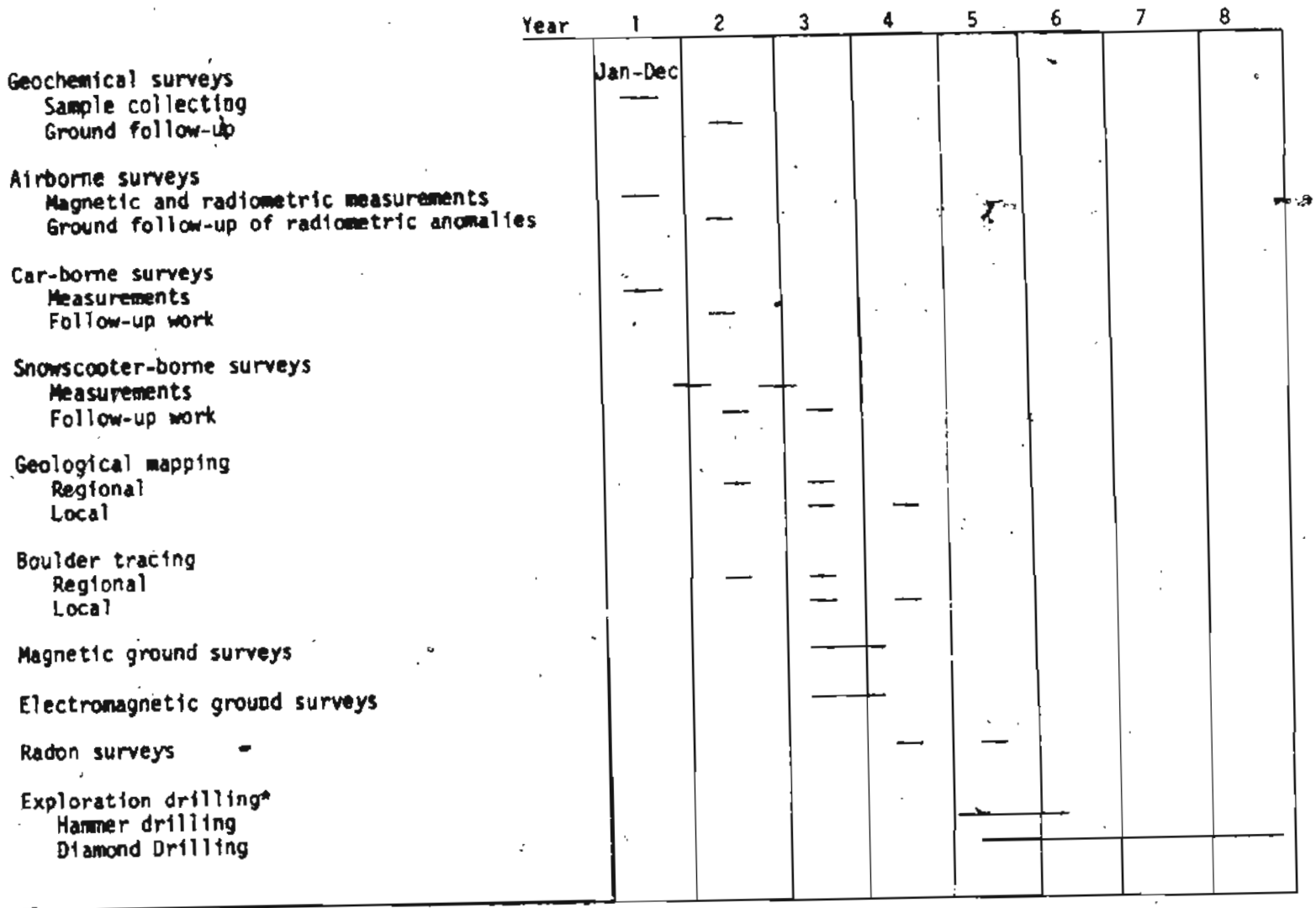

*Drilling to search for and make preliminary evaluation of new deposits.

Figure 47. Idealized time scheme for uranium exploration field activities in northern Sweden (after Lundberg, 1972).

of application of the different techniques, e.g. Snowscooter-borne surveys have to be done during the winter while radon surveys should not normally be done before a detailed boulder tracing (regional or local) survey has been completed, simply because no distinction can be made by using a radon technique between buried mineralized bedrock and mineralized boulders. If the distribution of glacial erratics is known then the interpretation of radon results, in conjunction with other factors (relief, drainage pattern, structural geology) can reveal useful information on the radon source which usually is related to uranium mineralization.

4.3 Radon Survey

Work on the soil-air detection in Labrador was threefold:

(a) Comparison of radon results obtained with Track Etch films and radon counter methods.

(b) Proof of the impracticability of radon techniques to make any distinction between covered uranium-bearing bedrock and covered erratics as well as correlation between the Track density and the radon source, and

(c) Degree of reliability of interpreting radon results over ground where glacial drift has an uneven distribution.

(a) Comparison of radon results obtained from Track Etch cups and radon counter methods.

Radon detection techniques for uranium exploration, belong to the so called vapor or gas surveys, the results of which are generally very difficult to repeat exactly. A radon survey over an uraniferous area in

Labrador showed a close correspondence between two different techniques, radon detection by radon emanometer and the track-etch method.

Radon detection by using a radon counter, INAX, Model CPD 284 (Adapted from A.A. Levinson's "Introduction to Exploration Geochemistry", 1974.)

Several papers have been published on the use of radon -222 as a uranium exploration tool (Peacock and Williamson, 1962; Dyck, 1968; Dyck, 1969; Smith and Dyck, 1969; Stevens et al., 1971; Morse, 1971; Bowie et al., 1971; Soonawala, 1974), and for the purpose of this chapter only a brief description on the radon detection by using a radon counter is given below.

In the decay scheme for ^{238}U, there are several unstable members as follows:

$$^{238}U \rightarrow ^{234}U \rightarrow ^{230}Th \rightarrow ^{226}Ra \rightarrow ^{222}Rn \rightarrow ^{218}Po \rightarrow ^{214}Pb \rightarrow ^{214}Bi \rightarrow ^{210}Po$$

$$^{210}Pb \rightarrow ^{206}Pb$$

Although several members of this series are alpha-emitters in addition to ^{222}Rn, their half-lives are in the range of minutes or seconds as opposed to the 3.8 days of ^{222}Rn, and so their interference is negligible. The same applies to ^{220}Rn, one of the daughter products of the decay of ^{232}Th.

To determine radon in soils, it is necessary to flush it from the soil with air, through a perforated or open-ended pipe inserted in the soil to a depth of 3-6 feet. The air-radon mixture is then forced into the special activated zinc sulfide chamber of a radon detector from which

all light is excluded, but which is open to a very sensitive photocell. When an atom of ^{222}Rn decays in the chamber, it releases an alpha-particle causing a fluorescence of the zinc sulfide which is detected by the photoelectric cell. In the case of water samples, after one liter has been collected in a polyethelene bottle, air is circulated from the counting chamber to the water bottle and back to the counting chamber, bringing with it any radon dissolved in the water. As with radon collected from soil, decay of the radon results in a fluorescence of the zinc sulfide and the light is detected by the photocell.

The Track Etch Technique

Diurnal and other variations in soil air radon led researchers at General Electric to develop the Track Etch technique (Gingrich, 1974).

Alpha-particles emitted by radon gas can penetrate certain plastic films and cause invisible damage along their paths, and subsequent chemical etching of the plastic films causes the damaged tracks to become visible, hence the name Track Etch. The visible tracks can be counted to determine the amount of radon present. Track Etch films record the amount of radiation exposure (radon present) much as photographic films record the amount of light exposure. However, they are uniquely different since they are not sensitive to light or other electromagnetic radiation, such as x-rays or gamma rays. To apply the Track Etch technique in uranium exploration, small pieces of specially sensitized plastic film are placed in sample cups to detect the alpha-particles emitted by radon. The sample cups containing Track Etch films

are placed upside down in shallow holes (0.6-1 m deep) over the area of investigation. The sample holes are located in a frid pattern of which the profile spacing and station interval depends on the size of the area being explored, the depth and size of the expected ore bodies and other factors related with the general geomorphological features of the area. After the cups are in place, the holes are covered and left undisturbed for several weeks. By leaving the sample cups undisturbed for an extended period of time, a true equilibrium radon concentration can be measured, and therefore results are more reliable than those obtained with other techniques.

The Track Etch film is recovered from the cups after the sampling period is completed and the films are returned to a central laboratory where they are processed and read to determine the number of alpha tracks recorded.

Field Work

Part of the Rainbow grid of approximately 10,000 m^2 was covered by using both conventional emanometer and Track Etch techniques. A profile spacing of 60 m and a station interval of 60 m was used. Because of the shallow soil conditions in the area, the depth of the holes was 0.3 m in both cases.

The Track Etch cups were placed in the same holes where radon had been earlier detected by using the conventional emanometer. The holes were covered by small pieces of plywood and the cups were left undisturbed for 20 days. It should be mentioned that care must be taken during the

placement of cups so that they are not substantially pressed into the soil, as this would result in measuring the less energetic alpha emitters in the soil as well as the gaseous emitters.

Results

The results are shown in Figs. 48 and 49. Fig. 48a shows the distribution of radon detected by using the conventional emanometer. It is quite clear that there are three radon highs which outline a linear zone along the base line of the grid. Fig. 48b shows the distribution of radon detected by using Track Etch cups. It can be seen that the Track Etch maxima outline more or less the same linear zone along the base line of the grid. Fig. 49 shows the correlation between emanometer readings in counts/minute (c/m) and the Track Etch readings in Tracks/Square millimeters (T/Sq. mm).

The Track Etch shows a weak high off the base line. This high does not show up in the emanometer results. Fig. 50 shows that the soil-air radon concentrations can vary by factors 4 to 30 in any 72 hour period at a station of a grid. This variability could explain the lack of the emanometer radon high off the base line (Fig. 48b).

The fact that the uranium showings in the area have a linear pattern striking E-W reinforces the possibility that the radon anomaly overlies a uranium deposit covered by the overburden.

Comparisons

The current price of one Track Etch cup is $15.00, while that of

a radon counter is close to $3,500.00. The cost of the 40 Track Etch cups used in this survey was $600.00. A cup cannot be used more than once, while a radon counter can be used many times. A minimum order of a number of cups whose total price exceeds the price of the radon counter, is uaually required. On the other hand the simplicity of the Track Etch technique eliminates all mechanical parts and special electronic equipment whose breakdown in the field can cause costly delsys. Perhaps the main advantage of a portable enamometer is that the data is immediately available allowing any unusual readings to be immediately rechecked and additional attention given to special features of anomalous areas.

Discussion

Soil conditions in this part of Labrador are far from ideal for radon tests. The overburden often consists of compacted clay or gravel interspersed with boulders. In an area with normal soil conditions these surveys could have been completed within two days, but the interspersed boulders caused a delay.

The emanometer survey was completed within two days. The Track Etch cups were also placed within two days. After 20 days it was necessary to visit the area again and pick up the cups. So from the point of view of time and expense the Track Etch technique has the disadvantage that a minimum of two visits per site is required.

No clear distinction between radon isotopes can be made with the Track Etch cups, while this is possible with the emanometer.

Radon detection with emanometer and Track Etch films over the

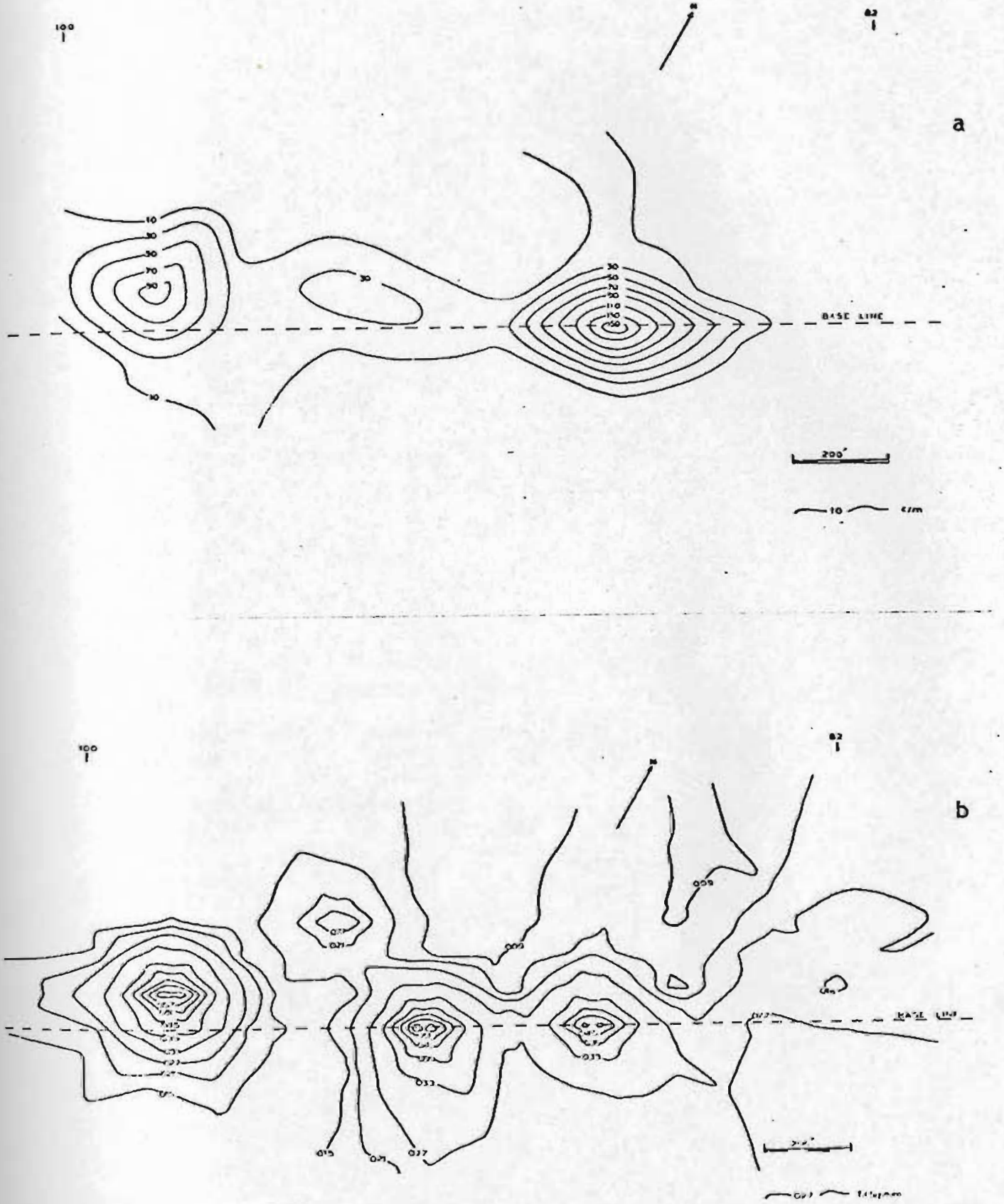

Figure 48. a. Distribution of radon detected by using the conventional emanometer.

b. Distribution of radon detected by using Track Etch cups.

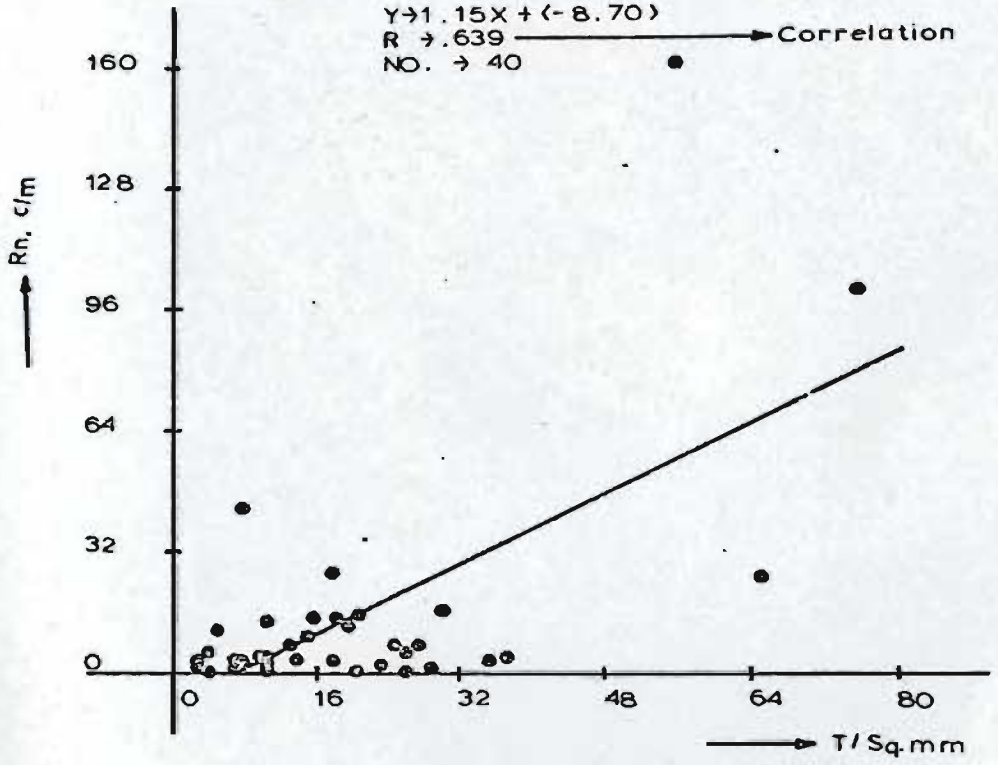

Figure 49. Diagram showing the correlation between emanometer readings in c/min. (c/m) and the Track Etch readings in Track/Square millimeters (T/Sq. mm).

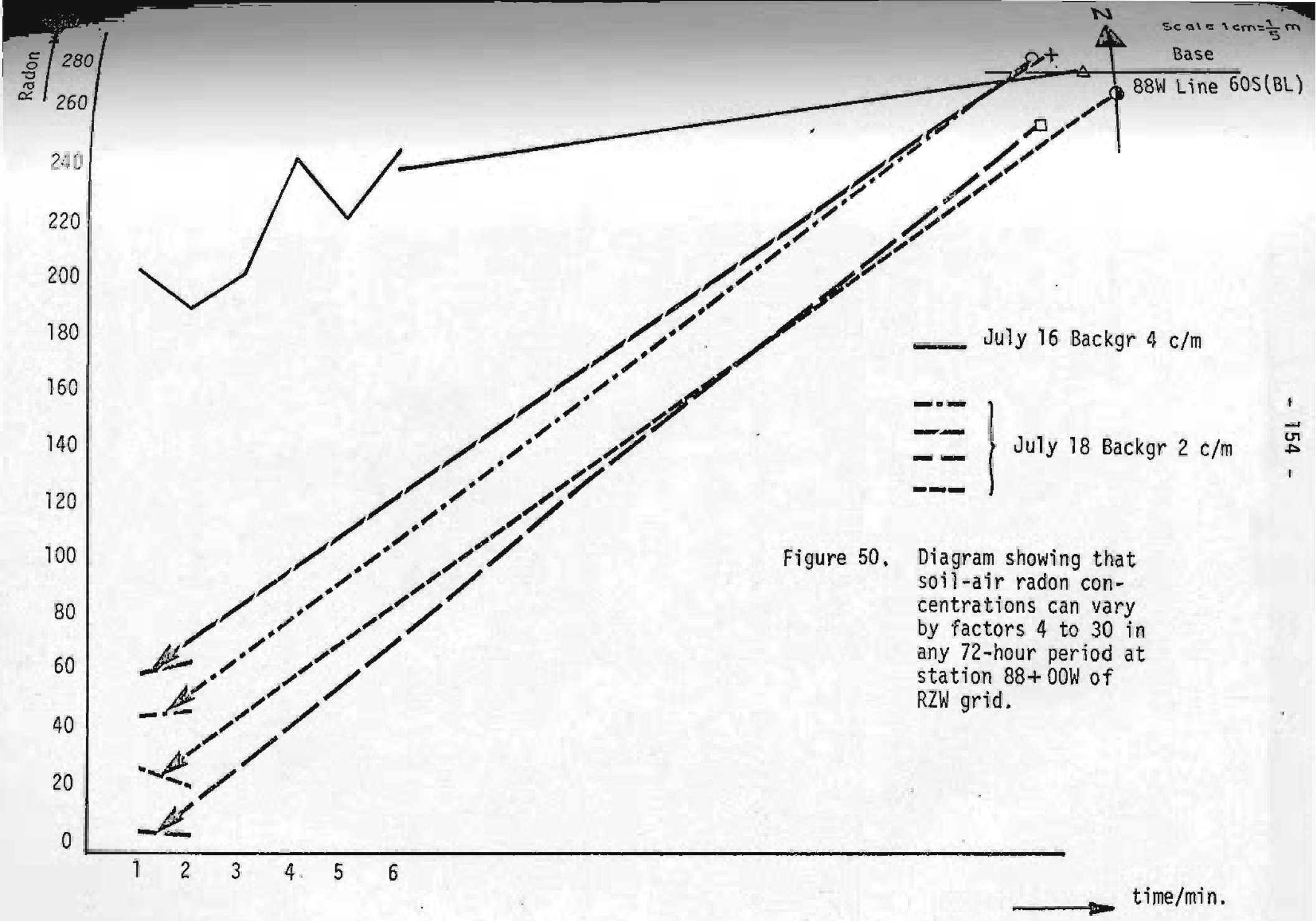

Figure 50. Diagram showing that soil-air radon concentrations can vary by factors 4 to 30 in any 72-hour period at station 88+00W of RZW grid.

same ground gave similar patterns of the radon distribution over a uraniferous area in Labrador. It is concluded that despite some differences either technique can give more or less the same satisfactory results for the detection of hidden uranium deposits in this part of Labrador.

(b) Proof of the impracticability of radon techniques to make any distinction between covered uranium-bearing bedrock and covered erratics.

In an attempt to confirm the impracticability of the radon technique as to the distinction between covered bedrock and covered erratics the following test was carried out:

Two barrels, namely "Radioactive" and "Non-Radioactive" were filled with soil (glacial drift) which was taken from the vicinity of a uraniferous showing. Some radioactive rock fragments were placed 40 cm below the surface fo the soil, in the "radioactive barrel" as indicated in Fig. 51.

Twenty, one-minute soil-air radon readings were taken from a 30 cm deep hole in the barrels using a conventional emanometer for 9 consecutive days. The temperature and radioactivity at the same spot were also measured. The radon, radioactivity and temperature readings were plotted and the results are shown in Fig. 52. In the first day both the radon and radioactivity values in both barrels was the same and the explanation for this is that during the first day not much radon had been emanated from the uraniferous rock fragments. Measurements in the "non-radioactive

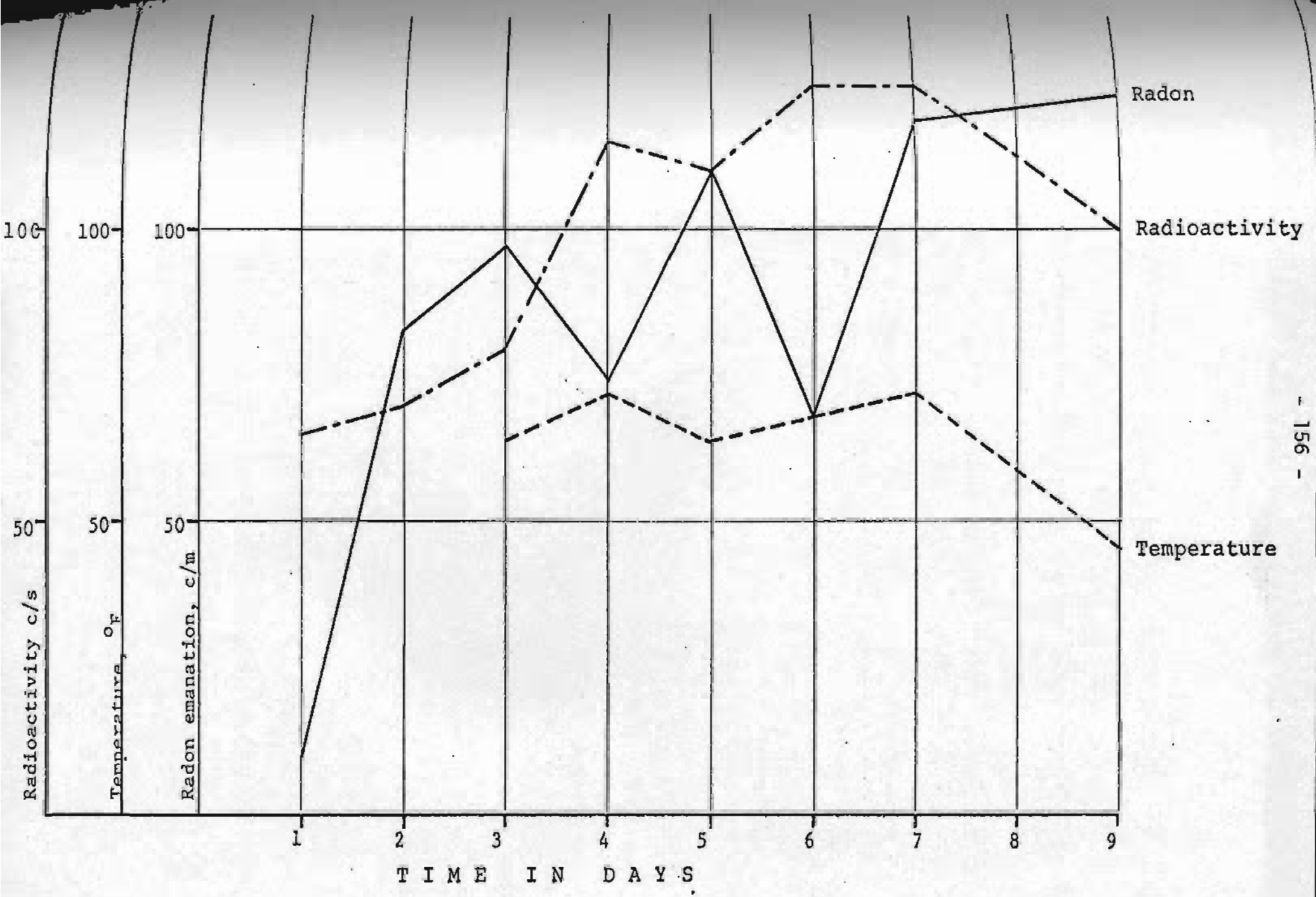

Figure 52. Variation of radon, radioactivity and temperature readings vs time (see text).

barrel" gave readings which range in general from 10-35 c/m. The readings in the "radioactive barrel" were of the order of 50 to 130 c/m, i.e. approximately four times as high as the readings in the non-radioactive barrel.

During the soil-air radon surveys, the radon readings taken over uranium bearing bedorck were of the same intensity with those taken over the uranium bearing fragments in the "radioactive barrel". From the above observations it is concluded that a 40 or 60 c/m soil-air radon reading could be attributable either to buried mineralized bedrock or to buried mineralized erratics.

After the end of the soil-air radon measurement with the conventional emanometer two holes, 30 cm deep were dug and a Track Etch cup was placed on the bottom of each hole. The cup was left undisturbed for 20 days as described above. Based on the results obtained in the two barrels a qualitative correlation is apparent between the Track density and the depth of the radon source. The distance between the Track Etch film in the radioactive barrel and the uraniferous specimen is 17 cm. The Track density was 280.724 T/Sq. mm in the case of the "radioactive barrel" and 22.358 T/Sq. mm in the case of the "non radioactive barrel".

Assuming that the physical conditions of the till above the bedrock are more or less similar to the conditions of till material above the rock fragment in the radioactive barrel than it should be expected that a reading fo the order of 280 Track/Sq. mm would be due to a U source beneath the cup not deeper than the distance between the cup and the

radioactive rock fragment in the "radioactive barrel". However, much field and experimental work need to be done to give a more quantative evaluation of the correlation between Track density and depth of the source.

(c) Evaluation of radon results over a ground covered unevenly with glacial drift.

Experience showed that at least in the Michelin area and Rainbow Zone ther is a close association of uranium deposits and radioactive boulders, and with regard to the general radon work in this area, when a high radon reading is obtained, four questions must be answered:

1. Is the radon reading due to a U-bearing buried body?
2. Is the radon reading due to U in the fine fraction of the till?
3. Is the radon reading due to a buried or even partly exposed mineralized boulder?
4. Is the radon reading due to some combination of the above?

An interesting example with the above mentioned problems was met in Rainbow grid, Fig. 53. The grid is divisable in three different areas.

First area. Between lines 40W and 60W. In this area, although many radioactive boulders occur mainly along the base line, the radon readings were low except for the three high readings 16, 25 and 37 c/m at stations 52W 1N, 58W 4N and 58W 1S respectively

Second area. Between 60W and 80W. Radioactive till is dispersed almost everywhere in this area and a great deal of contamination has been involved in the survey and has influenced the radon readings, preventing

any systematic interpretation.

Third area. Between 80W and 100W. Here the radioactive boulders are not uniformly dispersed, but they are concentrated between 99W and 88W from the base line southwards. In this "clean" part of the grid the linear soil-air radon anomaly along the base line which was confirmed with Track Etch films represents a true anomaly and should be tested with drilling.

M.BEN GRID (North Showing)

The radon survey in the Emben Grid revealed a number of radon anomalies of the same magnitude (order) with those in Ribbs Lake Grid but neither drilling nor further work is recommended on these anomalies for the following reasons:

1. The radioactive anomaly in the northeastern part of the Grid is due to radioactive boulders (Fig. 54). The lack of a radon anomaly in the same part of this grid is an evidence suggesting that no buried uranium bearing rock is underneath this radioactive anomaly.

Two points which must be emphasized are:

(a) Although the area is well outcropped in some cases the distinction between outcrop and glacial erratic is not clear.

(b) The thickness of the soil is not stable; in some cases it may be 4 feet, in some 1 foot and so on. Differences in soil thickness are expected to modify the radon readings in such a way that it is not easy to say a soil air radon reading 15 c/m is less significant than another 30 c/m in other words, no evaluation

between two areas which have been outlined by the 15 c/m and the 30 c/m contours can be done unless it is known what the thickness of the soil is over the same areas and the physical properties of this (moisture, temperature and so on). (Soils of the same thickness in the general area of a grid are expected to have the same porosity).

The radioactive anomaly and its radon counterpart in the south-eastern cordor of the grid (station 2E 2S) is due to an outcrop whose maximum radioactivity with the SPP-2 is 1800 counts per second.

In general readings of the order 20 c/m upwards are above or in the vicinity of uranium bearing sources.

Two small radioactive outcrops is likely to be the source of the radon anomaly in the southwestern corner of the grid and it is worth noting that this anomaly is more extensive than the others in the same grid and could be extended further west.

RIBBS LAKE GRID

Fig. 55 I (map in back pocket) shows the distribution of radon gas in the Ribbs Lake grid as well as the histogram and cumulative % frequency of radon readings. Radon quantity plotted: radon reading minus background (unsmoothed values). Among the radon highs shown in this grid only the one at station 26W on the base line is related with radioactive rock, possibly big radioactive boulders.

Fig. 55 II shows the distribution of radioactivity. The

individual highs as well as the linear zone between stations 14W and 26W are not significant from economic point of view.

Fig. 55 III shows the distribution of radon gas as well as the histogram and cumulative % frequency of radon readings as in 55 I; radon quantity plotted: radon readings minus background (smoothed values.

Fig. 55 IVa and 55 IVb show that there is poor correlation between radioactivity and radon (unsmoothed values) and radioactivity and radon (smoothed values), respectively.

4.4 Lake sediment geochemistry.

Lake sediment sampling in an area of approximately 160 km^2 centered on the Michelin and Rainbow deposits revealed the same zones which were previously outlined by airborne and lake water geochemistry surveys. It is suggested that detailed nearshore lake sediment sampling can outline anomalous zones in areas where there is no surface evidence of ore bearing rock. Further analyses show that the clay and organic content have no effect on the elemental concentrations of the samples and so the anomalies represent true anomalies close to the source. Some of the zones stand as extensions of the existing uranium deposits in the area.

Lake sediment sampling has been used as reconnaissance exploration means by previous workers (Allan, 1971; Allan et al., 1973; Allan and Richardson, 1974). My attempt was to examine how a detailed nearshore lake sediment sampling program can be used for locating of anomalous uranium and copper zones in an area of central Labrador. Sampling of lake water in the Canadian Shield provides a means of evaluating large regions at a rate in excess of 100 square miles per day using a single sampling team (Meyer, 1969). In the same way conventional lake sediment sampling can be used as a means of evaluating large regions.

Although airborne surveys are being widely applied in uranium exploration, even the most sensitive gamma ray spectrometer can miss targets in areas of deep overburden or rugged terrain. In this uraniferous area of relatively deep overburden and rugged terrain detailed nearshore lake sediment sampling is considered to be useful because (1) it outlines

areas more precisely than conventional lake water and lake sediment sampling, (2) it may reveal targets missed with airborne surveys, and (3) the lake sediment samples can be analysed for many elements.

Field Work

The shallow lakes in the area are glacial in origin with the majority occurring in irregular depressions within ground moraines (Kettles) and in ice-scoured rock basins. One hundred and eighty-four lake sediment samples were collected from 24 lakes using a float-equipped helicopter and a canoe. Three to four lakes were sampled each day, permitting completion of this orientation survey in a week. The upper 20 cm of the lake sediment, 1 to 4 meters away from the shore line, was collected with an auger.

GEOCHEMISTRY

Mode of metal occurrence

Metals in sediments may be contained:

(1) within the structure of primary sulphide and silicate minerals
(2) in oxides, hydroxides, carbonates and sulphates, and
(3) adsorbed onto clay and organic particles.

Geochemical analyses are usually conducted on -80 mesh fraction. This size fraction includes not only primary uranium and sulphide grains but also all the phase described above. In order to properly evaluate sedimentary geochemical data, it is important to distinguish the phases

in which metals are concentrated, e.g. see Hawkes and Webb, 1962; Levinson, 1974; Alley and Slatt, 1975.

Analytical procedure

The samples were split in half, with one half of the sample kept for reference and the other placed in a porcelain dish and left in an oven at 80°C overnight. The dry samples were sieved and geochemical analyses were conducted on the -80 mesh fractions.

Fluorimetry provides the most sensitive method for uranium analysis (Smith and Lynch, 1969). Concentration of Cu was determined by Atomic Absorption Spectrophotometry after partial digestion of samples for 1 1/2 hours in a hot solution of 10 ml HNO_3 and 1 ml 16N HCl (see Table in appendix III). In addition, splits of the 184 samples analysed in our laboratory for Cu, were analysed by Atlantic Analytical Services (Springdale, Newfoundland) using the same method.

Table XXXV shows the results of the chemical analyses. Fig 56 show the correlation between U and Cu and Cu duplicate analyses. It is noteworthy that Cu and U are not mutually related in the lake sediments, in other words there is no areal correspondence between U and Cu enriched zones. The results from the Cu duplicate analyses are generally comparable although ours are consistently slightly lower.

Metals in silicate structures would not be leached by the digestion technique employed.

Twenty three samples covering the spectrum of U and Cu analyses

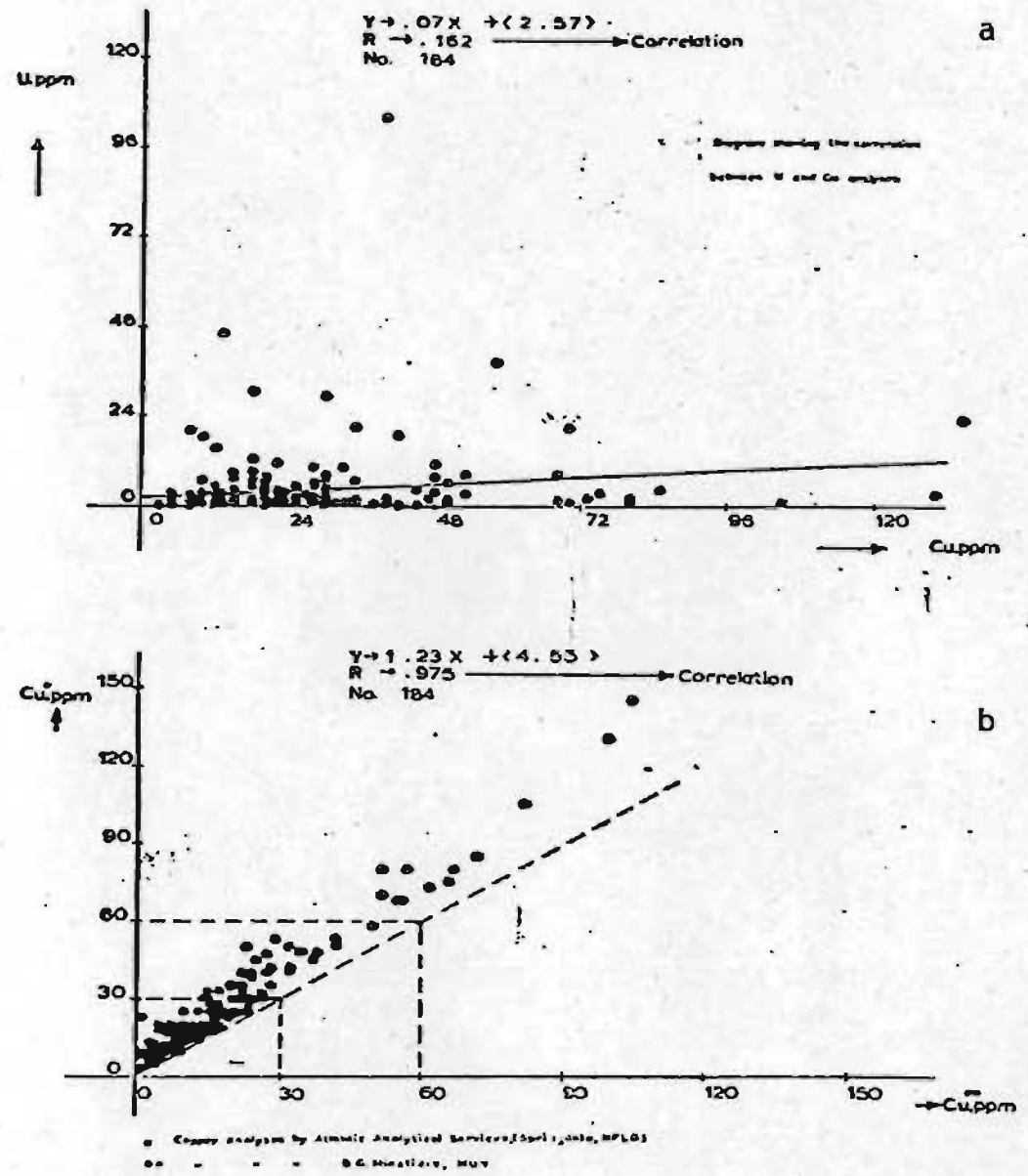

Figure 56. a. Correlation between U and Cu.

b. Correlation between Cu duplicate analyses.

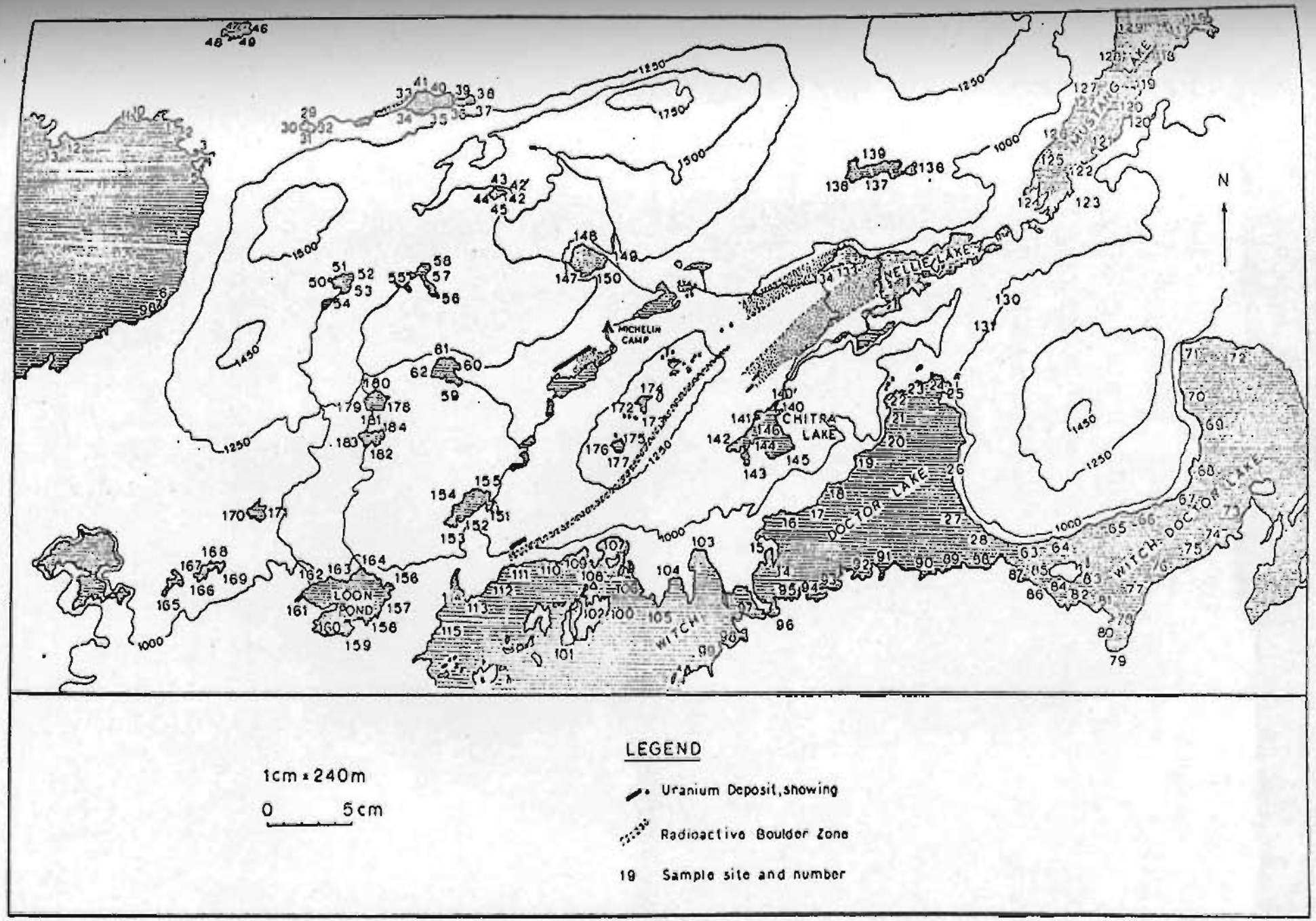

Figure 57. Numbered locations of nearshore lake sediment samples. Also shown are the locations of known uranium deposits and radioactive boulder trains. Topographic contours in ft.

were analysed for carbon with a Leco Carbon analyzer and for clay with Pipette analyses as described by Folk (1968). See Appendix III. The results are shown in Table XXXVI. The lack of carbonates, graphite etc., led to the assumption that the analysed carbon represents the organic content of the samples. To check the sample error duplicate samples were collected from different localities throughout the area (Fig. 57) and analyses for Cu and U. The results were similar except in the case of samples 120 and 120', the difference of which can be attributed to to the different content of organic material (Table XXXVI). Analytical precision for U, determined on five replicates of one sample and six replicates of another, was ± 25% and ± 23% respectively. Analytical precision for Cu, determined on 12 duplicate splits, averaged ± 32% of reported values.

In order to evaluate the mode of uranium occurrence 8 samples were separated into light and heavy fractions with tetrabromethane (Sp. G. = 2.92). The examination of heavy mineral thin sections and autoradiographs did not indicate the existence of primary uranium minerals in the lake sediment samples.

Discussion

The values were treated statistically and separated in three groups:

(a) values ranging from 0 to the mean

(b) values ranging from mean to the threshold, which is defined as the mean plus twice the standard deviation, and

TABLE XXXV

Sample	Cu*, ppm	Cu**, ppm	U*, ppm	Sample	Cu* ppm	Cu**ppm	U* ppm
1	80	67	1.2	44	12	7	2.6
2	22	16	0.5	45	13	6	3.7
3	25	23	5.3	45'	12	7	3.9
4	20	10	0.4	46	8	5	0.4
5	130	100	3.1	47	25	17	0.9
6	10	7	7.0	48	23	17	1.7
7	30	22	29.1	49	22	15	1.2
8	10	6	3.0	50	15	10	0.8
9	8	5	3.3	51	20	13	2.2
10	10	6	0.4	52	30	20	8.3
11	15	10	0.8	53	20	11	2.8
12	15	10	0.0	54	10	4	0.7
13	10	4	0.0	55	18	12	2.1
14	10	6	0.7	56	10	4	3.3
15	10	8	0.8	57	20	5	2.6
16	30	15	0.4	57'	18	12	2.0
17	28	23	1.2	58	15	8	2.2
18	10	4	1.0	59	20	14	0.6
19	33	17	1.2	60	13	9	0.7
20	35	20	1.0	61	15	8	2.7
21	33	22	0.8	62	40	27	104.0
22	25	15	1.4	63	70	52	20.8
23	40	27	1.1	64	25	21	1.2
24	42	28	0.3	65	20	16	6.4
25	12	3	0.2	66	20	14	0.4
26	13	3	0.3	67	13	9	0.3
27	12	3	0.6	68	45	37	0.6
28	18	5	6.7	69	15	9	0.2
29	48	34	7.8	70	10	5	1.4
30	70		1.1	71	20	16	0.2
31	23	16	0.6	71'	17	10	0.2
31'		13		72	8	3	0.4
32	145	106	23.1	73	18	12	0.4
33	30	15	3.1	74	18	10	0.9
34	25	13	2.6	75	40	32	2.0
35	35	22	1.8	76	15	12	4.7
36	105	82	0.9	77	10	4	1.0
37	50	32	0.7	78	12	8	4.5
38	45	25	4.5	79	10	7	1.5
39	25	10	1.3	80	12	8	0.5
40	18	12	1.5	81	8	3	0.1
41	85	72	4.3	82	15	9	0.9
42	15	11	9.0	83	13	4	0.4
42'	18	15	12.5	84	15	8	0.9
43	10	7	3.6	85	20	15	1.6

*Analyses by Atlantic Analytical Services (Springdale, Newfoundland)

**Analyses by S.E. Hrudey, M.U.N.

TABLE XXXV (Cont'd.)

Sample	Cu*, ppm	Cu**, ppm	U*, ppm	Sample	Cu*, ppm	Cu**, ppm	U*, ppm
86	5	3	0.2	128	50	23	6.2
87	10	6	0.9	129	12	8	3.9
88	15	9	0.6	130	5	1	0.2
89	10	5	1.1	131	38	24	0.7
90	8	4	2.8	132	33	15	10.2
91	15	12	1.1	133	25	17	5.6
92	18	12	1.6	134	53	42	8.5
93	18	10	1.3	135	20	15	5.7
94	25	17	2.2	136	27	23	2.9
95	28	23	5.7	137	22	15	0.8
96	10	6	0.6	137'	8	5	2.0
96'	10	9	0.7	138	18	12	30.5
97	15	11	1.8	139	20	13	2.5
98	18	11	1.5	140	18	10	5.2
99	5	4	0.4	140'	13	8	46.3
100	50	42	1.3	141	18	6	5.0
101	35	28	6.9	142	28	15	6.4
102	12	8	1.8	143	18	11	1.5
103	42	32	18.6	144	20	12	1.4
104	8	1	1.6	145	73	62	2.3
105	28	17	1.3	146	25	22	1.2
106	47	27	2.1	147	22	17	11.6
107	8	1	0.7	148	12	6	5.3
108	22	14	2.9	149	15	12	7.5
108'	20	15	1.9	151	18	13	5.4
109	28	17	3.0	152	5	3	1.6
110	20	14	4.4	153	58	50	38.3
110'	20	15	7.8	154	48	35	4.0
111	20	16	7.0	155	80	52	2.3
112	35	28	21.0	156	30	21	4.3
113	15	9	1.9	157	20	14	2.3
114	10	6	1.2	158	30	26	7.5
114'	10	19	1.5	159	22	15	2.4
115	23	19	2.2	160	23	19	3.5
116	80	57	1.5	161	13	10	2.2
117	30	15	2.2	162	48	38	11.3
118	68	56	8.6	163	28	23	10.5
119	18	11	9.4	164	40	24	1.5
120	75	65	3.7	164'	25	17	2.4
120'	30	21	5.2	165	30	23	3.5
121	23	1	1.8	165'		21	
122	68	55	1.6	166	18	12	1.7
123	20	5	0.4	167	15	9	1.3
124	53	28	3.4	167'	13	10	0.8
125	32	26	1.2	168	12	8	0.8
126	50	32	1.9	168'	20	17	1.4
127	30	24	0.5	169	40	22	2.2
127'	30	14	2.6	170	15	12	0.8

TABLE XXXV (Cont'd.)

Sample	Cu*, ppm	Cu**, ppm	U*, ppm
171	22	15	4.4
171'	20	17	5.0
172	10	8	18.6
173	12	8	15.5
174	5	2	3.5
175	15	13	2.7
176	3	1	0.4
178	10	3	3.1
179	18	11	6.8
180	10	6	2.8
181	20	10	5.8
182	25	18	2.1
183	20	9	4.7
184	20	7	3.8

TABLE XXXVI

Sample No.	Cu ppm	U ppm	C%	Clay wt%	Silt wt%	Sand wt%	U/Clay	Cu/clay	Color
1	67	1.2	22.97	0	0.425	0.300			brown gray
3	23	5.3	28.60	14.380	2.080	0.360	0.368	1.599	" "
7	22	29.1	1.62	7.600	8.380	11.490	3.828	2.894	gray
17	23	1.2	1.27	1.740	13.260	27.860	0.689	13.218	gray greenish
23	27	1.1	12.73	61.070	2.110	0.420	0.018	0.442	pale brown grey
41	72	4.3	2.67	2.970	5.270	4.500	1.447	24.242	gray greenish
52	20	8.3	3.48	6.810	4.845	7.740	1.218	2.936	" "
62	27	104.0	7.44	2.120	2.565	1.820	49.056	12.735	gray brownish
63	52	20.8	5.08	3.830	6.190	5.970	5.430	13.577	pale gray brownish
69	9	0.2	0.35	0.600	5.045	9.670,	0.333	15.000	yellow white
90	4	2.8	2.05	0.560	3.260	10.050	5.000	7.142	gray brown
95	23	5.7	9.85	48.690	4.065	1.160	0.117	0.472	pale grey
109	17	3.0	4.72	6.180	5.075	7.520	0.485	2.750	pale brown
112	28	21.0	0.14	3.560	6.365	7.560	5.898	7.865	white gray
118	56	8.6	1.71	6.380	9.545	4.520	1.347	8.777	yellow brown
120	66	3.7	1.47	0.210	6.815	7.500	17.619	314.285	gray
120'	21	5.2	0.40	1.780	7.230	6.820	2.921	11.797	yellowish gray
127	19	0.5	1.33	1.590	5.745	8.730	0.314	11.949	gray greenish
133	17	5.6	0.89	3.440	5.365	8.650	1.627	4.941	yellow
138	12	30.5	3.38	0.660	30.350	5.000	46.212	18.181	brownish
140	9	5.2	2.99	5.790	5.915	6.200	0.898	1.554	brownish
155	52	2.3	2.56	1.780	9.125	9.590	1.292	29.213	brown yellow
163	23	10.5	0.71	13.520	9.020	3.480	0.776	1.701	whitish

(c) values ranging from the threshold up to the highest value (Hawkes and Webb, 1962)

Enriched zones were outlined based on (b) and (c) groups.

Figs. 58-59 show the histograms and the cumulative frequency per cent curves for U and Cu values. Concentrations of the elements increase with increasing clay content. In some cases smaller concentrations are associated with the clay size rather than the coarser fraction. Plots of trace element concentrations/clay content vs clay content discriminate between concentrations in both fractions and filter out the grain size effect (Slatt and Sasseville, 1975). Plots of Cu/clay versus clay and U/clay versus clay (Figs. 60-61) show clearly two trends, one "background" trend and one "anomalous" trend. All the samples which constitute the anomalous trend are located geographically in the anomalous outlined zones, which are shown in Figs. 64-65.

Figs. 62-63 show that there is no correlation between U, Cu, C and clay; this suggests that the organic content and the clay have no effect on the elemental concentrations of the samples and so the anomalies represent true anomalies close to the source.

Fig. 66 shows the results from airborne survey, lake water geochemistry (Meyer, 1969) and present lake sediment geochemistry for uranium. This type of sampling has allowed me to extend previously known anomalies across glacial drift and lake-covered terrain. As well, large areas of individual lake drainage basins have been shown not to be potential source areas of uranium. This had not been possible on the basis of previous airborne surveys or lake water geochemistry. Further exploration

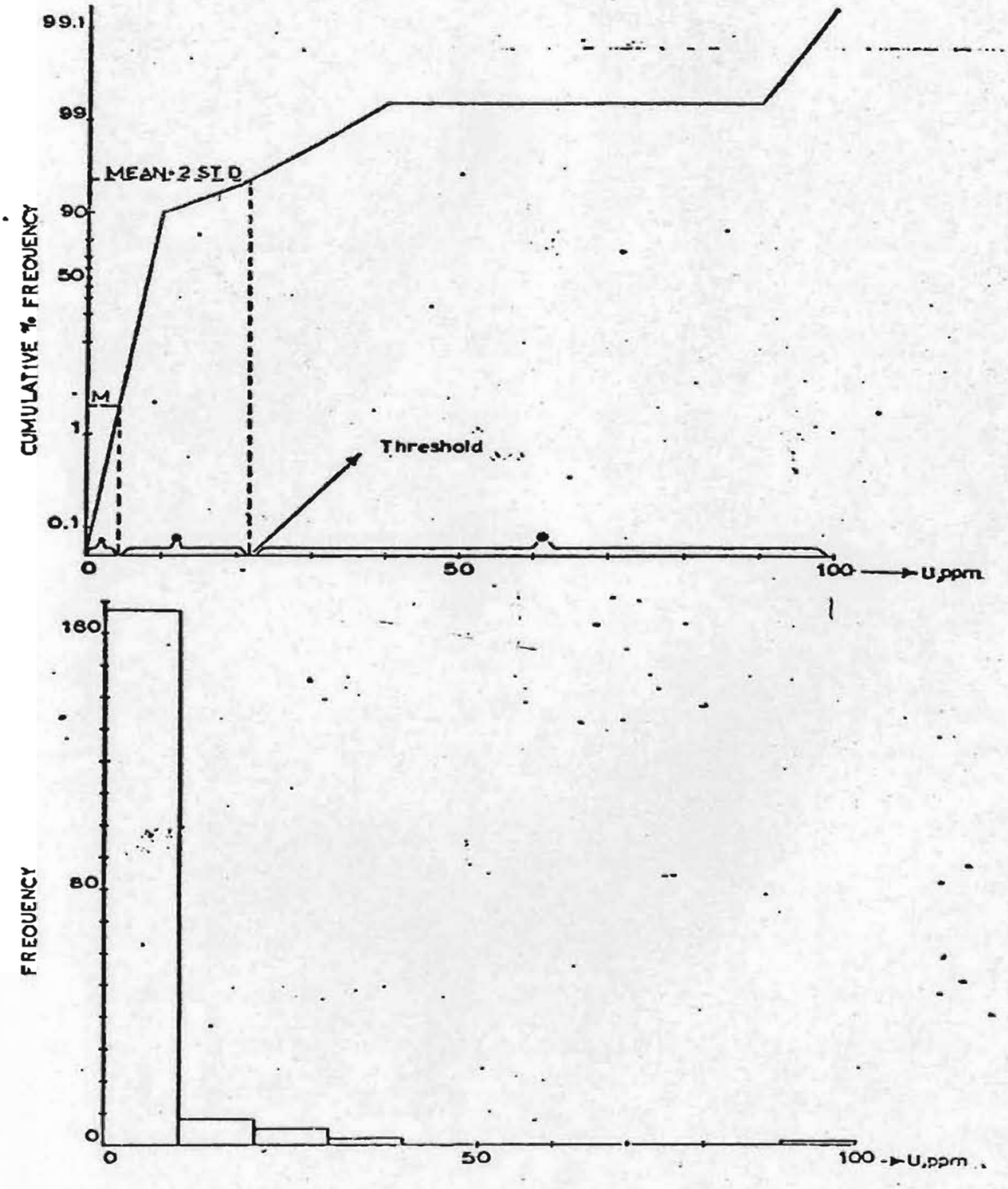

Figure 58. Histogram and cumulative frequency per cent curve for U values.

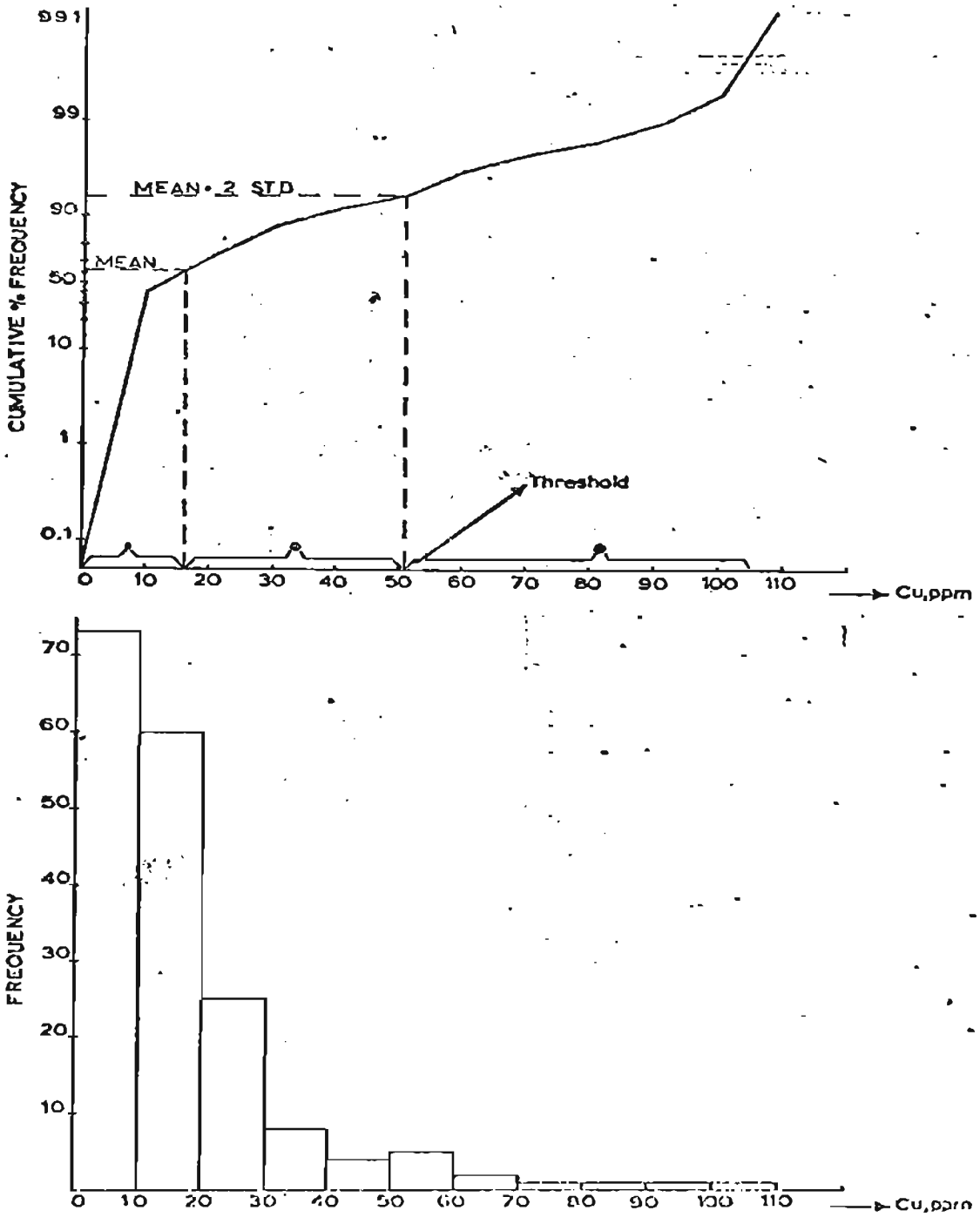

Figure 59. Histogram and cumulative frequency per cent curve for Cu values.

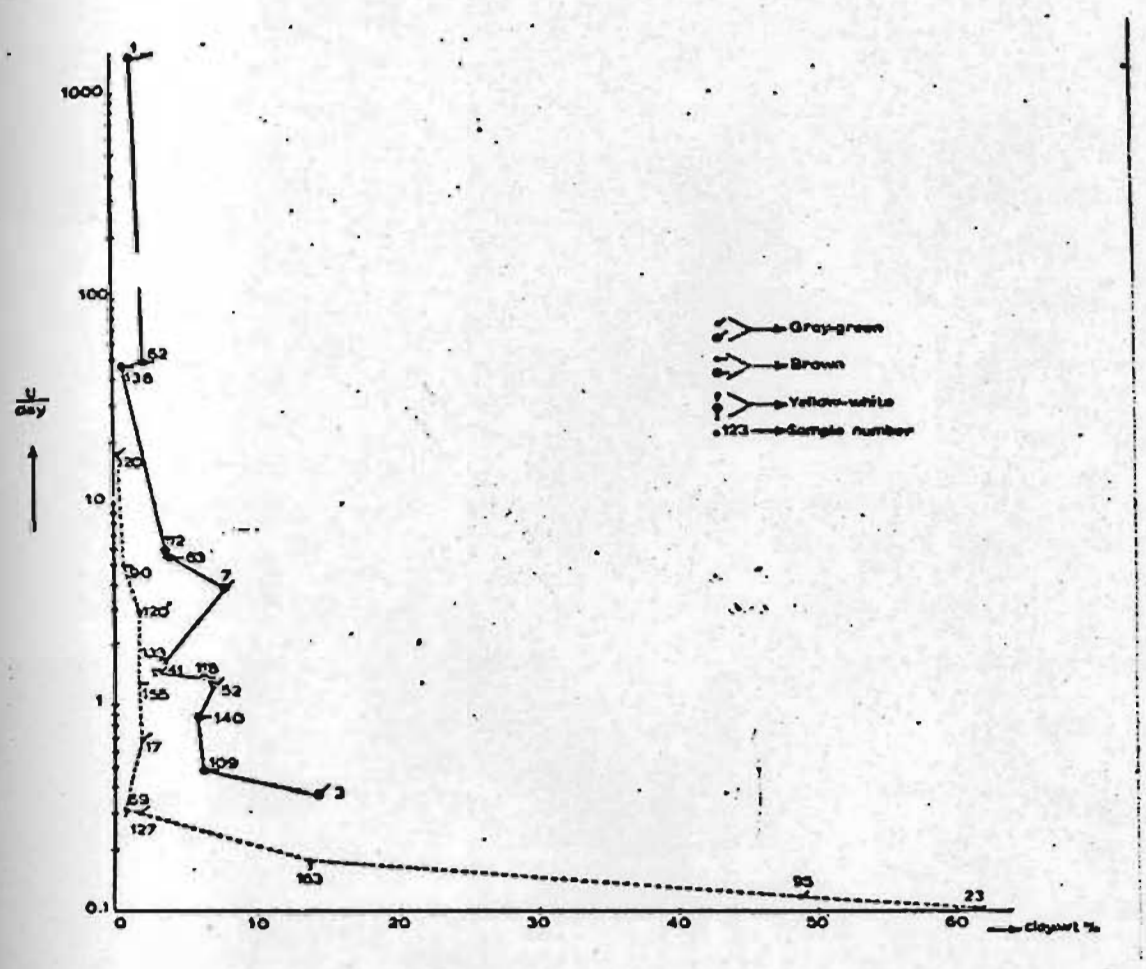

Figure 60. Plot of U/clay vs clay, wt.% of the nearshore lake sediments (see text).

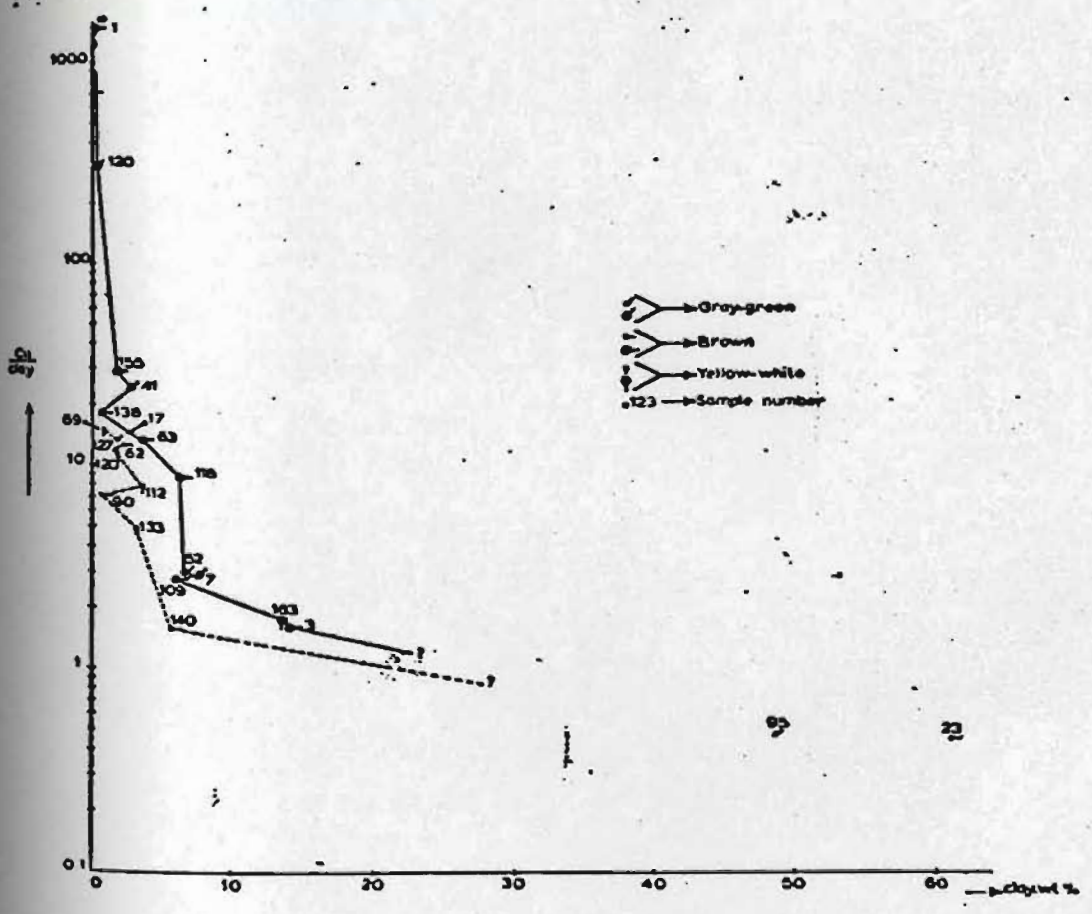

Figure 61. Plot of Cu/clay vs clay, wt.% of nearshore lake sediments (see text).

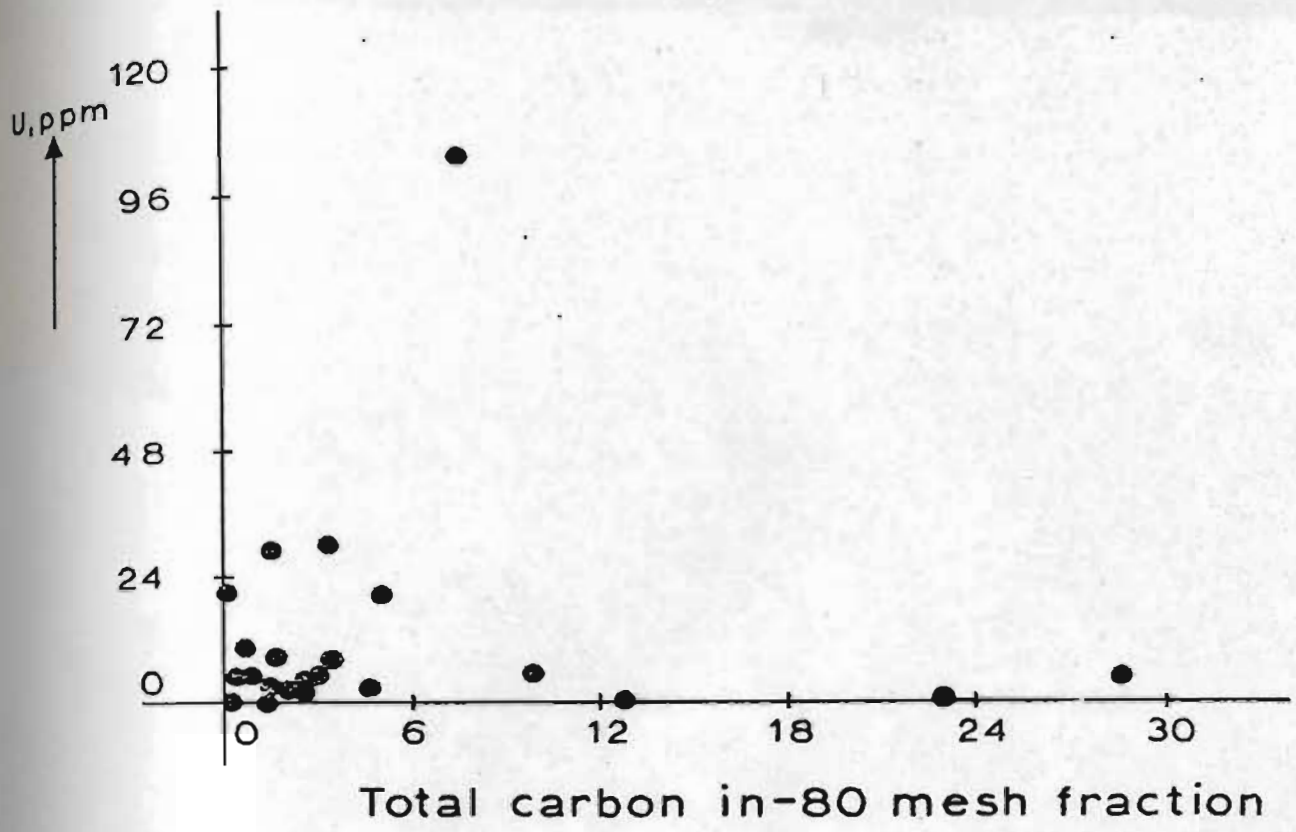

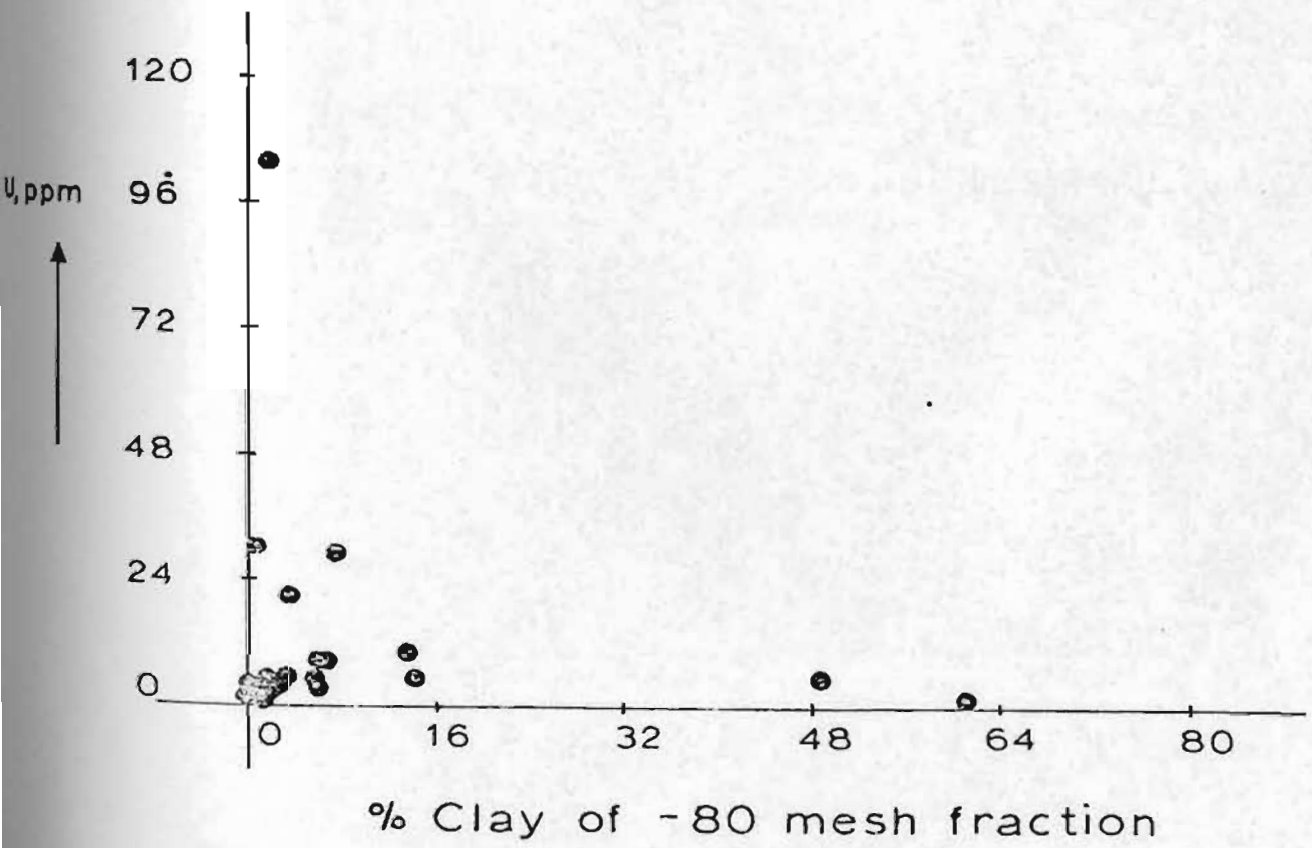

Figure 62. Variations in uranium concentrations with total carbon and clay contents of the -80 mesh fraction of nearshore lake sediment samples.

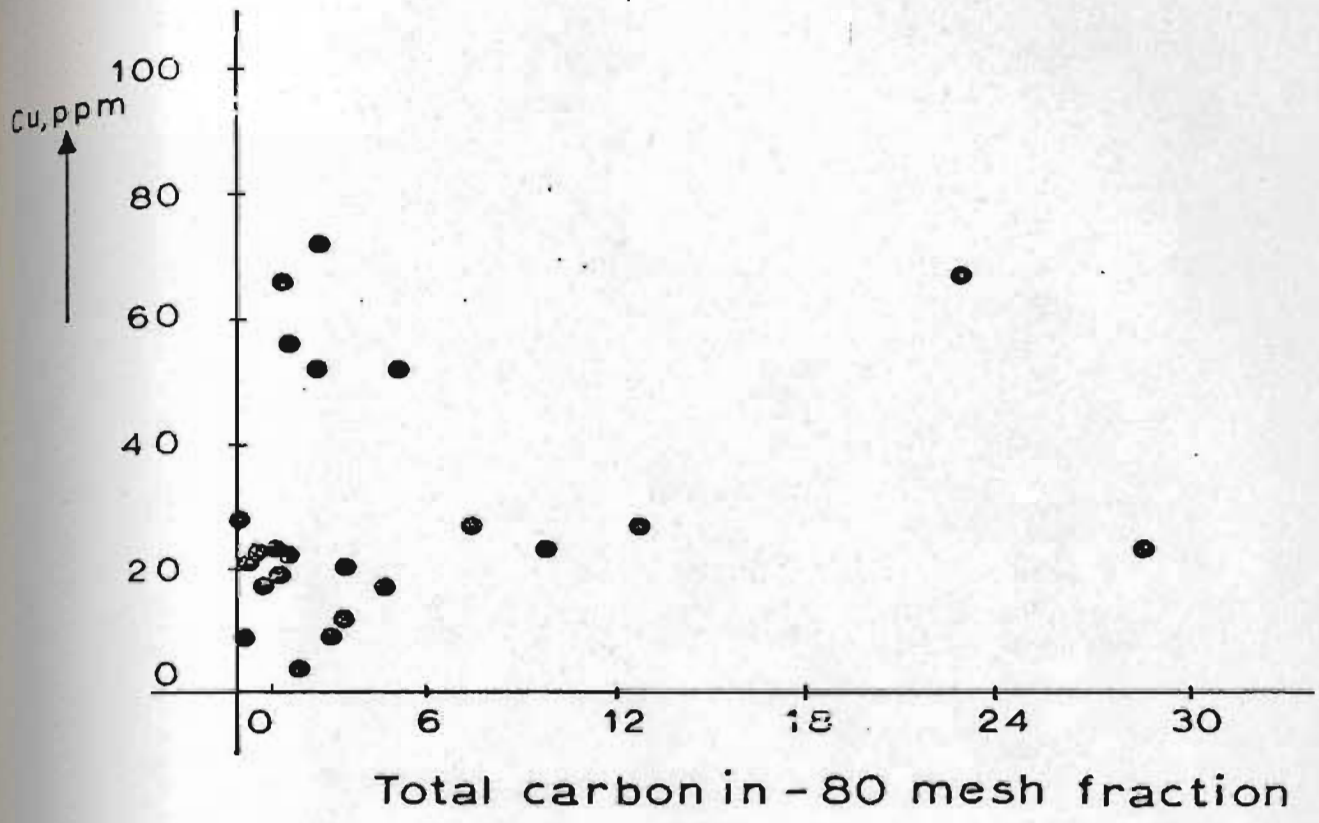

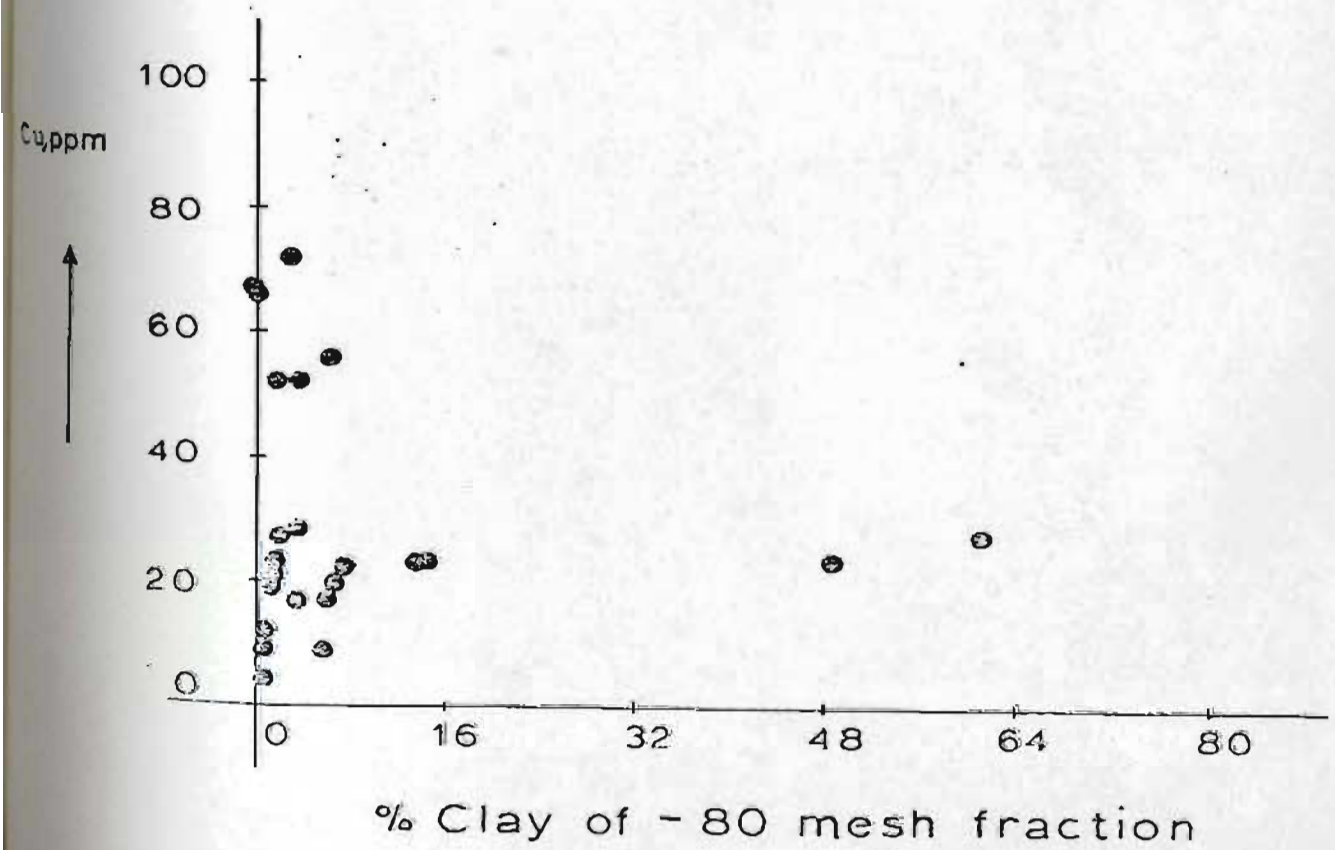

Figure 63. Variations in copper concentrations with total carbon and clay contents of the -80 mesh fraction of nearshore lake sediment samples.

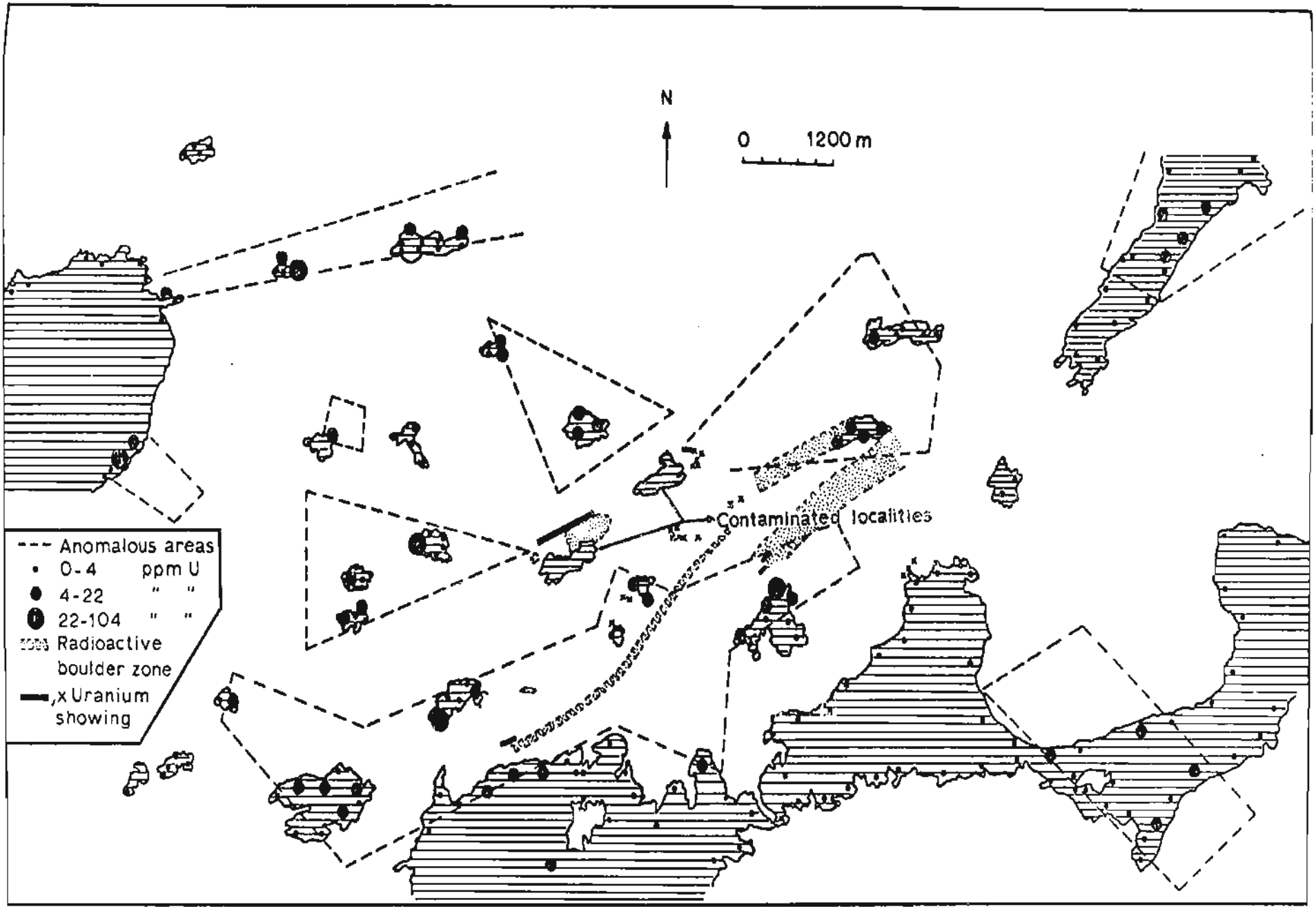

Figure 64. Distribution of uranium in nearshore lake sediments. Dashes outline areas enriched in uranium.

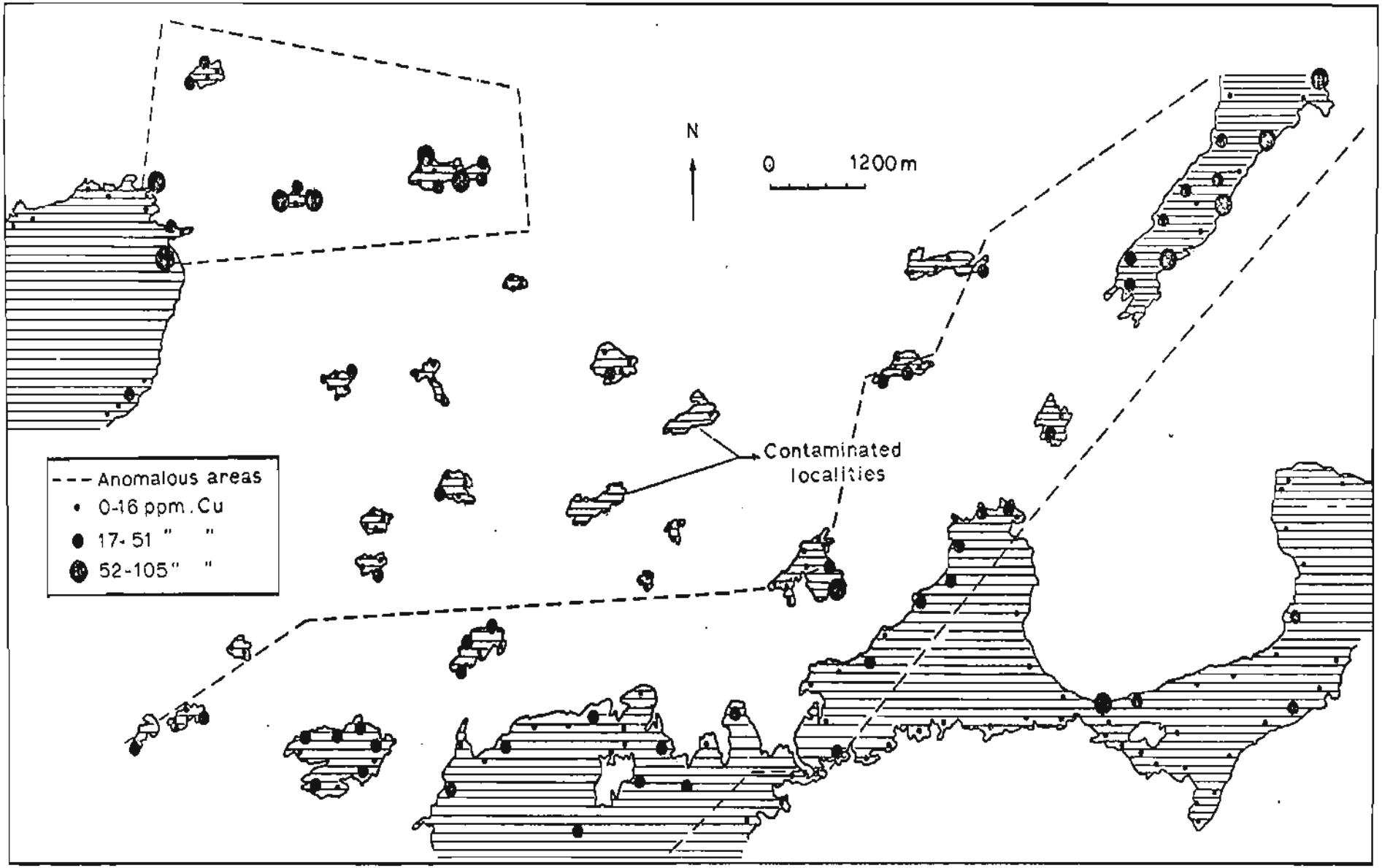

Figure 65. Distribution of copper in nearshore lake sediments. Dashes outline areas enriched in copper.

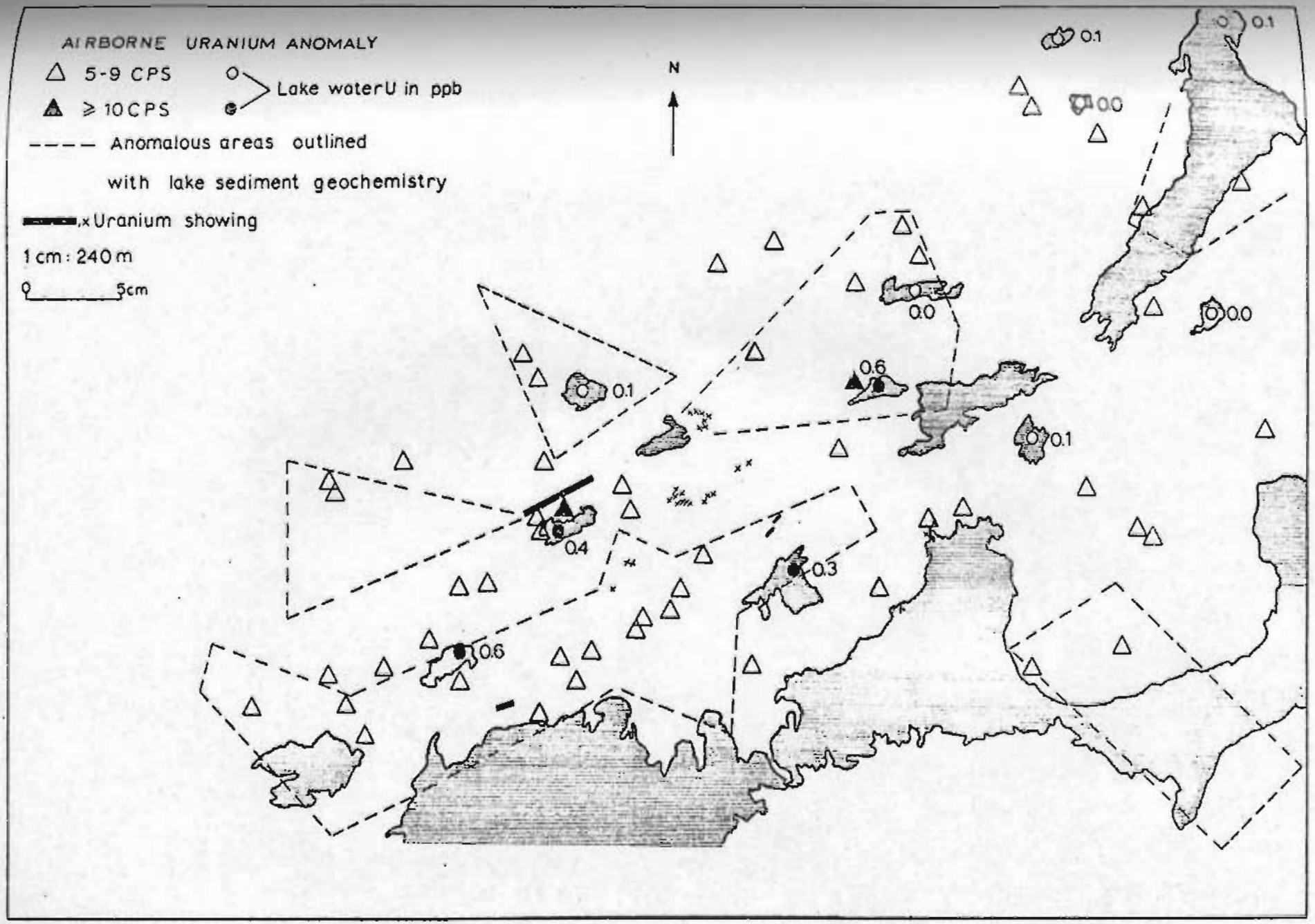

Figure 66. Airborne uranium anomalies and uranium concentrations in lake water. Dashes outline uranium-enriched zones determined by uranium concentrations in nearshore lake sediments.

is warranted in the zones I have outlined. In general there is coincidence among the outlined zones as it is suggested that detailed nearshore lake sediment sampling in rugged terrain, where mineralization is not exposed, is a suitable means for accurate outlining of anomalous zones.

CHAPTER V

SUMMARY AND EXPLORATION APPLICATION

5.1 Summary

The following is a brief summary of the findings of this study:

(1) The investigated uranium deposits have a stratiform shape and the uranium mineralization has been affected by more than a single event.

(2) Rb/Sr plots suggest that the original protolith for some of them was not an igneous rock, e.g. Michelin, M. Ben. The same plots suggest an igneous protolith of some others, e.g. Rainbow, Nash.

(3) The Kitts Pond and Long Island uranium deposits represent "black shale type uranium deposits".

(4) Davidite is possibly the primary uranium mineral in Michelin and McLean uranium deposits.

(5) Opaque submicroscopic inclusions of unknown composition within andradite and quartz and feldspar grains constitute the uranium mineral in M. Ben and Rainbow deposits respectively.

(6) Dark lenses of bituminous material are the uranium carriers in Kitts and Long Island deposits.

(7) High uranium content is associated with high magnetite content in the Witch Lake deposit.

5.2 Exploration Application

On the basis of the findings of this study, further detailed geochemical-geological studies appear justified to outline areas of potential mineralization.

All results obtained from different uranium exploration techniques should be interpreted in conjunction with the glacial geology.

REFERENCES

Adams, J.A.S., Osmond, J.K. and Rodgers, J.J.W., 1959. The geochemistry of thorium and uranium. Physics and Chemistry of the Earth, vol. 6, pp. 298-348.

Adams, J.A.S. and Gasparini, P., 1970. Gamma-ray spectrometry of rocks. Elsevier Publishing Company, Amsterdam, 295 pp.

Allan, R.J., 1971. Lake sediment: A medium for regional geochemical exploration of the Canadian Shield. C.I.M. Bull. 64(Nov.), pp. 43-59.

Allan, R.J., Cameron, E.M. and Durham, C.C., 1973. Reconnaissance geochemistry using lake sediments of a 36,000 square mile area of the northwestern Canadian Shield. Geol. Surv. Can. Paper 72-50.

Allan, R.J. and Richardson, K.A., 1974. Uranium and Potassium distribution by lake sediment geochemistry and airborne gamma-ray spectrometry: A comparison of reconnaissance techniques.

Alley, D.W. and Slatt, R.M., 1975. Drift prospecting and glacial geology in the Sheffield Lake-Indian Pond area, North-Central Newfoundland. Nfld. Dept. of Mines and Energy Report 75-3.

Baranov, V.I. and Du Lieh-T'ien, 1961. Geochemistry of uranium and thorium in the granites of the Kyzyltav massif (central Kazakhstan). Geochemistry, No. 12, pp. 1180-1190.

Barua, M.C., 1969. Geology of uranium-molybdenum bearing rocks of the Aillik-Makkovik Bay area, Labrador. Unpublished M.Sc. thesis, Queen's Univ., Kingston, Ont.

Bates, T.F., Strahl, E.O., Short, N.M., Silverman, E.N. and Camilli, E., 1954. Mineralogy and petrography of the Chattanooga shale. Geol. Soc. Amer. Bull., vol. 65, p. 1230.

Beavan, A.P., 1958. The Labrador uranium area. Geol. Assoc. Can. Proc., vol. 10, pp. 137-145.

Beck, L.S., 1970. Genesis of Uranium in the Athabasca Region and its significance in Exploration. C.I.M. Trans., vol. LXXIII, pp. 59-69.

Bowes, D.R., 1972. Metamorphic environments-chemical mobility. In: The Encyclopedia of Geochemistry and Environmental Sciences. Ed. Rhodes W. Fairbridge. Van Nostrand Reinhold.

Bowie, S.H.U., Ostle, D., Ball, T.K., 1971. Geochemical Methods in the detection of hidden uranium deposits. C.I.M. Special Vol. No. 11.

Boyle, R.W. and Garrett, R.G., 1970. Geochemical Prospecting- a review of its status and future. Earth Science Review, v. 6, pp. 51-75.

Bradshaw, P.M.D., Clews, D.R. and Walker, J.L., 1970. Exploration Geochemistry - Part 4: Primary dispersion. Mining in Canada, 1970.

Bridgwater, D., 1970. Observations on the Precambrian rocks of Scandinavia and Labrador and their implications for the interpretation of the Precambrian of Greenland. Grøn. Geol. Under., Rapport Nr. 28, pp. 43-47.

Christie, A.M., Roscoe, S.M. and Fahrig, W.F., 1953. Preliminary Map, Central Labrador Coast. Geol. Surv. Can. Pap 53-1.

Clark, A.M.S., 1970. A structural reinterpretation of the Aillik Series, Labrador. Unpublished M.Sc. thesis, Memorial University of Newfoundland, St. John's, Newfoundland.

_____, 1974. A reinterpretation of the stratigraphy and deformation of the Aillik Group, Makkovik, Labrador. Unpublished Ph.D. thesis, Memorial University of Newfoundland, St. John's Newfoundland.

Daly, R.A., 1902. The geology of northeast coast of Labrador. Bull. Mus. Comp. Zool. Harvard, 38, Geol. Ser., 5, No. 5.

D'Arcy, George, 1949. Mineralogy of uranium and thorium bearing minerals. U.S. Atomic Energy Commission, Raw Materials Operations Office, 198 pp.

Dawson, J.B., 1964. Reactivity of the Cations in Carbonate Magmas. Proc. Geol. Assn. Canada, vo. 15, pp. 103-113.

Deer, W.A., Howie, R.A., Zussman, J., 1971. An introduction to the rock-forming minerals. Longman, 528 p.

Douglas, G.V., 1953. Notes on localities visited on the Labrador Coast in 1946 and 1947. Geol. Surv. Canada, Paper 53-1, pp. 20-30.

Douglas, R.J.W. (Editor), 1970. Geology and Economic Minerals of Canada. Geol. Surv. Canada, Economic Geol. Rept. 1, 1838 p.

Duncan, D.C., 1953. Reconnaissance investigations for uranium in black shale deposits of the Western States during 1951 and 1952: U.S. Geol. Survey TEI-381, U.S. Atomic Energy Commission, Tech. Inf. Service, Oak Ridge, Tenn.

Dyck, W., 1968. Radon-222 emanations from a uranium deposit. Econ. Geol., vol. 63, pp. 288-289.

_____, 1969. Development of uranium exploration methods using radon. Geol. Surv. Can. Paper 69-46, 26 pp.

Dyck, W. and Smith A.Y., 1968. Use of radon-222 in surface waters for uranium geochemical prospecting. Can. Min. J., April, pp. 100-103.

Fahrig, W.G. and Larochelle, A., 1972. Paleomagnetism of the Michael Gabbro and Possible Evidence of the rotation of Makkovik Subprovince. Can. J. Earth Sci., vol. 9, no. 10, pp. 1287-1246.

Flint, R.F., 1971. Glacial and Quaternary Geology. Wiley

Folk, R.L., 1968. Petrology of sedimentary rocks: Hemphill's, Austin, Texas. 170 p.

Fredrickson, A.F., 1948. Some mechanisms for the fixation of uranium in certain sediments. Science, vol. 108, pp. 184.

Gandhi, S.S., Grasty, R.L. and Grieve, R.A.F., 1969. The geology and geochronology of the Makkovik Bay area, Labrador. Can. J. Earth Sci., vol. 6, no. 5, pp. 1019-1035.

Garrels, R.M., 1953. Some thermodynamic relations among the vanadium oxides and their relation to the oxidation states of the uranium ores of the Colorado Plateaus. Am. Mineralogist, vol. 38, pp. 1251-1265.

Garrett, R.G., 1969. The determination of sampling and analytical errors in Exploration Geochemistry. Econ. Geol., vol. 64, pp. 568-574.

Gerasimovkiy, V.I., 1957. Form taken by uranium in rocks. Atomic Energy, vol. 3, no. 12.

Gill, F.D., 1966. Petrography of molybdenite-bearing gneisses, Makkovik area, Labrador. Unpublished M.A. Thesis, University of Toronto, Toronto, Ontario,

Gingrich, J.E., 1974. Results from a new uranium exploration method. A.I.M.E. preprint.

Greene, B.A., 1972. Geological map of Labrador. Mineral Resources Division, Department of Energy, Mines and Resources, Province of Newfoundland and Labrador.

_____, 1974. An outline of the Geology of Labrador. Mineral Development Division, Department of Mines and Energy, Province of Newfoundland, Information Circular No. 15.

Greene, B.A. and McKillop, J.H., 1972. The first geological map of Labrador. Can. Mining J., vol. 93, pp. 89-97.

Hawkes, H.E. and Webb, J.S., 1962. Geochemistry in mineral exploration. Harper and Row, N.Y., 415 p.

Heier, K.S. and Adams, J.A.S., 1965. Concentration of radioactive elements in deep crustal material. Geoch. and Cosmoch. Acta., vol. 29, pp. 53-61.

Jones, M.J., 1973. Prospecting in areas of Glacial Terrain. Institution of Mining and Metallurgy, London.

Katz, J.J., Rabinowitch, E., 1951. The Chemistry of Uranium. Dover Publications, Inc., New York, 609 p.

King, A.F., 1963. Geology of Cape Makkovik Peninsula, Aillik, Labrador. Unpublished M.Sc. Thesis, Memorial University of Newfoundland, St. John's, Nfld.

King, A.F. and McMillan. , 1975. A mid-Mesozoic Breccia from the Coast of Labrador. Can. J. Earth Sci., vol. 12, no. 1, pp. 44-51.

Kistler, R.W. and Peterman, Z.E., 1973. Variations in Sr, Rb, K, Na, and initial Sr^{87}/Sr^{86} in Mesozoic granitic rocks and intruded wall rocks in central California. Bull. Geol. Soc. Amer., vol. 84, pp. 3489-3512.

Komarov, A.N. and Yu. A. Shukolyukov, 1966. Form taken by uranium in Micas. Geochemistry International No. 11.

Komarov, A.N., Yu. A. Shukolyukov, and N.V. Skororodk[illegible], 1967. Uranium content and distribution in some rocks and minerals examined by Neutron Activation and recording of Fission-Fragment Tracks. Geochemistry, No. 7.

Kranck, E.H., 1939. Bedrock Geology of seaboard region of Newfoundland, Labrador. Geol. Surv. Nfld. Bull., no. 19.

_____, 1953. Bedrock geology of the seaboard of Labrador between Domino Run and Hopedale, Newfoundland. Geol. Surv. Can., Bull. 26.

Krauskopf, K.B., 1967. Introduction to Geochemistry. McGraw-Hill, 721 pp.

Krylov, A. Ya. and Atrashenok, L. Ya., 1959. The mode of occurrence of uranium in granites. Geochemistry, no. 3, pp. 307-313.

Kvalheim, A. (Editor), 1967. Geochemical prospecting in Fennoscandia. Interscience.

Leech, G.B., Lowdon, J.A., Stockwell, C.H. and Wanless, R.K., 1963. Age determinations and geological studies. Geol. Surv. Can. Paper 63-17, pp. 114-117.

Leonova, L.L. and Tauson, L.V., 1958. The distribution of uranium in the minerals of Caledonian granitoids of the Susamyr batholith (Central Tien Shan). Geochemistry, no. 7, pp. 815-826.

Lenova, L.L. and Pogiblova, L.S., 1961. Uranium in minerals of the intrusive rocks of the Kzyl-ompul Mountains (Northern Kirgiziya). Geochemistry, no. 10, pp. 999-1004.

Levinson, A.A., 1974. Introduction to Exploration Geochemistry. Applied Publishing Ltd., Calgary, Alberta.

Lieber, O.M., 1860. Notes on the Geology of the Coast of Labrador. Report of the U.S. Coast Survey.

Lowden, J.A., 1961. Age determinations by the G.S.C. Dept. of Mines and Technical Surveys, Canada, Paper 61-17.

Lundberg, Bo, 1972. Uranium exploration in Arjeplog Area, Northern Sweden.

McKelvey, V.E., Everhart, D.L. and Garrels, R.M., 1955. Origin of uranium deposits. Economic Geology, 50th. Anniversary Volume.

McKie, D., 1966. Fenitization, In: O.F. Tuttle and J. Gittins (Eds.), Carbonatites. Interscience (Wiley), New York, pp. 261-294.

McPhar Geophysics. Geological Applications of Portable Gamma-ray spectrometers. Parts I and II.

Meyer, W.T., 1969. Uranium in lake water from the Kaipokok region, Labrador. Quaterly of the Colorado School of Mines, vol. 64, no. 1.

Morse, R.H., 1971. Comparison of Geochemical Prospecting Methods using Radium with those using Radon and Uranium. C.I.M. Special Vol., no. 11,

Murray, E.G. and Adams, J.A.S., 1958. Amount and distribution of thorium, uranium and potassium in sandstones. Geochim. Cosmochim. Acta, vol. 13, pp. 260-269.

Mursky, G., 1963. Mineralogy, Petrology and Geochemistry of Hunter Bay Area, Great Bear Lake, N.W.T., Canada. Unpubl. Ph.D. thesis, Stanford University.

Neuerberg, G.J., 1956. Uranium in igneous rocks of the U.S.A. Proc. Intl. Conf. Peaceful Uses Atomic Energy. vol. 6.

Nichol, I.and Bjorklund, A., 1973. Glacial geology as a key to geochemical exploration in areas of glacial overburden with particular reference to Canada. J. Geochem. Explor., vol. 2, pp. 133-170.

Nicholls, G.D., 1958. Sedimentary Geochemistry. Petroleum , vol. 21, pp. 316-320, 324.

Nicholls, G.D. and Loring, D.H., 1962. The geochemistry of some British Carboniferous sediments. Geoch. et Cosmoch. Acta, vol. 26, pp. 181-223.

Paarma, H., 1970. A new kind of carbonatite in North Finland, The Sokli Plug. Lithos, vo. 3, pp. 129-133.

Packard, A.S. Jr., 1891. The Labrador Coast, N.D.C., Hodges, New York.

Page, L.R., 1960. The Source of Uranium in Ore Deposits. Inter. Geol. Cong., 21st. Sess., pp. 149-164.

Peacock, J.D. and Williamson, R., 1962. Radon determining as a prospecting technique, Inst. Min. Met. Trans., vol. 71, pp. 75-85.

Perio, P., 1953. Chimie des mineraux uranifères. Bull. Soc. chim. France, No. 3.

Phair, G., 1952. Radioactive tertiary porphyries in the Central City district, Colorado, and their bearing upon pitchblende deposition. U.S. Geol. Survey TEI-247, U.S. Atomic Energy Comm., Tech. Inf. Service, Oak Ridge, Tenn. Nuc. Sci, Abs., vol. 6, p. 776

Picciotto, E.E., 1950. Distribution de la radioactivité dans les roches eruptives. Soc. belge de Geol. Bull., 59, pp. 170-198.

Pliler, R. and Adams, J.A.S., 1962. The distribution of the thorium, uranium and potassium in the Mancos shale. Geochim. et Cosmochim. Acta, vol. 26, pp. 1115-1135.

Robinson, S.C., 1955. Autoradiographs as a means of studying distribution of radioactive minerals in thin section. Amer. Mineralogist, vol. 37, pp. 544-547.

Rodgers, J.J.W. and Adams, J.A.S., 1969. Thorium: In Handbook of Geochemistry, Ed. K.H. Wedepohl II-I. Springer-Verlag.

Ruzicka, V., 1971. Geological Comparison between East European and Canadian Uranium deposits. Geol. Surv. Can., Paper 70-48.

Sakrison, H.C., 1971. Rock geochemistry - its current usefulness on the Canadian Shield. Can. Inst. Min. Metall. Bull., Nov., pp. 28-31.

Slatt, R.M. and Sasseville, D.R. (in press). Trace element geochemistry of detrital sediments from Newfoundland inlets and the adjacent continental margin: Application to provenance studies, mineral exploration, and Quaternary marine stratigraphy. In: Kramer, J.R. (Ed.) Environmental aspects of mineralogy and sedimentary geochemistry. Miner. Assoc. Can. Symposium, Waterloo, Ontario.

Smith, A.Y. and Lynch, J.J., 1969. Uranium in soil, stream sediment and water. Geol. Surv. Can. Paper 69-40.

Smith, A.Y. and Dyck, W., 1969. The application of radon methods to geochemical exploration for uranium. Paper presented at the annual C.I.M. convention, Montreal. Abstract in C.I.M. Bull., vol. 62, no. 683, p. 215.

Soonawala, N.M., 1974. Data processing techniques for the Radon method of uranium exploration. Can. Min. Metal. Bull., April, 1974.

Steinhauer, H., 1814. Notes on the geology of the Labrador coast. Trans. Geol. Soc., II, pp. 488-491.

Stevens, D.N., Rouse, G.E. and DeVoto, R.H., 1971. Radon-222 in soil gas: Three Uranium Exploration Case Histories in the Western United States. C.I.M. Special vol. no. 11.

Stevenson, I.M., 1970. Rigolet and Groswater Bay Map-areas, Newfoundland (Labrador). Geol. Surv. Can. Paper 69-48.

Stockwell, C.H., 1964. Age determinations and Geological studies. Geol. Surv. Can. Paper 64-17, Pt. II.

Strøm, K.M., 1948. A concentration of uranium in black muds. Nature, vol. 162, p. 922.

Sutherland, D.S., 1965. Potash-Trachytes and Ultra-potassic rocks associated with the carbonatite complex of Toror Hills, Uganda. Mineral. Mag., vol. 35, pp. 363-378.

Sutton, J.S., 1972a. Notes on the geology of Labrador. Memorial University of Newfoundland Geological Report No. 5.

_____, 1972b. The Precambrian gneisses and supracrustal rocks of the western shore of Kaipolok Bay, Labrador, Newfoundland. Can. J. Earth Sci., vol. 9, no. 12, pp. 1677-1692.

Sutton, J.S., Marten, B.E., and Clark, A.M.S., 1971. Structural History of the Kaipokok Bay Area, Labrador, Newfoundland. Geol. Assoc. Canada Proc., vol. 24, pp. 103-106.

Sutton, J.S., Marten, B.E., Clark, A.M.S., and Knight, I., 1972. A correlation of the Precambrian supracrustal rocks of coastal Labrador and southwestern Greenland. Nature Phys. Sci., vol. 238, pp. 122-123.

Svenke, E., 1956. The occurrence of uranium and thorium in Sweden. Intern. Conf. Peaceful Uses Atomic Energy, Proc. 6, pp. 198-199.

Swanson, V.E., 1953. Uranium in the Chattanooga shale (Abs.). Geol. Soc. Amer. Bull., vol. 64, p. 1481.

Taylor, F.C., 1971. A revision of Precambrian structural provinces in northeastern Quebec and northern Labrador. Can. J. Earth Sci., vol. 8, no. 5, pp. 579-584.

_____, 1972a. A revision of Precambrian structural provinces in northeastern Quebec and northern Labrador: Reply Can. J. Earth Sci., vol. 9, no. 7, pp. 930-932.

_____, 1972b. The Naine Province. In: Variations in Tectonic Styles in Canada (Price, R.A. and Douglas, R.J.W., editors). Geol. Assoc. Canada, Spec. Paper no. 11, pp. 435-452.

_____, 1972c. Reconnaissance geology of a part of the Precambrian shield, northeastern Quebec and northern Labrador, Part III. Geol. Surv. Canada Paper 71-48.

Taylor, S.R., 1962. The chemical composition of australites. Geochim. et Cosmoch. Acta, vol. 26, pp. 685-722.

_____, 1965. The application of trace element data to problems in Petrology. Physics and chemistry of the Earth, vol. 6, p. 133.

Turekian, K.K. and Wedepohl, K.H., 1961. Distribution of the elements in some major units of the Earth's Crust. Bull. Geol. Soc. Amer. vol. 72, p. 175.

Turner, F.J., 1968. Metamorphic petrology. McGraw-Hill Book Company, New York.

Vinogradov, A.P., 1962. The average contents of the chemical elements in the main types of eruptive rocks. Geochemistry, vol. 7.

Von Eckermann, H., 1961. The petrogenesis of the Alnö alkaline rocks. Bull. Geol. Inst. Uppsala, vol. 40, pp. 25-36.

Wanless, R.K. and Loveridge, W.D., 1972. Rubidium-Strontium Isochron Age studies: Report I. Geol. Surv. Can. Paper 72-23.

Wedepohl, K.H., 1971. Geochemistry. Holt-Rinehart-Winston. 231 p.

Wheeler, E.P., 1933. A study of some diabase dikes on the Labrador coast. J. Geol., vol. 41, no. 4, pp. 418-431.

_____, 1935. An amazonite aplite dike from Labrador. Amer. Miner., vol. 20, no. 1, pp. 44-49.

Whitehead, W.L., 1952. Studies of the effect of radioactivity in the transformation of marine organic materials into petroleum hydrocarbons: In Am. Petroleum Inst., Fundamental research on occurence and recovery of petroleum, 1950-1951. pp. 192- 201.

Yermolayev, N.P. and Zhidikova, A.P., 1966. Behavior of U in progressive metamorphism in the western part of the Aldan Shield. Geokhimiya, no. 8.

Yermolayev, N.P., 1971. Processes of redistribution and extraction of Uranium in progressive metamorphism. Geokhimiya, No. 8, pp. 949-962.

_____, 1973. Uranium and thorium in regional and contact metamorphism. Geokhimiya, No. 4, pp. 551-558.

APPENDIX I

FIELD, LABORATORY AND STATISTICAL METHODS

FIELD, LABORATORY AND STATISTICAL METHODS

Sample Collection and preparation

Most samples were collected from the strongly mineralized areas. Samples collected for analysis were washed, logged and put into clean sample bags prior to crushing. All samples were crushed according to the following procedure:

1) Each sample was broken into chips using a small sledge hammer on an iron thick board. A slab was saved for thin section.

2) A clean representative sample of chips was crushed to 1-2 cm or smaller pieces in a Denver steel jaw crusher.

3) A representative sample of these pieces was crushed in a tungsten carbide Siebtechnik swing mill for three minutes producing a rock powder of -100 mesh, as determined by random sieving checks.

Analytical procedures

Estimation of Mode. Modal analyses were carried out on a point-counter. A total of 3000 counts were made on two thin sections from each showing: One thin section from the low mineralized rock and one thin section from the high mineralized rock.

Trace element analyses. Zirconium, strontium, rubidium, zinc, copper barium, niobium, nickel and chromium were determined on pressed powder discs using a Philips 1220-C Automatic X-ray fluorescence spectrometer.

The sample discs were prepared in the following manner:

1) 1.5 g of rock powder was thoroughly mixed with two to three drops of N-30-88 Mowiol binding agent until the colour was uniform.

2) Using a boric acid backing, this powder was pressed into a disc for one minute at 15 tons per square inch.

The samples of Michelin, Rainbow and Witch Lake uranium showings were analysed for U and Th in IAEA laboratory at Seibersdorf by DGS, X-ray fluorescence (XRF), Neutron Activation Analysis (NAA) and fluorimetry, as appropriate. Differential gamma spectrometry (DGS) compensates for the disequilibrium of daughter products with the uranium (Adams and Gasparini, 1970). In addition all except those containing less than 0.01% U were analysed by XRF. Where the two methods produce similar results, no further work was done and the mean reported. Where the difference was probably significant, an additional measurement was made by NAA and the mean of all three measurements reported. Fluorimetry was only used to spot-check a few of the samples with low uranium concentrations (Otto Suschny, IAEA, personal communication).

The samples from all the other showings were analysed for U with fluorimetry.

Statistical procedures and methods of data presentation.

Upon completion of the analytical program, the trace element results were punched on computer cards according to the format shown

below. Means, standard deviation and 95% confidence interval for Mean were calculated for all elements in each deposit. A standard statistical program was then employed to plot trace element variation diagrams in each uranium deposit using a Hewlett-Packard Model 20 desk computer-plotter.

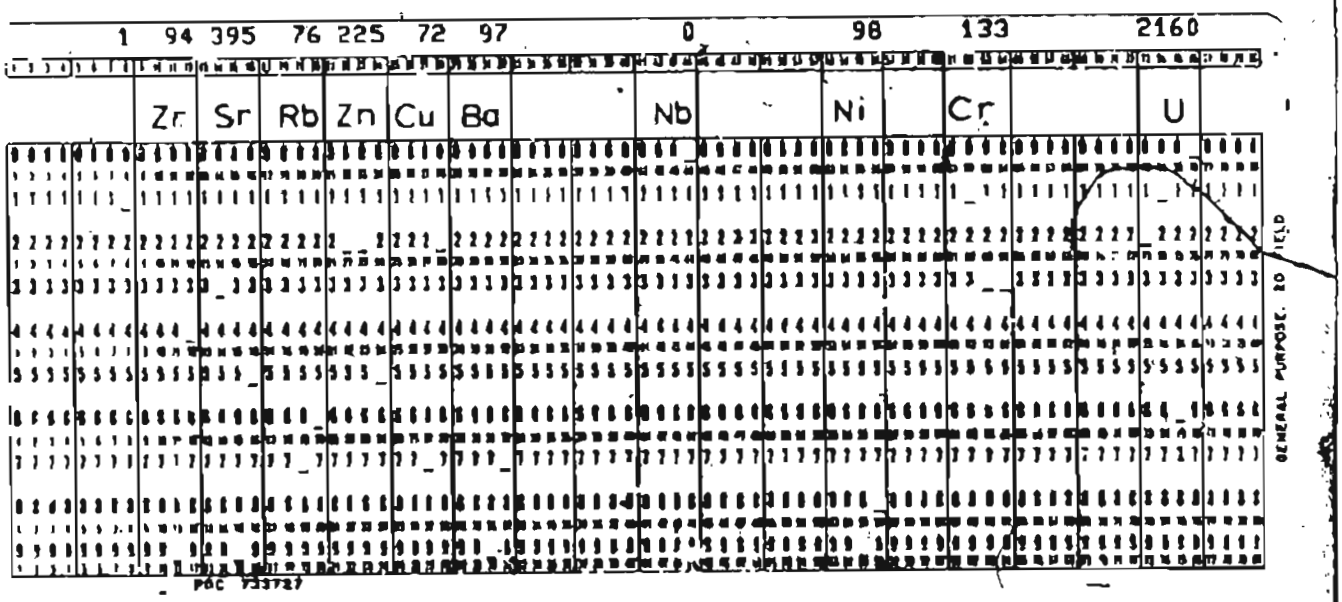

APPENDIX II

FLUORIMETRY

Special Equipment

Fluorimetry dishes: Platinum, approximately 18 mm wide and 3 mm deep. When not in use they should be stored in a glass beaker under distilled water.

Pipet: For measuring 0.10 ml and 0.20 ml aliquots; a 100 μl and a 200 μl microchemical pipet equipped with syringe attachment.

Aluminum tray: 5 1/2 in. X 3 1/2 in. X 5/32 in.; containing 24 holes (6 rows of 4 each) each 5/8 in. in diameter.

Burner: Rotating propane burner (Modified Fletcher radial burner).

Shaker: Special shaker for mixing the solutions.

Hood: A standard fume hood lined above the fire.

Fluorimeter: Jarrell-Ash Galvanek-Morrison Fluorimeter.

Reagents

Aluminum nitrate salting solution: Transfer 5 lb. of reagent grade aluminum nitrate, having a low uranium content, to a 4 liter beaker. Add 1150 ml

H_2O, cover, place the beaker on a combined hot plate and magnetic stirrer, and heat, with stirring, until solution is complete. Adjust the concentration by evaporation or dilution to give a solution which boils at 130°C and transfer to a round bottom flask. The solution should be kept saturated

Ethyl Acetate

Solium fluoride pellets: 98% NaF, 2% LiF = prepared pellets, each containing 0.588 g NaF and 0.012 LiF, can be obtained. Those supplied by:

"Analoid"
Ridsdale and Co. Ltd.
Middlesbrough, England

Standard uranium solutions

Weigh 210 mg of uranyl nitrate $(UO_2(NO_3)_2 \cdot 6H_2O$ into a 100 ml volumetric flask. Add approximately 25 ml of 4N nitric acid and dissolve the uranyl nitrate. Dilute to the mark with 4N nitric acid and mix well. This solution should be prepared every two weeks since uranium salts tend to precipitate. This solution contains 1000 μg/ml uranium. From this solution prepare a standard solution containing 0.1 μg/ml by dilution in the following steps:

Standard used	Aliquot taken	Diluted to*	New Standard**
1000 μg/ml (1000 ppm)	10 ml	100 ml	100 μg/ml (100 ppm)
100 μg/ml (100 ppm)	10 ml	100 ml	10 μg/ml (10 ppm)
10 μg/ml (10 ppm)	10 ml	100 ml	***1 μg/ml (1 ppm)
1 μg/ml (1 ppm)	10 ml	100 ml	***0.1 μg/ml (0.1 ppm)

Place 12 test tubes into rack and add standard solution

1. 0.25 ml of stock 10 ppm standard solution
2. 0.50 ml " " " " " "
3. 0.75 ml " " " " " "
4. 1.00 ml " " " " " "
5. 1.50 ml " " " " " "
6. Blank

} Duplicate standards

Add 5 ml of saturated aluminym nitrate plus 5 ml of ethyl acetate.

Shake for 20 min. in shaker. Let settle for 5 min. After 5 min. two layers are formed in the tube: One layer of aluminum nitrate (lower layer) and one layer of ethyl acetate (upper layer). Uranium is concentrated in the upper layer (ethyl acetate).

Put one sodium fluoride pellet into each platinum dish.

Pipette 0.2 ml of standard solution (from the upper layer of the solution) in the platinum dish on the top of the pellet.

Evaporate to complete dryness on a hot plate.

---

*Dilute with 4 N HNO_3
**Make the solutions freshly, twice weekly
***Prepare these standards only if it is necessary to increase the range of standards.

Transfer platinum dishes on the burner and fuse 90 seconds after the pellet has been melted. Total fusion time 3 minutes.
Samples are cooled in a dessicator for twenty minutes, and the fluorescence read on the fluorimeter.

Preparation of Standard Curve

1. Having calibrated the fluorimeter by using the "blank" and the highest standard, proceed to read the standard discs. Reread the blank and the highest standard and adjust the instrument to correct for any drift that might have occurred.

2. Prepare a graph of scale reading as ordinate against the uranium standards as abscissa, the points of which should fall on a straight line (use arithmetic scale). Draw lines at 5 per cent above and below the first line. Reject those standards which do not fall within these 5 per cent limits. If more than two standards fall outside the ± 5 per cent range, repeat the entire set.

Calibration of the fluorimeter

1. Turn the "sensitivity" switch fully counter-clockwise.
2. Switch the instrument power switch to "on" and allow 20-30 minutes warm up time.
3. Insert the highest standard (containing 1.5 ml) in the dual-flux sample dish and push the slide into the reading position.

4. Increase the sensitivity control (usually to step 5 or 6) while depressing the 0.1 scale key until the meter reads approximately mid-scale.
5. Set the meter to read 60 by adjusting the "Fine Volts" control.
6. Pull the sample slide out to the loading position and rotate the "zero" adjusting knob until the meter reads zero.
7. Push empty slide into the reading position. Depress the highest sensitivity key (0.01) and adjust the locknut control marked "Background" until the meter reads zero.
8. Repeat steps 5, 6 and 7 alternately until the readings are correct and no change occurs. This should be done at least three times. The instrument is not set up to read unknown samples.
9. When the sample slide is pushed in, the lowest sensitivity scale is automatically switched in. Operate the scale keys, starting with the highest valued key going from right to left. This is done to prevent the meter from being damaged by a high concentration sample.

Uranium determination in core and rock samples

1. Weigh 1 gm portion of pulverized sample into a 100 ml glass beaker.
2. Digest with 20 ml of concentrated HNO_3 plus 30 ml of distilled H_2O for 2 hours on hot plate at medium heat.
3. Add 50 ml H_2O and boil gently for 30 minutes.

4. Remove from plate and cool, then pour contents into a 100 ml volumetric flask. Wash beaker and funnel well with H_2O. Fill flask to mark, stopper and shake well.
5. Let settle overnight
6. Pipette exactly 1 ml of solution into a test tube. Add 5 ml of aluminum nitrate solution, plus 5 ml of ethyl acetate. Stopper test tube and shake in shaker for 20 min.
7. Remove from shaker and let settle for 5 min. After 5 min. two layers are formed in the test tube: One layer of aluminum nitrate (lower layer) and one layer of ethyl acetate (upper layer). Uranium is concentrated in the upper layer (ethyl acetate).
8. Wash acid off platinum dish with water. Place dish in drying pan.
9. Add fusion pellet (sodium fluoride-lithium fluoride 98:2).
10. Transfer by use of a 200 μl automatic micropipet, 0.2 ml of sample from the upper layer of the solution (ethyl acetate) into the platinum dish. Evaporate to complete dryness on a hot plate. *** When the sample has an exceptionally high uranium content, i.e. when the needle in the dial of the fluorimeter is off the scale then transfer 0.1 ml of sample and multiply the calculated uranium value times 2.
11. Remove from pan and fuse on the burner. Pellets should fuse in 1 1/2 min. Total fusion time is 3 min.
12. Let platinum dish and contents cool, transfer to aluminum tray and into the dessicator and leave them there for 20 min.

13. Place in instrument room for reading of results.

Calculations:

$$\frac{\text{av. unknown reading - blank}}{\text{av. standard reading - blank}} \times \text{Factor} \times 1.1792 = \% \; U_3O_8$$

The factor is calculated as follows:

Sample: 1 gm ⟶ 100 ml = .01 gm/ml

1 ml ⟶ 5 ml acetate = 0.002 gm/ml

0.2 aliquot = 0.0004 gm/ml

Standard: 1.5 ml of 10 ppm ⟶ 5 ml acetate = 3 ppm U

0.2 ml aliquot = 0.4 ppm

Factor: $\frac{0.4}{0.0004} = 1000$

$$\frac{\text{av. unknown reading - blank}}{\text{av. standard reading - blank}} \times 1000 = \text{U, ppm}$$

Conversion factors

$$U_3O_8 \underset{1.1792}{\overset{0.8480}{\rightleftharpoons}} U$$

Depending on the range of uranium content of the samples, standards and calculations should be done as appropriate. The method described above was developed by Sydney Abbey of the Geological Survey of Canada, and was modified by the Atlantic Analytical Services, Springdale, Newfoundland.

Fusion technique (Step 11, page 204)

1. Remove platinum dishes from pan (or hot plate) and place them in order on the platinum holders in the burner.
2. Turn on the motor of the burner in medium speed so that the dishes will start rotating above the burners.
3. Turn on gas and light the fire; at the same time start measuring the time (total fusion time 3 minutes). At the end of the second minute make sure that the pellets have been fused.
4. At the end of the third minute turn off the gas and after one minute the motor.
5. When the dishes are cooled transfer to aluminum tray, always in order and place in dessicator for twenty minutes.
6. Take out aluminum tray and using a tweezer tip over the platinum dishes, put the pellets in the fluorimeter and measure fluorescence.

Percautions

1. Two Sylvania black light blue type 360 fluorescent lamps are sued to provide UV light. These lamps should provide uniform light intensity for five to six months under normal use. Under everyday use where the instrument is left on at all times, it is recommended that these lamps be changed every six weeks.
2. Care must be taken to assure cleanliness of the platinum ware for two reasons: Firstly, platinum is an expensive commodity which can be lost through misuse. Secondly, contamination, particularly

by quenching elements, can be carried from sample to sample on the platinum dishes. After each use dishes should be soaked in 1:1 HCl, rinsed with tap water, then with metal-free water. Stains which are not removed in this way may be eliminated by heating the platinum dishes from 3-4 min. in the burner. Also stains which are not removed in this way may be eliminated by fusing 3 g of potassium pyrosulphate in the dish followed by cleaning with HCl as above.

3. Attention must be paid to spurious fluorescence from other materials in the laboratory. Dust, paper and cloth lint, and vaseline are among common materials which fluoresce strongly under UV light. Care must be taken to keep such materials away from the sample receptacle of the fluorimeter. Similarly chips from the flux discs must be cleaned out of the fluorimeter sample slide frequently.

4. The background readings on blank flux discs may increase with time. This may be due to contaminants mentioned in 3 above. It may also be due to scratches on the black coating of the sample receptacle, caused during loading and unloading of the sample discs with tweezers. Should this occur the coating must be renewed.

5. On long-continued heating, platinum becomes gray as a result of recrystallization, which begins at the surface, if allowed to continue, the dish may eventually develop cracks; the deterioration can be stopped by burnishing the metal with quartz sand.

In the case of a dish, this treatment may well be repeated after ever five or six ignitions.

APPENDIX III

PIPETTE ANALYSIS

PIPETTE ANALYSIS

The common method of grain size analysis of mud (finer than 4 ϕ fraction) is the pipette method.

The principle of pipette analysis is based on Stokes Law of Settling Velocity. Particles in a solution of known temperature, viscosity, and density will settle through the column at a constant velocity which is a function of grain size (for the purpose of standardization it is assumed that particles are spherical-shaped- an erroneous but necessary assumption). Large particles settle faster than smaller particles. By calculating settling velocities for particles of known diameter it is possible to determine how long it will take for particles of a given size to travel a given distance through a column of solution. Therefore it is possible to collect, with a pipette, selected size fractions, as they settle through the column. By determining the weight of each size fraction the grain size distribution is determined.

1. The lake sediment samples contained gravel (pebble and granule), sand and mud. Geochemical analyses were conducted on -80 mesh fraction. It was necessary to separate this fraction from the rest of the sample.
2. The dry sample was placed in the -80 mesh sieve and was sieved on the vibrator for 25 minutes. The coarser fraction which was retained on screen was discarded.
3. An appropriate amount of the -80 mesh of each one sample was placed in 4L beakers and covered with 15% H_2O_2 to remove organic

matter and disaggregate mud. The beakers were covered with a watch glass, placed in heated water bath until effervesence ceased (2 hours).

4. Using cold water, the samples were wet sieved through stainless steel 4 ϕ (.063 mm) screen. Sand was retained on the screen and mud in a plastic washpan. The wet sieving was continued until water flowed clear through the screen. All of the mud was poured back into rinsed beakers and a capful of 1N $MgCl_2$ was added. This helped the floculation of mud. The beakers were covered and stored for 4 days.

5. Using a squirt bottle, the sand was washed from the sieve into evaporating dishes. The sand was let to settle, the water was decanted and the evaporating dishes were put into the oven in order to dry the sand.

6. After 4 days most of the water was siphoned off from the 4L beakers.

7. 500 ml of 10 gm/L Calgon was added to a labelled squirt bottle.

8. Using the squirt bottle, each one sample was transferred to a malt mixer and filled to 2/3 with the Calgon solution.

9. Each sample was dispersed for 10 minutes on the malt mixer.

10. Each sample was transferred from the malt mixer to a 1 L cylinder using the squirt bottle. The remainder of the 500 ml of 19 gm/L Calgon solution was poured into the cylinder. There was 500 ml of Calgon solution in the cylinder.

11. The cylinder was brought to volume with distilled water. The concentration of Calgon solution in the cylinder was now 5 gm/L (500 ml water plus 500 ml 10 gm/L Calgon solution).

12. Forty six beakers were weighed to three decimal places.

13. Twenty three beakers were used for the 4 ϕ fraction (silt + clay) and 23 for the 8 ϕ fraction (clay).

14. Withdrawl times and depths for the water temperature were given in the sedimentology Laboratory.

15. The sample was stirred for 1 minute with a stirring rod. The end of 1 minute is equal to T = 0 and all withdrawls were made at times determined from this base.

16. Each 20 ml pipette fraction was placed into a labelled pre-weighed beaker. After emptying a pipette it was washed with 20 ml distilled water and added to the fraction in the beaker.

17. Beakers were placed in the drying oven in order to get dried overnight.

18 When dry, each beaker was weighed and taking into consideration that

$$\begin{array}{r} \text{Silt + clay } (> 4\ \phi) \\ - \text{ clay } (> 8\ \phi) \\ \hline \text{silt } 4\text{-}8\ \phi \end{array}$$

calculations were made as appropriate.

Pretreatment and analytical method for Cu

OVEN DRIED, SIEVED, -80 MESH, STORED IN PLASTIC VIALS

SPLIT INTO 3 SUBSAMPLES

0.1 GM INTO 20 ML TEST TUBE

DIGESTION

10 ML IN HNO_3

THEN 1 ML IN HCL

PLACE IN 100°C WATER BATH FOR 1.5 HOUR. STIR WITH VORTEX ACTION STIRRER EVERY 30 MINUTES

COOL, THEN BRING TO 20 ML WITH DISTILLED H_2O, STIR WITH VORTEX ACTION STIRRER

ATOMIC ABSORPTION ANALYSIS, WHOLE SAMPLE SEE APPENDIX

PPM, Cu

0.01-0.25 GR (DEPENDING ON THE VISUALLY RECOGNISED AMOUNT OF ORGANIC CONTENT OF THE SAMPLE), INTO DISPOSABLE CRUCIBLE. ADD TIN FLUX AND IRON CHIP ACCELERATOR

FIRE AT 3000° IN LECO INDUCTION FURNACE

% CARBON

HEAVY MINERAL SEPARATION WITH TETRABROMOETHANE (Sp. G.= 2.92)

SPIN WITH CENTRIFUGE AT 2000 RPM FOR 3 MINUTES

ATOMIC ABSORPTION ANALYSIS HEAVY FRACTION

ELEMENTAL ANALYSIS OF EACH FRACTION

APPENDIX IV

AUTORADIOGRAPHY

AUTORADIOGRAPHY

The method described here was developed by Robinson (1955). The thin sections were made without a cover glass and with all the Canada balsam removed from the exposed surface of the rock slice. In order to facilitate orientation of the thin section on the autoradiograph, two or three single grains of uraninite (or other radioactive substance) were cemented in the Canada balsam around the rock slice and ground down with the rock slice.

For exposure, the rock surface was placed against the emulsion side of the plate or film and held there under light pressure. The mount was then put away in total darkness for exposure. Time of exposure depends on the radioactivity of the minerals in the rock. It has been suggested (Robinson, 1955) that for uraninite, an exposure of 3 days is ample, but for weakly radioactive minerals, exposures of up to a month in duration, may be necessary.

Areas of alpha tracks from the uraninite grains will be clearly visible to the unaided eye and by means of these, the thin section may be roughly oriented and held in position, back to back, on the autoradiograph, by rubber cement. With the mount lying on the microscope stage, rock slice down, emulsion side up, the thin section was precisely oriented on the autoradiograph under a low-power objective, before the cement sets.

The mount was studied under a medium-power objective such that

the alpha tracks are out of focus when the microscope was focussed on the rock slice and vice versa.

It was best to set the focus on one of the dense patches of tracks from the uraninite and then traverse the mount to look for the weaker centres of tracks. When these are found, it was only necessary to focus down to the rock slice in order to identify the mineral that has caused them. If the mineral is opaque, it is often possible to dig enough of it out of the section with a needle, to be mounted on a glass fibre coated with vaseline, for determination by X-ray diffraction.

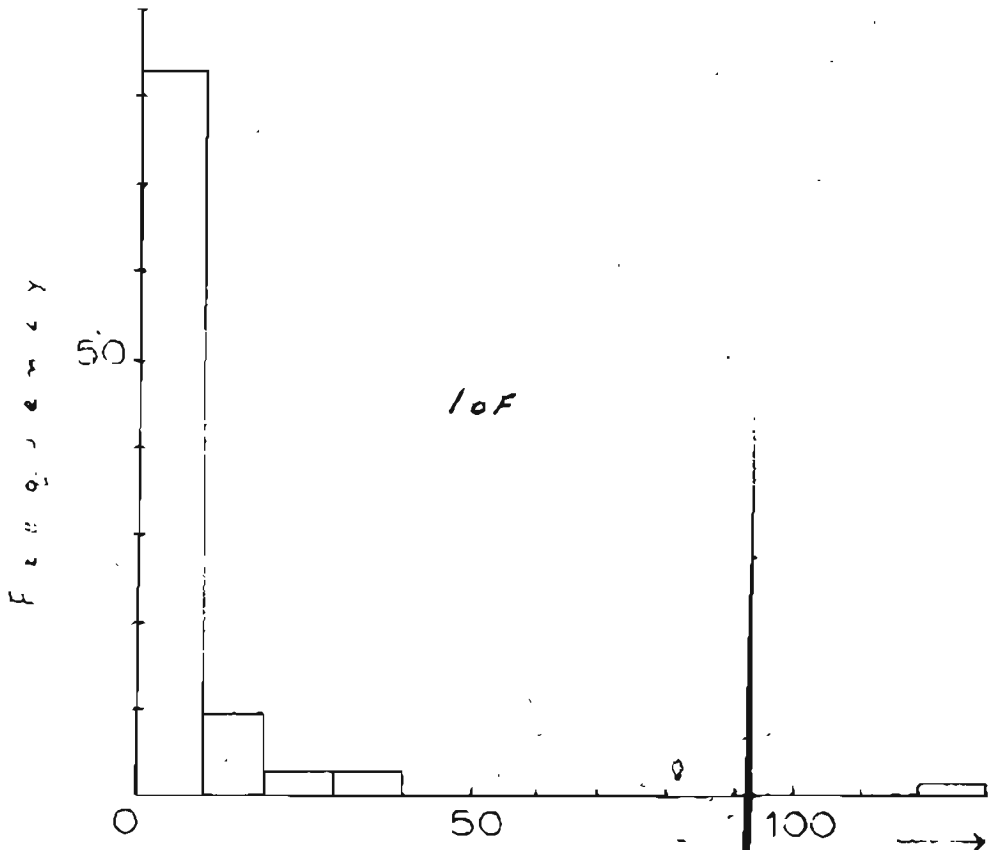

1 of

20W

8 .9 1 .4

3 .0 .0 .0

.0 .1 .0

0 2 .0

40
10
20

20

8 Radioactive boulder

Radioactive boulder zone

0 2 .9 .1

.3 .0 .2

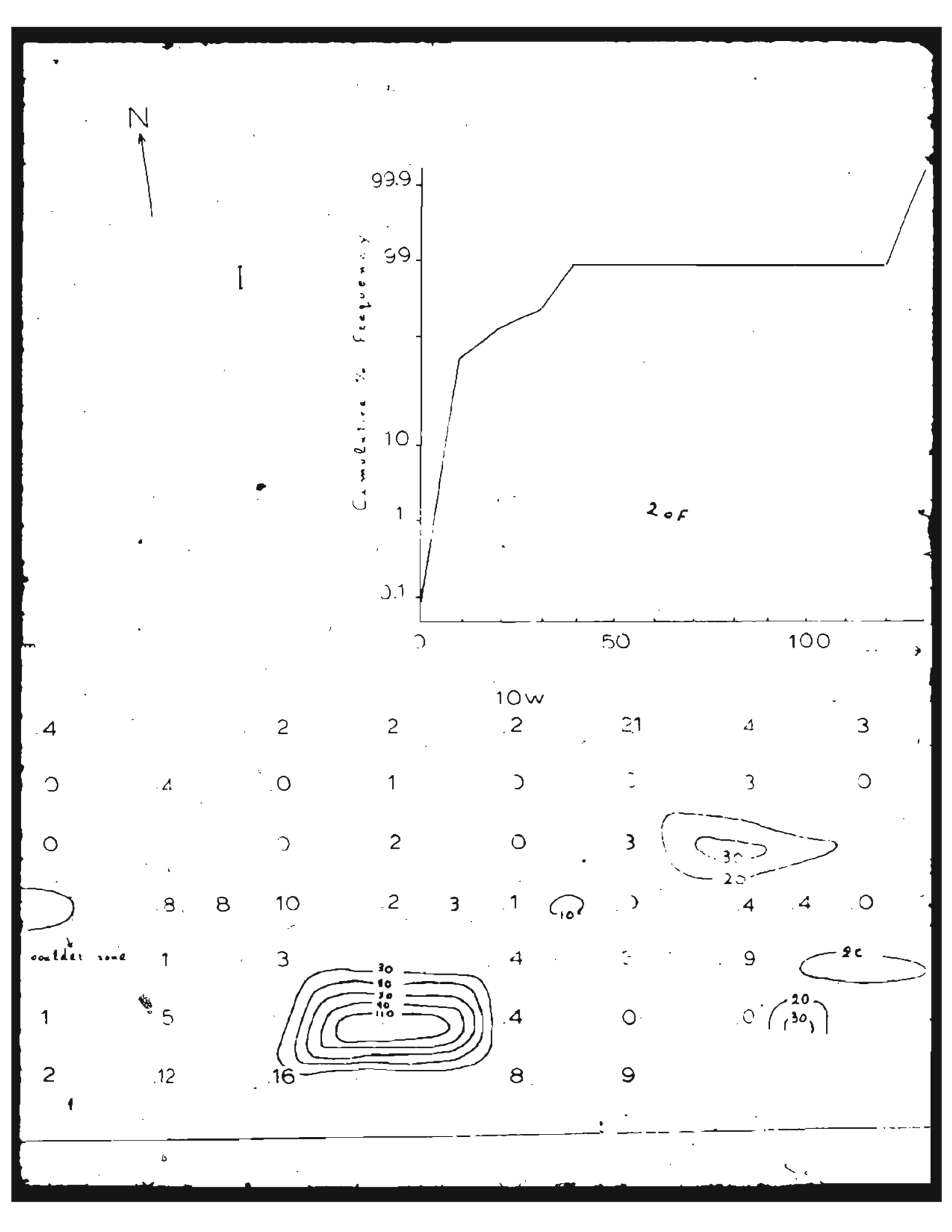
N
99.9
99
10
1
0.1
Cumulative % frequency
2 of
0
50
100
10w
4
2
2
2
21
4
3
0
4
0
1
0
3
0
0
0
2
0
3
30
20
8
8
10
2
3
1
10
4
4
0
cooler zone
1
3
4
9
2c
30
50
30
10
10
1
5
4
0
0
20
30
2
12
16
8
9

3 of F

100 → Room c/m

00+00

4	1		3		0		1
	3		0		13		0
					0		4
	4	4	0	1	0	3	5 ← Base line
	9		9c		3		1
	0				4		1
					0		

30
20

20
30

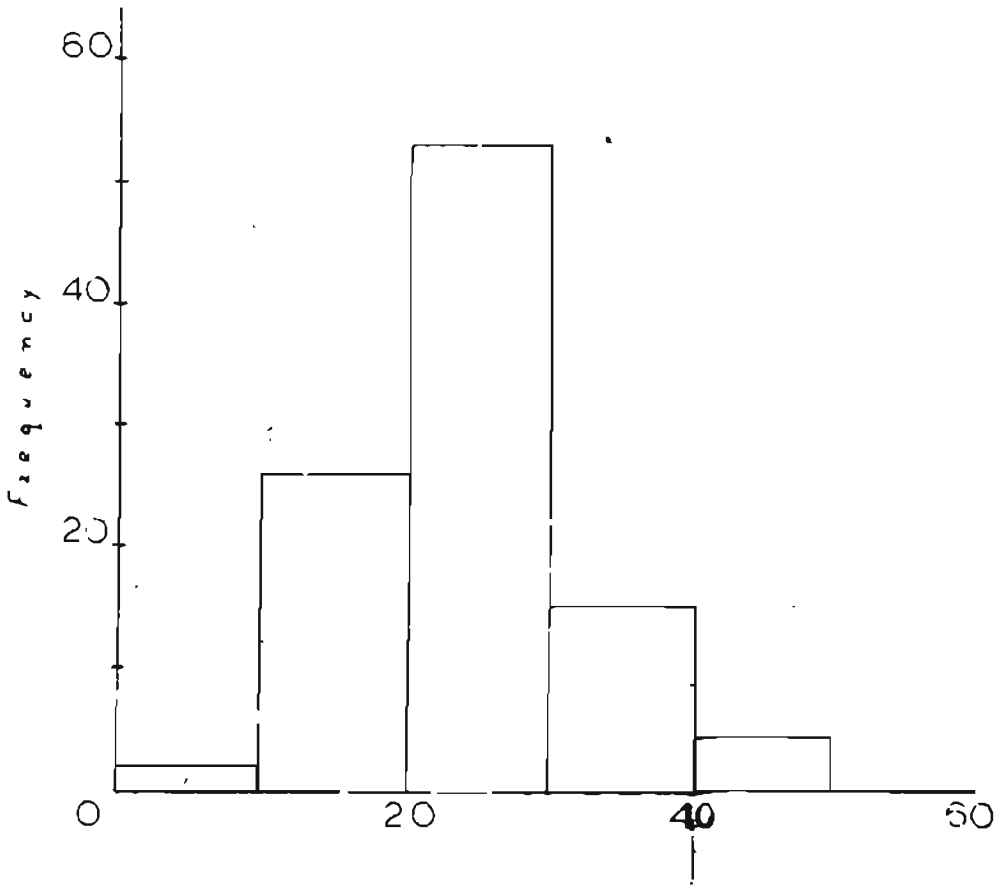

40 F

20W

30

30

40

30

Radioactive boulder zone

30

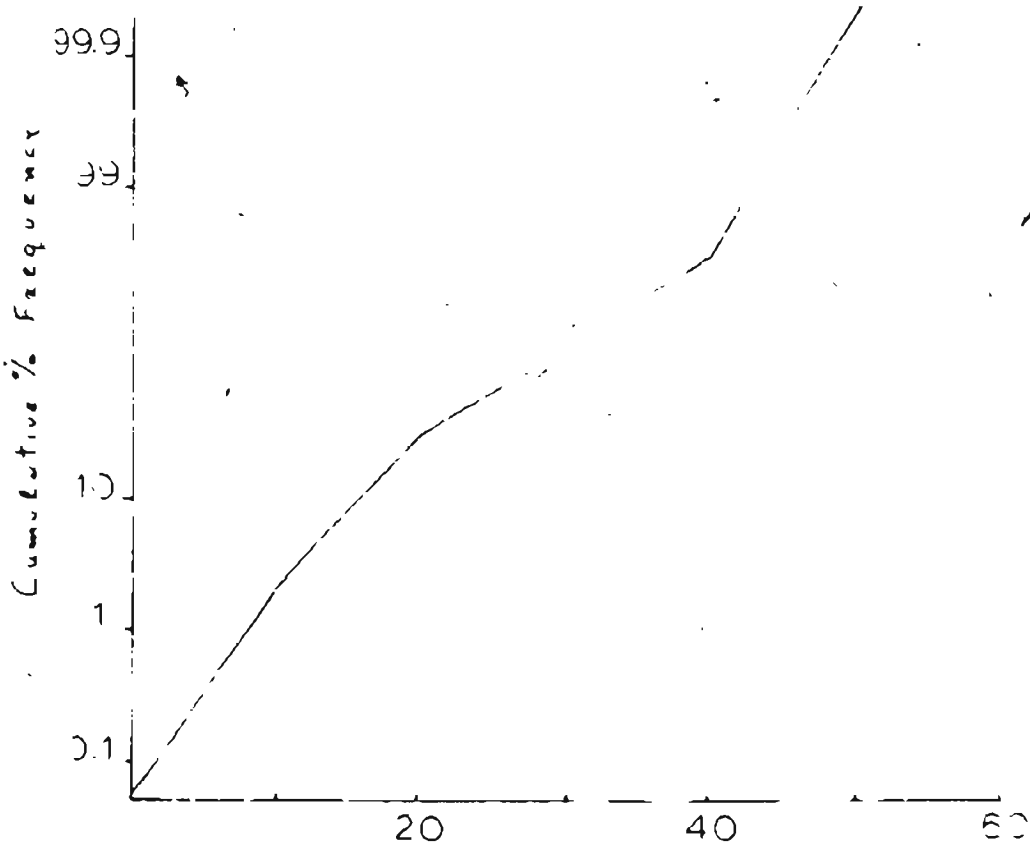

10w

5.F

30
30
40
50
30
40
30
30

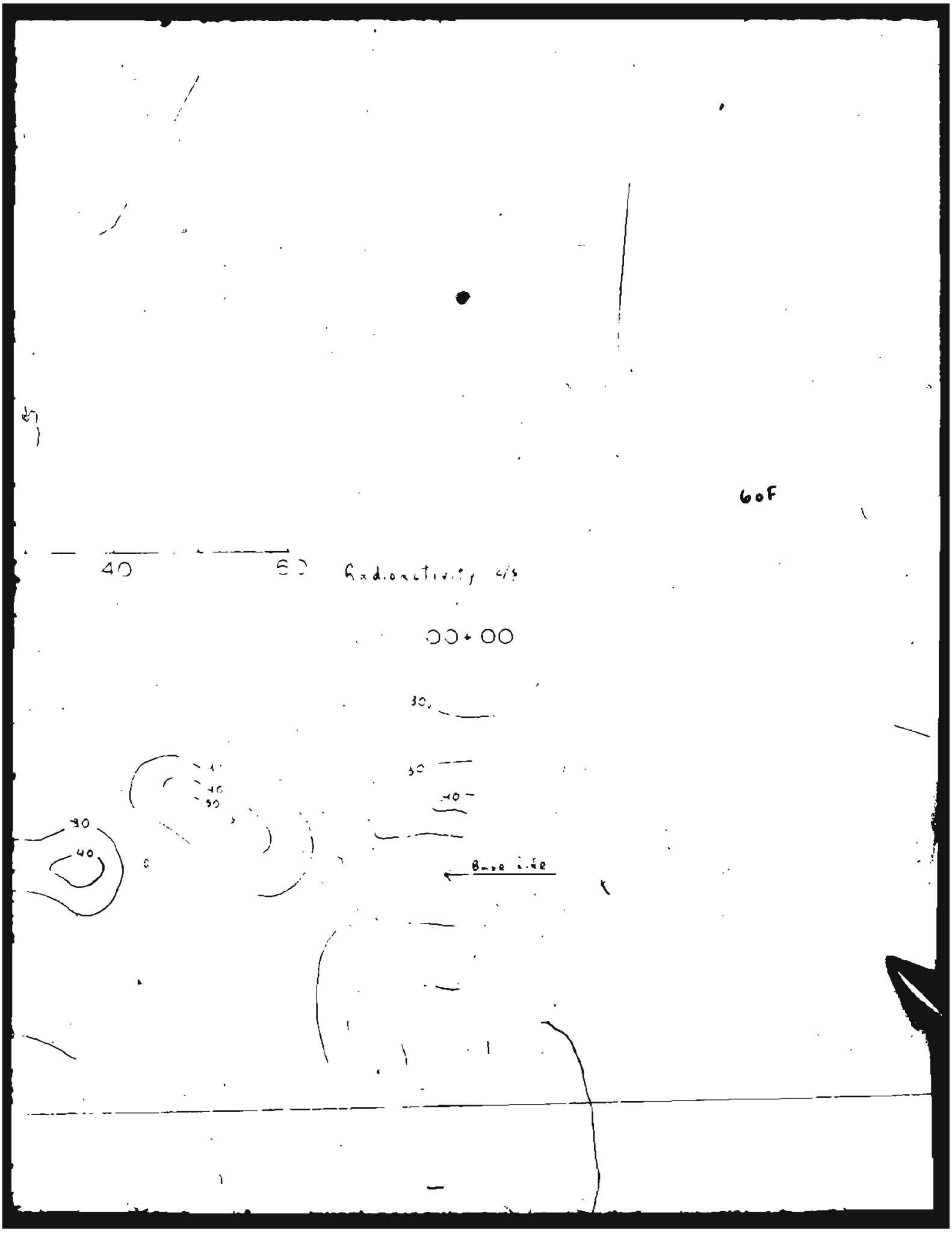
60F
40
60
Radioactivity c/s
00+00
30
30
40
30
40
30
40
Base line

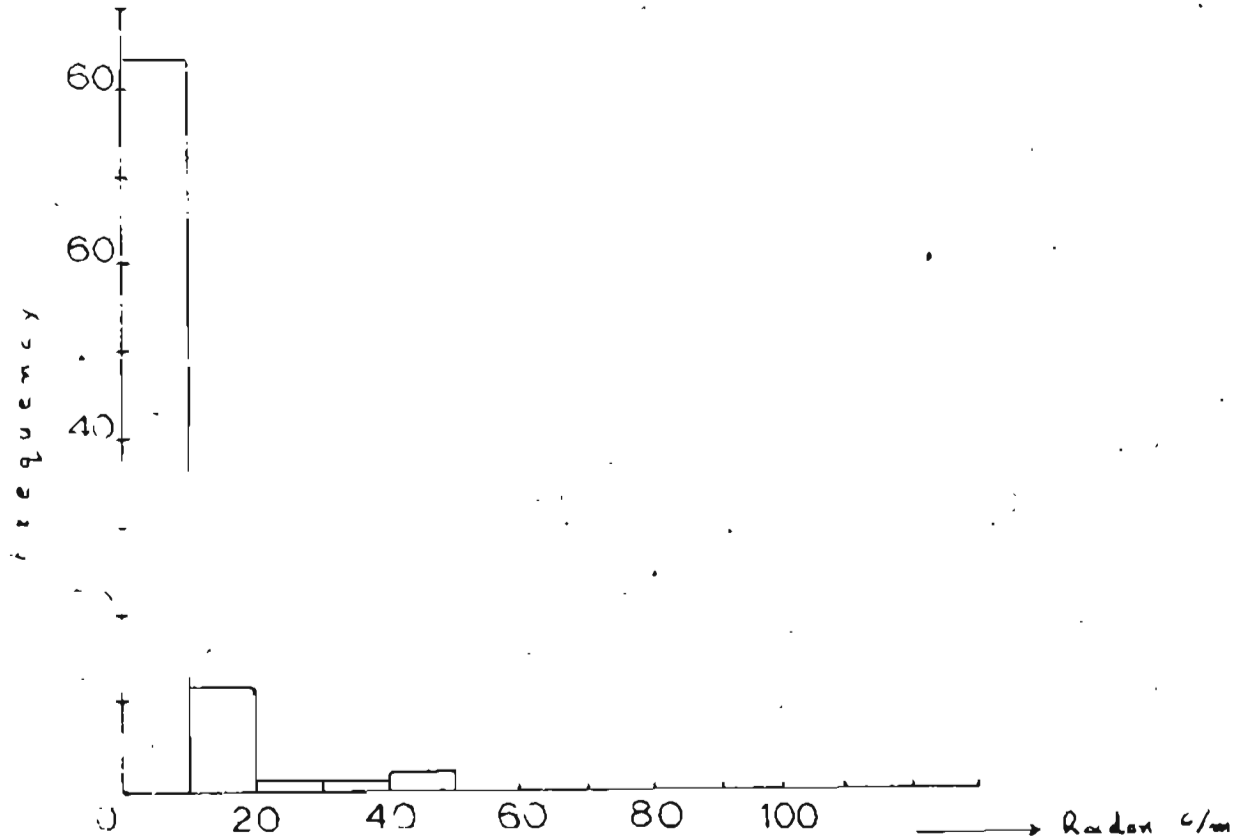

20w

	8	9	1	4
	4	7	1	2
0	1	5	2	10
14	4	9	3	11
0	4	6	5	12
	5	5	9	3
	3	0		2

7 of

Radioactive boulder zone

Radioactive

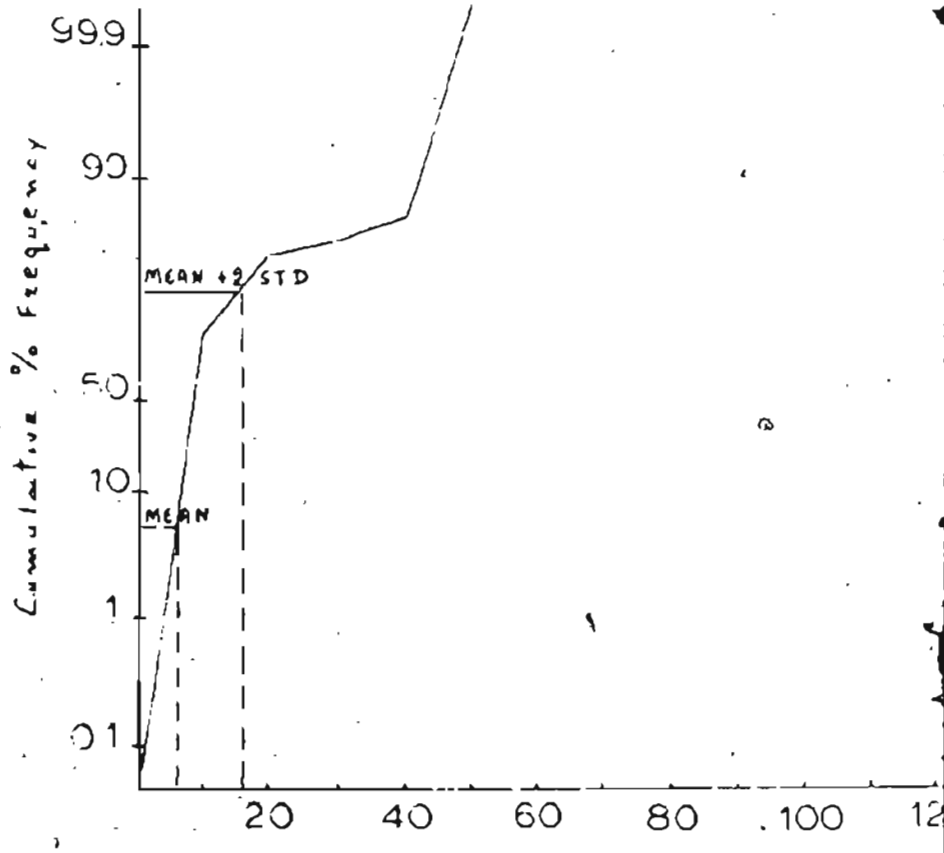

III

8.F

N

10W

4 2 2 2 21 4 3

2 4 1 2 1 10 13 5

10 8 4 2 1 3 13 5

11 7 8 5 12 7 3 2 12 2 1 15 4 12 1

Radioactive boulder zone

12 5 6 3 1 5 10

3 6 8 6 4 0 7

2 12 16 6 8 9

9.F

0 80 100 120 ——→ Radon c/min

00+00

4		3		0		1	
13		6		5		2	
13		5		5		3	
15	4	12	1	1	3	4	← Base line
5		10		3		3	

20
30

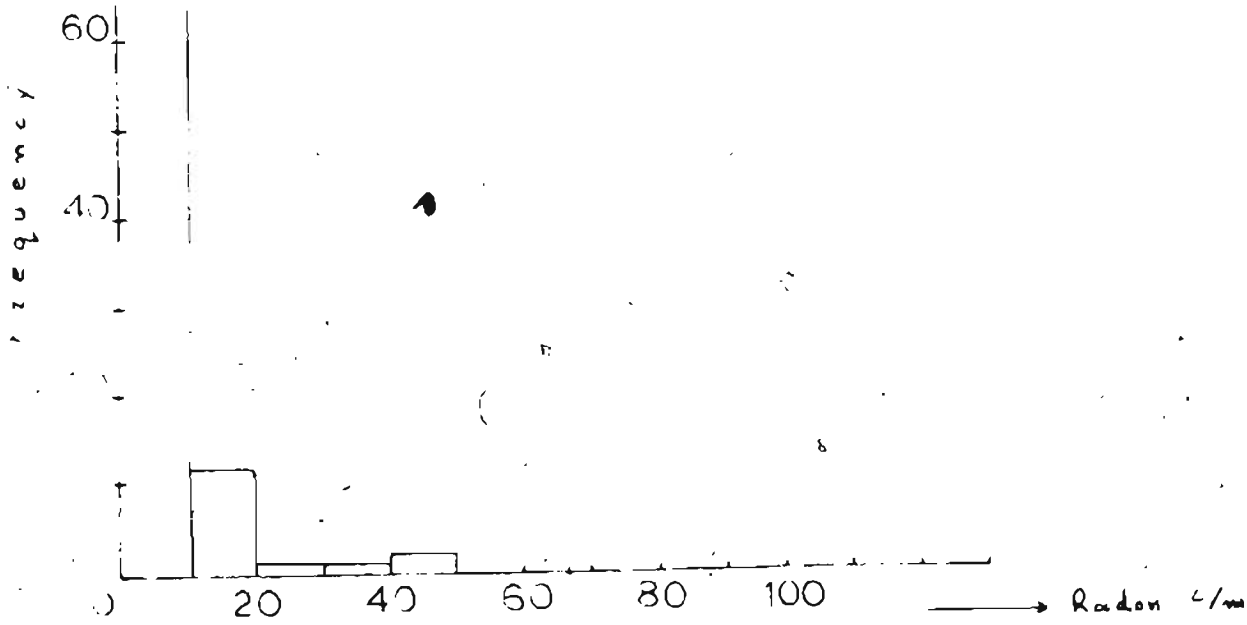

20w

	8	9	1	4
	4	7	1	2
0	1	5	2	12
14	4	9	3	11
0	4	6	5	12
	5	5	9	3
	3	0		2

Radioactive boulder zone

Radioactive

100 F

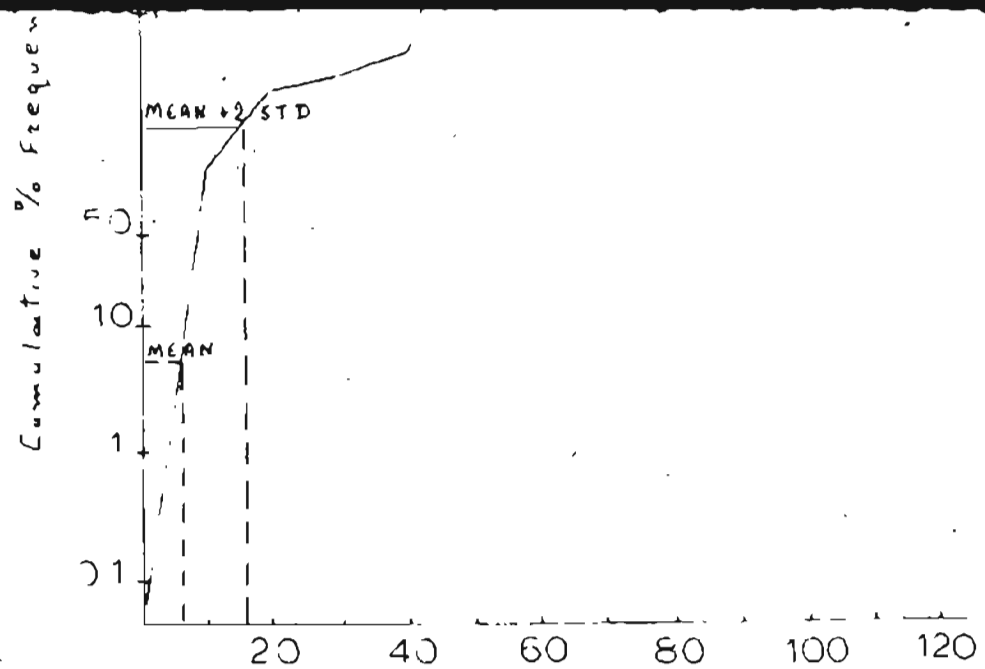

N

10W

4 2 2 2 21 4 3

2 4 1 2 1 10 13 5

10 8 4 2 1 3 13

11 7 8 5 12 7 3 2 12 2 1 15 4 12 1 1

12 5 6 46 3 1 5 10 3

20 30 40

20 30

3 6 8 48 6 4 0 7 3

2 12 16 6 3 9

Three point linear mov

RIBBS LAKE GRID

Fig. 60

80 100 120 → Radon c/min

00+00

4		3		0		1	
13		6		5		2	
13		5		5		3	
15	4	12	1	1	3	4	← Base line
5		10		3		3	
0		7		3		1	
				0			

12 of 12

Three point linear moving average was used

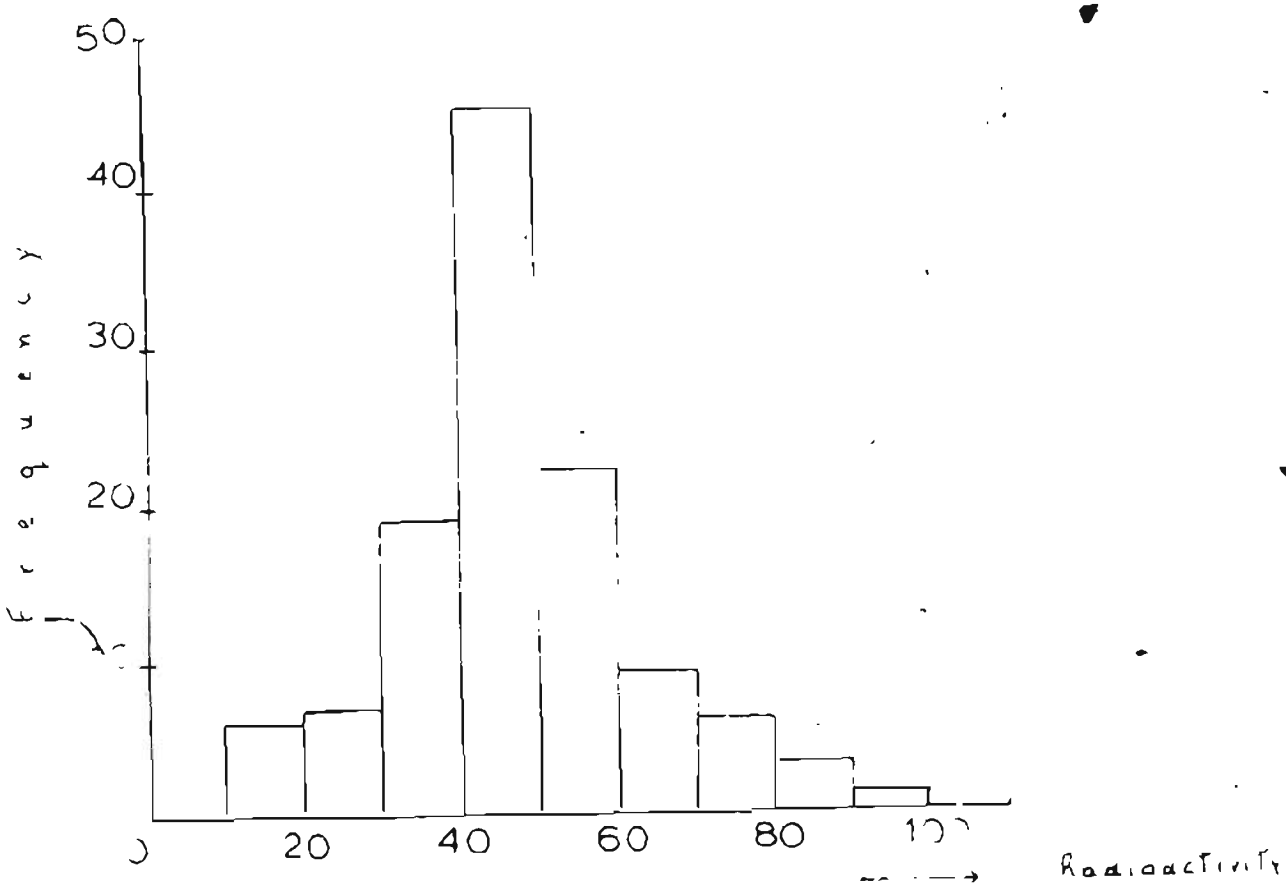

10F

8W						4W				00+00		2E
35	15	20	40	50	50	50	25	45	55	55	80	70
25	30	55	47	47	45	54	40	55	52	69	74	55
	42	65	50	47	35	54	45	60	58	84	77	65
		60										
34	54	49	44	49	35	50	49	57	77	84	94	67

N

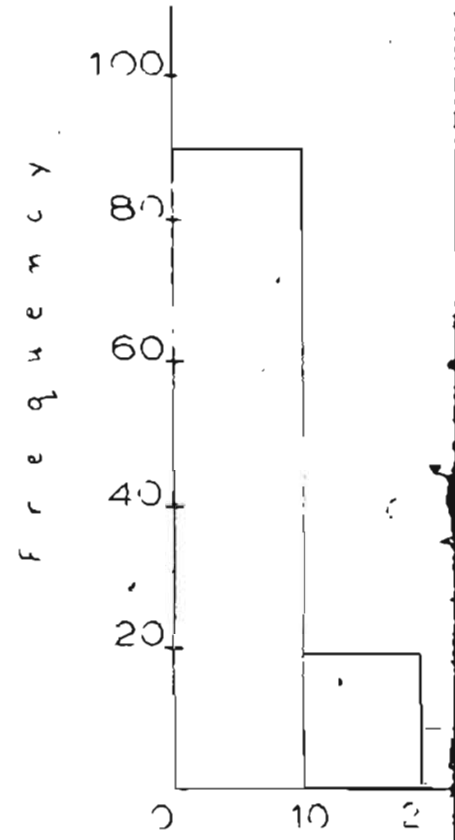

.oactivity c/s

1

2E

8W

80	70	1	1	3	1	0	2
74	55 → Radioactive Boulder zone	1	11	5	1	2	6
77	65		12	10	1	3	9
64	67	1	15	8	1	3	10

3 of F -

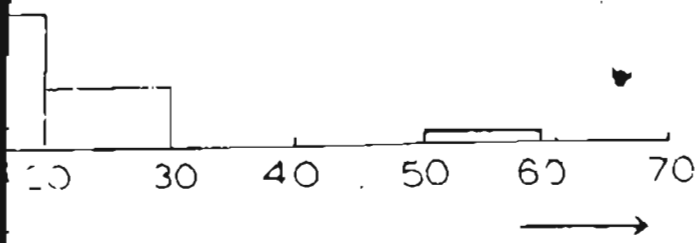

1

4w				00+00			2E
2	2	2	6	18	1	15	2
6	3	2	3	10	5	10	7
9	4	3	3	5	7	5	6
10	5	4	3	2	6	4	5

Radioactive Boulder zone

44	54	50	47	42	35	47	40	54	64	70	80	74
49	54	50	55	39	45	50	4	44	54	57	64	57
49	44	50	59	34	50	50	44	34	39	45	37	45
44	44	47	52	42	44	50	42		39	32	27	57
35	50	40	30	50	30	50	25	20	35	20	20	90

X Radioactive outcrop

X Radioactive outcrop

60

80

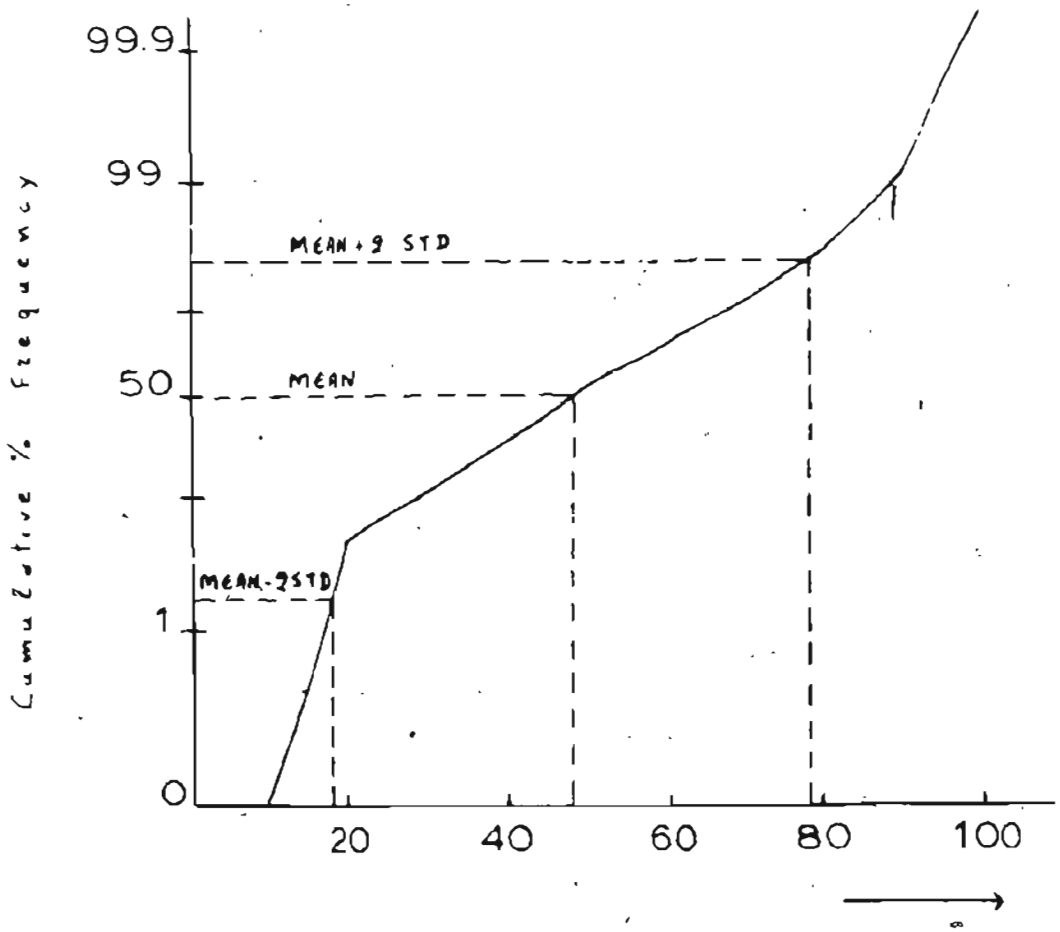

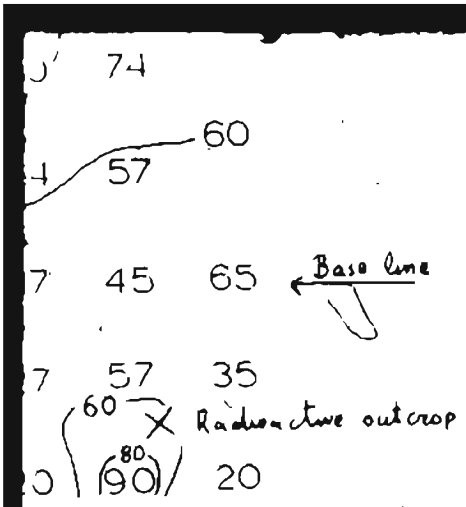

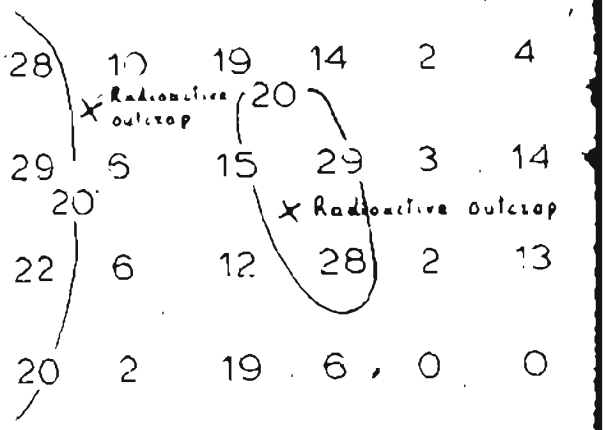

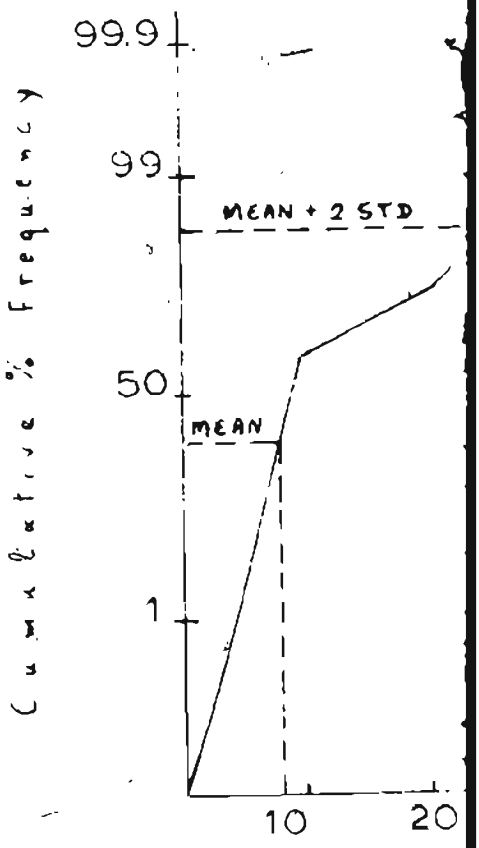

M. BEN GRID

Fig. 59

activity c/s

5 of

4	8	8	6	3	5	5	10	
14	9	9	8	5	11	12	10	3 ← Base line
outcrop								
13	15	7		13	9	9	23	3
0	19	0	7	28	4	0	59	0

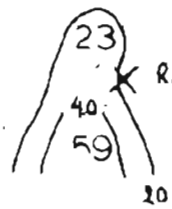

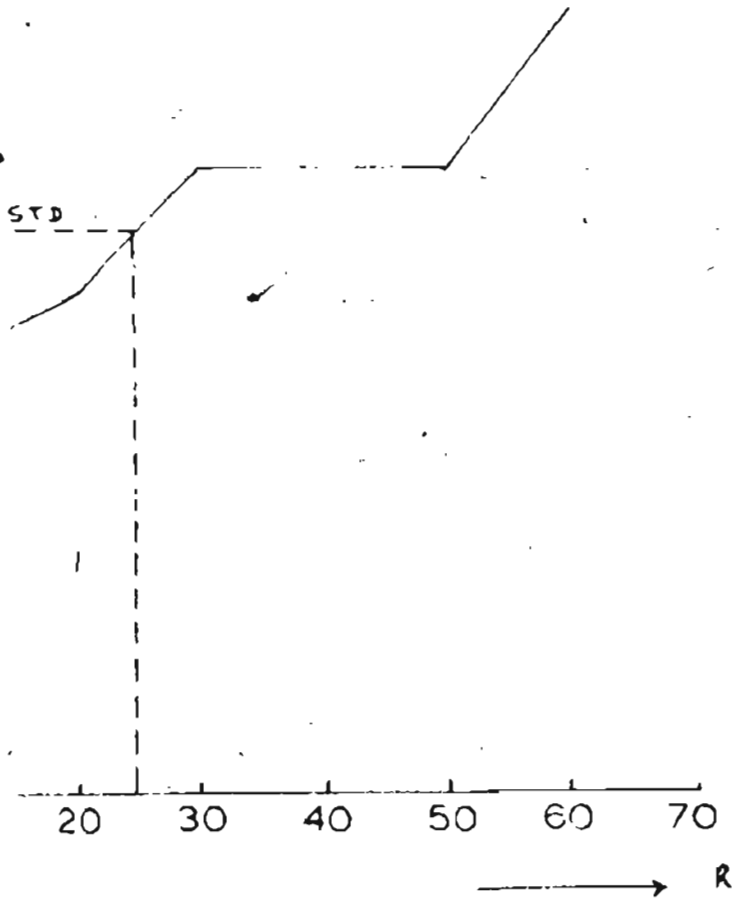

6 of 8

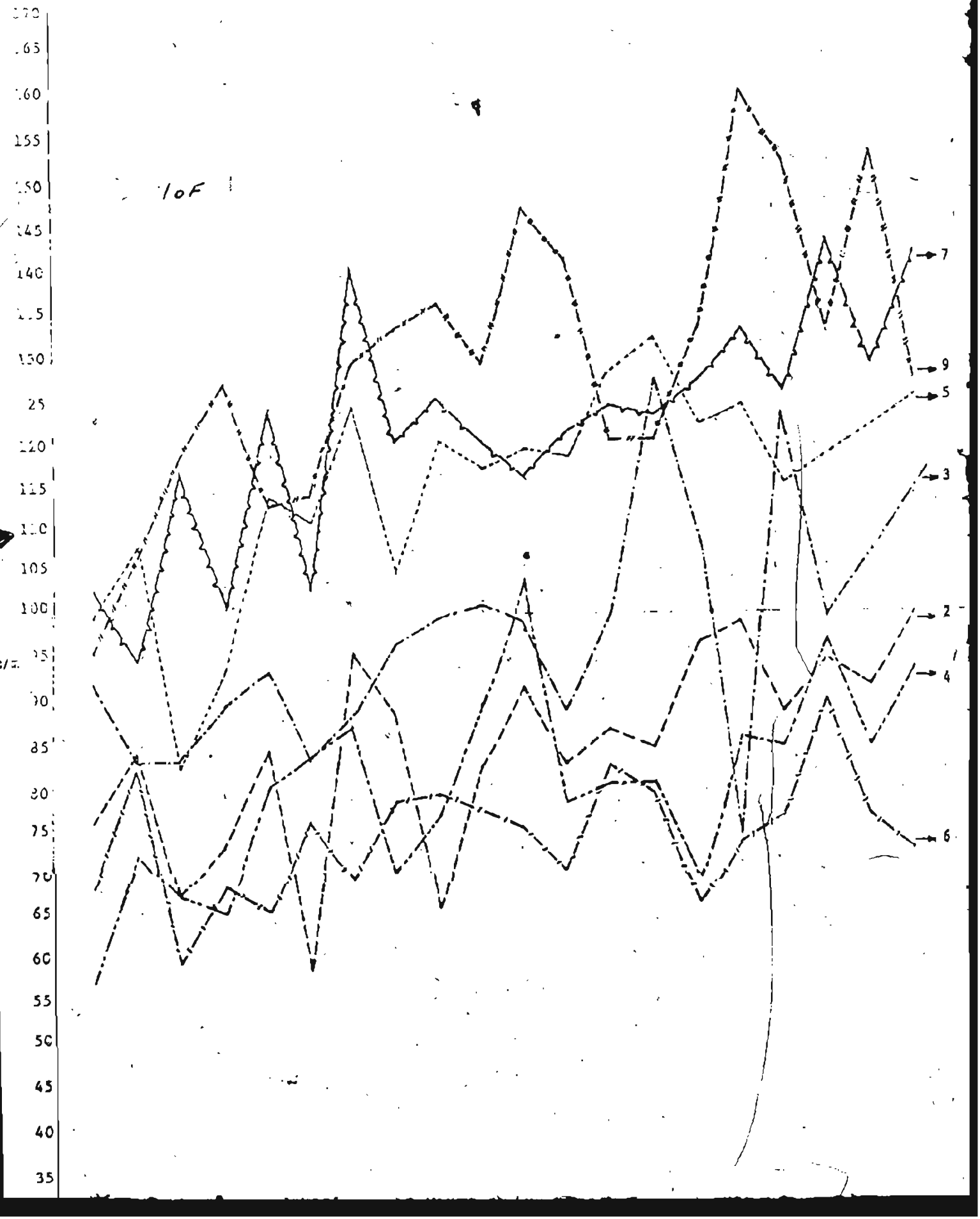
1 OF
7
9
5
3
2
4
6

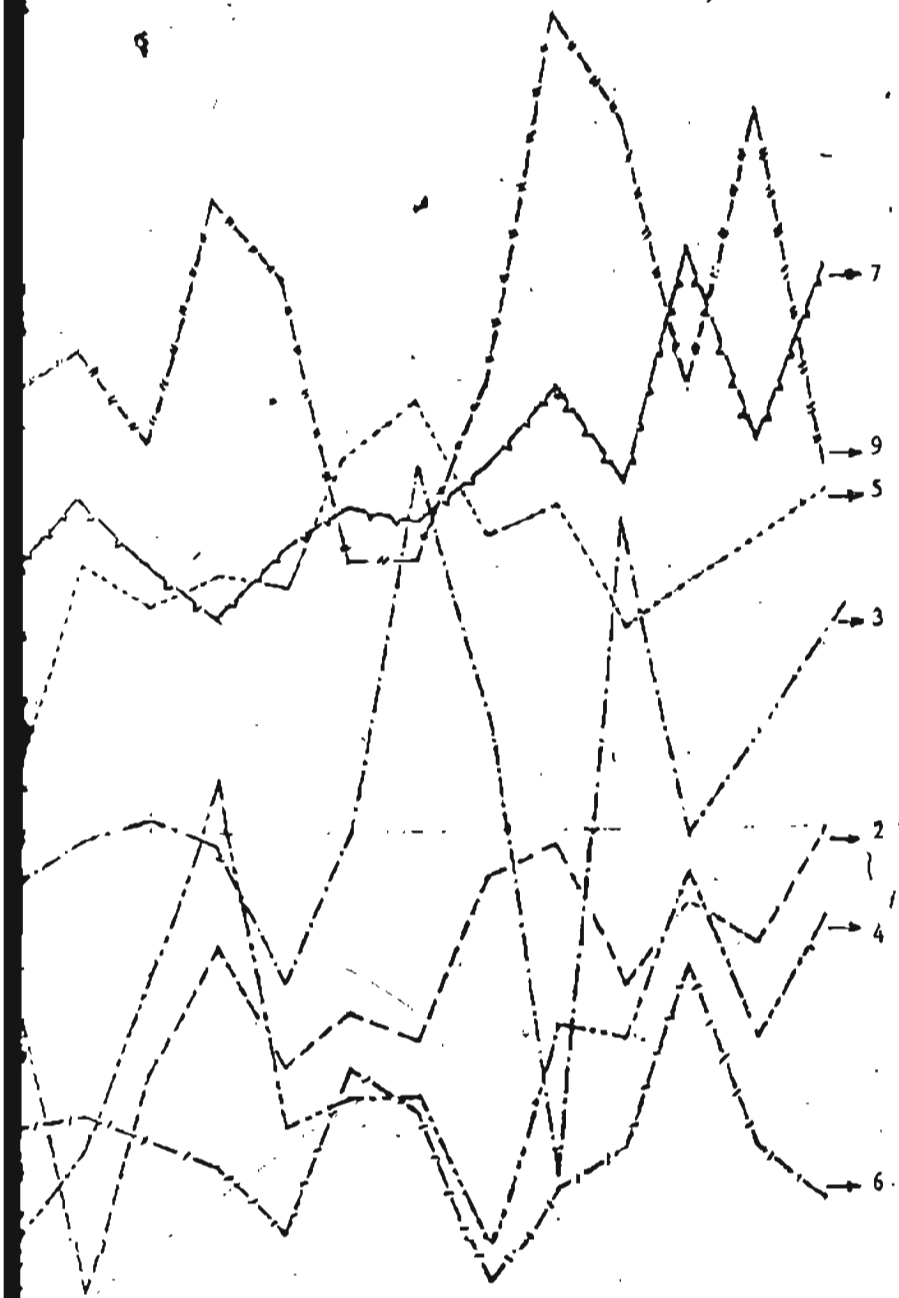

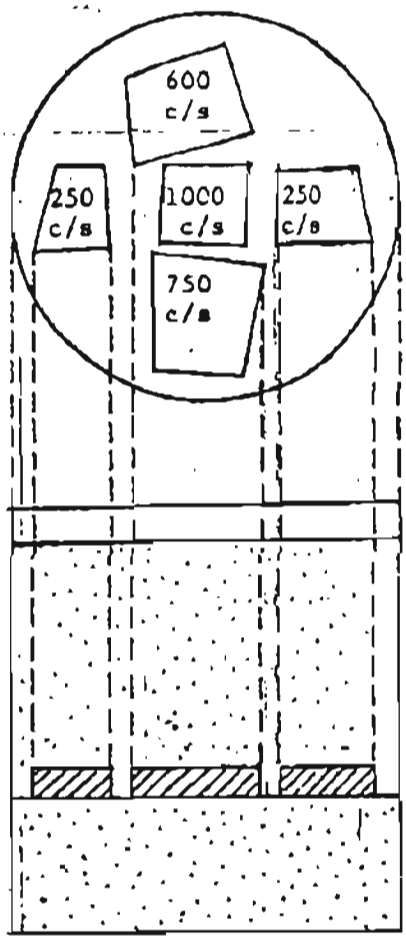

1) July 29, backgr 8c/m Radic 65 c/s SPP-2

2) July 30, Backgr 2c/m R 70c/s

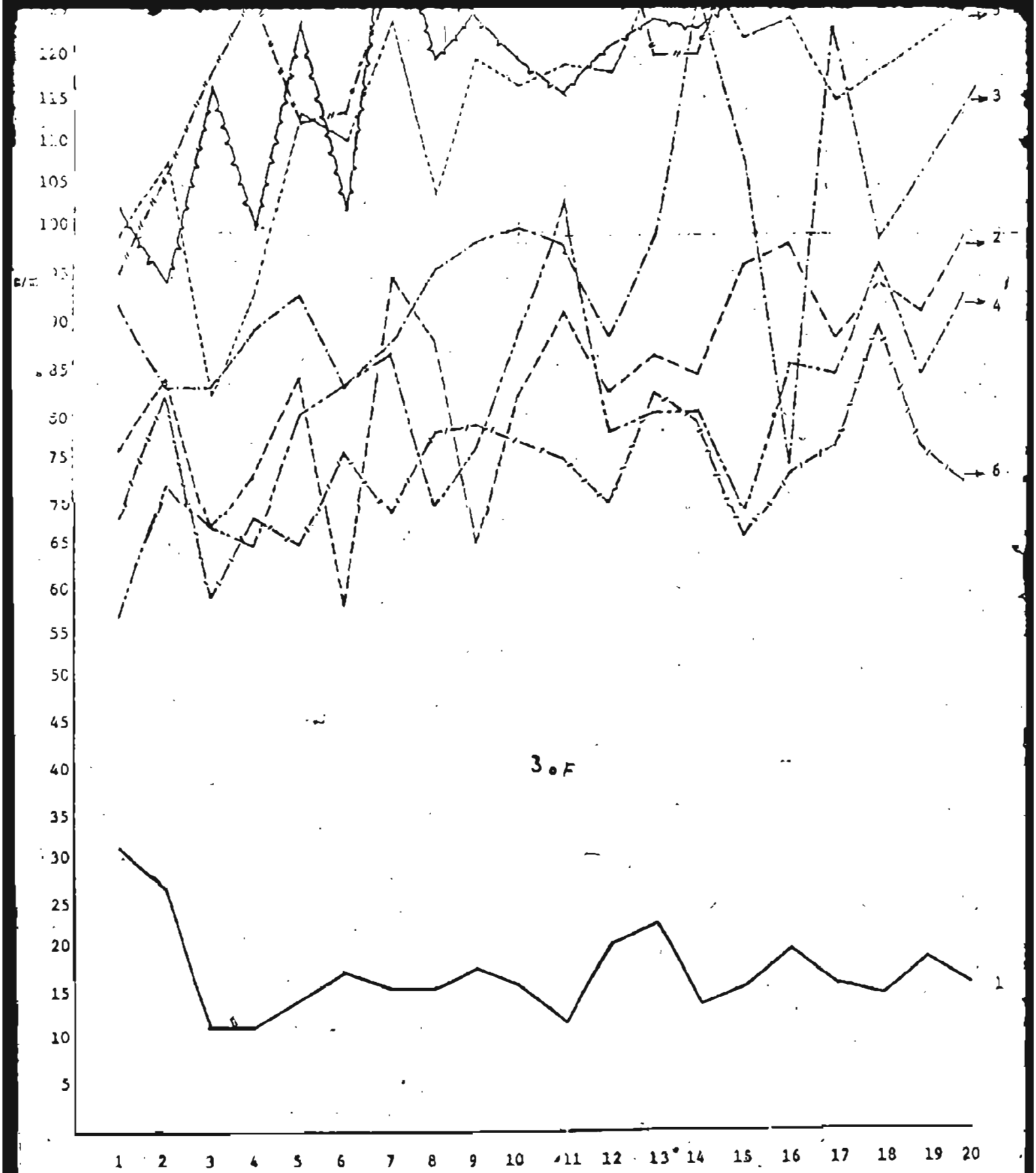

Figure 56 Variability of the radon intensity in the "radioactive barrel" (see text).

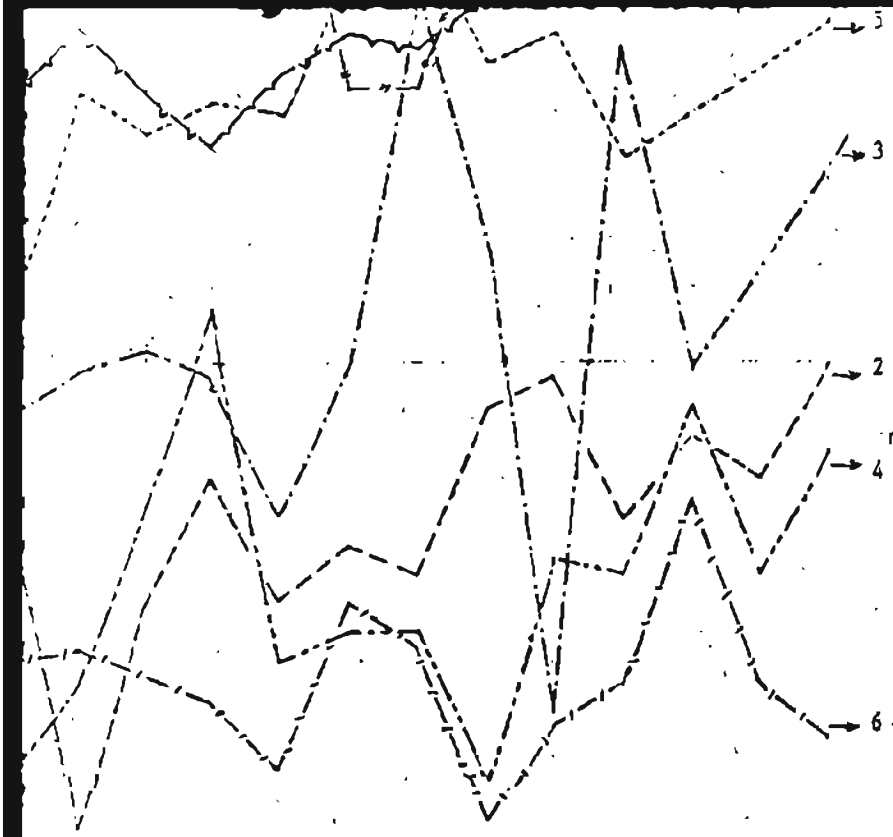

4 of 4

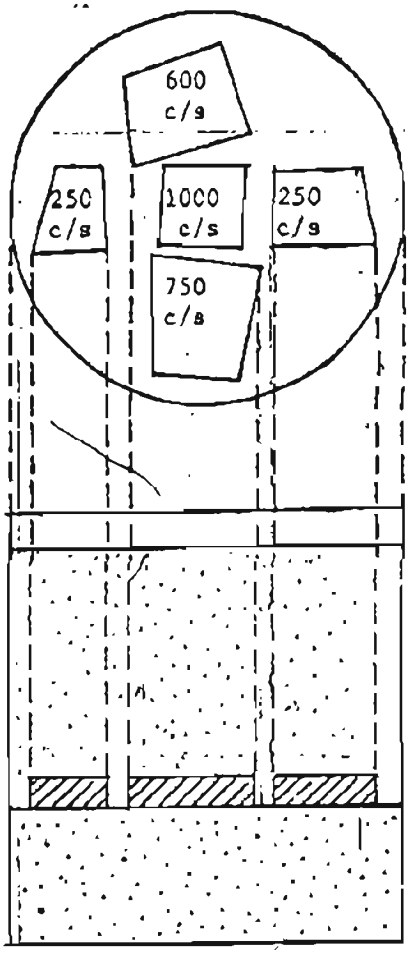

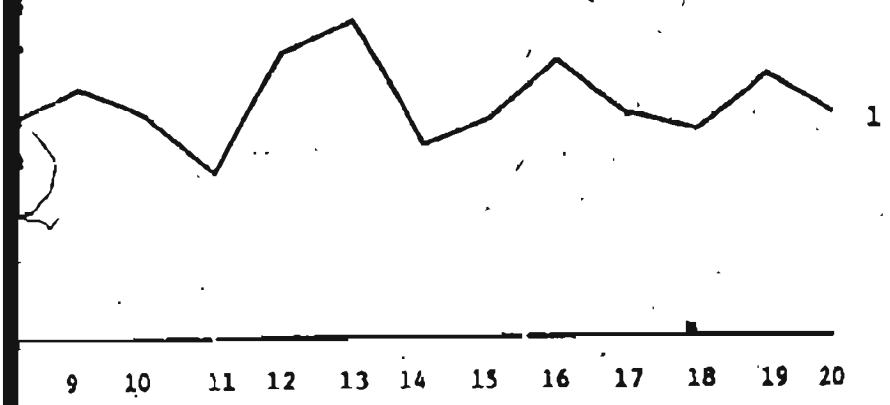

n intensity in the "radioactive barrel" time, min.

1) July 29, backgr 8c/m Radic 65 c/s SPP-2
2) July 30, Backgr 2c/m R 70c/s
3) July 31 Backgr 1c/m R= 80 T = 64°F
4) Aug. 1 Backgr. 7c/m R= 115c/s T = 72°F
5) Aug. 2 Backgr. 4c/m R= 110c/s T = 64°F
6) Aug. 3 Backgr. 7c/m R= 125c/s T = 68°F
7) Aug. 4 Backgr. 3c/m R= 125c/s T = 72°F
8) Aug. 5 Strong rain (survey impossible)
9) Aug. 6 Backg. 6 c/m R= 100c/s T = 46°F

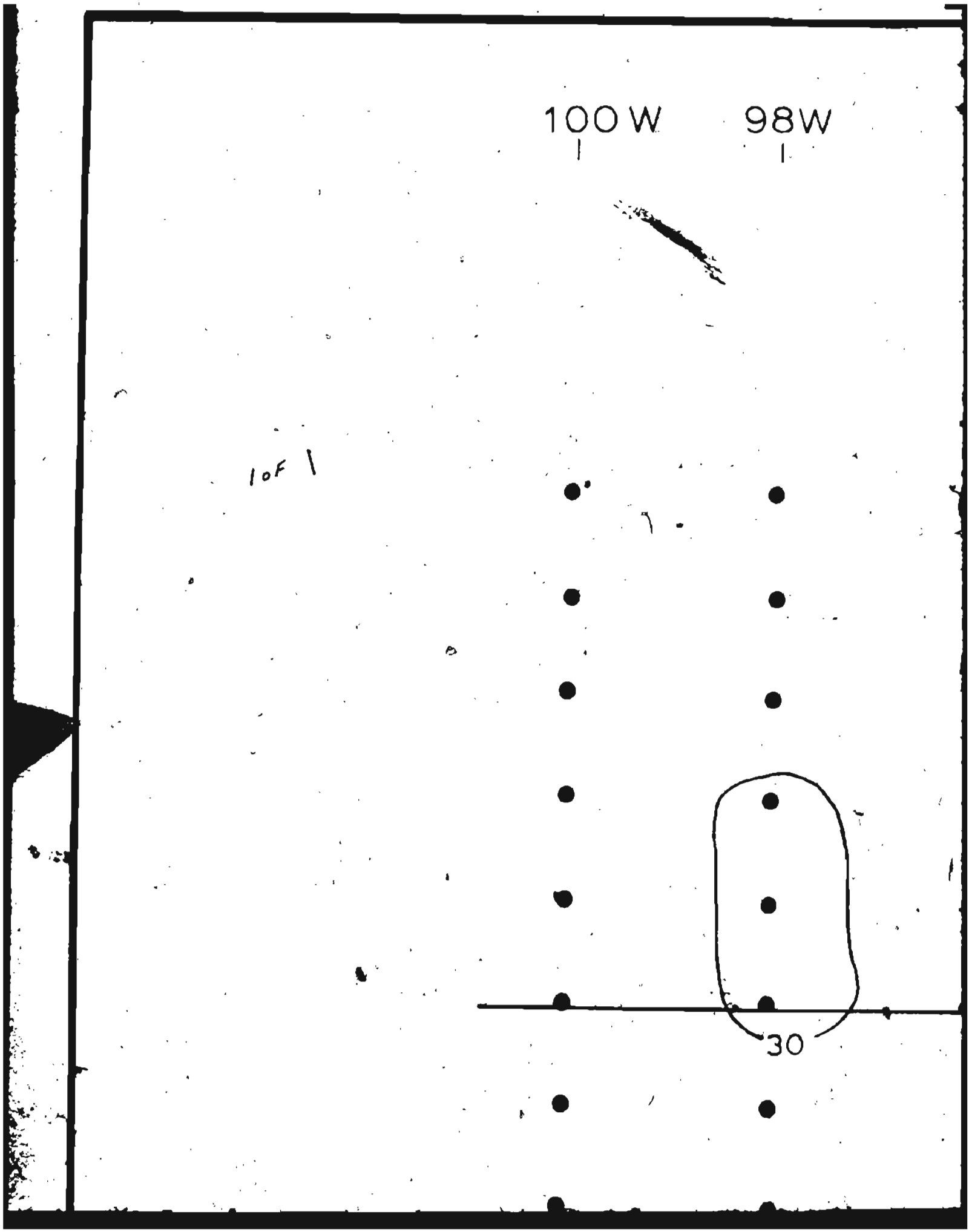
100W
98W
1 OF 1
30

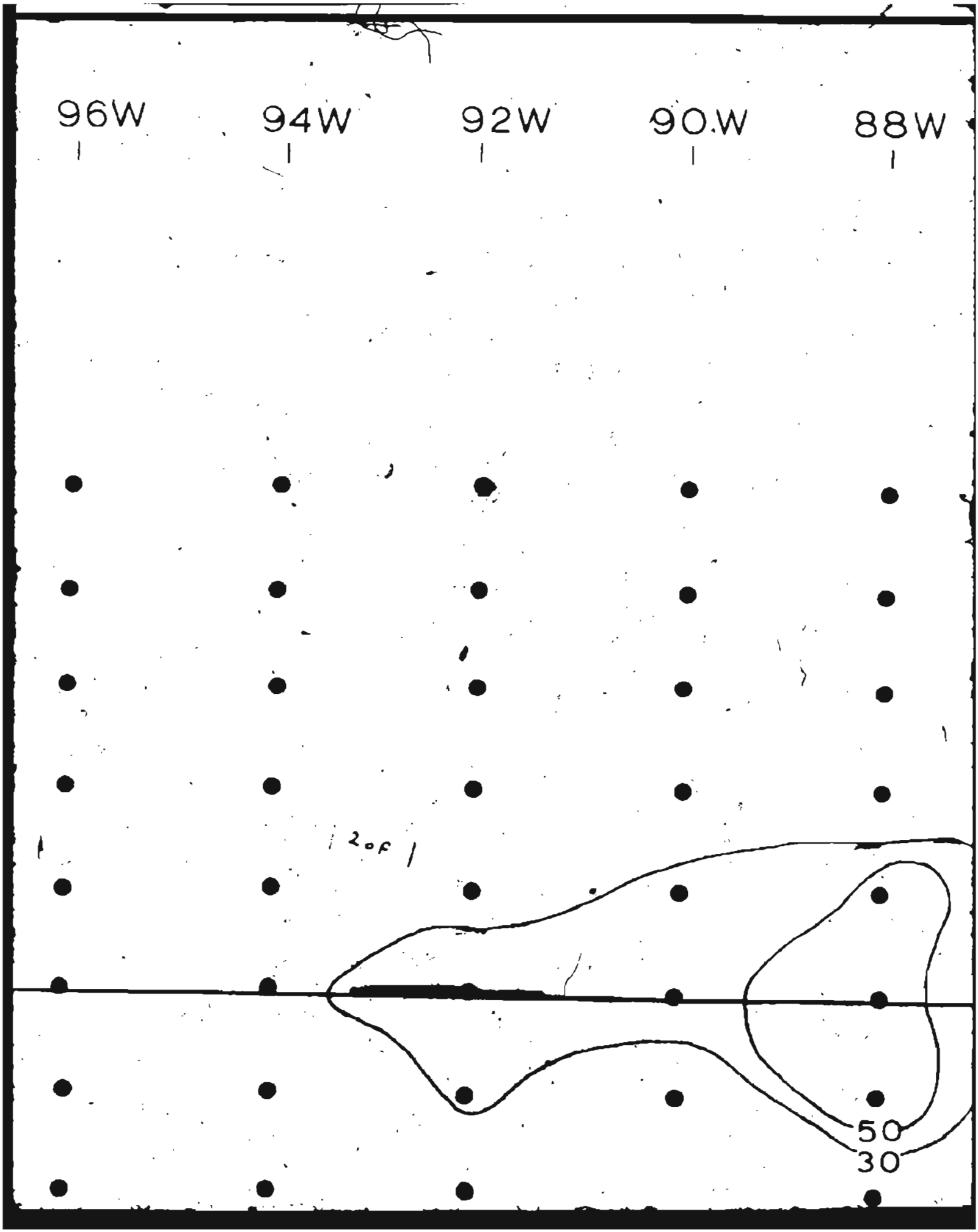
96W
94W
92W
90W
88W
50
30

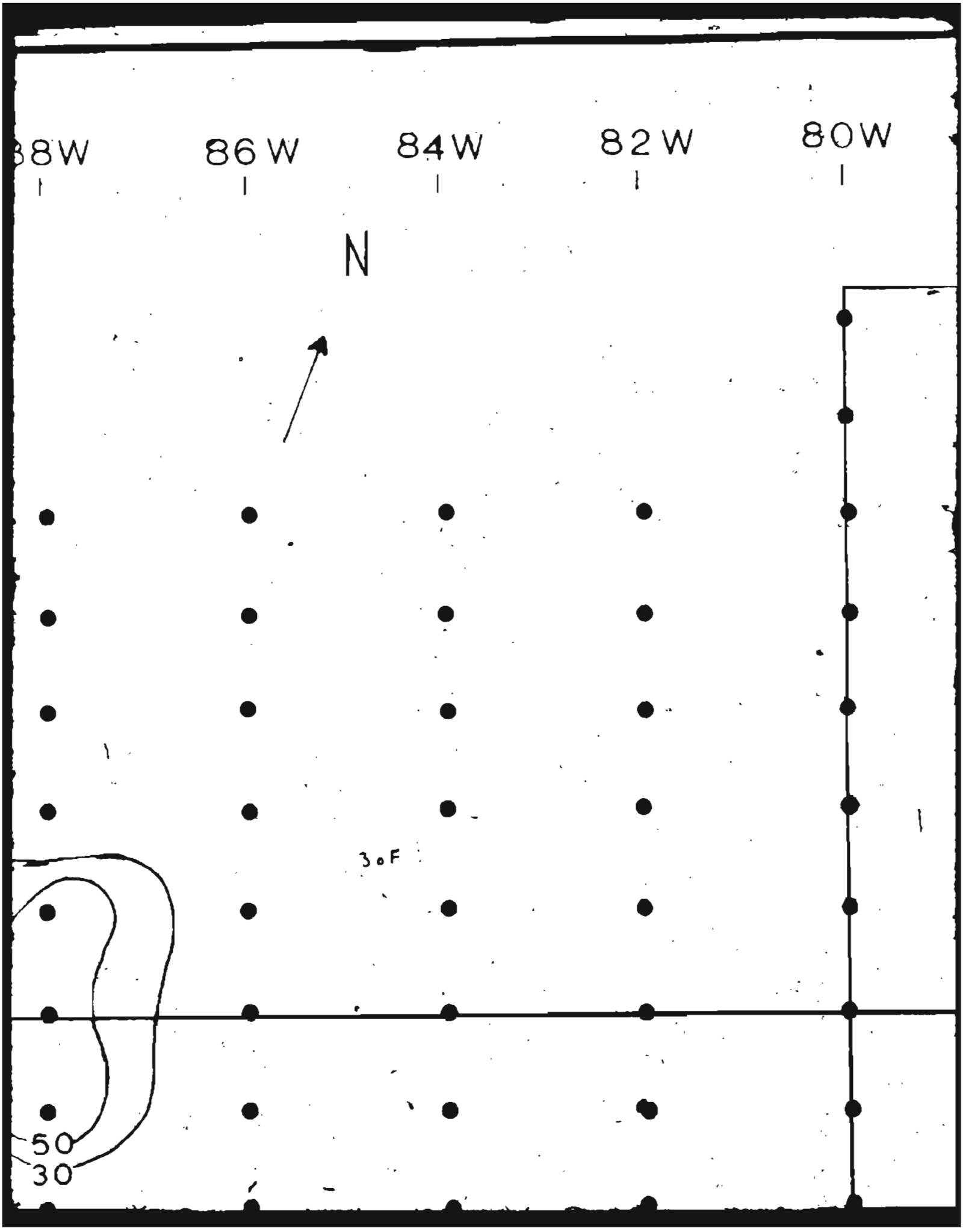
88W
86W
84W
82W
80W
N
3°F
50
30

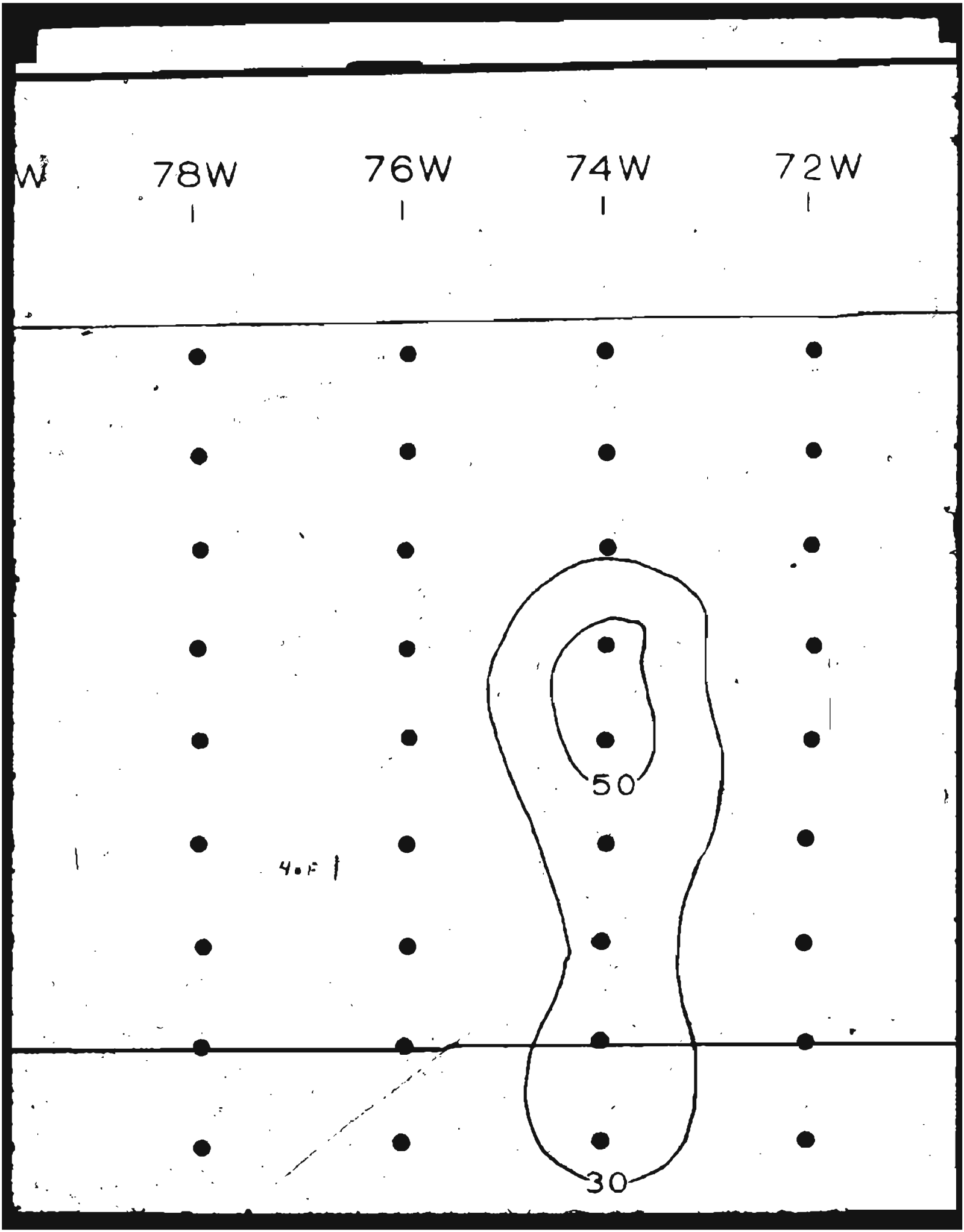
W
78W
76W
74W
72W
50
30

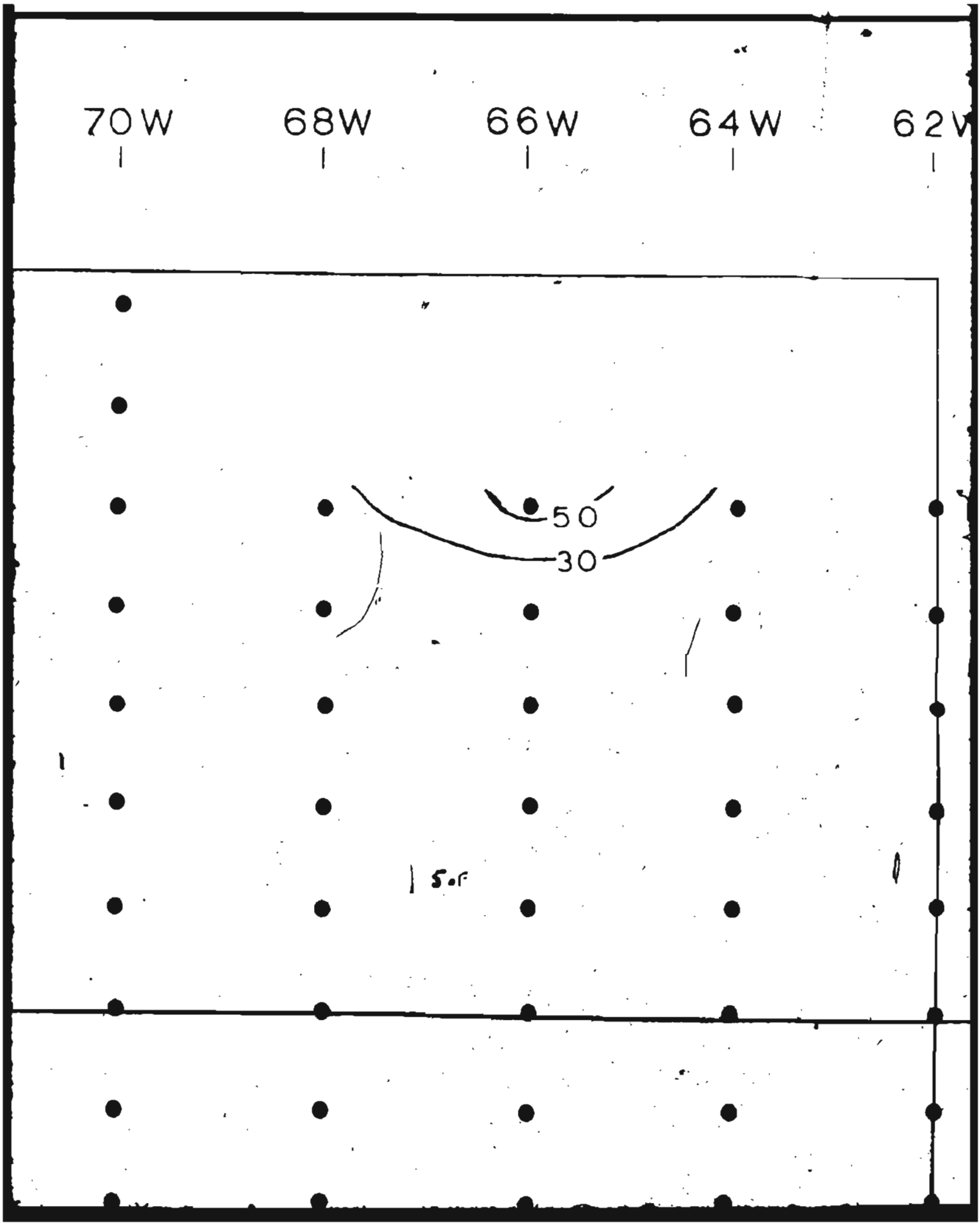
70W
68W
66W
64W
62W
50
30
5.F

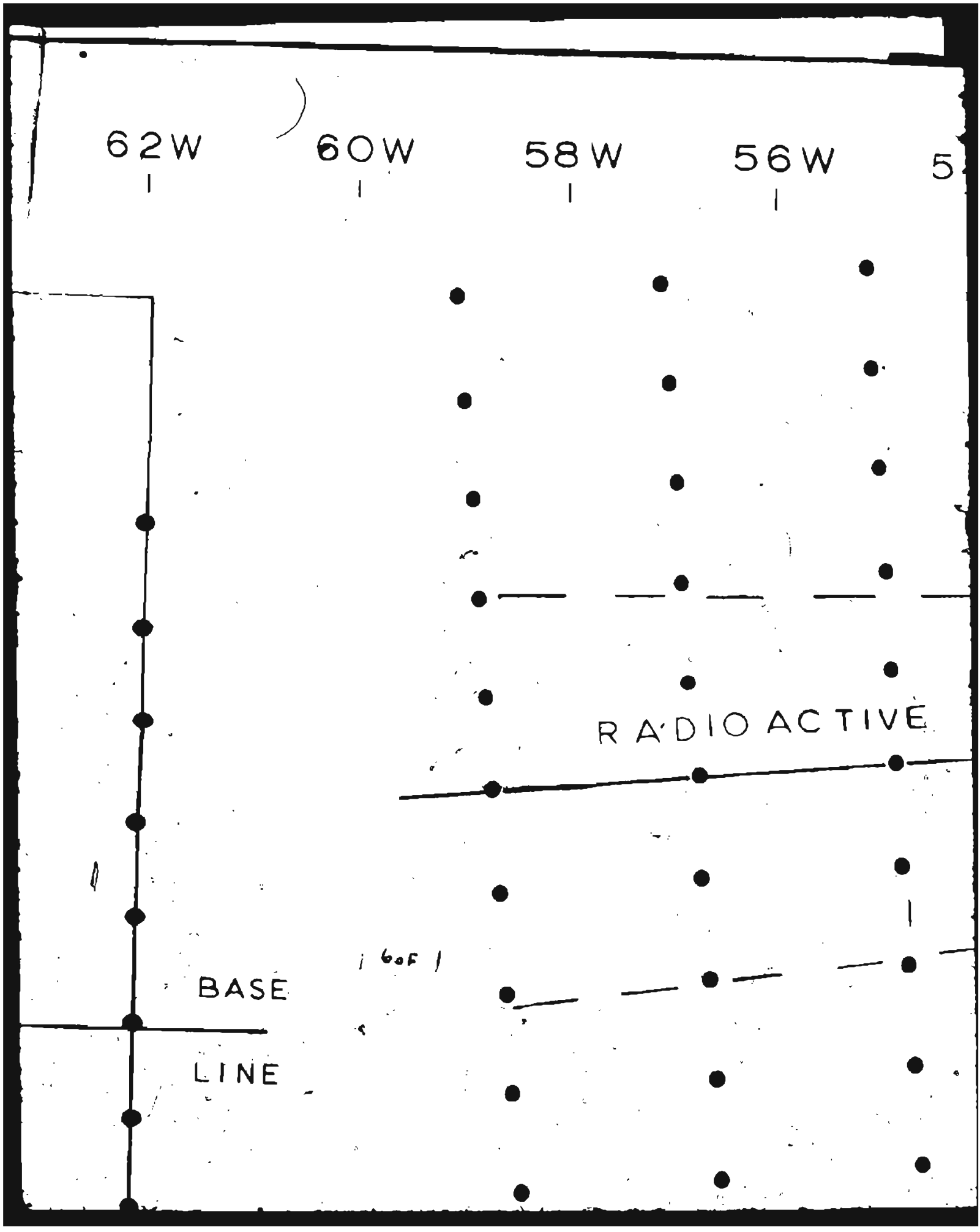
62W
60W
58W
56W
5
RADIO ACTIVE
BASE
LINE
60F

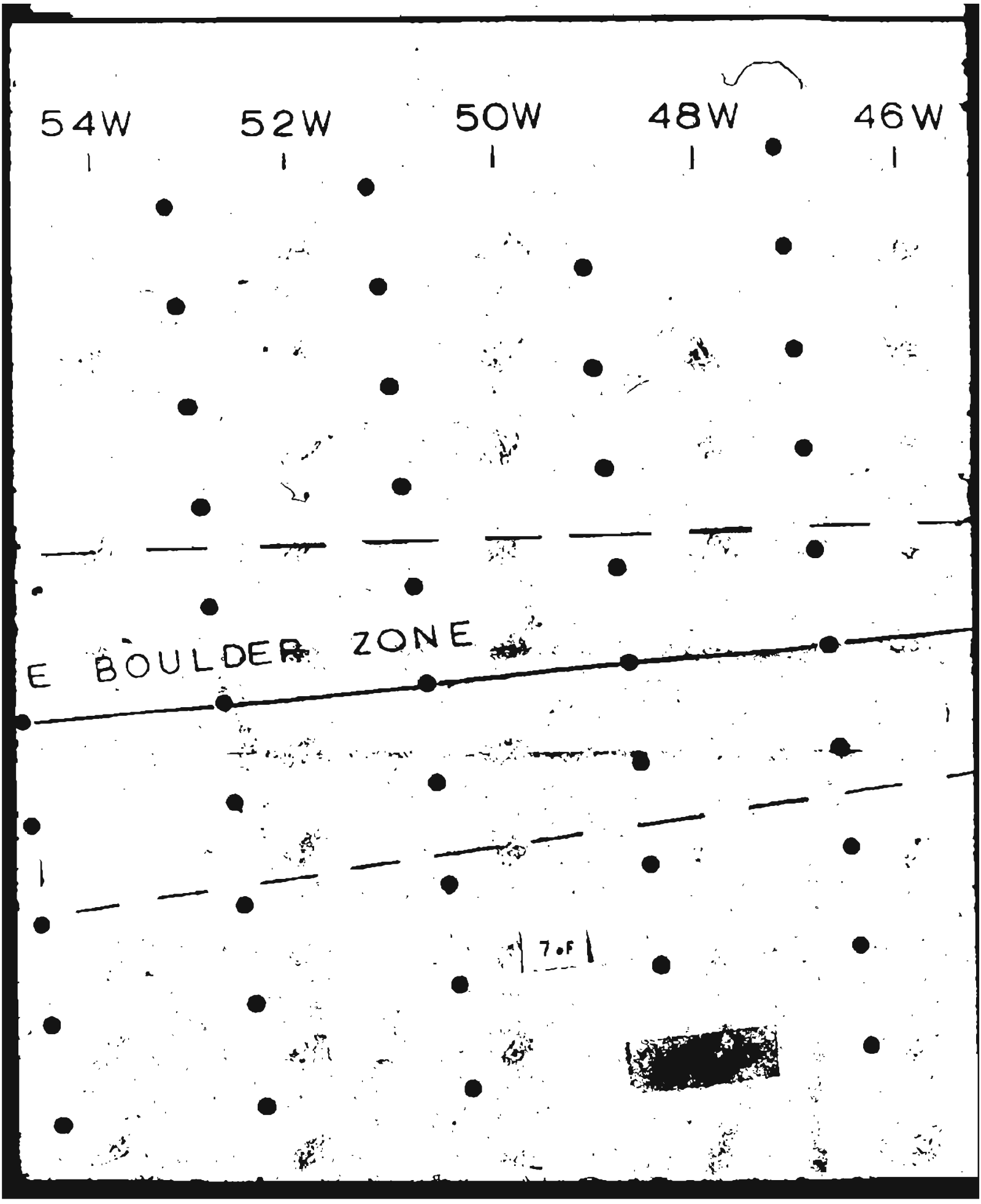
54W
52W
50W
48W
46W
E BOULDER ZONE
7 of

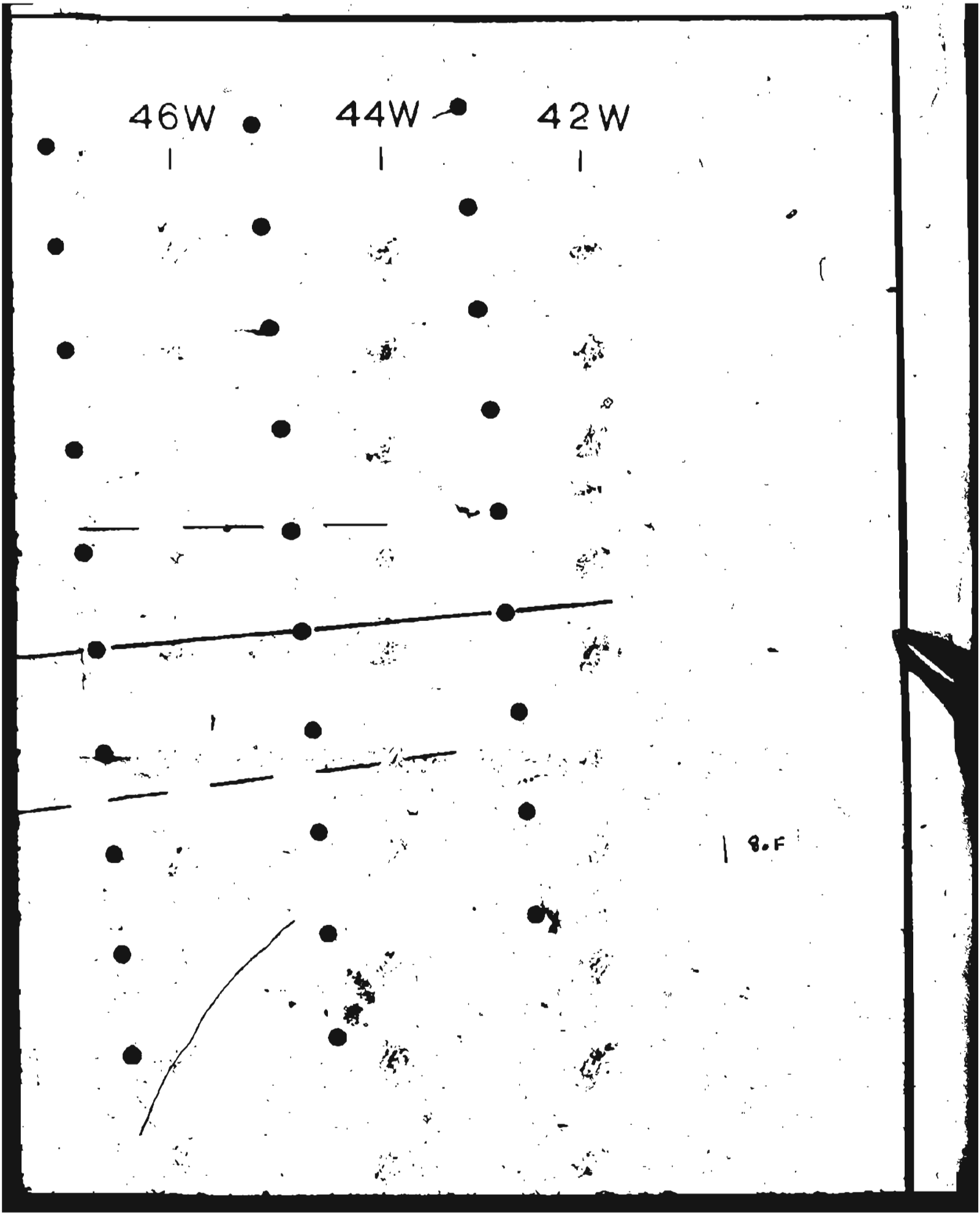
46W
44W
42W
8.F

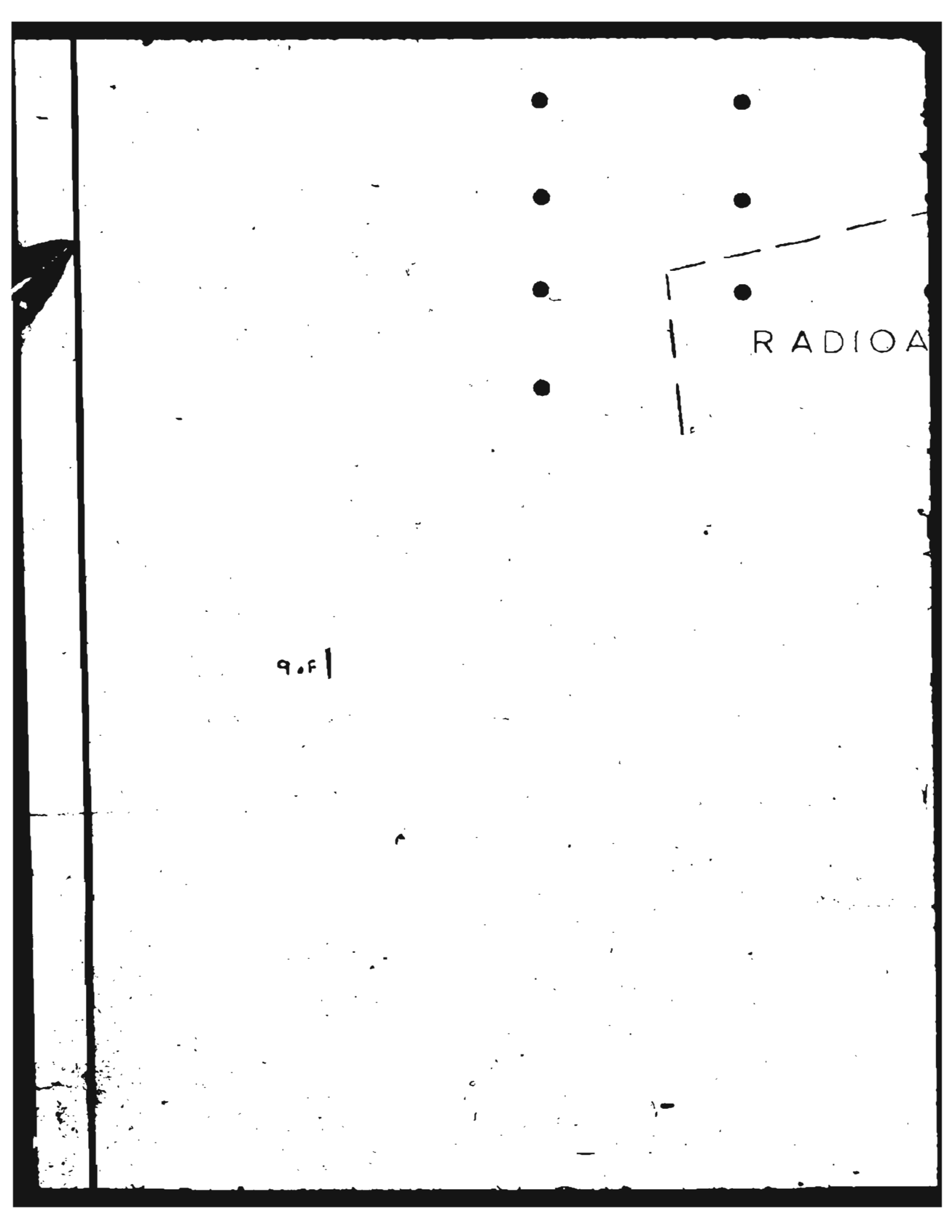
RADIOA
9.F

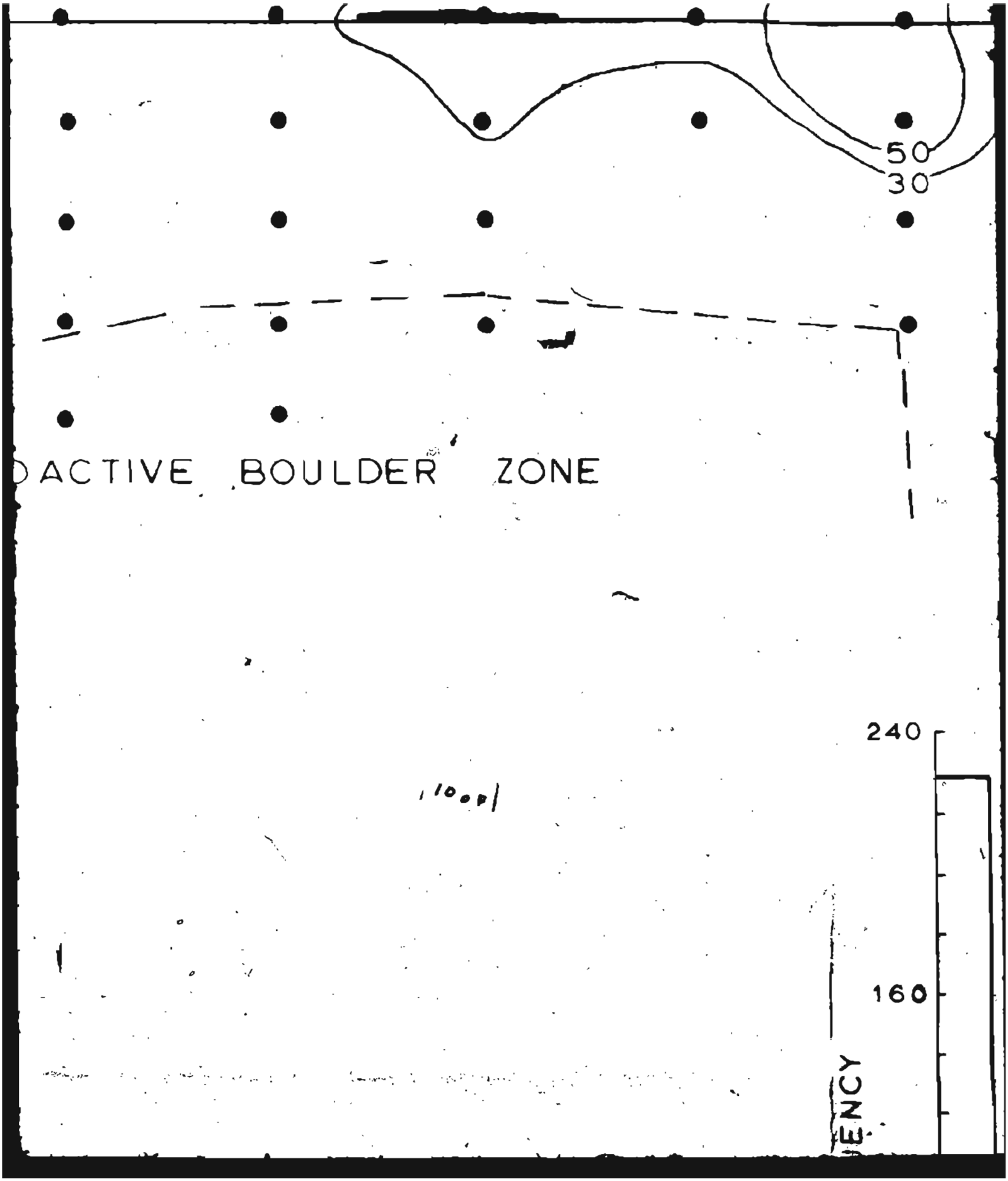
50
30
ACTIVE BOULDER ZONE
240
160
ENCY

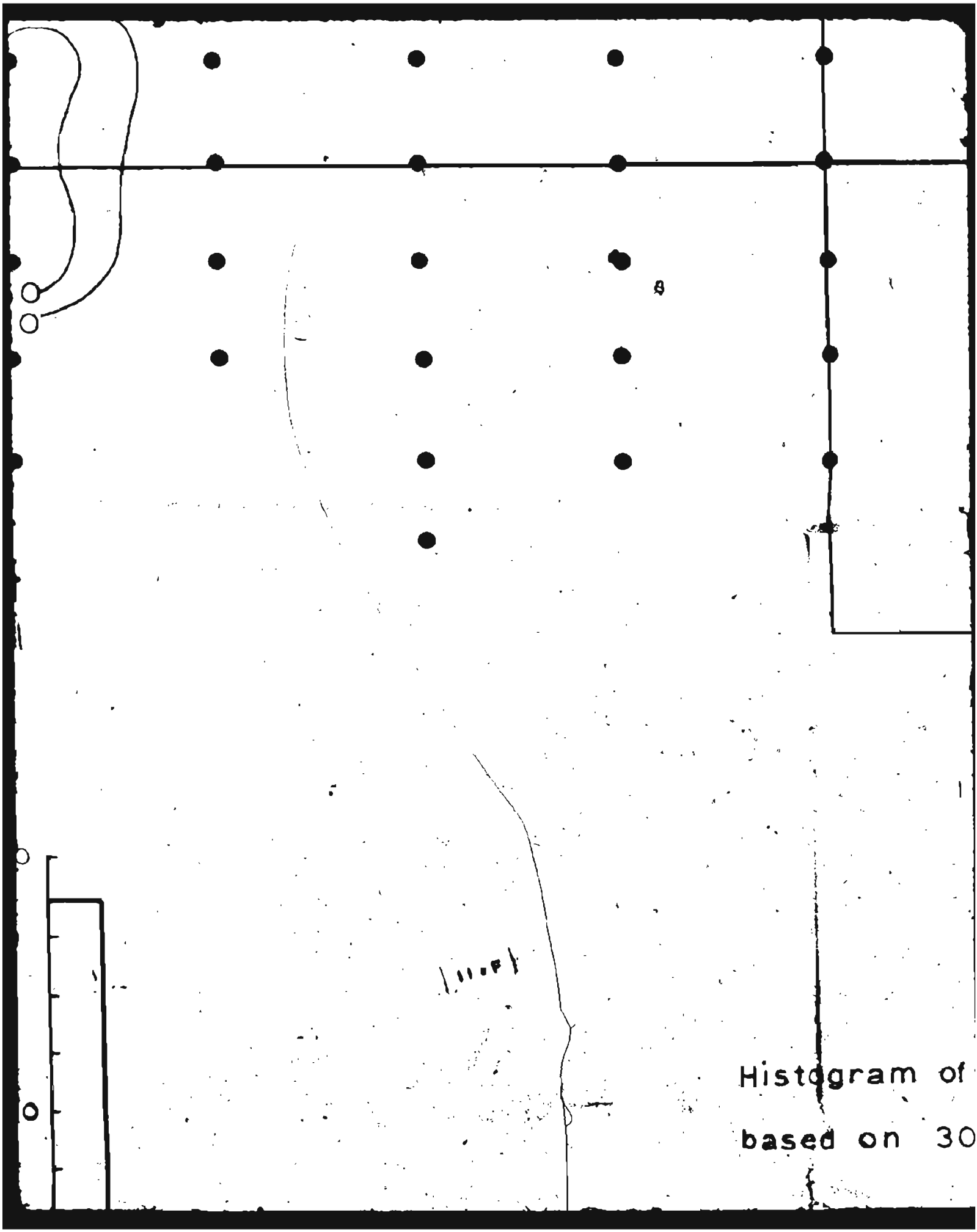
Histogram of
based on 30

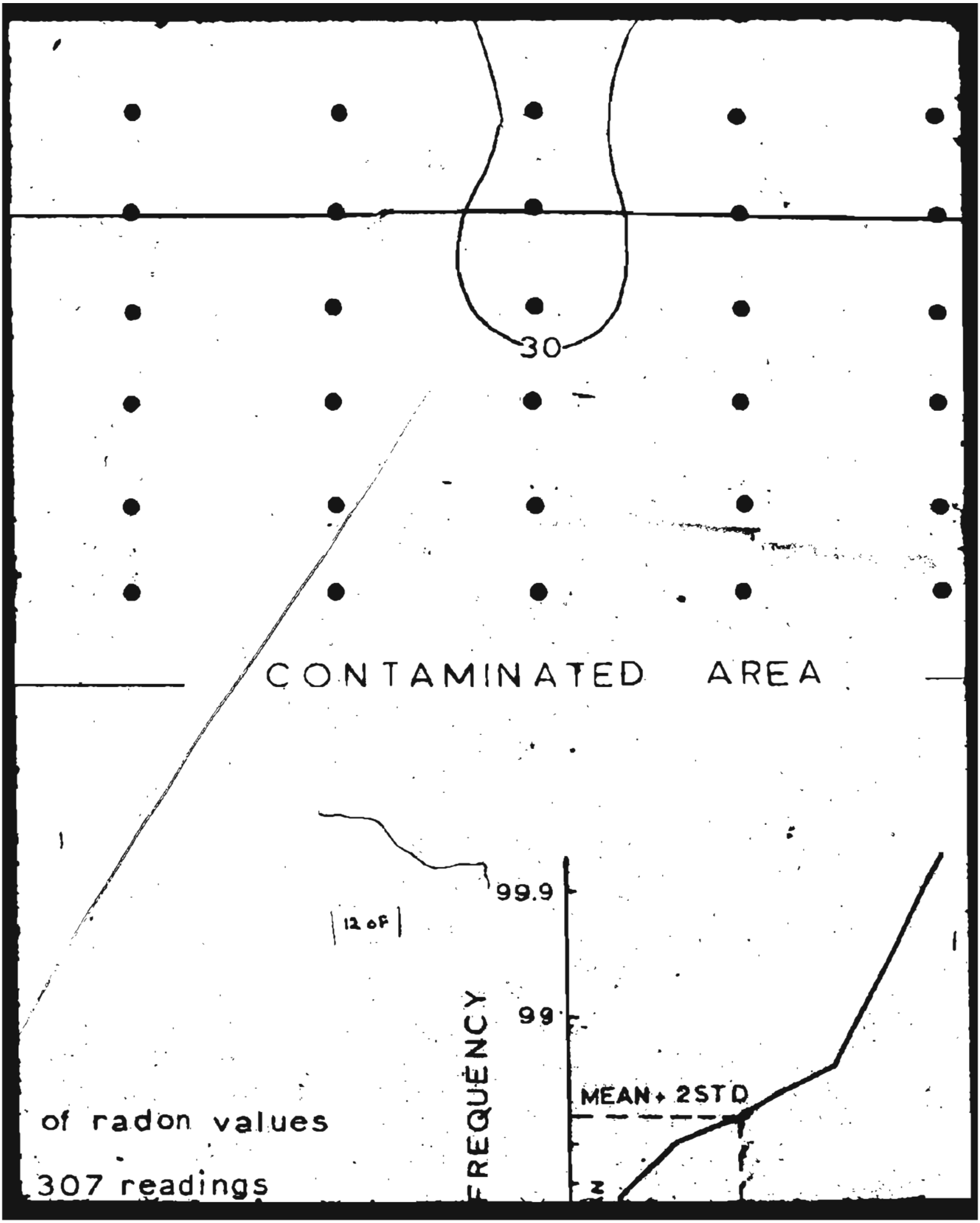
30
CONTAMINATED AREA
12 oF
99.9
99
FREQUENCY
MEAN + 2STD
of radon values
307 readings

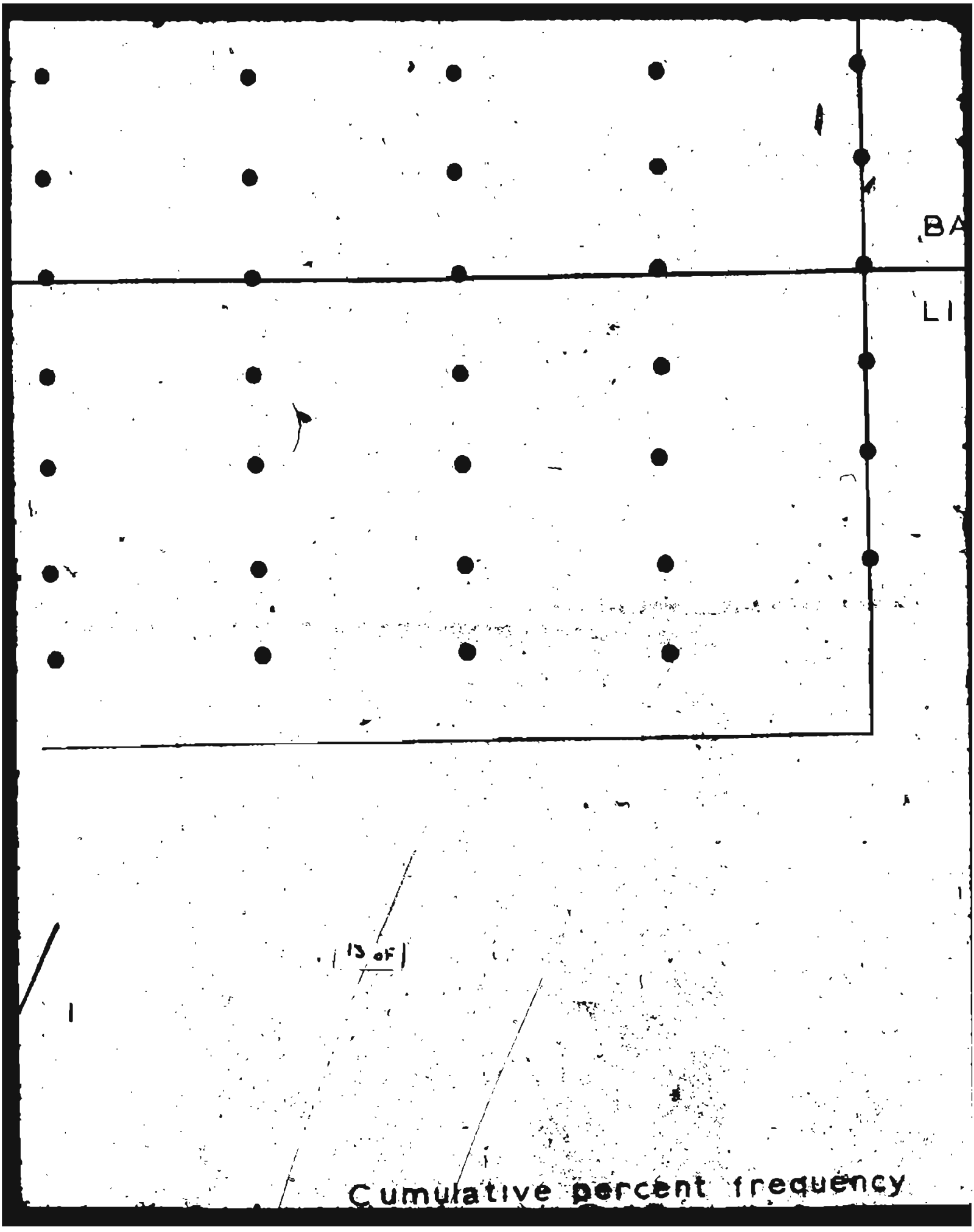
BA
LI
13 of
Cumulative percent frequency

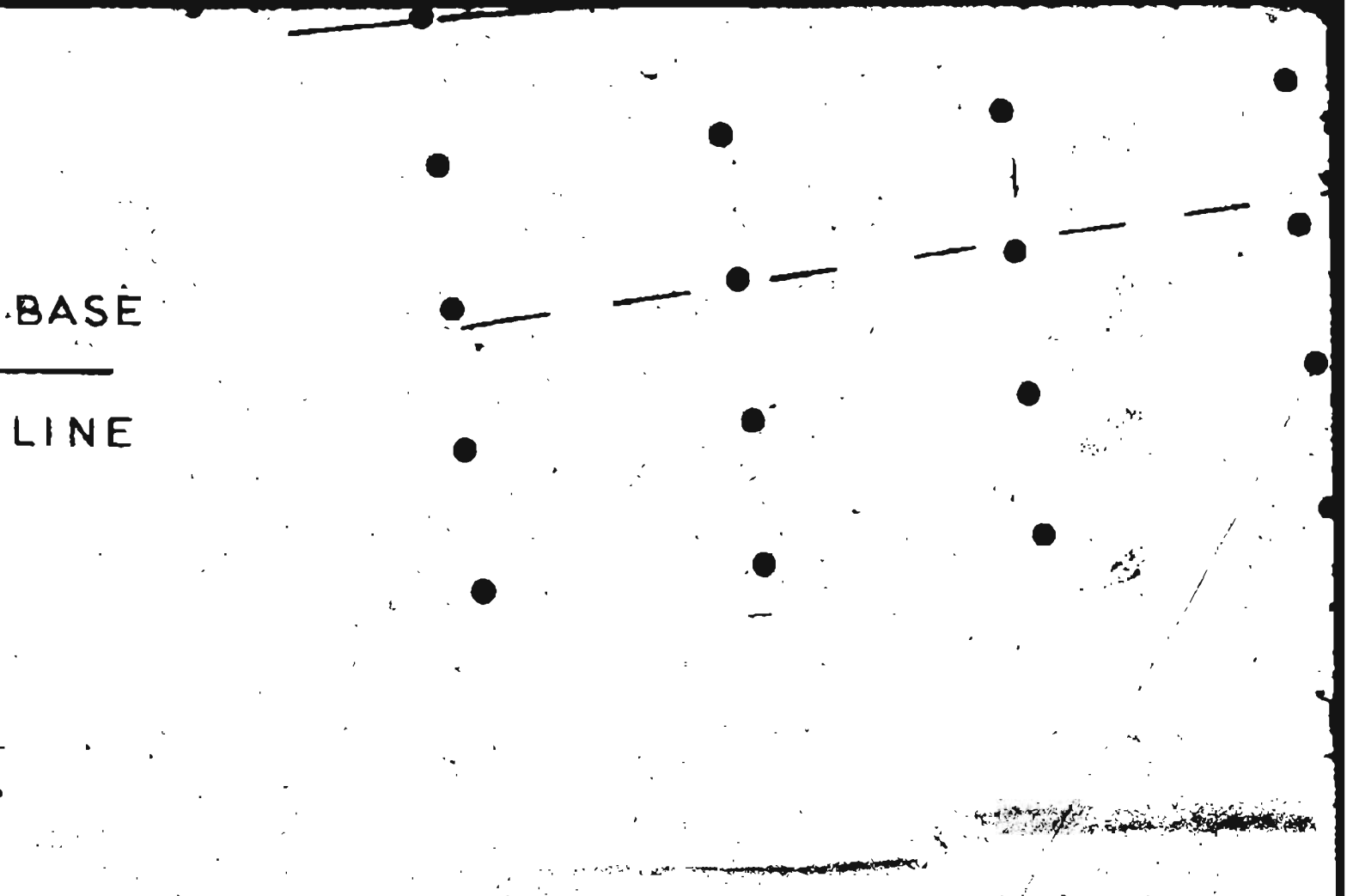

RAINBOW G

Radon in soil air

Instrument : INA
CP

Holes 0.3m

10 squeezes on t

14 of

Scale 1":100'

Corrected rado

plotted :

GRID

r

NAX Counter
PD 284

/15 OF/

the hand pump

on quantity

minus

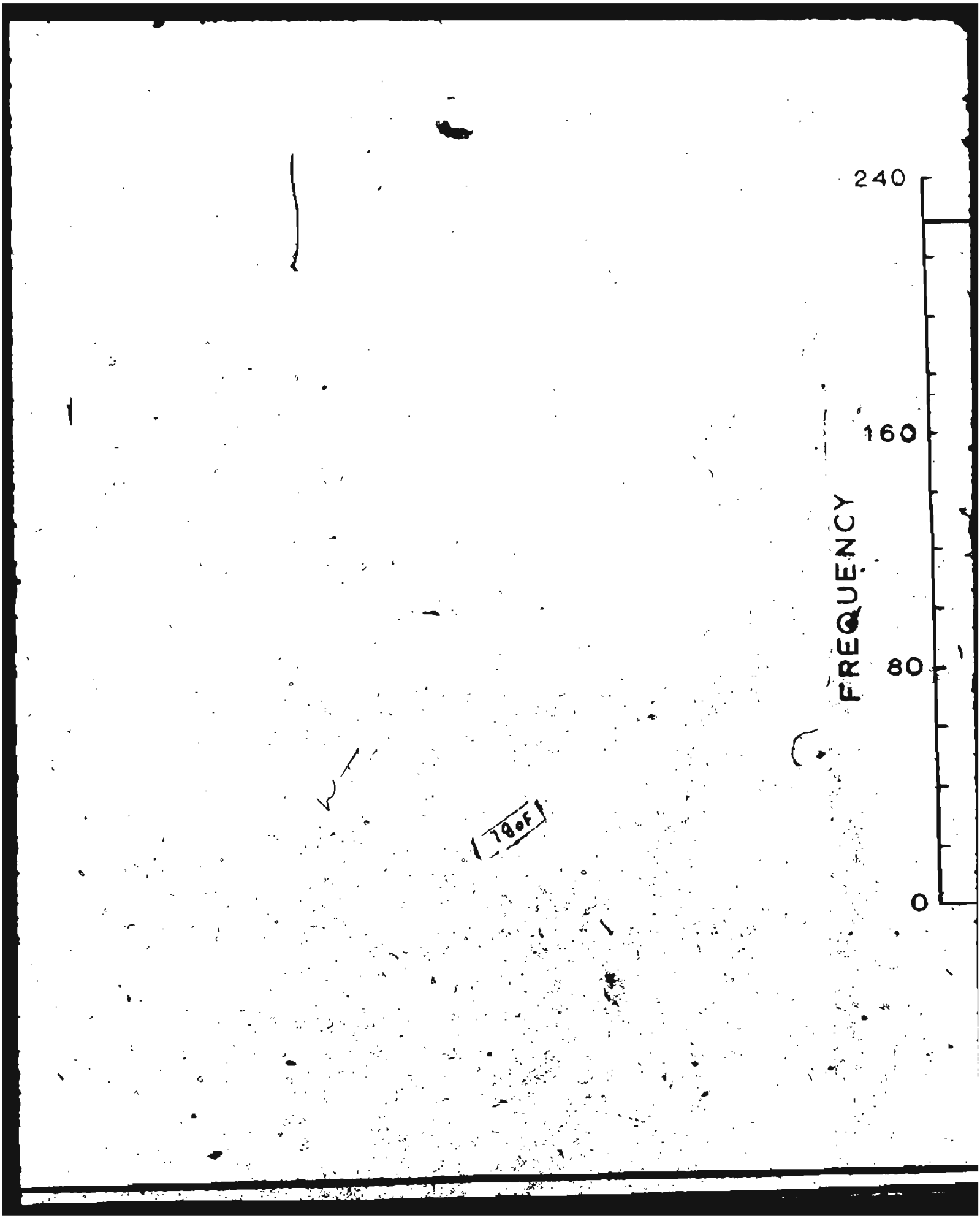
240
160
80
0
FREQUENCY
1 of 1

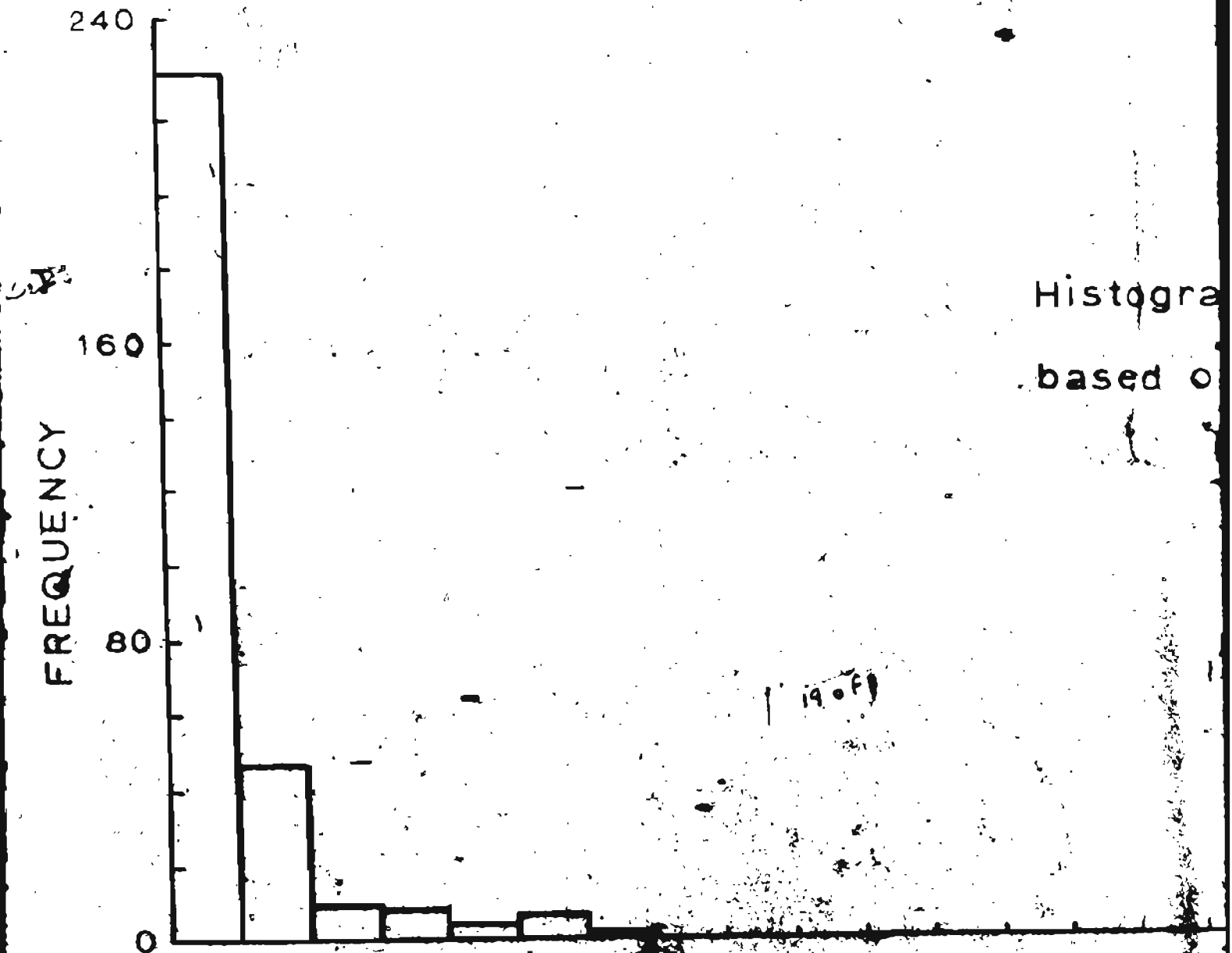

Histogra

based o

80

on c/m

ogram of radon values

ed on 307 readings

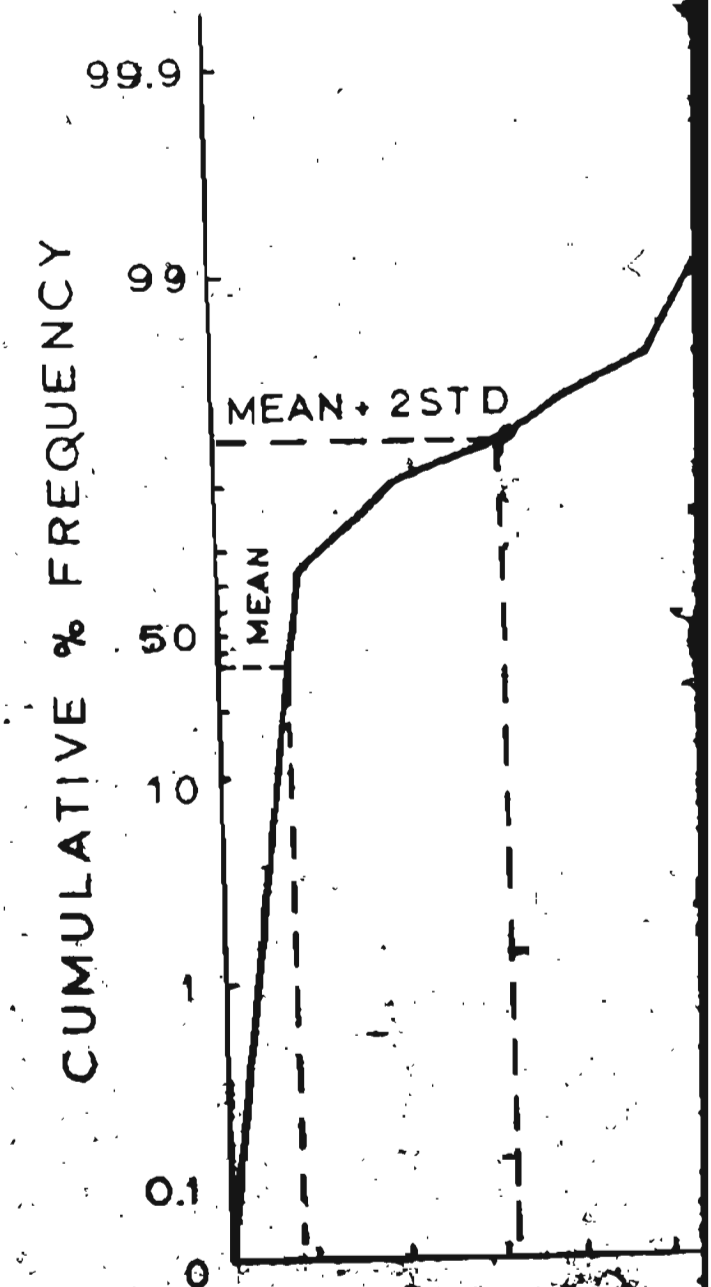

20°F

160

Cumulative percent frequenc
distribution of radon readi
on normal probability paper

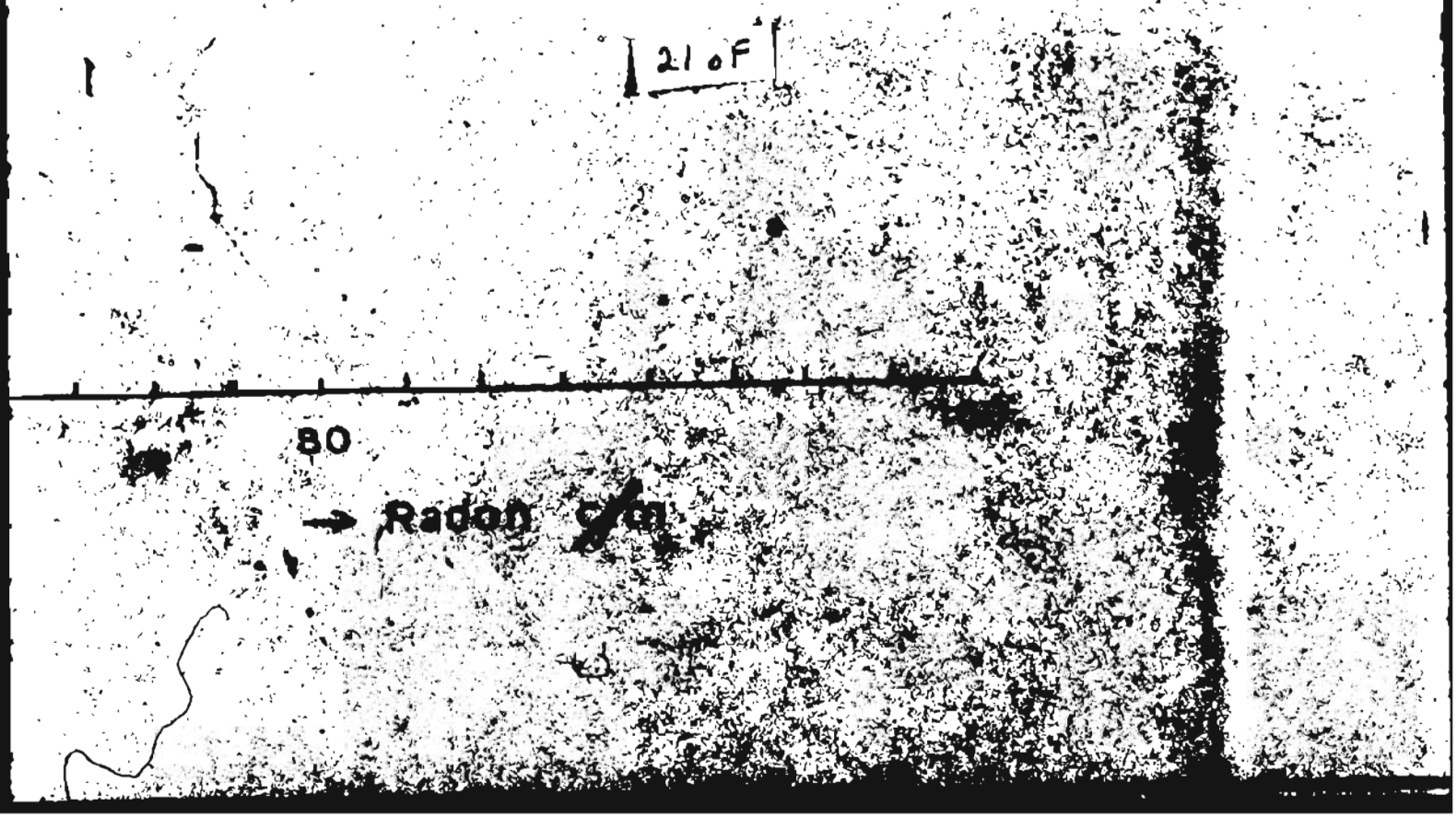

Instrument

Holes 0.3

10 squeeze

Scale 1":1

Corrected

plotted:

quency

readings

aper

Radon rea

backgroun

(Radon valu

smoothed

method o

Three po

average

Fig. 5B

Instrument : INAX Counter
CPD 284

Holes 0.3m

10 squeezes on the hand pump

Scale 1":100'

Corrected radon quantity plotted :

Radon reading minus background

(Radon values have been smoothed by using the method of moving averages) : Three point linear moving average was used

23 of 23


CENTRE FOR NFLD. STUDIES
JUN 2 1979
MEMORIAL UNIVERSITY
OF NEWFOUNDLAND